Modern Countercurrent Chromatography

EDITED BY
Walter D. Conway
and Richard J. Petroski

ACS Symposium Series [illegible]

ACS SYMPOSIUM SERIES **593**

Modern Countercurrent Chromatography

Walter D. Conway, EDITOR
State University of New York at Buffalo

Richard J. Petroski, EDITOR
Agricultural Research Service, U.S. Department of Agriculture

Developed from a symposium sponsored
by the Division of Agricultural and Food Chemistry
at the 206th National Meeting
of the American Chemical Society,
Chicago, Illinois,
August 22–27, 1993

American Chemical Society, Washington, DC 1995

Downloaded by 89.163.35.42 on June 28, 2012 | http://pubs.acs.org
Publication Date: May 15, 1995 | doi: 10.1021/bk-1995-0593.fw001

QP 519.9 C68M63 1995 copy 1

Modern countercurrent
chromatography

Library of Congress Cataloging-in-Publication Data

Modern countercurrent chromatography / Walter D. Conway, editor; Richard J. Petroski, editor.

p. cm.—(ACS symposium series; 593)

"Developed from a symposium sponsored by the Division of Agricultural and Food Chemistry at the 206th National Meeting of the American Chemical Society, Chicago, Illinois, August 22–27, 1993."

Includes bibliographical references and index.

ISBN 0–8412–3167–2

1. Countercurrent chromatography—Congresses. I. Conway, Walter D. II. Petroski, Richard J. III. American Chemical Society. Division of Agricultural and Food Chemistry. IV. Series.

QP519.9.C68M63 1995
543′.0894—dc20 95–7048
CIP

This book is printed on acid-free, recycled paper.

Downloaded by 89.163.35.42 on June 28, 2012 | http://pubs.acs.org
Publication Date: May 15, 1995 | doi: 10.1021/bk-1995-0593.fw001

Copyright © 1995

American Chemical Society

All Rights Reserved. The appearance of the code at the bottom of the first page of each chapter in this volume indicates the copyright owner's consent that reprographic copies of the chapter may be made for personal or internal use or for the personal or internal use of specific clients. This consent is given on the condition, however, that the copier pay the stated per-copy fee through the Copyright Clearance Center, Inc., 222 Rosewood Drive, Danvers, MA 01923, for copying beyond that permitted by Sections 107 or 108 of the U.S. Copyright Law. This consent does not extend to copying or transmission by any means—graphic or electronic—for any other purpose, such as for general distribution, for advertising or promotional purposes, for creating a new collective work, for resale, or for information storage and retrieval systems. The copying fee for each chapter is indicated in the code at the bottom of the first page of the chapter.

The citation of trade names and/or names of manufacturers in this publication is not to be construed as an endorsement or as approval by ACS of the commercial products or services referenced herein; nor should the mere reference herein to any drawing, specification, chemical process, or other data be regarded as a license or as a conveyance of any right or permission to the holder, reader, or any other person or corporation, to manufacture, reproduce, use, or sell any patented invention or copyrighted work that may in any way be related thereto. Registered names, trademarks, etc., used in this publication, even without specific indication thereof, are not to be considered unprotected by law.

PRINTED IN THE UNITED STATES OF AMERICA

American Chemical Society
Library
1155 16th St., N.W.
Washington, D.C. 20036

Downloaded by 89.163.35.42 on June 28, 2012 | http://pubs.acs.org
Publication Date: May 15, 1995 | doi: 10.1021/bk-1995-0593.fw001

1995 Advisory Board

ACS Symposium Series

M. Joan Comstock, *Series Editor*

Robert J. Alaimo
Procter & Gamble Pharmaceuticals

Mark Arnold
University of Iowa

David Baker
University of Tennessee

Arindam Bose
Pfizer Central Research

Robert F. Brady, Jr.
Naval Research Laboratory

Mary E. Castellion
ChemEdit Company

Margaret A. Cavanaugh
National Science Foundation

Arthur B. Ellis
University of Wisconsin at Madison

Gunda I. Georg
University of Kansas

Madeleine M. Joullie
University of Pennsylvania

Lawrence P. Klemann
Nabisco Foods Group

Douglas R. Lloyd
The University of Texas at Austin

Cynthia A. Maryanoff
R. W. Johnson Pharmaceutical
Research Institute

Roger A. Minear
University of Illinois
at Urbana–Champaign

Omkaram Nalamasu
AT&T Bell Laboratories

Vincent Pecoraro
University of Michigan

George W. Roberts
North Carolina State University

John R. Shapley
University of Illinois
at Urbana–Champaign

Douglas A. Smith
Concurrent Technologies Corporation

L. Somasundaram
DuPont

Michael D. Taylor
Parke-Davis Pharmaceutical Research

William C. Walker
DuPont

Peter Willett
University of Sheffield (England)

Downloaded by 89.163.35.42 on June 28, 2012 | http://pubs.acs.org
Publication Date: May 15, 1995 | doi: 10.1021/bk-1995-0593.fw001

Foreword

THE ACS SYMPOSIUM SERIES was first published in 1974 to provide a mechanism for publishing symposia quickly in book form. The purpose of this series is to publish comprehensive books developed from symposia, which are usually "snapshots in time" of the current research being done on a topic, plus some review material on the topic. For this reason, it is necessary that the papers be published as quickly as possible.

Before a symposium-based book is put under contract, the proposed table of contents is reviewed for appropriateness to the topic and for comprehensiveness of the collection. Some papers are excluded at this point, and others are added to round out the scope of the volume. In addition, a draft of each paper is peer-reviewed prior to final acceptance or rejection. This anonymous review process is supervised by the organizer(s) of the symposium, who become the editor(s) of the book. The authors then revise their papers according to the recommendations of both the reviewers and the editors, prepare camera-ready copy, and submit the final papers to the editors, who check that all necessary revisions have been made.

As a rule, only original research papers and original review papers are included in the volumes. Verbatim reproductions of previously published papers are not accepted.

M. Joan Comstock
Series Editor

In Modern Countercurrent Chromatography; Conway, W., et al.;
ACS Symposium Series; American Chemical Society: Washington, DC, 1995.

Downloaded by 89.163.35.42 on June 28, 2012 | http://pubs.acs.org
Publication Date: May 15, 1995 | doi: 10.1021/bk-1995-0593.pr001

Preface

PROBLEMS INVOLVING SEPARATION, ISOLATION, and purification pervade the sciences of natural products, phytochemistry, biochemistry, synthetic chemistry, and related fields. Many mixtures defy resolution by any single method and require the combined advantages of several complementary techniques. Modern countercurrent chromatography (CCC) greatly extends the range of sample types amenable to chromatographic purification, particularly on a preparative scale.

CCC is a relatively new technique. Although its origins can be traced to the early 1930s, development of modern apparatus began in the 1960s when Yoichiro Ito introduced a helical coil of inert plastic tubing as a column for the practice of liquid–liquid partition chromatography. The method provided counterflow of two immiscible liquids and did not require a porous matrix to retain a stationary liquid phase. It thereby provided a pure form of liquid–liquid chromatography in which solute retention depends only on the partition coefficient.

The evolution of CCC apparatus and underlying theory is continuing. The purpose of this volume and the symposium upon which it is based is to discuss the lastest advances in CCC technology. Several chapters in the book discuss advances in CCC since the symposium.

The book begins with a brief overview of CCC followed by four chapters that discuss various theoretical aspects of the technique. Specific applications of CCC to plant components, a peptide and lipids, the optimization of solvent systems, coupling of CCC with fast atom bombardment mass spectrometry, and the use of CCC to directly measure octanol–water partition coefficients are presented in the next section. A new technique, pH-zone-refining CCC for purification of acids and bases, is presented in the final four chapters. This section includes extensive discussion of an equilibrium model that was only very recently developed to explain this new methodology.

Acknowledgments

The symposium could not have been held without the sponsorship and financial assistance of the ACS Division of Agricultural and Food Chem-

istry as well as the financial assistance of Hauser Chemical Company, for which we are grateful.

WALTER D. CONWAY
Department of Pharmaceutics
School of Pharmacy
State University of New York at Buffalo
565 Hochstetter Hall
Buffalo, NY 14260

RICHARD J. PETROSKI
National Center for Agricultural Utilization Research
Agricultural Research Service
U.S. Department of Agriculture
1815 North University Street
Peoria, IL 61614

December 16, 1994

Downloaded by 89.163.35.42 on June 28, 2012 | http://pubs.acs.org
Publication Date: May 15, 1995 | doi: 10.1021/bk-1995-0593.pr001

Downloaded by 89.163.35.42 on June 28, 2012 | http://pubs.acs.org
Publication Date: May 15, 1995 | doi: 10.1021/bk-1995-0593.ch001

Chapter 1

Overview of Countercurrent Chromatography

Walter D. Conway

Department of Pharmaceutics, School of Pharmacy, State University of New York at Buffalo, 565 Hochstetter Hall, Buffalo, NY 14260

Retention and separation in countercurrent chromatography (CCC) is based purely on the liquid-liquid partition coefficients of the solutes since no adsorptive matrix is employed to retain the stationary phase. The liquid stationary phase is held in an inert, coiled tubular column by an inertial force field while the immiscible mobile phase passes through. Droplet CCC as well as more modern coil planet centrifuge and chambered plate chromatographs are described. The theoretical basis of retention and resolution is briefly presented along with a discussion of solvent systems and some applications of this relatively new chromatographic technique.

This chapter is intended to introduce the novice to the nature and scope of countercurrent chromatography (CCC) and to present a brief outline of chromatographic theory relating CCC to other forms of chromatography. A comprehensive review of CCC literature is not intended and only selected references will be given. Several monographs and reviews have been published (1-7). The reader is also directed to several special issues of J. Liq. Chromatog. **1984** [no. 2] *7*, 227-431; **1985** [no. 12] *8*, 2127-2335; **1988** [no. 1] *11*, 1-300; **1990** [no. 12] *13*, 2309-2448; **1990** [no. 18] *13* 3559-3704; **1992** [nos. 15, 16] *15*, 2639-2925 and the January 18 (**1991**) issue of J. Chromatog. **1991** [no. 1] *538*, 1-229, which contain a broad range of articles mainly based on presentations given at annual symposia on CCC held at the Pittsburgh Conference since 1980 and on an international colloquium on centrifugal partition chromatography in 1990 at San Mateo, CA.

CCC is fairly well known and practiced in the field of natural product chemistry, including fermentation. It is almost universally applicable on a mg to multigram scale as a preparative purification technique for both polar and nonpolar organic materials as well as inorganic mixtures such as rare earths. It has been applied to many classes of compounds, including agricultural chemicals, alkaloids,

0097–6156/95/0593–0001$12.00/0

amino acids, peptides, proteins, antibiotics, drug metabolites, dyes, food products, flavonids, glycosides, herbicides, pesticides, pharmaceuticals, optical isomers, saponins, tannins, metals and other inorganic materials. While less well known in many of these fields, the circle of CCC practitioners is expanding as the perception of its advantages increases. Recent development of a technique called pH-Zone Refining (8-10), which allows ready purification of multigram quantities of halogenated fluorescein dyes, will likely accelerate the use of CCC. It is broadly applicable to acidic and basic compounds and in the case of dyes allows separation and purification of the components with a speed and to a degree of purity not achievable previously.

What is Countercurrent Chromatography?

Countercurrent chromatography or CCC is simply liquid-liquid partition chromatography carried out in such a way that no solid matrix is required to retain the stationary phase. It can be broadly defined as: a. any chromatographic technique employing two immiscible liquid phases in which, b. one phase is distributed longitudinally in a relatively uniform manner in a hollow tube or series of chambers while, c. the second phase passes through and is mixed with the first phase.

It is difficult to make the definition simple and yet include all the techniques which have been referred to as CCC, as well as all types of apparatus described as countercurrent chromatographs (also abbreviated CCC). Part of the difficulty stems from the fact that some CCC apparatus are very versatile and allows one to carry out other separation processes which are not classically regarded as chromatography. These include, for instance, foam fractionation, batch extraction, and some forms of countercurrent extraction. Countercurrent chromatographers tend to regard anything done in a CCC apparatus as chromatography. To avoid confusion, it is sometimes preferable to distinguish the process from the apparatus.

Conventional column chromatography is usually carried out by introducing the sample as a bolus at the inlet of the column, and the packing or stationary phase does not flow. In conventional HPLC, sample constituents partition into, or are adsorbed onto, the stationary phase and are eluted from the column in order of their increasing affinity for the stationary phase.

Partition Coefficient and Sample Recovery

CCC is usually carried out in exactly the same way, but both phases are liquid and migration through the column is controlled only by the partition coefficient, K,

$$K = C_s/C_m \qquad (1)$$

where C_s and C_m represent the concentrations of a solute in the stationary and mobile phases respectively. Solutes with higher partition coefficients are eluted later. Since no adsorptive materials are present, the mixed adsorption/partition modes are avoided and retention can be predicted from the partition coefficient

Downloaded by 89.163.35.42 on June 28, 2012 | http://pubs.acs.org
Publication Date: May 15, 1995 | doi: 10.1021/bk-1995-0593.ch001

Downloaded by 89.163.35.42 on June 28, 2012 | http://pubs.acs.org
Publication Date: May 15, 1995 | doi: 10.1021/bk-1995-0593.ch001

and the amounts of stationary and mobile phases within the column. Loss of sample in CCC is avoided also since usually both phases are volatile and retained solutes can be recovered by pumping out the column contents and evaporating the solvents.

Versatility. CCC is extremely versatile. Almost any two phase solvent system may be employed, although some solvent systems give better results in a particular type of apparatus. In general, either the lighter or the heavier phase may be chosen as the mobile phase, thereby reversing the order of solute elution. In fact, the separation may be started in one mode and then the phases reversed at any time later in the run. While one of the phases is often aqueous, nonaqueous systems such as hexane or heptane vs. either acetonitrile or methanol are useful for lipophilic solutes. Two phase aqueous systems such as aqueous sodium phosphate vs. aqueous polyethylene glycol or aqueous dextran vs. aqueous polyethylene glycol are useful for very hydrophilic solutes such as proteins or enzymes (11,12).

Sample introduction is also versatile. The sample is usually introduced with a conventional sample loop and valve and may be dissolved in either an aliquot of stationary phase, or of mobile phase, or a mixture of both phases.

Additives such as counterions for ion pairing may be added to one or both phases. Chiral resolution of isoleucine on a mg scale has been reported using dodecylproline as a chiral selector (13). Recently N-dodecanoyl-L-proline-3,5-dimethylanilide has been used to completely resolve racemic dinitrobenzoyl derivatives of t-butylvalinamide and t-butylleucinamide on a gram scale (14).

Although most applications of CCC employ a mode with one phase held stationary, it is possible, using a modified column, to flow both phases simultaneously in opposite directions while introducing the sample either as a bolus or continuously at either one end or the center of the column. If a gas is introduced as one fluid stream, foam fractionation (or foam CCC) may be carried out. Though the feasibility of these modes has been demonstrated, they are not yet being routinely employed. Details may be found in the general references cited earlier.

Mainly Preparative. CCC is mainly a preparative technique and is not competitive with quantitative analytical HPLC in terms of sensitivity. CCC effluent is commonly monitored using UV absorption with a preparative cell. Use of an evaporative light scattering detector has also been described (15) and coupling CCC with a mass spectrometer is described in this symposium volume (McGuire et al.). In many applications to natural products and organic synthesis, fractions are simply collected and examined by TLC. In fact, a device to directly monitor CCC by TLC has been described (16).

History and Modern Apparatus

The origins of CCC can be traced to a counterflowing liquid-liquid apparatus described in 1934 by Cornish (17) and used to purify oil-soluble vitamins. But the modern era began in 1966 when Ito and colleagues described the first coil planet centrifuge CCC (18,19). Although sold commercially as the CPC Analyzer, this was not a flow-through device and was cumbersome to use. The significant conceptual advance was the use of a rotating helical coil of polyethylene tubing to cause counterflow of immiscible liquids, initially loaded in opposite halves of the coil. A sample placed initially at the coil center was fractionated by partitioning of the constituents. Ito has since described a large number of instruments mainly using the helical coil as a chromatographic column. Only two of Ito's designs and one other will be described here.

Droplet CCC. The first really successful CCC was the droplet countercurrent chromatograph described in 1970 (20) and introduced commercially by Tokyo Rikakikai in 1972. It is shown schematically in Figure 1. The apparatus typically consists of about 300 glass tubes approximately 1.8 mm i.d. and 60 cm length connected in series using narrow-bore PTFE tubing and inert plastic fittings. Many separations, particularly in the area of natural products were done in the 1970s and early 1980s using DCCC (3,21). Although very efficient separations were obtained, the technique was very slow, often 2 or 3 days, and worked with only a limited number of solvent systems. The apparatus was also difficult to clean and was prone to leaks at the many connections. It has therefore given way to the more rapid centrifugal techniques which Ito and others began to develop in the late 1970s.

Coil Planet Centrifuges. The most successful of Ito's centrifugal machines thus far has been the multilayer coil planet centrifuge or MLCPC described in 1981 (22,23). A schematic view is shown in Figure 2A. The coil, which is the chromatographic column, is attached through a bearing to a rotating frame. A planetary gear on the coil shaft meshes with a stationary or sun gear so that as the frame rotates with an orbital frequency of ω, typically 800 rpm, the planetary coil rotates twice on its axis with each circuit of the orbit or at an absolute frequency of 2ω. This sets up an unsymmetrical centrifugal force field, which causes immiscible liquids in the coil to counterflow, while at the same time producing quite vigorous mixing within one sector of the coil (2,4). Although coils may be made in a range of sizes, a common one consists of a winding of about 130 m of PTFE tubing, 1.7 mm i.d. x 2.5 mm o.d. on a 5 cm wide spool with a 10 cm core and an o.d of 17.8 cm, giving a column volume of about 300 ml. This is used with an orbital radius of 10 cm. Retention of stationary phase ranges from about 80% for the hydrocarbon systems to about 50% for n-butanol at flow rates of about 2 ml per minute. Larger and smaller variants of the apparatus have been built. Apparatus containing two or three spools in series, thereby eliminating the counterweight, have been described (24,25). Multiple windings on a single spool, with volumes as low as 15 ml have also been made (26). Separations on 300-ml columns typically require a few hours or more. On 15-ml columns a solute with a partition coefficient of 1 elutes in less than 10 minutes while one with a partition coefficient of 10 requires about an hour. On small columns, it is practical and convenient to make multiple injections without replenishing the stationary phase and, except for the necessity of rotating the column, operation resembles use of an HPLC.

Downloaded by 89.163.35.42 on June 28, 2012 | http://pubs.acs.org
Publication Date: May 15, 1995 | doi: 10.1021/bk-1995-0593.ch001

The multilayer coil performs well with organic/aqueous solvent systems ranging from the nonpolar hexane or heptane/water systems through the polar n-butanol/water system. However, with more hydrophilic systems such as sec-butanol/water or n-butanol/acetic acid/water or n-butanol/methanol/water containing significant amounts of acetic acid or methanol, the stationary phase is poorly retained. This is unfortunate for peptide chemists who frequently employ the BAW or n-butanol/acetic acid/water - 4:1:5 (v/v/v) or similar systems (27). Another variant of the coil planet centrifuge (28) employs a series of somewhat longer coils up to a few layers thick, wound on a small-diameter core and mounted in eccentric positions on the column holder as illustrated in Fig. 2B. While the stationary phase retention of these eccentric columns is only about 50% of column volume for less viscous solvents like hexane, they exhibit retention of about 40% with the more hydrophilic systems used in peptide purification (29). The stationary phase retention is important in CCC since resolution increases significantly as the stationary phase volume, V_S, increases (4). In CCC, V_S can be 80% or more of column volume, V_C, whereas in conventional solid-supported chromatography, V_S is less than 10% of V_C.

A novel feature of coil planet centrifuge chromatographs is the lack of a rotating seal in the fluid stream. The flow lines of approximately 1.6 mm od PTFE tubing in Figure 2A are continuous from the instrument inlet or outlet to the connections on the multilayer coil. Because of the 2/1 ratio of coil rotational frequency to orbital frequency the sections of tubing between the coil axis and the central axis undergo only a half-twist and reversal with each revolution. The lines therefore do not twist or tangle and will operate for several thousand hours before replacement is required.

Chambered Plate Chromatographs. A series of chromatographs in which the column consists of a series of chambers and interconnecting channels, cut into blocks held in a centrifuge rotor or later cut directly into the rotor itself was introduced in 1982 (7, 30-33). Two rotating seals allow liquid to flow through the rotating column as shown schematically in Figure 3. Stationery phase is retained in the chambers by centrifugal force and surface tension and mixing is achieved by turbulence produced by flow within the chambers. The stationary phase is segmented as in DCCC and the process has been described as Centrifugal Droplet CCC (4) although droplet formation need not arise in the mixing process (30,31). Some authors use the abbreviation CPC to refer specifically to CCC carried out in a chambered rotor (hydrostatic apparatus) (7,34), and use the term CCC only for chromatography done in apparatus involving hydrodynamic mixing such as the MLCPC. Others use CPC generically in reference to Centrifugal Partition Chromatography in any type of centrifugal apparatus. The acronym has also been widely used for a longer time to abbreviate Coil Planet Centrifuge (5).

Liquid Flow in Coil Planet Centrifuge Chromatographs

When coils are mounted in an eccentric position in the CPC as shown in Figure 2B, the stationary phase is segmented, as shown in Figure 4A. Either upper or lower phase, pumped in a head to tail direction, percolates through the stationary

Downloaded by 89.163.35.42 on June 28, 2012 | http://pubs.acs.org
Publication Date: May 15, 1995 | doi: 10.1021/bk-1995-0593.ch001

Downloaded by 89.163.35.42 on June 28, 2012 | http://pubs.acs.org
Publication Date: May 15, 1995 | doi: 10.1021/bk-1995-0593.ch001

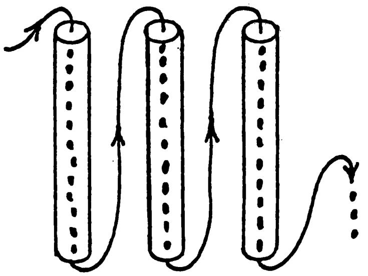

Figure 1. Gravitational droplet CCC. Lower phase flow is shown.

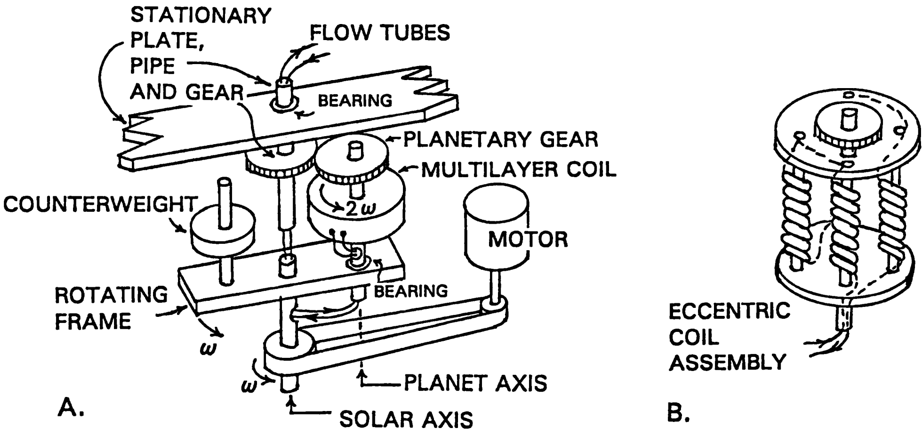
STATIONARY PLATE, PIPE AND GEAR
FLOW TUBES
BEARING
PLANETARY GEAR
MULTILAYER COIL
COUNTERWEIGHT
2ω
MOTOR
ROTATING FRAME
ω
BEARING
ω
PLANET AXIS
SOLAR AXIS
A.
ECCENTRIC COIL ASSEMBLY
B.

Figure 2. A. Cutaway view of essential features of the multilayer coil planet centrifuge, MLCPC. B. Modified planetary column assembly with single or multilayer coils mounted in eccentric positions and connected in series.

segments. Mixing of the two phases is described as dynamic, meaning that it is induced by the motion of the CPC and is independent of flow rate. The mixing has also been referred to as cascade mixing to depict the continuous flow of one phase into the other, somewhat like a waterfall. The term head signifies the end of the coil approached by a heavy bead or air bubble placed within the coil and followed by coil rotation. It is analogous to the head of a screw if one imagines a wall or object approaching the head of the screw as the screw is turned.

When the coil is wound coaxially around the rotating planetary axis, as in Figure 2A, it is acted on by a quite different force field pattern which causes the two immiscible liquids to form parallel layers as in Figure 4B, C. These have a natural tendency to slowly flow in opposite directions. Either phase may be pumped without displacing a large quantity of the stationary phase. In this case best results are usually obtained when the column is rotated in the direction that places the column head at the spool center and either the heavier phase is pumped in the head to tail direction or the lighter phase is pumped in the tail to head direction. Mixing here is also dynamic and is caused by vigorous agitation of the two layers in that segment of the spool nearest the solar axis (Figure 2A). This segment comprises about one-third of the column, and contains a mixing zone in each column loop. Since the spool is rotating, the mixing zones continuously travel through the column length at high speed (4 to 7 m/s at 800 rpm), maintaining the phases in hydrodynamic equilibrium and facilitating mass transer of sample components between the phases.

Indeed both phases may be pumped simultaneously to generate true countercurrent flow as illustrated in Figure 4D. Although this has been demonstrated (35) it has not been extensively studied.

Downloaded by 89.163.35.42 on June 28, 2012 | http://pubs.acs.org
Publication Date: May 15, 1995 | doi: 10.1021/bk-1995-0593.ch001

Brief Outline of CCC Theory

Retention. Since adsorption is precluded by the absence of a solid support, retention of solutes in CCC depends only on the partition of coefficient, K, equation 1. Because the volumes of both phases, as well as the column volume, are readily measured, the capacity factor term is unnecessary in CCC and the chromatogram is readily visualized in terms of the partition coefficient.

A universal countercurrent chromatogram is shown in Figure 5A. Band spreading of the later peaks is not illustrated. Regardless of the phase volume ratio, a solute with $K=1$ will elute with one column volume of mobile phase. Since it is invarient, the $K=1$ position serves as the focal point of the countercurrent chromatogram. A solute with $K=0$ does not partition into the stationary phase and will elute with one mobile phase volume or at the position commonly called the solvent front. Solutes with partition coefficients increasing by integers will elute at multiples of V_s.

This pattern is a consequence of the general equation for elution in partition chromatography.

$$V_R = V_m + KV_s \qquad (2)$$

where V_R is the solute retention time.

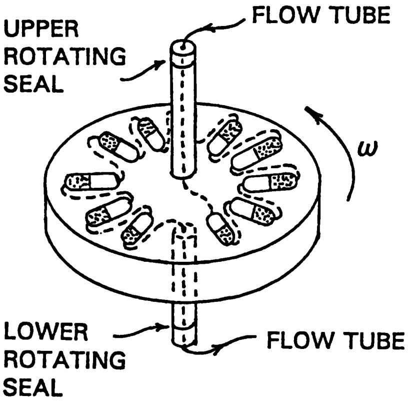
UPPER ROTATING SEAL
FLOW TUBE
ω
LOWER ROTATING SEAL
FLOW TUBE

Figure 3. Schematic view of essential features of the Sanki Centrifugal Partition Chromatograph based on a chambered column.

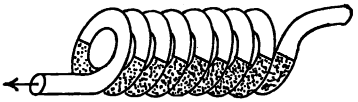

A. SEGMENTED PHASES, UPPER OR LOWER PHASE MOBILE

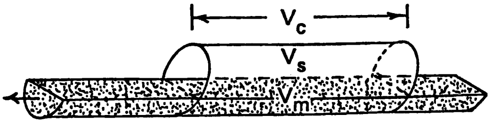

B. CCC, LOWER PHASE MOBILE

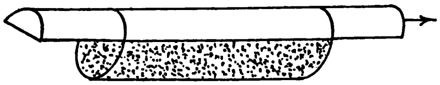

C. CCC, UPPER PHASE MOBILE

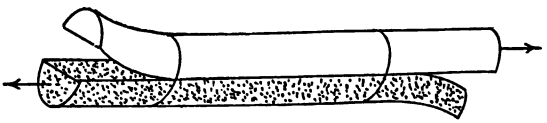

D. TRUE CCC, BOTH PHASES MOBILE

Figure 4. Liquid flow in coil planet centrifuge chromatographs.

Downloaded by 89.163.35.42 on June 28, 2012 | http://pubs.acs.org
Publication Date: May 15, 1995 | doi: 10.1021/bk-1995-0593.ch001

The fraction of column volume filled with stationary phase, S_F, will depend on the particular solvent system and on operating conditions, particularly rotational speed and mobile phase flow rate. Figure 5B illustrates the universal chromatogram for $S_F = 0.67$ while Figure 5C presents the retention times in minutes under the same conditions when the flow rate is 2 ml/min. Figure 5D illustrates the visual estimation of K after notation of the V_m and V_c points on the chromatogram. It is visually apparent that solute 1 eluting at V_1 has a K of about 0.5 while solute 2 has a K of about 2.25. The K values can be accurately calculated from the chromatogram using the equation

$$K = (V_R - V_m)/(V_c - V_m) \qquad (3)$$

The point V_c is the known column volume. The point V_m can be determined in various ways. One approach is based on the common method of performing CCC wherein the column is first filled with stationary phase (without rotation), after which the sample is injected, rotation is begun and mobile phase is pumped into the column. The stationary phase displaced on the first passage of mobile phase through the column is equal to V_m. In a second approach, a nonretained easily detected marker is added to the sample to indicate V_m. In another versatile method, two pumps are used in parallel to fill the column with both phases simultaneously (36). This method allows the phase volume ratio to be set at any desired value by choice of the relative flow rates of the pumps and is particularly useful for strongly retained solutes for which a low S_F is useful.

Resolution. The resolution of adjacent peaks is commonly defined in chromatography as

$$R_s = 2\ (V_{R,2} - V_{R,1})/(W_1 + W_2) \qquad (4)$$

where $V_{R,2}$ and V_{R}, are the retention volumes of the later and earlier eluted peaks respectively and W_2 and W_1 are their respective base widths.

When the expression in equation 2 is substituted for the V_R terms in equation 4, the V_m term cancels, giving

$$R_s = 2\ (K_2 - K_1)V_s/(W_1 + W_2) \qquad (5)$$

The base width increases with increasing retention volume, but as a first approximation for solutes with similar K values the term $(W_1 + W_2)$ can be assumed to be constant in equation 5. The equation then shows that resolution will be directly proportional to the stationary phase volume, V_s, and to the difference between the solute partition coefficients $(K_2 - K_1)$. The very high V_s values, usually over 0.5, explains why high resolution is obtained in CCC in spite of the modest 300 to 1000 theoretical plates usually obtained. The partition coefficient difference relates to the selectivity of a solvent system. Since many solvent systems are available for CCC, it is advantageous to screen several to optimize retention time and resolution. Screening is conveniently done either with a small CCC column or by non-CCC means. The latter include visual estimation

Downloaded by 89.163.35.42 on June 28, 2012 | http://pubs.acs.org
Publication Date: May 15, 1995 | doi: 10.1021/bk-1995-0593.ch001

of resolution by TLC (5) or several means of estimating K by assay of each phase after equilibrating a small amount of sample with small volumes of the proposed phases. Assays employed include HPLC, absorption spectrophotometry, bioassay and TLC densitometry. Examples of this last method are given by D. Martin in another chapter of this monograph. The initial practical goal is usually to find a solvent system providing a K of about 1 (or in the range of about 0.5 to 2) for the component of interest in the mixture. This usually provides adequate resolution from early eluting substances but allows elution within a few hours. Subsequent optimization would examine solvent selectivity, particularly if more than one substance is to be isolated.

A more complete expression of the resolution equation for CCC is

$$R_s = 0.25\ (\alpha\text{-}1)\ (N)^{0.5}\ K_1/[0.5\ K_1\ (\alpha + 1) + (1\text{-}S_F)/S_F] \qquad (6)$$

in which the selectivity term $\alpha = K_2/K_1$ and the theoretical plate count $N = 16\ (V_R/W)^2$. The ratio of K_1 over the bracketed term is referred to as the partition coefficient term (4).

Downloaded by 89.163.35.42 on June 28, 2012 | http://pubs.acs.org
Publication Date: May 15, 1995 | doi: 10.1021/bk-1995-0593.ch001

Solvent Systems

Two-phase systems ranging in polarity from hexane to 1-butanol with water as the counterphase perform well in the MLCPC (Figure 2A). More hydrophylic systems, such as 2-butanol/water, 1-butanol/acetic acid/water and 1-butanol/methanol/water are poorly retained in the MLCPC but perform better in the eccentric coil apparatus (Figure 2B). Best performance for these more hydrophilic systems as well as two-phase aqueous systems is obtained in various models of the cross axis CCC (37-39). Some hydrophilic systems are also accommodated by apparatus of the chambered rotor type (Figure 3).

Probably the two most commonly used solvent systems in the area of natural products are the ternary chloroform/methanol/water and the quaternary hexane/ethyl acetate/methanol/water systems. Many applications of these and other systems are summarized in recent monographs and reviews (4,5,7).

pH-Zone-Refining CCC

This new technique allows sample size for ionizable solutes to be increased several fold with no increase in the size of the apparatus. Several sample components present in either small or large amount can be separated in high purity in a reasonable time. It therefore represents a very significant advance in the art of preparative CCC. Although initially described for purification of acids (8,9,10) the technique is applicable to bases as well. The methodology will be described only briefly here since it is presented in detail in other chapters of this monograph.

Initially the components of a moderately polar solvent system, such as methyl tert-butyl ether and water are mutually equilibrated in a separatory funnel, then placed in separate containers. In one approach for DNP-amino acids (9), the aqueous phase was made alkaline with ammonia and the CCC coil entirely filled with the alkaline aqueous phase, in anticipation of employing it as the stationary phase. The organic phase, used as the mobile phase, was acidified with trifluoroacetic acid. The DNP-amino acid mixture was added to an aliquot of organic phase. The compounds were not completely soluble but were used as a fine dispersion formed by sonication of the sample. After loading the sample and bringing the CCC up to running speed, the acidified organic phase was pumped through the column as mobile phase.

Initially the acidic sample components transfer to the alkaline stationary phase forming a compact sample zone. The separation then proceeds in the manner of a continuously eluted two-phase aqueous titration. In this example, the acid with the highest pK_a will be neutralized first and will then be extracted into the mobile organic phase where it is continuously eluted as a broad zone. The pH will remain relatively constant throughout this elution since the acid salt and its free acid formed by neutralization serve to buffer the solution. Acids of lower pK_a, still largely in salt form, will be too polar for extraction by the mobile phase. While the solute pK_a appears to be the dominant factor, elution depends also on the relative lipophilicity of the acids present and where two solutes have the same pK_a, the more lipophilic will be eluted first by the mobile organic phase. The chromatographic process is superimposed on that of neutralization and tends to sweep impurities toward the edges of the zone of constant pH. In this example, the pH will fall stepwise as each zone is eluted as in Figure 6. The ammonia in the aqueous phase is referred to as a retainer base, while trifluoroacetic acid in the mobile phase is called a displacer acid. The process is described in much more detail in later chapters.

Downloaded by 89.163.35.42 on June 28, 2012 | http://pubs.acs.org
Publication Date: May 15, 1995 | doi: 10.1021/bk-1995-0593.ch001

Advantages of CCC

The advantages of CCC stem from its lack of solid phase, the wide range of solvent systems available, and its simplicity and versatility. The absence of solid phase coupled with the relatively wide passageways in most apparatus allow relatively crude samples to be chromatographed. As long as there is no actual solid in the samples and as long as no precipitation occurs during chromatography, no damage to the chromatograph will occur. Since most solvent systems are volatile, the sample can be completely recovered by evaporation of the expelled column contents. The column can then be readily rinsed with a suitable solvent and dried with air or nitrogen flow. Extensive rinsing is not required. Retention time is determined only by partitioning, since there is no adsorption, and is therefore predictable from measurements of the partition coefficient obtained either by CCC or other means. Retention time for columns of different size can then be easily calculated.

While CCC is often the method of choice for purification of very polar solutes, the wide range of available solvent systems permits chromatography of compounds ranging from very lipophilic to strongly hydrophilic.

Chromatographic theory for CCC is not fundamentally different from that for other forms of chromatography. However, the equations can be expressed in terms of K, the partition coefficient, which emphasizes the simplicity of CCC and facilitates visual perception of the separation process.

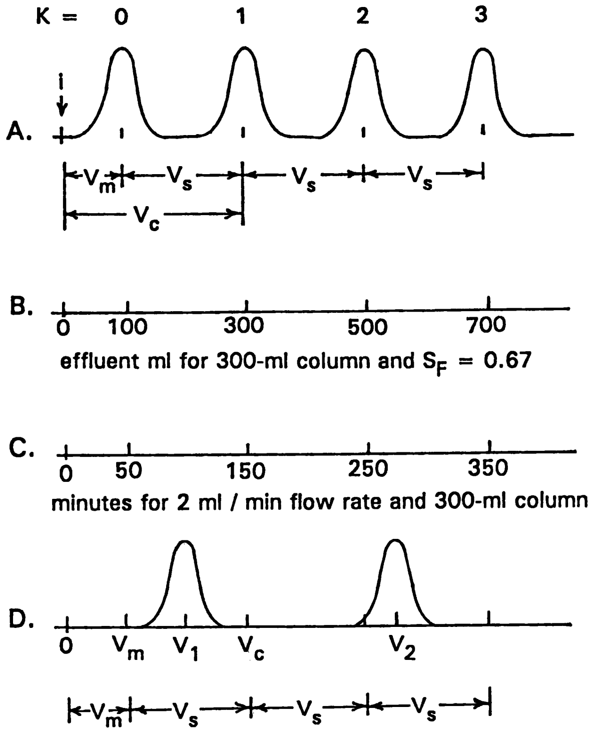

Figure 5. Universal countercurrent chromatogram. A. In terms of the partition coefficient, K. B. Corresponding elution volume scale for a 300-ml column containing 200 ml of stationary phase. C. Corresponding elution time scale for the same column with a flow rate of 2 ml/min. D. Elution volumes V_1 and V_2 for solutes with K of about 0.5 and 2.25 respectively.

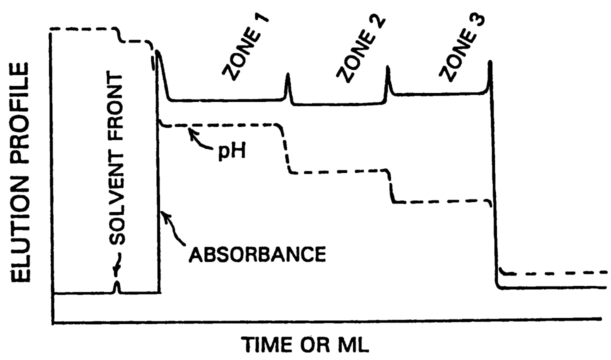

Figure 6. Illustration of pH and absorbance profiles for purification of organic acids by pH-zone-refining CCC using an alkaline aqueous stationary phase and an acidified organic mobile phase. Adapted from Fig. 1 of ref. 9.

Downloaded by 89.163.35.42 on June 28, 2012 | http://pubs.acs.org
Publication Date: May 15, 1995 | doi: 10.1021/bk-1995-0593.ch001

CCC presents a versatility in technical manipulation unprecedented in chromatography. A few of these possibilities include: operation in either the normal or reverse phase mode, simultaneous filling with both phases to vary the phase volume ratio, partial separation in one mode followed by mode reversal to recover strongly retained solutes, addition of interactive solutes (such as retainer and displacer components in pH-zone-refining) to opposite phases prior to the start of chromatography, various types of gradient programs which include conventional pH and solvent polarity programs but also phase volume ratio manipulation during the separation process as well as gradients which lead to dissolution of the stationary phase, and also concurrent flow of the otherwise stationary phase either in the same direction as mobile phase or in the opposed direction (producing true countercurrent chromatography or countercurrent extraction). All of these processes can be carried out in the same apparatus. This manipulative capability permits optimization of particular separations in a variety of ways which are not available in other forms of chromatography.

Downloaded by 89.163.35.42 on June 28, 2012 | http://pubs.acs.org
Publication Date: May 15, 1995 | doi: 10.1021/bk-1995-0593.ch001

Literature Cited

1. Ito, Y., CRC Crit. Rev. Anal. Chem. **1986**, *17*, 65-143.
2. Mandava, N.B. and Ito, Y., Eds., Countercurrent Chromatography, Theory and Practice, Marcel Dekker, New York, Chromatographic Science Series, *44* (1988).
3. Hostettmann, K., Hostettmann, M., and Marston, A., Preparative Chromatography Techniques, Applications in Natural Product Isolation, Springer-Verlag, Berlin, **1986**.
4. Conway, W.D., Countercurrent Chromatography, Apparatus, Theory and Applications, VCH Publishers Inc., New York, (1990).
5. Marston, A. and Hostettmann, K., J. Chromatogr. A, **1994**, *658*, 315-341.
6. McAlpine, J.B. and Hochlowski, J.E., Countercurrent Chromatography, in: Natural Product Isolation, Wagman, G.H., and Cooper, R., Eds., Elsevier, Amsterdam. J. Chromatog. Library, 1989, Vol. *43*, 1-53.
7. Centrifugal Partition Chromatography, Foucault, A.P., Ed., Marcel Dekker, Inc., New York, NY, 1994.
8. Weisz, A.; Scher, A.L.; Shinomiya, K.; Fales, H.M. and Ito, Y., J. Amer. Chem. Soc. **1994**, *116*, 704-708.
9. Ito, Y. and Ma, Y., J. Chromatogr. A, **1994**, *672*, 101-108.
10. Weisz, A.; Andrzejewski, D.; Highet, R.J. and Ito, Y., J. Chromatogr. A, **1994**, *658*, 505-510.
11. Shibusawa, Y. and Ito, Y., J. Liq. Chromatogr., **1992**, *15*, 2787-2800.
12. Lee, Y.W.; Shibusawa, Y.; Chen, F.T.; Myers, J.; Schooler, J.M. and Ito, Y., J. Liq. Chromatogr., **1992**, *15*, 1831-2841.
13. Takeuchi, T.; Horikawa, R. and Tanimura, T., J. Liq. Chromatogr., **1984**, *284*, 285-288.
14. Oliveras, L.; Puertolas, P.F.; Minguillon, C.; Camacho-Frias, E.; Foucault, A.; and Le Goffic, F., J. Liq. Chromatogr., **1994**, *17*, 2301-2318.

15. Schaufelberger, D.E.; McCloud, T.G. and Beutler, J.A., J. Chromatogr., **1991**, *538*, 87-90.
16. Diallo, B.; Vankaelenfastre, R. and Vankaelen, M., J. Chromatogr., **1991**, *558*, 446-450.
17. Cornish, R.E.; Archibald, R.C.; Murphy, E.A. and Evans, H.M., Ind. Eng. Chem., **1934**, *26*, 397-406.
18. Ito, Y.; Harada, R.; Weinstein, M.A. and Aoki, I., Ikakikaigakuzaski, **1966**, *36*, 1-4.
19. Ito, Y.; Weinstein, M.A.; Aoki, Il; Harada, R.; Kimura, E. and Nunogaki, K., Nature, **1966**, *212*, 985-987.
20. Tanimura, T.; Pisano, J.J.; Ito, Y. and Bowman, R.L., Science, **1970**, *169*, 54-56.
21. Hostettmann, Kl., Planta Medica, **1980**, *39*, 1-18.
22. Ito, Y.; J. Chromatogr., **1981**, *214*, 122-125.
23. Ito, Y.; Sandlin, J. and Bowers, W.G., J. Chromatogr., **1982**, *244*, 247-258.
24. Ito, Y. and Chou, Y.E., J. Chromatogr., **1988**, *454*, 382-386.
25. Ito, Y.; Oka, H. and Slemp, J.L., J. Chromatogr., **1989**, *475*, 219-227.
26. Conway, W.D.; Yeh, H.C. and Tedesche, N.J., J. Liq. Chromatogr., **1992**, *15*, 2751-2768.
27. Knight, M., Adv. Chromatogr., **1992**, *31*, 253-292.
28. Ito, Y. and Oka, H., J. Chromatogr., **1988**, *457*, 393-397.
29. Knight, M. and Gluch, S., J. Liq. Chromatogr., **1990**, *13*, 2351-2362.
30. Murayama, W.; Kobayaski, T.; Kosuge, Y.; Yars, H.; Numogaki, Y. and Nunogaki, K., J. Chromatogr., **1982**, *239*, 643-649.
31. Berthod, A. and Armstrong, D.W., J. Liq. Chromatogr., **1988**, *11*, 547-566.
32. Berthod, A. and Armstrong, D.W., J. Liq. Chromatogr., **1988**, *11*, 567-583.
33. Foucault, A.P.; Bousquet, O.; Le Gaffic, F. and Gazes, F., J. Liq. Chromatogr., **1992**, *15*, 2721-2733.
34. Foucault, A.P.; Durand, P.; Comacho Frias, E. and Le Gaffic, F., Anal. Chem., **1993**, *65*, 2150-2154.
35. Lee, Y.-W.; Cooke, C.E. and Ito, Y., J. Liq. Chromatogr., **1988**, *11*, 37-53.
36. Slacanin, I.; Marston, A. and Hostettmann, K., J. Chromatogr., **1989**, *4898*, 234-239.
37. Shinomiya, K.; Menet, J.M.; Fales, H.M. and Ito, Y., J. Chromatogr., **1993**, *644*, 215-229.
38. Menet, J.M. and Ito, Y., **1993**, *644*, 231-238.
39. Menet, J.M.; Shinomiya, K. and Ito, Y., J. Chromatogr., **1993**, *644*, 239-252.

RECEIVED November 28, 1994

Downloaded by 89.163.35.42 on June 28, 2012 | http://pubs.acs.org
Publication Date: May 15, 1995 | doi: 10.1021/bk-1995-0593.ch001

Chapter 2

Liquid Polarity and Stationary-Phase Retention in Countercurrent Chromatography

Alain Berthod, Jean Marc Deroux, and Madeleine Bully

Laboratoire des Sciences Analytiques, Unité de Recherche Associée au Centre National de la Recherche Scientifique 435, Université de Lyon 1, 69622 Villeurbanne, France

Downloaded by YORK UNIV on June 29, 2012 | http://pubs.acs.org
Publication Date: May 15, 1995 | doi: 10.1021/bk-1995-0593.ch002

In countercurrent chromatography (CCC), there are only two parameters influencing solute retention volumes: the liquid stationary phase volume and the solute liquid-liquid partition coefficient. The retention of 18 non-water miscible solvents were measured by a hydrodynamic CCC apparatus using an aqueous mobile phase. The corresponding water retention was measured using the organic solvent mobile phase. All 36 experiments were done at a 2 mL/min flow rate and a rotation speed of 800 rpm. The stationary phase retention volume was found to be directly related to the phase density difference. With most binary liquid systems, a loss of the stationary phase was observed. This loss could be modeled by a simple exponential decay. The loss of the stationary phase could be related to the mutual solubility of the water-solvent systems and solvent polarity.

Countercurrent chromatography (CCC) is a separation technique in which the stationary phase is a liquid (*1-4*). The mobile phase, which is another liquid phase, should neither dissolve the stationary phase nor remove it from the CCC "column" (*5*). Some liquid systems are well retained in CCC apparatuses when others are not. Of course, liquid stationary phase retention in a given CCC apparatus is critical. The stationary phase volume is related to the resolution capability, the pressure drop, the maximum loading of solute and the efficiency of the CCC "column" (*4*).

The goal of this research was to investigate the liquid phase retention by a hydrodynamic coil planet centrifuge apparatus. The usual procedure to make a CCC "column" is first to fill the CCC apparatus with the stationary phase, followed by initiation of mobile phase flow. Equilibrium is reached when the mobile phase is seen exiting the CCC apparatus. With many biphasic liquid

0097–6156/95/0593–0016$12.00/0

systems, there is a loss of stationary phase continuing after the first equilibrium. The phase retention depends mainly on the apparatus used and on the initial conditions. It also depends on the physicochemical properties of the liquid system used. The physicochemical properties of 46 solvents commonly used in CCC were listed. 18 solvents were selected from this list for their low water solubility. Their CCC retention was studied with water as the other liquid phase. The stability of the liquid-liquid equilibrium, i.e., the stationary phase-mobile phase equilibrium, was studied in particular. The stationary phase losses after the initial equilibration were quantified by plotting the retention percentage versus time.

The concept of polarity is widely used in CCC but it is not well defined. The polarity of the CCC solvents was studied using the definitions of three different authors: Hildebrand (*6*), Snyder (*7*) and Reichardt (*8*). In CCC, V_R, the solute retention volume depends on only two parameters: V_S, the stationary phase retention volume and P, the solute liquid-liquid partition coefficient:

$$V_R = V_M + PV_S \tag{1}$$

where V_M is the mobile phase volume inside the apparatus and the partition coefficient, P, is defined as the concentration ratio for solute in the stationary and mobile phases, C_s/C_m. The total volume of the apparatus, V_T, is equal to $V_M + V_S$. The possible relationships between liquid system polarity and solute partition coefficients were also studied.

Experimental

Chromatographic system. The CCC apparatus was the Model CPHV 2000 from Société Française de Chromato Colonne (SFCC, 95610 Eragny, France). It is a coil planet centrifuge apparatus, first designed by Ito (*3*). It contains three multilayer coils connected in series and spinning to a planetary motion around a central axis. A special gear arrangement is designed to avoid any rotary seal. The apparatus has been completely described in a recent publication (*9*). Each spool was filled with 133 turns of PTFE tubing, i.d. 1/16 in. (1.6 mm), length 26 m, coiled in seven layers of 19 turns. The Ito β value is the ratio of the coil radius, r, to the spool revolution radius, R. The β ratio was 0.37 for the inner first layer with r = 2.2 cm and R = 6 cm. It was 0.75 for the outermost layer with r = 4.5 cm and R = 6 cm. The average β value for this CCC apparatus was 0.56. The internal volume of one coiled spool was 52 ml. The three-coil apparatus had a total internal volume, V_T, of 158 ml. The whole system was housed in an air-thermostated box. The temperature was regulated to 22°C ± 0.5°C.

A Shimadzu LC6A pump was used to fill the CCC apparatus with the stationary phase and to provide a mobile phase flow rate of 2 ml/min.

Downloaded by YORK UNIV on June 29, 2012 | http://pubs.acs.org
Publication Date: May 15, 1995 | doi: 10.1021/bk-1995-0593.ch002

A Shimadzu SPD-6A UV detector was used, set at 254 nm, for detection of solutes along with a CR5-A recorder integrator.

Chemicals. The solvents were obtained from Merck (Darmstadt, Germany), Fluka (Saint Quentin Fallavier, France), Prolabo (Paris, France) and Laurylab (Chassieu, France). 2-Methyl cyclohexanol acetate and trimethylbenzene (TMB or mesitylene, 1,3,5-trimethyl benzene) were industrial solvents (80% average purity) supplied by ELF-Atochem (Vernaison, France). 1,1,2-trichloro-1,2,2-trifluoro ethane is also called Freon 113. Formanilide was used as a test solute of intermediate polarity. It is soluble in water and in most of the 18 solvents tested. It was supplied by MTM Lancaster Synthesis (Strasbourg, France). The Reichardt's dye, 2,6-diphenyl-4-[2,4,6-triphenylpyridinio]-phenolate inner salt, was obtained from Sigma Chemical Co. (St. Louis, Missouri, USA).

Downloaded by YORK UNIV on June 29, 2012 | http://pubs.acs.org
Publication Date: May 15, 1995 | doi: 10.1021/bk-1995-0593.ch002

Method. The water-organic solvent system was equilibrated overnight to obtain an aqueous phase saturated in organic solvent and an organic water-saturated phase. The apparatus was first filled with the liquid chosen to be the stationary phase. This took about 25 min at an 8 mL/min flow rate. Next, the centrifuge was turned on to a stable rotation speed of 800 rpm. The pump was rinsed with the mobile phase. The mobile phase was then begun at 2 ml/min. The mobile phase entered through the tail of the apparatus if its density was less than the one of the liquid stationary phase and *vice versa*. This is the normal mode described by Ito (*3*) (Figure 1). The reversed mode (head to tail) was used only with the butanol-water system (Figure 2). The 2 mL/min flow rate and 800 rpm rotor speed setup were used for every water-solvent pair studied.

As long as the apparatus was not equilibrated, the stationary phase was displaced from the apparatus and collected in a graduated cylinder. When the immiscible mobile phase appeared at the exit of the apparatus, an important optical noise signal was generated by the UV detector, and two liquid layers appeared in the graduated cylinder. This was taken as time, t=0, for the two-phase equilibrium inside the CCC "column". The displaced liquid stationary phase volume was measured next. This volume, $V_{M,\,t=0}$, corresponded to the mobile phase volume inside the apparatus at time t=0. The stationary phase volume inside the apparatus, V_S, is:

$$V_{S,\,t=0} = V_T - V_{M,\,t=0}. \qquad (2)$$

The stationary phase retention is defined by:

$$Sf_{t=0} = V_{S,\,t=0}/V_T *100. \qquad (3)$$

The cumulative displaced stationary phase was measured for one hour and the corresponding stationary phase retention, Sf_t computed at every time t. Sf_t was then plotted versus time for the liquid systems studied, as shown by Figures 1 and 2.

Downloaded by YORK UNIV on June 29, 2012 | http://pubs.acs.org
Publication Date: May 15, 1995 | doi: 10.1021/bk-1995-0593.ch002

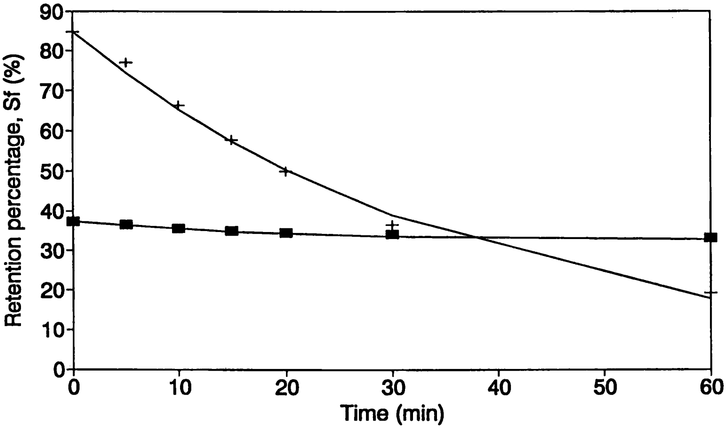

Figure 1. Stationary phase retention percentage versus time, for the butanol water system. Hydrodynamic Ito CCC apparatus, rotor speed: 800 rpm, mobile phase flow rate: 2 mL/min, +: butanol mobile phase entering tail; ■ : water mobile phase entering head.

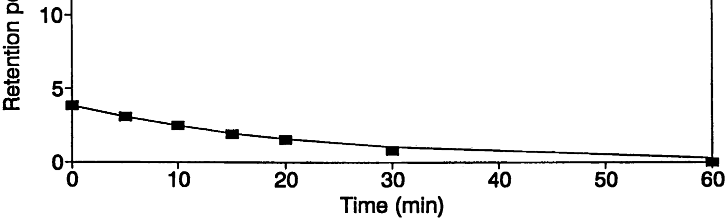

Figure 2. Same as Figure 1 but reverse mode. +: butanol mobile phase entering head; ■ : water mobile phase entering tail.

The test solute, formanilide, was injected in aqueous solution. Its retention volume, V_r, is dependent on its liquid-liquid partition coefficient, P, by equation 1.

Theoretical Model

The variation of the retention percentage, Sf_t, could be modeled by a simple exponential decay:

$$Sf_t = (Sf_{t=0} - Sf_{t=\infty}) \exp(-at) + Sf_{t=\infty} \tag{4}$$

in which a, in min^{-1}, is a constant that indicates how fast the stationary phase stops to bleed off the CCC apparatus (Figure 3). At time $t_{1/2}$, in minutes,

$$t_{1/2} = 0.69/a \tag{5}$$

the stationary phase retention percentage is equal to $(Sf_{t=0} + Sf_{t=\infty})/2$. The constant "a" is indirectly related to the rate of the stationary phase loss. At time t=0, the rate of stationary phase loss, $Vt_{t=0}$, is expressed with the first derivative of equation 4:

$$Vt_{t=0} = (dSf/dt)_{t=0} = -a\,(Sf_{t=0} - Sf_{t=\infty}) \tag{6}$$

The rate of loss, Vt_t, decreases with time. It is divided by 2 after a time t equal to $t_{1/2}$ (equation 5). For $t = 3t_{1/2}$, the rate of loss of stationary phase is only 13% of its initial value. Only then is the CCC "column" really equilibrated, i.e. the liquid stationary phase volume remains reasonably constant.

Solvents and Solvent Polarity

Table I lists some physicochemical parameters of a selection of solvents commonly used in CCC. The polarity of each solvent was also indicated. The characterization of a solvent by its polarity is not precise since the term "polarity" itself has, until now, not been precisely defined. Solvent polarity is related to the permanent dipole moment of solvent molecules, to the dielectric constant and/or to the sum of selected molecular properties responsible for interaction forces between solvent molecules (e.g. coulombic, inductive, hydrogen bonding, electron pair donor/acceptor interaction forces) (*8*). Different polarity scales have been established. Hildebrand linked solvent polarity to its solubilizing capability, defining the solubility parameter, δ, as the

Downloaded by YORK UNIV on June 29, 2012 | http://pubs.acs.org
Publication Date: May 15, 1995 | doi: 10.1021/bk-1995-0593.ch002

Downloaded by YORK UNIV on June 29, 2012 | http://pubs.acs.org
Publication Date: May 15, 1995 | doi: 10.1021/bk-1995-0593.ch002

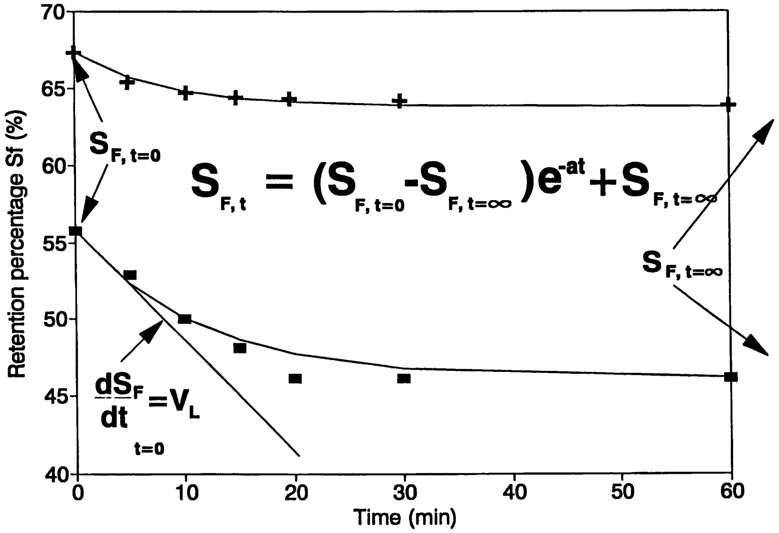

Figure 3. The ethylacetate-water liquid system shown to illustrate the proposed exponential decay model.

Downloaded by YORK UNIV on June 29, 2012 | http://pubs.acs.org
Publication Date: May 15, 1995 | doi: 10.1021/bk-1995-0593.ch002

Table I. Selected Physicochemical Properties of Solvents Commonly Used in CCC

Solvent	*M. W.*	*density*	*dipole moment*	*dielectric constant*	*polarity*			*solubility %w/w*	
	dalton	g/cm3	debye		Hilde-brandt	Reich-ardt	Snyder	solv. in water	wat. in solvent
acetic acid	60	1.049	1.74	6.15	20.6	**64.8**	5.1	inf	inf
acetone	58	0.790	2.69	20.7	18.6	**35.5**	5.1	inf	inf
acetonitrile	41	0.782	3.44	37.5	24.1	**46**	5.8	inf	inf
benzene	78	0.879	0	2.28	18.8	**11.1**	2.7	0.18	0.063
1-butanol	74.1	0.810	1.75	17.5	27.2	**60.2**	3.9	7.8	20.1
2-butanol	74.1	0.808	1.64	15.8	25.2	**50.6**	4	12.5	44.1
chloroform	119.4	1.485	1.15	4.9	18.9	**25.9**	4.1	0.815	0.056
cyclohexane	84	0.778	0	2.02	15.8	**0.6**	0.2	0.006	0.01
decahydronaphthalene	138	0.883	0	2.15	15.6	**1.5**	0.2	<.02	0.0063
1,4-dichlorobutane	127	1.140	2.2	-	20.5	**34**	3	0.3	0.11
1,2-dichloroethane	99	1.246	1.86	10.4	20.4	**32.7**	-	0.81	0.187
dibutylphthalate	278.3	1.043	2.82	6.44	17.4	**20**	4.6	0.01	0.46
dichloromethane	85	1.317	1.14	8.9	20	**30.9**	3.1	1.6	0.24
diethyl ether	74	0.713	1.15	4.34	15.4	**11.7**	2.8	6.9	1.3
diethylcarbonate	118	0.975	0.9	2.82	18	**19.4**	5.5	hydrolyze	1.4
dimethoxyethane	90	0.863	1.71	7.2	22.8	**23.1**	-	inf	inf
N,N-dimethylacetamide	87	0.937	3.72	37.8	21.6	**40.1**	6.5	inf	inf
dimethylformamide	73	0.948	3.86	36.7	24.2	**40.4**	6.4	inf	inf
dimethylsulfoxyde	78	1.095	4.3	48.7	24	**44.4**	7.2	inf	inf
dioxane	88	1.033	0.45	2.25	20	**16.4**	4.8	inf	inf
di-isopropyl ether	102	0.724	1.32	3.88	14.6	**9.8**	-	1.2	0.57
ethanol	46	0.789	1.66	26.6	26	**65.4**	4.5	inf	inf

Downloaded by YORK UNIV on June 29, 2012 | http://pubs.acs.org
Publication Date: May 15, 1995 | doi: 10.1021/bk-1995-0593.ch002

ethyl acetate	88	0.895	1.88	6	18.2	**22.8**	4.4	8.7	3.3
furfural	92	1.154	3.5	38	23.6	**50**	3.8	8.2	6.3
heptane	100.2	0.679	0	1.92	14.7	**1.2**	0.1	0.0004	0.0091
hexane	86	0.655	0.08	1.88	15	**0.9**	0.1	0.001	0.01
isooctane	114	0.692	0	1.94	15.4	**0.9**	0.1	0.0002	0.006
methanol	32	0.791	2.87	32.7	29.3	**76.2**	5.1	inf	inf
methyl ethyl ketone	72	0.788	2.76	15.2	19.2	**32.7**	4.7	24	10
methyl-ter-butyl ether	88	0.741	1.32	4.5	15.1	**14.8**	2.5	4.8	1.5
N-methylpyrrolidone	99	1.028	4.1	32	22.4	**35.5**	6.7	inf	inf
2-methyl cyclohexanol acetate	156.2	0.936	-	-	17.4	**20**	4.2	-	-
octanol	130	0.822	1.76	10.3	20.9	**54.3**	3.4	0.054	4.1
n-pentane	72	0.626	0	1.84	14.9	**0.9**	0	0.004	0.009
1-pentanol	88	0.814	1.82	14.7	22.1	**56.8**	3.7	2.2	7.5
1-propanol	60	0.803	3.1	20.3	24.4	**61.7**	4	inf	inf
2-propanol	60	0.785	1.66	19.9	23.7	**54.6**	3.9	inf	inf
propylene carbonate	102	0.943	4.9	65	27.8	**49.1**	6.1	17.5	8.3
tetrachloromethane	154	1.594	0	2.24	17.6	**5.2**	1.6	0.08	0.008
tetrahydrofuran	72	0.888	1.75	7.6	18.2	**20.7**	4	inf	inf
toluene	92	0.862	0.31	2.38	18.3	**9.9**	2.4	0.074	0.03
tributylphosphate	266.3	0.973	3.07	8.1	15.3	**27.5**	4.6	0.039	4.7
111-trichloroethane	133.4	1.330	1.7	7.3	17.9	**26.9**	3.2	0.132	0.034
freon 113 (CCl_2F-$CClF_2$)	187.3	1.563	-	2.4	14.5	**0.1**	0.1	0.017	0.011
trimethylbenzene	120	0.861	0	2.27	17.8	**6.8**	2.2	0.0048	0.029
water	18	0.997	1.87	80.1	48.6	**100**	10.2	-	-

Data from Reichardt, C. *Solvents and Solvent Effects in Organic Chemistry*; VCH Publishers, Weinheim, Germany, 1988 and *Handbook of Chemistry and Physics*; Weast, R. Ed.; CRC Press, Boca Raton, FL, 1987, 67th ed.

Downloaded by YORK UNIV on June 29, 2012 | http://pubs.acs.org
Publication Date: May 15, 1995 | doi: 10.1021/bk-1995-0593.ch002

work necessary to separate two solvent molecules (*6*). Snyder defined an eluant strength parameter, E_o, based on the eluting power of the solvent when used as a mobile phase in thin layer chromatography on silica or alumina plates (*7*). Reichardt proposed a solvent polarity parameter, E_T, based on the transition energy for the longest wavelength solvatochromic absorption band of a pyridinium-N-phenoxyde betaine dye. The E_T parameter was normalized using water (E_T=100) and tetramethylsilane (E_T=0) as the reference solvents (*8*).

Table I lists the δ parameter in $J^{1/2}cm^{-3/2}$ and the dimensionless Snyder and Reichardt polarity indexes. Figure 4 compares the three polarity indexes. The solvents were sorted by decreasing Reichardt values. Figure 4 shows that there is only approximate correspondence among the three polarity scales. For example, the 2-butanol E_T value is 50.2 and the δ value is 25.2. The 1-propanol E_T value is higher, 61.7, and its δ value is lower, 24.4. Which one is more polar? Both have identical E_o values of 4. Conversely, diethylcarbonate, with 5.5 in the Snyder scale, is it more polar than ethanol, rated at 4.5 (Table I) ? In the two other scales, ethanol is considered the more polar solvent, and diethylcarbonate as a low polarity solvent. Water solubility is linked to polarity through hydrogen bonding and electron or proton donor capabilities. Polar solvents should be miscible with water. However, butanol, a polar solvent in all three scales, has limited water miscibility; dioxane, an intermediate/low polarity solvent, is completely water miscible due to its high proton donor capacity (Table I). Most of the experiments presented in this work were done with water-solvent binary liquid systems using solvents with an intermediate or low polarity. Butanol, the most polar, is the only one that shows a significant reversed mode retention (*3*). The 18 water immiscible solvents that were used, can be found in Table II along with the four biphasic solvent pairs under "Non-aqueous systems" heading.

Results and Discussion

Table II lists the experimental data obtained with the hydrodynamic CCC machine at 800 rpm rotor speed and 2 mL/min flow rate. Table II is divided into three parts: (i) *Aqueous mobile phase*; the mobile aqueous phase is from tail to head (T→H) if the liquid stationary phase is more dense than water. It is moving from head to tail (H→T) if the solvent stationary phase is the lighter upper phase, unless otherwise indicated (e.g. butanol). The organic solvent is the stationary phase. (ii) *Solvent mobile phase*; the aqueous phase is the stationary phase. (iii) *Non aqueous systems*; Four non aqueous solvent systems were tested in the two possible flow modes to generalize the observed behavior of water-solvent systems.

Initial Stationary Phase Retention. Figure 5 shows the initial stationary phase retention percentage, $Sf_{t=0}$, plotted versus the difference of density

Downloaded by YORK UNIV on June 29, 2012 | http://pubs.acs.org
Publication Date: May 15, 1995 | doi: 10.1021/bk-1995-0593.ch002

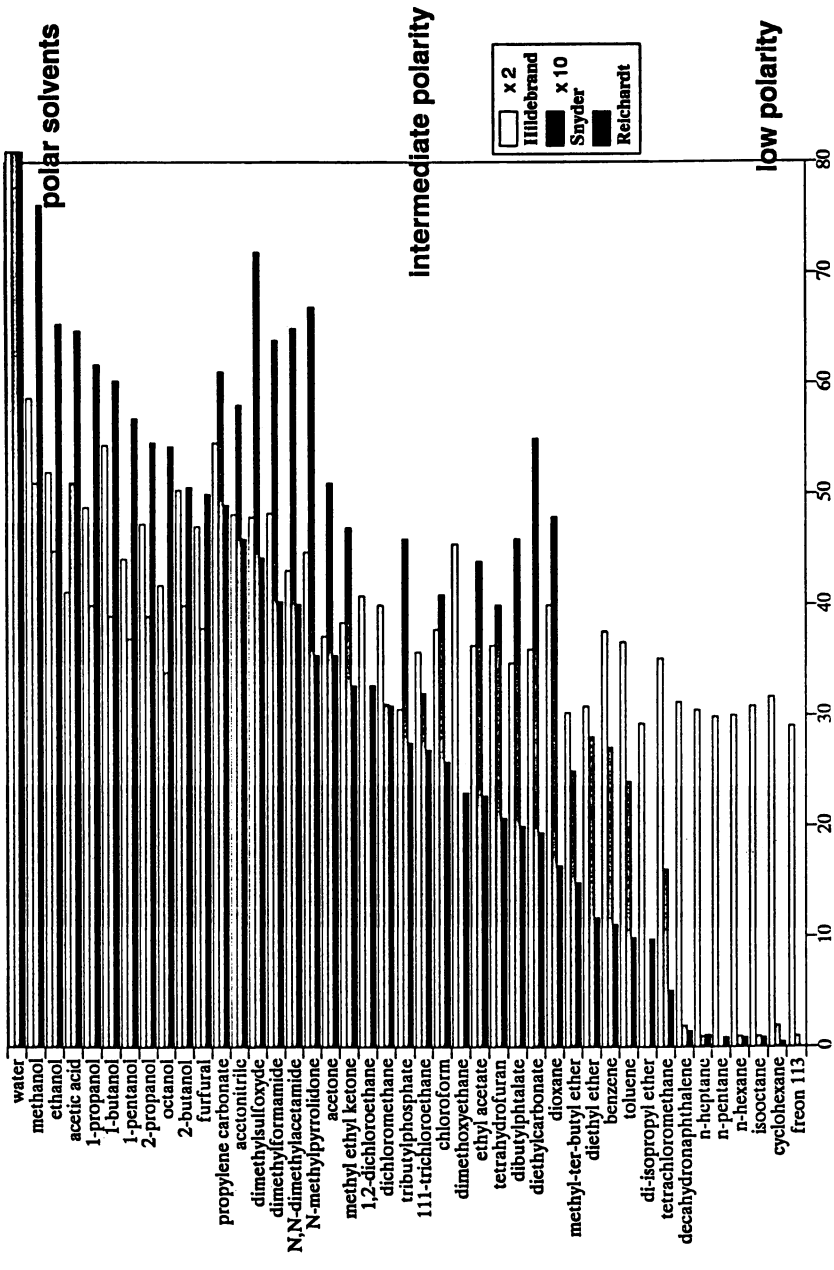

Figure 4. Comparison three different polarity scales for the Table I solvents. The solvents were sorted by decreasing polarity of the Reichardt index (closed bars).

Downloaded by YORK UNIV on June 29, 2012 | http://pubs.acs.org
Publication Date: May 15, 1995 | doi: 10.1021/bk-1995-0593.ch002

Table II. Stationary Phase Retention at Initial Time ($t=0$) and at Equilibrium ($t=\infty$), Decay Factor, Time $t_{1/2}$, and Rate of Stationary Phase Loss at Time $t=0$

Aqueous mobile phase					
Solvent	*Sf retention %*		*a*	$t_{1/2}$	*Vt (t=0)*
	t=0	t=∞	min-1	min	% min-1
Butanol (normal)	37.5	32.5	0.049	14	0.24
Butanol (rev. water T->H)	3.8	0.0	0.044	16	0.17
Butanol-water NaCl 1M normal	55.8	51.4	0.050	14	0.22
Butanol-water NaCl 1M rev	1.9	0.0	0.150	5	0.29
Chloroform	75.0	61.7	0.037	19	0.49
Cyclohexanol 2-methyl, acetate	19.2	16.9	0.092	8	0.22
Dibutylphthalate	13.5	7.7	0.110	6	0.63
1,4-Dichlorobutane	26.9	0.0	0.029	24	0.79
1,2-Dichloroethane	67.3	62.4	0.120	6	0.59
Dichloromethane	75.0	70.8	0.024	29	0.10
Ethyl acetate	55.8	46.2	0.090	8	0.87
Furfural	21.2	0.0	0.020	35	0.42
Heptane	75.0	75.0	0.000	inf	0.00
Methyl ethyl ketone	53.8	47.9	0.008	87	0.05
Methyl t-butyl ether	74.0	72.0	0.028	25	0.06
Octanol	58.7	51.5	0.030	23	0.21
Toluene	57.7	57.7	0.000	inf	0.00
Tributylphosphate	11.5	0.0	0.050	14	0.58
1,1,1-Trichloroethane	73.1	50.6	0.005	139	0.11
1,1,2-Trichloro 1,2,2-trifluoroethane (Freon 113)	76.9	0.0	0.013	54	0.98
Trimethylbenzene	45.2	42.3	0.020	35	0.06

Table II. *Continued*

Solvent mobile phase

Solvent	*Sf retention %*		*a*	$t_{1/2}$	*Vt (t=0)*
	$t=0$	$t=\infty$	min-1	min	% min-1
Butanol (normal T→H)	84.6	0.0	0.026	27	2.19
Butanol (rev. H→T)	20.2	17.5	0.068	10	0.18
Butanol-Water NaCl 1M normal	96.2	56.0	0.055	13	2.21
Butanol-Water NaCl 1M rev	15.4	9.3	0.067	10	0.40
Chloroform	75.0	74.0	0.220	3	0.21
Cyclohexanol 2-methyl, acetate	21.2	0.0	0.120	6	2.54
Dibutylphthalate	0.0	0.0	0.000	-	no ret.
1,4-Dichlorobutane	28.8	16.3	0.068	10	0.85
1,2-Dichloroethane	71.2	68.3	0.073	9	0.21
Dichloromethane	76.9	72.0	0.016	43	0.08
Ethyl acetate	67.3	63.8	0.126	6	0.44
Furfural	36.5	30.8	0.073	9	0.42
Heptane	84.6	84.6	0.000	inf.	0.00
Methyl ethyl ketone	84.6	53.5	0.050	14	1.54
Methyl t-butyl ether	84.6	84.6	0.000	inf	0.00
Octanol	26.9	13.0	0.073	10	1.01
Toluene	75.0	75.0	0.000	inf	0.00
Tributylphosphate	0.0	0.0	0.000	-	no ret.
1,1,1-Trichloroethane	71.2	70.2	0.057	12	0.06
1,1,2-Trichloro 1,2,2-trifluoro-ethane (Freon 113)	76.9	74.0	0.147	5	0.42
Trimethylbenzene	47.1	46.0	0.036	19	0.04

Non aqueous systems

Solvent	*Sf retention %*		*a*	$t_{1/2}$	*Vt (t=0)*
stationary phase-mobile phase	$t=0$	$t=\infty$	min-1	min	% min-1
Heptane-DMF	75.0	39.1	0.002	347	0.07
Heptane-DMSO	74.2	72.8	0.043	16	0.06
Heptane-NMP	73.1	47.4	0.008	87	0.21
DMSO-Freon 113	76.9	76.9	0.000	inf	0.00
DMF-Heptane	96.2	84.5	0.060	12	0.70
DMSO-Heptane	88.5	87.5	0.048	14	0.05
NMP-Heptane	82.7	69.4	0.037	19	0.49
Freon 113-DMSO	90.4	58.2	0.069	10	2.21

Downloaded by YORK UNIV on June 29, 2012 | http://pubs.acs.org
Publication Date: May 15, 1995 | doi: 10.1021/bk-1995-0593.ch002

In Modern Countercurrent Chromatography; Conway, W., et al.;
ACS Symposium Series; American Chemical Society: Washington, DC, 1995.

Downloaded by YORK UNIV on June 29, 2012 | http://pubs.acs.org
Publication Date: May 15, 1995 | doi: 10.1021/bk-1995-0593.ch002

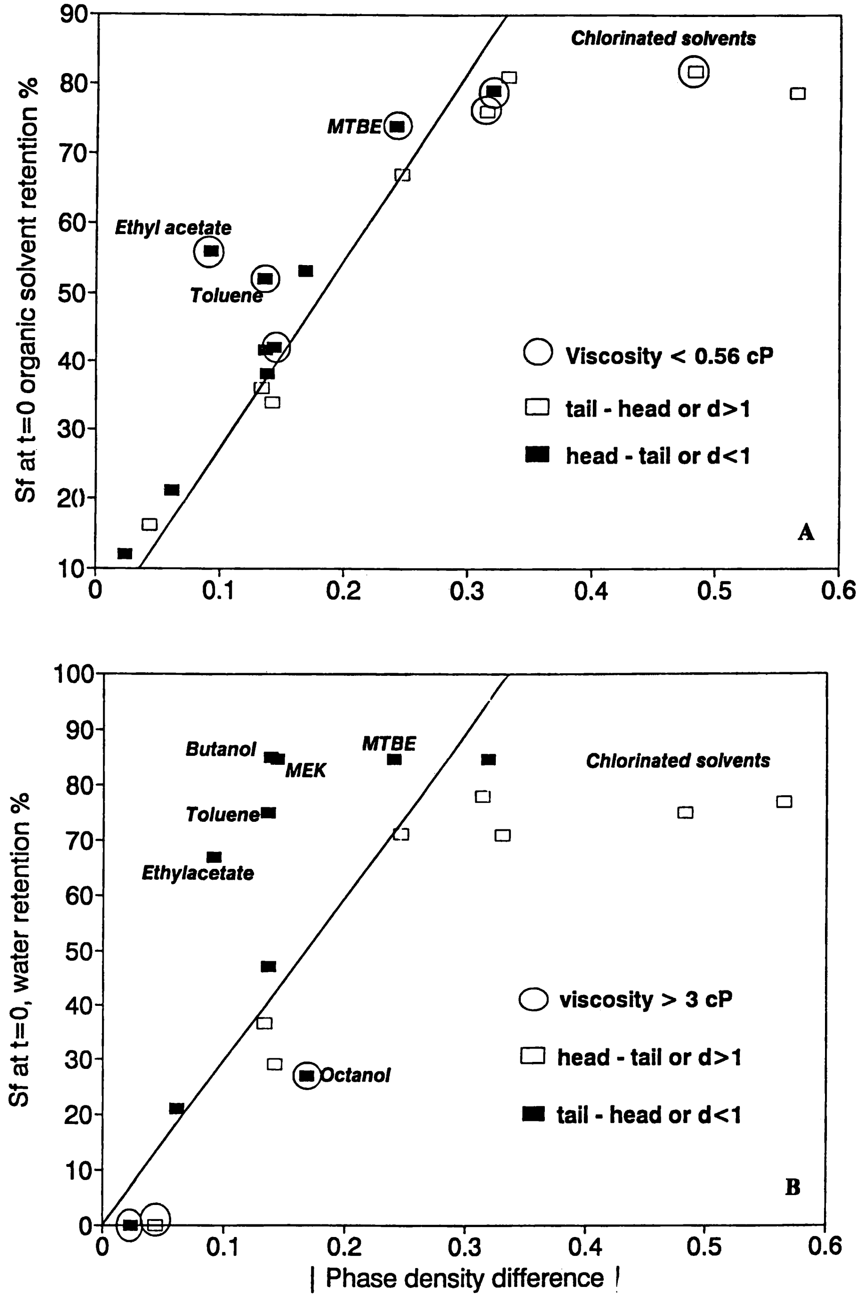

Figure 5. The initial stationary phase retention plotted versus the phase density difference. Top (A): The solvents are the stationary phase; bottom (B): the aqueous phase is the stationary phase. Density difference in g/cm^3.

Downloaded by YORK UNIV on June 29, 2012 | http://pubs.acs.org
Publication Date: May 15, 1995 | doi: 10.1021/bk-1995-0593.ch002

between the aqueous and the solvent phase. Water is the mobile phase in Figure 5A. Water is the stationary phase in Figure 5B. Figure 5 shows a relationship between the stationary phase retention, $Sf_{t=0}$, and the absolute value of the phase density difference, $|\Delta d|$. $Sf_{t=0}$ increases almost linearly with $|\Delta d|$ up to $|\Delta d| = 0.35$. For $|\Delta d|$ values higher than 0.35, a plateau is reached of $Sf_{t=0}$ values close to 80%. The linear regression for the $|\Delta d| < 0.35$ data in Figure 5A, with the intercept forced to 0, gave the following equation:

$$\begin{gathered} Sf_{t=0} = 273\ |\Delta d| \\ \pm 13.3 \\ n = 15;\ \ r^2 = 0.787 \end{gathered} \tag{7}$$

The ethyl acetate and toluene data greatly reduce the correlation coefficient. The retention values of Figure 5A were all obtained with an aqueous mobile phase of similar viscosity (organic-solvent-saturated water). It seems that the solvents with low viscosity (< 0.56 cP) have a retention that is somewhat higher than the other solvents (circled points on Figure 5A).

The regression fit for Figure 5B was:

$$\begin{gathered} Sf_{t=0} = 297\ |\Delta d| \\ \pm 62 \\ n = 15;\ \ r^2 = 0.384 \end{gathered} \tag{8}$$

The correlation is poor. The $Sf_{t=0}$ versus $|\Delta d|$ plot obtained when the aqueous phase was the stationary phase produced scattered data (Figure 5B). The least square line (equation 8) has a low 0.384 regression parameter which means that the phase density parameter is not the only parameter responsible for water retention inside the CCC "column". However, it was not possible to find any correlation with any of the following solvent physicochemical properties: interfacial tension, molecular weight, boiling point, vapor pressure, dielectric constant and dipole moment (*10*). A high viscosity of the solvent mobile phase is unfavorable to high aqueous phase retention (circled points in Figure 5B).

The sign of the density difference seems to have a significant effect on the aqueous phase retention. $Sf_{t=0}$ is higher with low density solvent mobile phases (closed squares, Figure 5B). When the aqueous phase is the stationary phase, a denser liquid must enter the CCC apparatus through the head, a lighter liquid ($d < 1$) must enter the apparatus through the tail and leave through the head. Ito has shown that the rotation of a coiled tube filled with a liquid produced a pressure difference between the two ends of the tube due to a "screw effect" (*1-3*). When two immiscible liquids are loaded in a coiled tube, the rotation produces also a pressure difference. For most binary liquid systems, the lighter liquid accumulates on the high pressure side of the rotating coil, called "head". The denser liquid is located on the low pressure side of the coil, called "tail", where it pushes the lighter liquid toward the head (*1-3*). For all solvents denser than water ($d > 1 g/cm^3$), the pressure is lower with the water mobile phase than with the corresponding organic mobile phase (*10*). With organic phases having a density higher than 1, the water mobile phase entered the CCC apparatus through the tail, the lower pressure side. The corresponding organic phase entered through the head, the high pressure side. For organic solvents with a $d > 1$ (open squares of Figure 5B) low aqueous phase retention was observed compared to $d < 1$ organic solvents entering at the tail (closed squares, Figure 5B). Although the regression line shown in Figure 5B is not really significant, the open squares ($d > 1$ solvents) are all located below the line and most of the closed squares ($d < 1$ solvents) are above the line. This trend was not observed when water was the mobile phase. Water phases entering the head or tail had little effect on the organic solvent retention (open and closed squares, Figure 5A).

Downloaded by YORK UNIV on June 29, 2012 | http://pubs.acs.org
Publication Date: May 15, 1995 | doi: 10.1021/bk-1995-0593.ch002

Stable Stationary Phase Retention. Figure 6 shows the stable stationary phase retention percentage, $Sf_{t=\infty}$, plotted versus the density difference between phases. Figure 6A corresponds to the solvent retention percentage $Sf_{t=\infty}$ when the aqueous phase is the mobile phase. Figure 6B represents the aqueous retention percentage. The regression lines obtained at time $t = 0$ (equations 7 and 8) are also included. The linear relationship between Sf and $|\Delta d|$ is difficult to discern. However, the trend: increase of Sf with $|\Delta d|$ remains. Figure 6A shows that the aqueous phase completely displaces some solvents such as 1,4-dichlorobutane, furfural, tributylphosphate, freon 12 and butanol in reversed mode. Also, butanol (normal mode, Figure 1), dibutylphthalate, tributylphosphate and cyclohexanol acetate completely displaced the aqueous phase.

The low viscosity solvents that were located above the regression line in Figure 5A (circled points) remains retained. The $Sf_{t=\infty}$ values of MTBE, heptane, toluene and trimethylbenzene are identical to their $Sf_{t=0}$ values due to their $a=0$ value (Table II). The Sf losses of ethyl acetate, MEK, chloroform and dichloromethane are only 9%, 6%, 13% and 4%, respectively (Figures 5A and 6A, Table II). However, the losses for octanol and butanol, two viscous solvents were only 7% and 5%, respectively. Similar observations can be made on the aqueous mobile phase. Figures 5B and 6B and Table II show that the low viscosity solvents, MEK excluded, displace little (less than 4%) water out of the CCC apparatus. The viscous solvents, butanol and octanol, expel a large amount of water, 85% and 14%, respectively. The large Sf change, 31%, produced by MEK, a low viscosity solvent may be due to its capability to dissolve large amounts of water (10% w/w). A low mutual solubility seems to be a parameter enhancing solvent retention in the hydrodynamic CCC apparatus studied.

Rate of Stationary Phase Loss. Table II lists the exponential decay parameter, a, the $t_{1/2}$ time and the initial loss speed for the water-solvent

Downloaded by YORK UNIV on June 29, 2012 | http://pubs.acs.org
Publication Date: May 15, 1995 | doi: 10.1021/bk-1995-0593.ch002

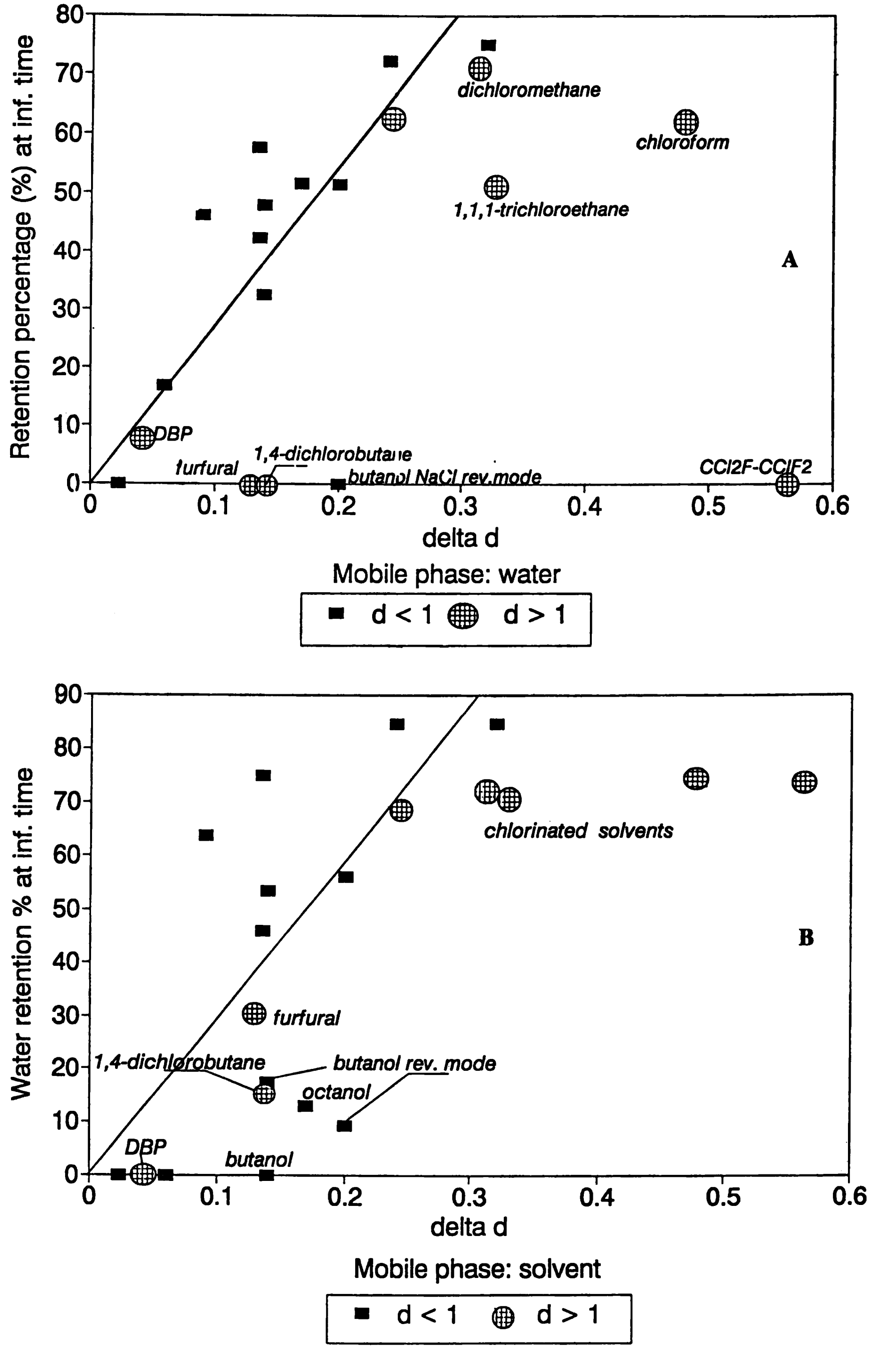

Figure 6. The stable retention of the stationary phase plotted versus the phase density difference. Top (A): The solvents are the stationary phase; bottom (B): the aqueous phase is the stationary phase. Density difference in g/cm^3.

systems studied. Equations 5 and 6 show that these three parameters are related. However, a large decay parameter does not mean necessarily a high initial rate of loss. The largest "a" parameter was 0.22 min^{-1}, obtained with chloroform as the mobile phase. The corresponding initial rate of loss was 0.21 % min^{-1}. One of the lowest "a" parameter was 0.026 mn^{-1}, obtained with butanol as the mobile phase. This corresponds to one of the highest initial loss speeds, 2.19 % min^{-1}, because the aqueous phase loss was 85% with butanol and only 1% with chloroform (Table II and equation 6). We could not find any direct relationship between the decay, $t_{1/2}$ or initial rate of stationary phase loss and the physicochemical parameters; such as phase density difference, viscosity, interfacial tension and boiling point. The only parameter that is related somewhat to the stationary phase loss, is the solvent-water solubility. Overall, the $t_{1/2}$ equilibration times are often shorter with solvent mobile phases than with aqueous mobile phases (Table II).

The experimentally useful parameter is $t_{1/2}$. As shown previously, after a waiting time of 3 $t_{1/2}$, the apparatus can be considered fully equilibrated. Practically, if $t_{1/2}$ is lower than 30 min, it can be worthwhile to wait for the 3 $t_{1/2}$ equilibrium time to assure a constant stationary phase volume. To determine accurate octanol-water partition coefficients, a stable octanol volume is necessary. Hence, it is important to wait one hour ($t_{1/2}$ = 23 min) before making the first solute injection (*11*). If $t_{1/2}$ is higher than 30 min and $Sf_{t=\infty}$ is not too different from $Sf_{t=0}$, e.g., MEK, 1,1,1-trichloroethane and trimethylbenzene with an aqueous mobile phase and dichloromethane with the solvent mobile phase, the solute injection can be made after a short (~ 10 min) wait time. The small decrease of stationary phase volume that occurs during the run can easily be corrected by interpolation if needed.

Non Aqueous Solvent Systems. Four binary solvent systems were studied to generalize the results obtained with water-solvent systems. Figure 7 shows the results obtained with the heptane-DMF system. The previously mentioned exponential model can be used. However, the phase density difference $|\Delta d|$ versus $Sf_{t=0}$ relationship is not verified. The phase retention is approximately 75% for the four binary systems in the head-tail direction with the denser liquid as the mobile phase. Different and higher $Sf_{t=0}$ values were obtained in the tail-head direction (Table II). The $t_{1/2}$ times are longer in the head-tail direction than in the other direction. The stability of the heptane-DMSO system in both directions should be noted.

Liquid Polarity and Partition Coefficient

As shown by equation 1, beside the stationary phase volume, the only parameter responsible for solute retention is its liquid-liquid partition coefficient, P. In a previous study, we have shown that the solvent-water

Downloaded by YORK UNIV on June 29, 2012 | http://pubs.acs.org
Publication Date: May 15, 1995 | doi: 10.1021/bk-1995-0593.ch002

Downloaded by YORK UNIV on June 29, 2012 | http://pubs.acs.org
Publication Date: May 15, 1995 | doi: 10.1021/bk-1995-0593.ch002

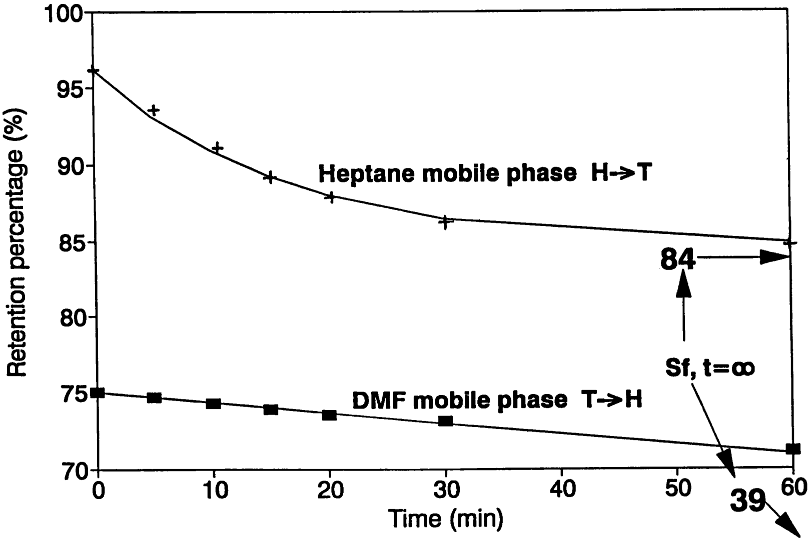

Figure 7. The change in heptane-DMF retention percentage with time. The heptane losses were almost linear (a=0.002) when DMF was the mobile phase (■).

partition coefficient of formanilide was related to the Reichardt polarity index of the water saturated solvent (*10*). The octanol-water partition coefficient has been used for many years as a measure of relative hydrophobicity. The partition coefficient values are commonly adjusted by adding a third solvent in a binary biphasic mixture. The third solvent should have a miscibility in the two initial solvents, *i.e.*, the third solvent being at intermediate polarity. For example, methanol or acetic acid are added to water-chloroform biphasic mixtures in the optimization of separation (*1-3*). The variation of solute partition coefficients with liquid composition changes can be found in other chapters of this book. However, it should be kept in mind that the addition of a third solvent in a biphasic mixture changes not only the phase polarity and the solute partition coefficient, but also it changes the phase density. The phase density difference remains the most important parameter for stationary phase retention for any CCC separation.

Downloaded by YORK UNIV on June 29, 2012 | http://pubs.acs.org
Publication Date: May 15, 1995 | doi: 10.1021/bk-1995-0593.ch002

Literature Cited

1- Mandava, N.B.; Ito, Y. *Countercurrent Chromatography*; Chromatographic Science Series, M. Dekker; New York, NY, 1988; Vol. 44.
2- Conway, W.D. *Countercurrent Chromatography, Apparatus, Theory and Applications*; VCH Publishers, Weinheim, Germany, 1990.
3- Ito, Y. In *Advances in Chromatography*; Giddings, J.C.; Grushka, E.; Cazes, J., Eds.; M. Dekker, New York, NY, 1984, Vol. 24, Ch. 6, pp 181-245.
4- Foucault, A.C. *Anal. Chem.* **1991**, *63*, 569A.
5- Berthod, A. *J. Chromatogr.*, **1991**, *550*, 677.
6- Hildebrand, J.H.; Prausnitz, J.M.; Scott, R.L. *Regular and Related Solutions*; Van Nostrand-Reinhold, Princeton, NJ, 1970.
7- Snyder, R.L. *Principle of Adsorption Chromatography*; M. Dekker, New York, NY, 1968.
8- Reichardt, C. *Solvents and Solvent Effects in Organic Chemistry*; VCH Publishers, Weinheim, Germany, 1988.
9- Berthod, A.; Bully, M. *Anal. Chem.*, **1991**, *63*, 2508.
10- Berthod, A.; Schmitt, N. *Talanta*, **1993**, *40*, 1667.
11- Berthod, A.; Dalaine, V. *Analusis*, **1992**, *20*, 325.

RECEIVED November 28, 1994

Chapter 3

Orbital Turns per Theoretical Plate for Countercurrent Chromatography Device Comparison

J.-M. Menet, M.-C. Rolet-Menet, D. Thiébaut, and R. Rosset

Laboratoire de Chimie Analytique, Unité de Recherche Associée au Centre National de la Recherche Scientifique 437, Ecole Supérieure de Physique et Chimie Industrielles, 10 Rue Vauquelin, 75231 Paris Cedex 05, France

Downloaded by UNIV OF GUELPH LIBRARY on June 28, 2012 | http://pubs.acs.org
Publication Date: May 15, 1995 | doi: 10.1021/bk-1995-0593.ch003

Counter-Current Chromatography involves many parameters including the geometrical characteristics of the devices and an essential one which is the volume of stationary phase retained inside the column. Studies of the plots of the number of theoretical plates *versus* the flow-rate of the mobile phase have showed they cannot be considered as Van-Deemter plots as the capacity factors of the separated solutes are not constant.

The number of orbital turns per theoretical plate is introduced as a mean of comparison between different type J Coil Planet Centrifuges. It is applied to two Counter-Current Chromatographs, based on the planetary motion of a coiled Teflon tube and consequently named type J Coil Planet Centrifuges, using separations of saturated fatty acids and of phenols.The number of orbital turns per theoretical plate reveals as a useful comparison parameter as the flow-rate of the mobile phase, the rotational speed of the apparatus, the internal diameter and the length of the tubing constituting the column are involved. The retention of stationary phase inside the column and the number of theoretical plates are also included.

The theory of plates was developed fifty years ago (*1*, *2*). It consists in the cut of the column into a number of fictive areas where the equilibria are realized. These areas are called theoretical plates. This model can be used for countercurrent chromatography (*3*). Thus, the number of theoretical plates (N) is a measure of the column efficiency and of the spreading of the injection bands during the chromatographic process. The shape of elution peaks may be approximated by a normal distribution.

To compare columns of various lengths, the height equivalent to a theoretical plate may be used. In HPLC the plot of N versus the mobile phase flow-rate (*4*) (Van Deemter curve) using a retained solute which capacity factor is constant in the operating conditions shows a maximum at the so-called optimum flow-rate.

Reports of plots of the number of theoretical plates in High Speed Counter-Current Chromatography (HSCCC) *versus* the mobile phase flow-rate (*5*,*6*) pointed out the problem of the variation of the stationary phase retention during the

0097–6156/95/0593–0035$12.00/0

experiments. As a result, the increase of the mobile phase flow-rate led to variations of the solutes capacity factors. Thus, no real comparison could be done with HPLC.

The comparison of type J Coil Planet Centrifuges (CPCs) between each others is difficult because of their various geometrical properties (length, i.d. of the column, number of columns, *etc.*); N or H do not take into account the rotational speed of the apparatus. Thus, in this paper we propose to introduce the count of orbital turns per plate (**n**) in order to compare CPCs and to investigate the efficiency of the process from the point of view of a time scale, **n** being the rotational speed times the reversal of the efficiency per unit of time.

Theoretical Background

Due to the geometrical properties of the Gaussian distribution, the number of theoretical plates (TP) can be calculated using equation (*4*):

$$N = 16\ (t_r/W)^2 = 5.54\ (t_r/\delta)^2 \qquad (1)$$

where t_r is the retention time of the solute used to determine N, W and δ are, respectively the peak width at the base and at one-half the height of the peak in time units. The second formula is better because errors in drawing tangents are avoided.

The height equivalent to a TP is defined by the formula (*4*):

$$\mathrm{HETP} = L/N = H \qquad (2)$$

where L is the length of the column.

The count of orbital rounds per plate was calculated using some simple theoretical points which are described below. All the tubes used to make a column are supposed to be of a cylindrical shape.

For a single-phase system, the linear velocity u in a tube was defined using the flow-rate:

$$u = F/S \qquad (3)$$

where F is the flow-rate of the phase and S the section of the tube. If the phase is taken as a perfect fluid (no viscosity), the velocity in the tube is homogeneous and equal to u. For a viscous fluid, the velocity distribution is parabolic (*7*). u is then the average velocity and the velocity on the axis of the cylinder is 2u, while near the wall of the tube it is equal to zero ; thus, u was used as an average velocity for a fluid in a cylindrical tube.

For a biphasic system, the calculation of the velocities of each phase is rather complicated (*8*). The model used here is very simple. In countercurrent chromatography, the use of a biphasic system allows to define a mobile phase and a stationary phase. The latter was considered as motionless in the tube while the mobile phase was flowing through it. The model requires that each coil of the column contains stationary phase. Thus the effective section of the tube was reduced because of the stationary phase retained in the tube. It is convenient to use S_F (*9*) (fractional volume of column occupied by stationary phase), defined as :

$$S_F = V_S/V_C \qquad (4)$$

$$V_C = V_S + V_M \qquad (5)$$

where V_S is the volume of the stationary phase, V_M the volume of the mobile phase

Downloaded by UNIV OF GUELPH LIBRARY on June 28, 2012 | http://pubs.acs.org
Publication Date: May 15, 1995 | doi: 10.1021/bk-1995-0593.ch003

Downloaded by UNIV OF GUELPH LIBRARY on June 28, 2012 | http://pubs.acs.org
Publication Date: May 15, 1995 | doi: 10.1021/bk-1995-0593.ch003

and V_C the volume of the column. The effective section S_{eff} of the tube is then calculated:

$$S_{eff} = S.(1-S_F) \qquad (6)$$

where S is the real section of the tube. Thus the mobile phase is flowing through a section S_{eff}. Its linear velocity can be written:

$$u_{eff} = \frac{F}{S_{eff}} = \frac{F}{S\,(1-S_F)} \qquad (7)$$

As this simplified model gives the velocity of the mobile phase, the time T required to obtain one plate is obtained using equation 8:

$$T = \frac{H}{u_{eff}} = \frac{L}{N}\frac{S\,(1-S_F)}{F} \qquad (8)$$

The period T_M of the motion of the column around the central axis of the apparatus is:

$$T_M = 1/\omega \qquad (9)$$

where ω is the orbital speed.

Then the count of orbital rounds per plate (dimensionless number) is defined by:

$$\mathbf{n} = \frac{T}{T_M} = \frac{L}{N}\frac{S\,(1-S_F)}{F}\,\omega \qquad (10)$$

where L is the length of the column (in cm), N the number of theoretical plates, S_F the fractional volume of column occupied by stationary phase, S the internal section of the tube (in cm^2), F the flow-rate (in mL/min) and ω the orbital speed of the HSCCC device (in rpm).

The given formula is appropriate for the calculation from experimental data. But it will be easier to understand the influence of each parameter by modifying it. The term $1-S_F$ is equal to V_M/V_C and L.S is equal to V_C. Thus equation 10 may be written:

$$\mathbf{n} = \frac{V_M\,\omega}{N\,F} = \frac{t_0}{N}\,\omega \qquad (11)$$

where t_0 is the dead time, defined as $t_0 = V_M/F$.

The higher the **n** value, the lower the yield of the chromatograph from the point of view of speed of separation. Due to the fact that the column rotates 2 times around it own axis during a revolution, the maximum yield should occur for 2 plates per revolution, meaning that **n** = 0.5.

Equation 11 could also be written:

$$\frac{1}{\mathbf{n}} = \frac{N}{t_0}\frac{1}{\omega} \qquad (12)$$

This form enables to recognize the N/t_0 parameter, which can be used for comparison between chromatographic techniques (*10*). The rotational speed intervenes in the definition of **n** because it is an intrinsic parameter of CCC.

Experimental

Solvent Systems and Solutes. Two sets of experiments were carried out. The first one used a two-phase solvent system composed of heptane / methanol / acetic acid (1:1:1, v/v) to separate a test mixture of saturated fatty acids. The second two-phase solvent system was composed of chloroform / methanol / water (3:1:3, v/v) and was used to separate a mixture of phenols. The solvent mixtures were equilibrated at room temperature and the phases were separated shortly before use.

All organic solvents were of HPLC grade. Methanol, acetic acid and heptane were purchased from Prolabo (Paris, France), other organic solvents from Rathburn (Chromoptic, Montpellier, France). All solvents were filtered before use and water was doubly distilled. Nitrogen (L'Air Liquide, Paris, France) supplied the nebulizer of the ELSD system. The paranitrophenol, phenol and stearic acid were purchased from Prolabo (Paris, France) and the two other fatty acids (myristic acid and palmitic acid) from Merck (Nogent-sur-Marne, France).

Downloaded by UNIV OF GUELPH LIBRARY on June 28, 2012 | http://pubs.acs.org
Publication Date: May 15, 1995 | doi: 10.1021/bk-1995-0593.ch003

Apparatus. The HSCCC apparatus consisted of two Gilson Model 303 pumps (Villiers-le-Bel, France) for pumping the organic and the aqueous phases.

The pumps were connected to a type J CPC. Two different type J CPCs were used. One was a P.C. Inc. system (Potomac, MD., USA), equipped with one column. The latter is made of a 1.6 mm i.d. PTFE tubing to give a total volume of 325 mL and it has a 161.6 m length. A counterweight is used to counterbalance the effect of the column filled with stationary and mobile phases. The β values ranged from 0.57 to 0.85. The second type J unit was a Model CCC 3000 system (Pharma-tech Research Corp., Baltimore, MD., USA) which is equipped with three identical columns. Each one is prepared from 0.8 mm i.d. PTFE tubing. As they are mounted in series, the total capacity of this apparatus is 45 mL and the total length is 89.5 m. The β values ranged from 0.55 to 0.75.

A stroboscope (Strob 1, AOIP, Paris, France), which measures are independent from the studied devices, allowed checking of the rotational speeds.

Samples were injected into the columns via Rheodyne Model 7125 injection valves. The samples, previously dissolved in the mobile phase, were carried out into the mobile phase after filling the column with the stationary phase.

The detection used for the separation of fatty acids was based on evaporative light-scattering detection (ELSD) on-line with HSCCC (*11*). The unit was a Sedex 45 ELSD system (Sédéré, Vitry-sur-Seine, France) manufactured for HPLC and used without modification. For the separation of phenols, a Model 2550 UV detector (Varian, Les Ulis, France) was used (*12*). Isopropanol was continuously added to the column effluent using a Model 8500 syringe pump (Varian, Les Ulis, France) via a Model 811 dynamic mixing chamber (Gilson, Villiers-le-Bel, France) in order to improve solute detectability (*12*). All data were stored either on Shimadzu CR 4A or CR 6A integrators (Touzart et Matignon, Vitry s/Seine, France).

Experimental Conditions. They are reported for the two CPCs in Table I for the separations of three saturated fatty acids, namely myristic acid ($C_{14}H_{28}O_2$), palmitic acid ($C_{16}H_{32}O_2$) and stearic acid ($C_{18}H_{36}O_2$). A typical separation is shown in Figure 1. The chromatogram demonstrates very high flow-rates such as 21 mL/min are compatible with satisfactory resolutions and high efficiencies. The resolution between the stearic and palmitic acids (first two peaks) is 1.22 and between the palmitic and the myristic acids (last two peaks) is 1.54. The efficiencies are 1900 theoretical plates (TP) for the stearic acid peak, 1480 TP for the palmitic acid peak and 1480 TP for the myristic acid. The three saturated fatty acids are separated in less than 16 minutes.

Downloaded by UNIV OF GUELPH LIBRARY on June 28, 2012 | http://pubs.acs.org
Publication Date: May 15, 1995 | doi: 10.1021/bk-1995-0593.ch003

Separation of phenol, paranitrophenol and orthonitrophenol is shown in Figure 2. Only paranitrophenol and phenol were used for the calculations because orthonitrophenol is not retained by the stationary phase. The second peak corresponds to 615 TP and the third one to 625 TP. The resolution between the two last peaks is 1.50.

Table I. Experimental conditions for the separation of myristic, palmitic and stearic acids on the CCC 3000 and P.C.Inc. CPCs

Model	Speed	Sample loop volume	ELSD conditions		
	ω	V	Temperature	Nitrogen Pressure	Gain
	(rpm)	(mL)	(°C)	(Bars)	
CCC 3000	1700	20	25	2	7
P.C. Inc.	750	450	25	2	7

Results and Discussion

Retention of Stationary Phase. S_F (defined in equation 4) is a measure of the volume of stationary phase retained inside the tubing of the column. The variation of S_F *versus* the flow-rate was studied on the P.C. Inc. with the heptane / acetic acid / methanol (1:1:1, v/v) and the chloroform / methanol / water (3:1:3, v/v) systems as shown in Figures 3A and 3B. The plots are similar in shape, as S_F linearly decreases with the flow-rate. The higher the flow-rate, the more the stationary phase is driven by the mobile phase, hence the decrease in the retention of stationary phase. However, the shape is changed for low flow-rates when using the CCC 3000 HSCCC with the heptane / acetic acid / methanol (1:1:1, v/v) solvent system. The plot, shown in Figure 3C, is a plateau below 2 mL/min before showing the same linear decrease observed on the P.C. Inc. apparatus. One explanation could be the higher running rotational speed combined with a smaller internal diameter of the coil tubing reducing the role of the drag of the stationary phase by the mobile one.

Effective Linear Velocity of the Mobile Phase. u_{eff} is calculated from equation 7 for the two different separations achieved on the P.C.Inc. (Figures 4A and B) and that achieved on the CCC 3000 (Figure 4C). All the plots display the same shape, which is an increasing curve, quite horizontal at higher flow-rates. According to equation 7, u_{eff} tends toward the asymptotic value u (defined in equation 3) for increasing flow-rates. This means that increasing a small flow-rate significantly increases u_{eff}, while an increase of an already high flow-rate does not change u_{eff} so much.

Efficiency. Three plots of the efficiency (number of theoretical plates) *versus* the flow-rate of the mobile phase are given. Two of them were achieved on a P.C. Inc. apparatus; one is based on the separation of the mixture of three fatty acids and is shown in Figure 5A. The other one involves the separation of phenols and is reported in Figure 5B. The same mixture of fatty acids was also separated on the CCC 3000 and the corresponding plot is displayed in Figure 5C.

Using the same test mixture of saturated fatty acids, the higher efficiencies are obtained with the CCC 3000 CPC. The number of theoretical plates ranges from 500 to 2500, while it ranges from 500 to 2000 for the P.C. Inc. unit. However, the total lengths of the columns are different between these type J CPCs. For this reason, it is necessary to introduce the length of the column for a first comparison of the devices.

Downloaded by UNIV OF GUELPH LIBRARY on June 28, 2012 | http://pubs.acs.org
Publication Date: May 15, 1995 | doi: 10.1021/bk-1995-0593.ch003

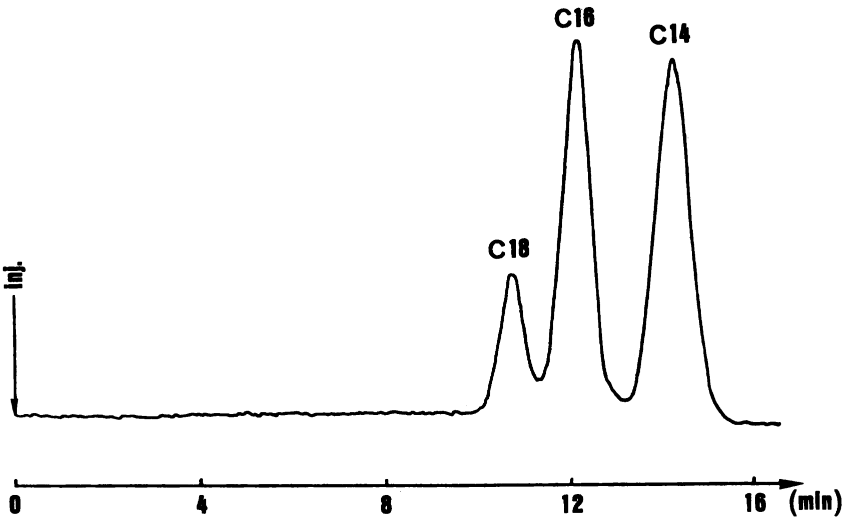

Figure 1. On-line HSCCC-ELSD chromatogram of a test mixture of fatty acids. P.C. Inc. apparatus; mobile phase: heptane rich; flow-rate: 21 mL/min; concentration: 1 g/L for each fatty acid; $S_F = 0.51$. Other experimental conditions described in Table I.

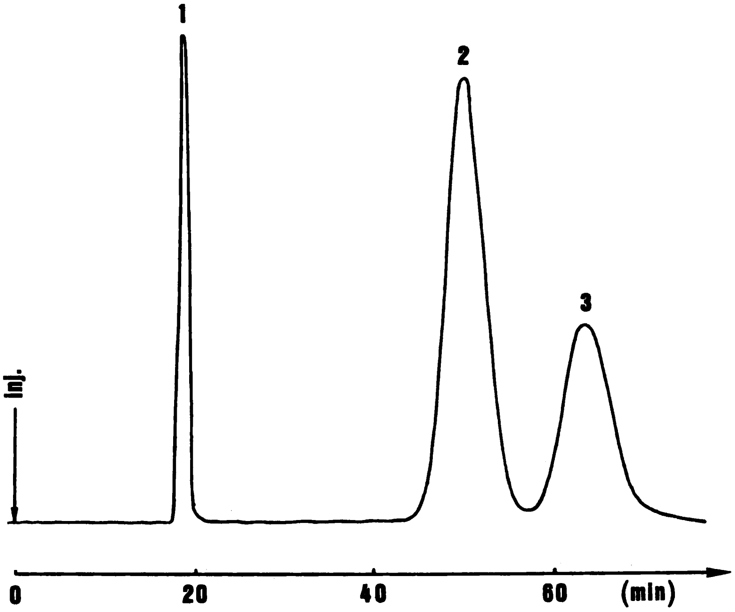

Figure 2. On-line HSCCC-UV chromatogram of a mixture of phenols: (1) orthonitrophenol, (2) paranitrophenol and (3) phenol.
P.C. Inc. apparatus; mobile phase: choroform / methanol; flow-rate: 2.5 mL/min; concentration: paranitrophenol: 0.7 g/L and phenol: 1.6 g/L; $S_F = 0.86$. UV detection: 2.56 A.U., 270 nm. Isopropanol flow-rate: 0.5 mL/min.

Downloaded by UNIV OF GUELPH LIBRARY on June 28, 2012 | http://pubs.acs.org
Publication Date: May 15, 1995 | doi: 10.1021/bk-1995-0593.ch003

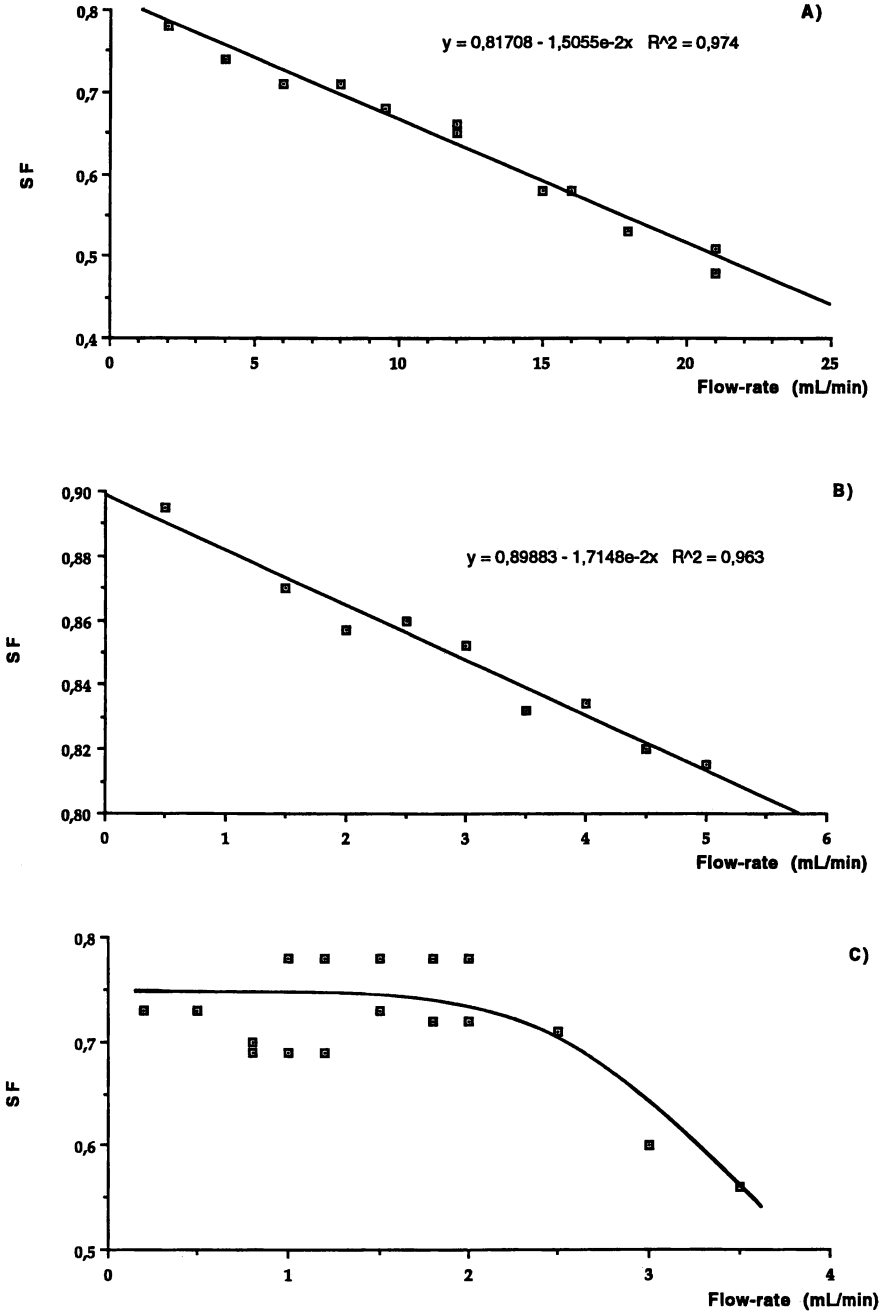

Figure 3. Plot of the retention of stationary phase (S_F) *versus* the flow-rate. A) P.C.Inc. apparatus, heptane / acetic acid / water system (1:1:1, v/v); B) P.C.Inc. apparatus, chloroform / methanol / water system (3:1:3, v/v); C) CCC 3000 apparatus, heptane / acetic acid / water system (1:1:1, v/v).

Downloaded by UNIV OF GUELPH LIBRARY on June 28, 2012 | http://pubs.acs.org
Publication Date: May 15, 1995 | doi: 10.1021/bk-1995-0593.ch003

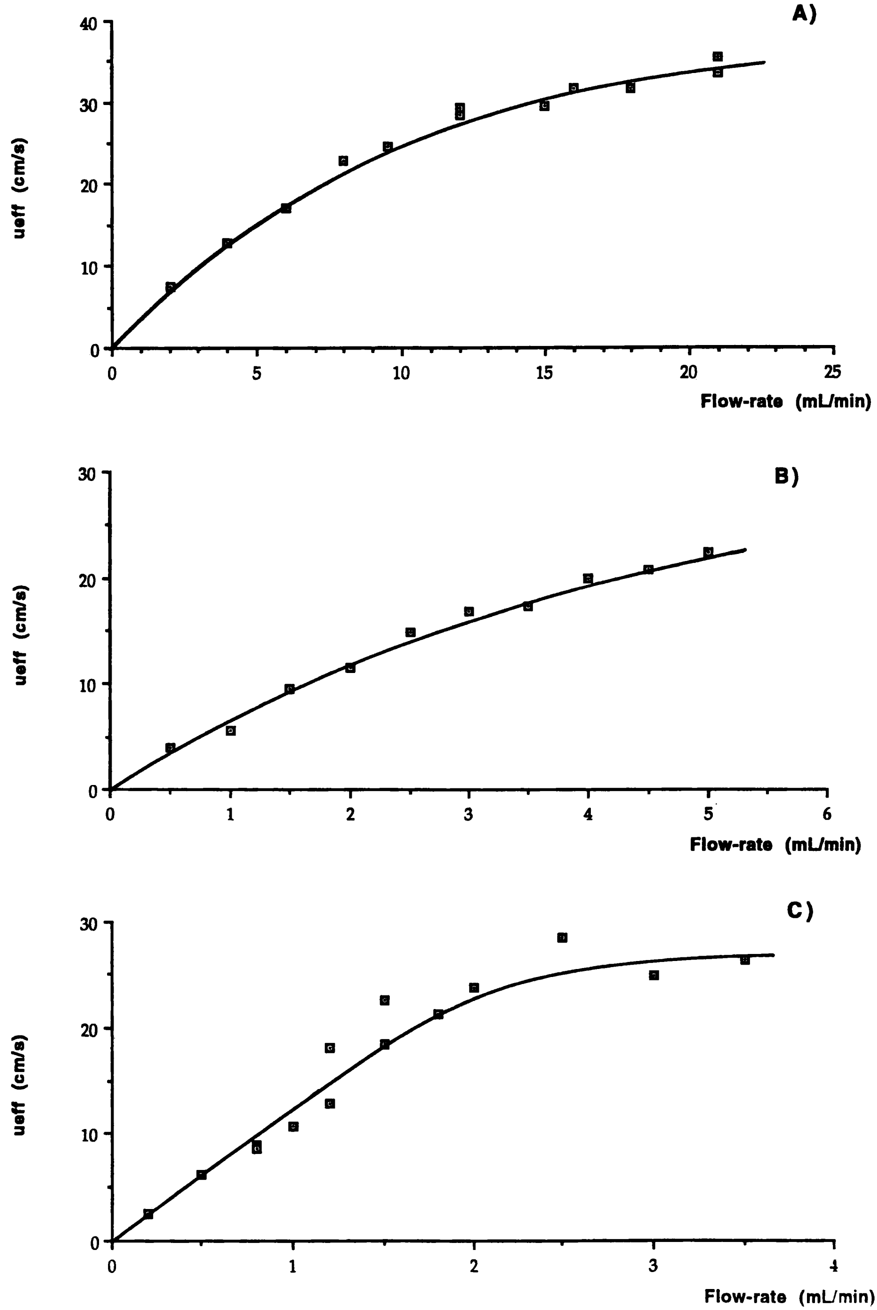

Figure 4. Plot of the efficicient linear velocity of the mobile phase (u_{eff}) *versus* the flow-rate.
A) P.C.Inc. apparatus, heptane / acetic acid / water system (1:1:1, v/v); B) P.C.Inc. apparatus, chloroform / methanol / water system (3:1:3, v/v); C) CCC 3000 apparatus, heptane / acetic acid / water system (1:1:1, v/v).

Downloaded by UNIV OF GUELPH LIBRARY on June 28, 2012 | http://pubs.acs.org
Publication Date: May 15, 1995 | doi: 10.1021/bk-1995-0593.ch003

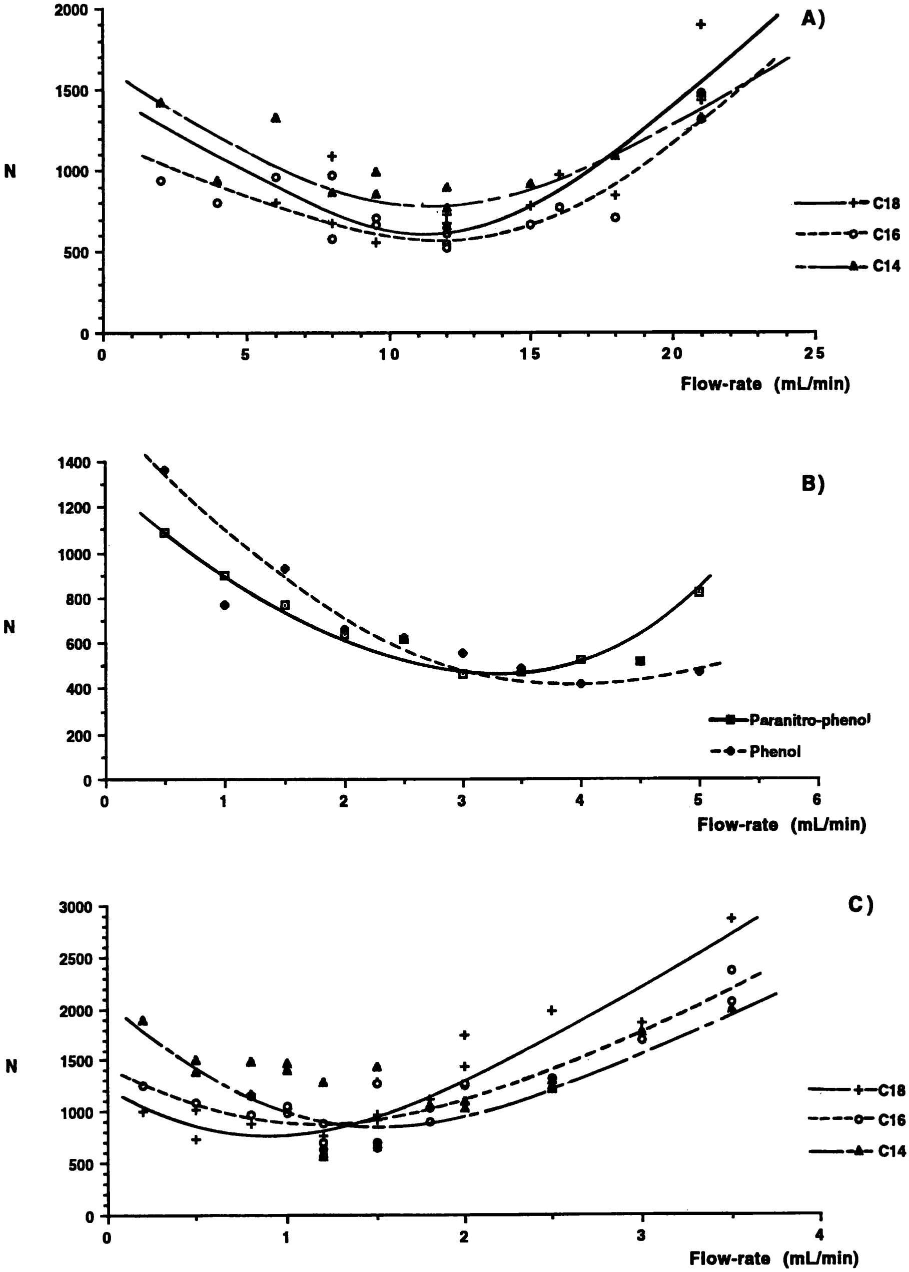

Figure 5. Number of theoretical plates (N) *versus* the flow-rate (F). A) P.C.Inc. apparatus, heptane / acetic acid / water system (1:1:1, v/v), mobile phase: heptane rich, separation of myristic, palmitic and stearic acids; B) P.C.Inc. apparatus, chloroform / methanol / water system (3:1:3, v/v), mobile phase: chloroform / methanol rich, separation of orthonitrophenol, paranitrophenol and phenol; C) CCC 3000 apparatus, heptane / acetic acid / water system (1:1:1, v/v), mobile phase: heptane rich, separation of myristic, palmitic and stearic acids.

For a 2 mL/min flow-rate, the heights equivalent to a theoretical plate are calculated for the palmitic acid (C_{16}). The P.C. Inc. device leads to 17.2 cm (*i.e.*, 5.8 plates per meter) and the CCC 3000 unit to 7.05 cm (*i.e.*, 14.2 plates per meter). The latter, with a higher operation rotational speed and a smaller internal diameter (*see* Table I), is twice as efficient as the other type J CPC. When compared to the average length of one coil, the height equivalent to a theoretical plate represents 40% of the length of one coil for the P.C. Inc. unit which is similar to the 45% for the CCC 3000 CPC.

The shapes of the curves have already been described by Foucault *et al.* (*5*) and Menet *et al.* (*6*). The efficiency N (number of theoretical plates) usually shows a minimum *versus* the flow-rate F, when the column is equilibrated at its maximum capacity for retaining the stationary phase (*i.e.*, hydrodynamic equilibrium). However, all these curves shall not be called Van-Deemter plots. The hydrodynamic equilibrium, which is flow-rate dependent, determines the retention of stationary phase, as shown in Figure 3. Consequently, the volume of stationary phase retained in the column, hence the capacity factors, vary during the calculation of N *vs.* F, whereas Van-Deemter plots are obtained at constant capacity factors.

Such results imply that the flow-rate can be increased in order to raise the efficiency and to shorten the separation time, but with a reduced retention of stationary phase and consequently a diminished resolution (*5*,*6*). An optimum has to be determined between efficiency and resolution.

Count of Orbital Turns per Plate. In order to take into account the separation time and the mechanical characteristics of the apparatus, we propose to introduce **n**, the count of orbital turns per plate calculated according to equation 10 or 11; **n** can be calculated for each solute which is separated. The length of the coiled Teflon tube L and its section S are geometric constants. The flow-rate of the mobile phase F and the rotational speed of the apparatus ω are experimental parameters, chosen for each separation. But the number of theoretical plates N and the retention of stationary phase S_F have to be calculated after the separation.

The calculations of **n** are derived from Figures 3 and 5 showing the dependence of the retention of stationary phase and of the number of theoretical plates on the flow-rate. Figures 6 A and B represent the variation of **n** *versus* the flow-rate of the mobile phase on the P.C. Inc. unit for a separation of fatty acids and a separation of phenols. Figure 6C shows the same plot achieved on the CCC 3000 CPC for the separation of fatty acids.

The shapes of the curves are similar for both type J CPCs and for two different separations achieved on the P.C.Inc. apparatus. It is a decreasing curve which tends to a plateau. It means that all the units used for this work are able to reach the same increased mechanical yield (below 10 turns per plate) despite their differences (column length and number, internal diameter or orbital and planet radius) at their higher flow-rates. But the lower the internal diameter of the column, the lower the value of the flow-rate required to obtain the same **n** value: for example, at **n** = 10, the flow-rate is 8 -10 ml/min for the P.C.Inc. and 2.5 ml/min for the CCC 3000. In that case, both CPCs lead to the same u_{eff}, approximately 28 cm/s. Using the same mixture of fatty acids at a 2 mL/min flow-rate, **n** is calculated for the palmitic acid. The value is 28 for the P.C. Inc. unit (u_{eff}=8 cm/s) and 15 for the CCC 3000 device (u_{eff}=21 cm/s). The latter is more efficient than the other CPC, but the increase in efficiency is reduced compared to the classification based on the height equivalent to a theoretical plate. The reason is that **n** involves the rotational speed and the internal diameter (*via* the section of the tube) which allows a more precise comparison of the type J CPCs.

Conclusion

Using mixtures of saturated fatty acids or phenols, separations carried out on

Downloaded by UNIV OF GUELPH LIBRARY on June 28, 2012 | http://pubs.acs.org
Publication Date: May 15, 1995 | doi: 10.1021/bk-1995-0593.ch003

Downloaded by UNIV OF GUELPH LIBRARY on June 28, 2012 | http://pubs.acs.org
Publication Date: May 15, 1995 | doi: 10.1021/bk-1995-0593.ch003

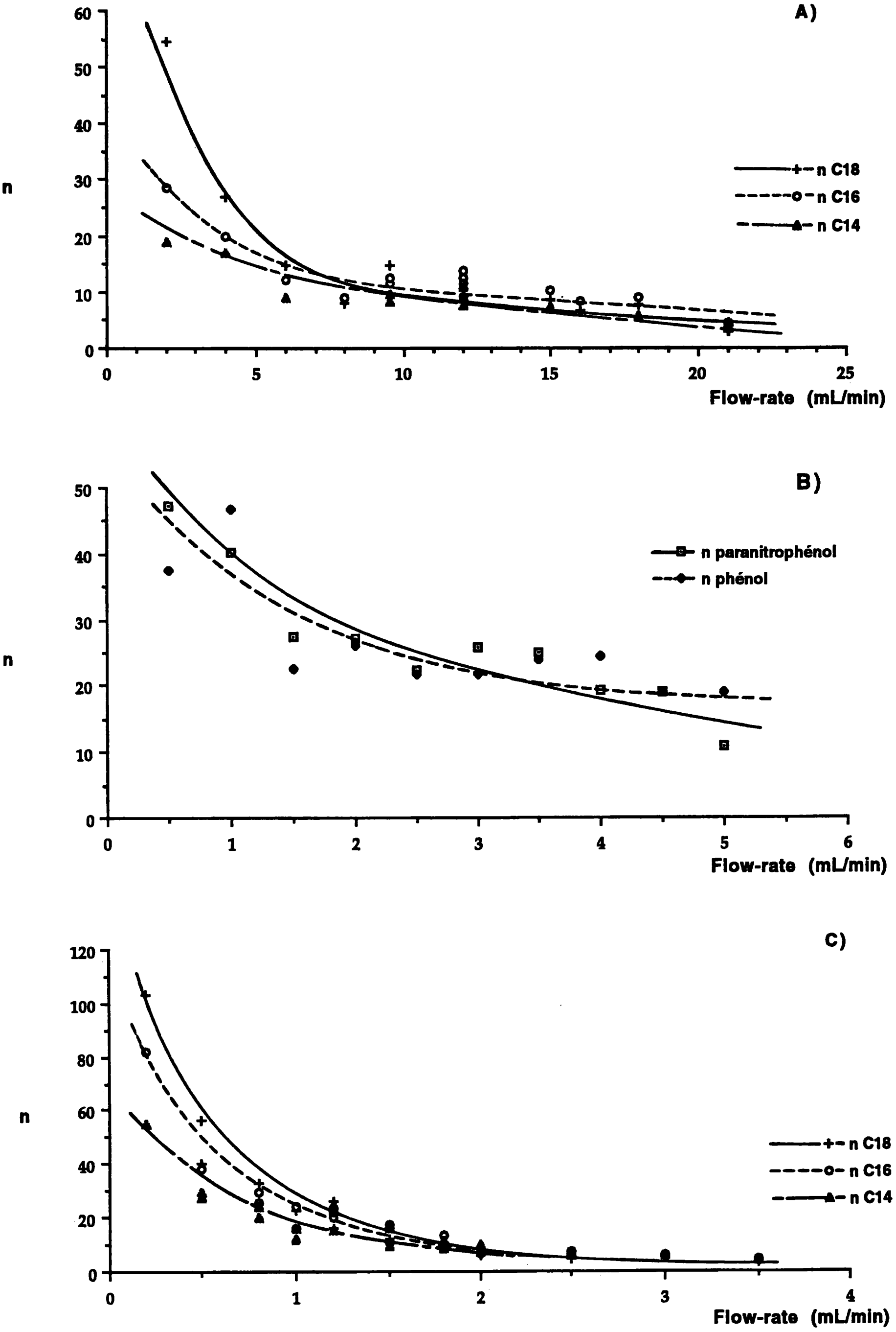

Figure 6. Count of orbital turns per plate (n) *versus* the flow-rate (F). A), B) and C) defined in the caption of figure 4.

the two different type J CPCs, namely the P.C.Inc. and the CCC 3000, allowed to study the influence of the flow-rate on the efficiency. Plotting the number of theoretical plates *versus* the flow-rate revealed a reversed curve compared to classical Van-Deemter curves. However, these plots are dependent on the retention of stationary phase and for Counter-Current Chromatography, they shall not be called Van-Deemter plots. A better comparison of the devices is based on the use of the height equivalent to a theoretical plate.

However, we needed a parameter including the rotational speed, the internal diameter of the column as well as the retention of the stationary phase inside the column. The number of orbital turns per theoretical plate has revealed as a good comparison parameter as many typical parameters of CCC are involved. The higher flow-rates lead to the best efficiencies. Nevertheless, it should be kept in mind that high flow-rates decrease the volume of stationary phase inside the column and consequently the resolution.

Downloaded by UNIV OF GUELPH LIBRARY on June 28, 2012 | http://pubs.acs.org
Publication Date: May 15, 1995 | doi: 10.1021/bk-1995-0593.ch003

Acknowledgments

The authors of this paper wish to thank the RHONE-POULENC RORER Company for its financial support.

Literature Cited

(*1*) Martin, A.J.P.; Synge, R.L.M. *Biochem. J.* **1941**,*35*,1358.
(2) Mayer, S.N.; Tompkins, E.R. *J. Amer. Chem. Soc.* **1952**, *52*, 238.
(*3*) Conway, W.D. *Countercurrent Chromatography; Apparatus, Theory and Applications*; VCH: New-York, NY, 1990; p195.
(*4*) Rosset, R.; Caude, M.; Jardy A. *Chromatographies en Phases Liquide et Supercritique*; Masson: Paris, 1991.
(*5*) Foucault, A. P.; Bousquet, O.; Le Goffic, F. *J. Liq. Chromatogr.* **1992,** *15*, 2691-2706.
(*6*) Menet, J.-M.; Rolet, M.-C.; Thiébaut, D.; Rosset R.; Ito, Y. *J. Liq. Chromatogr.* **1992**, *15*, 2883-2908.
(*7*) Poiseuille, J.L. *Comptes rendus* **1840**, *11*, 961 and 1041.
(*8*) Govier, G.W.; Aziz, K. *The Flow of Complex Mixtures in Pipes*; Robert E. Krieger Publishing Co., Inc.: New-York, NY, 1977.
(*9*) Ibid (3), except p198.
(*10*) Caude, M.; Rosset, R. *Analusis* **1986**, *14 (6)*, 310-311.
(*11*) Drogue, S.; Rolet, M.-C.; Thiébaut, D.; Rosset, R. *J. Chromatogr.* **1991**, *538*, 91-97.
(*12*) Rolet, M.-C.*Thèse de l'Université Paris VI*. 1993.

RECEIVED November 28, 1994

Downloaded by OHIO STATE UNIV LIBRARIES on June 29, 2012 | http://pubs.acs.org
Publication Date: May 15, 1995 | doi: 10.1021/bk-1995-0593.ch004

Chapter 4

Cross-Axis Coil Planet Centrifuge

Use of Experimental Design to Determine Optimal Settings

J. Goupy[1], J.-M. Menet[1], Kazufusa Shinomiya[2], and Yoichiro Ito[3]

[1]Laboratoire de Chimie Analytique, Unité de Recherche Associée
au Centre National de la Recherche Scientifique 437, Ecole Supérieure
de Physique et Chimie Industrielles, 10 Rue Vauquelin,
75231 Paris Cedex 05, France
[2]College of Pharmacy, Nihon University, 7–7–1, Narashinodai,
Funabashi-shi, Chiba 274, Japan
[3]Laboratory of Biophysical Chemistry, National Heart, Lung, and Blood
Institute, National Institutes of Health, Building 10, Room 7N322,
Bethesda, MD 20892

It has proved difficult to optimize the sixth cross-axis Coil Planet Centrifuge designed by Dr. Ito for retention of stationary phase. Graphical analysis of the trial data did not give precise indications of the optimal settings. We have therefore applied the method of experimental designs to the same experimental data obtained from the sixth cross-axis prototype. This method allows the calculation of the effect of each studied parameter along with their multiple interactions. The effects of the interactions of the four solvent systems studied were found to be greater than those of the main individual factors. Experimental designs method provided more precise optimal settings than the original graphical method and allowed us to calculate the interaction effects.

Interpreting the values of retention of stationary phase obtained from a cross-axis coil planet centrifuge (CPC) raised an interesting problem (*1*). The classical approach to such an interpretation proved to be inefficient, and Ito *et al.* were not satisfied with the original conclusions (*2*). We therefore looked for another way to solve this rather delicate problem. We studied seven parameters, with each factor being fixed at two levels. Three of them were related to the coil - direction of winding, hub diameter and position - and the four others were chosen by the experimenter - a heavier or lighter mobile phase, introduction mode, elution mode and rotation direction.

A mathematical approach was applied to the previously obtained experimental data, experimental design methodology (*3*), allows calculation of the effect of each factor along with the interactions between two or more factors. As expected, the results are similar to the original graphical observations. However, they provide us with values for each effect, which allows a more precise and complete optimization. They also demonstrate that they are necessary to optimize for stationary phase retention on

0097–6156/95/0593–0047$12.00/0

Downloaded by OHIO STATE UNIV LIBRARIES on June 29, 2012 | http://pubs.acs.org
Publication Date: May 15, 1995 | doi: 10.1021/bk-1995-0593.ch004

the cross-axis CPC as the interactions have greater effects than the factors themselves, which could not be observed with the previous graphical method.

Graphical Analysis

We used the sixth cross-axis CPC designed by Dr. Ito in 1992. Its general principle are shown in Figure 1.

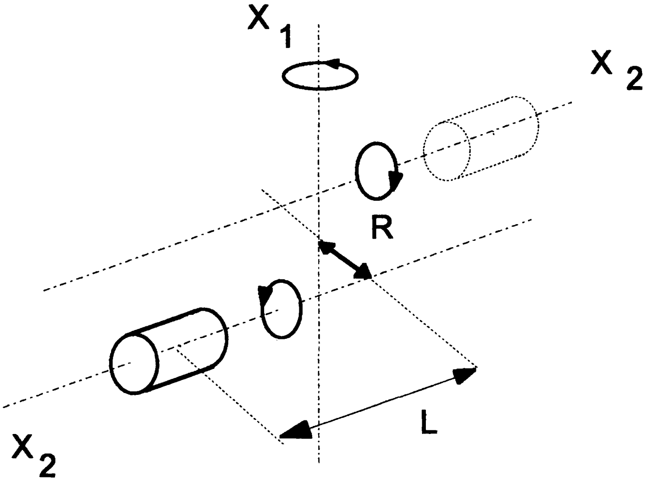

Figure 1. Diagram of the Ito cross-axis coil planet centrifuge (Adapted from Y. Ito, *Journal of Chromatography*).

Preliminary optimization to have the greatest volume of stationary phase inside the column revealed that as many as seven parameters had to be set. The coil may be left- or right-handed, 5.5 or 10 cm hub diameter and in the L or X-1.5L position. The experimenter can select the lighter or heavier mobile phase, its elution mode -tail to the head of the column (T) or reverse (H)-, its introduction mode -inward, against the centrifugal force (I) or outward, same direction as the centrifugal force (O)- and the direction of rotation -P_I, anti-clockwise or P_{II}, clockwise. Four solvent systems were studied. One consisted of n-butanol / 0.13M $NaCl_{aq}$ (1:1, v/v) + 1.5% (w/v) hexadecyl pyridinium chloride. The three others were based on an aqueous solution of a polymer: poly(ethyleneglycol)-1000 / K_2HPO_{4aq}, poly(ethyleneglycol)-8000 4.4% (w/w) / Dextran T500 7.0% (w/w) and poly(ethyleneglycol)-8000 4.0% (w/w) / Dextran T500 5.0% (w/w). All the values of retention of stationary phase are given in Reference 1.

The graphical method consisted of plotting the retention of stationary phase as one parameter is changed between the horizontal axis and the vertical axis. It was applied to the fourth prototype (type X-LL) with various solvent systems (*4*) including hexane / water, hexane / methanol, hexane / ethyl acetate / methanol / water (1:1:1:1, v/v), ethyl acetate / water, ethyl acetate / acetic acid / water (4:1:5, v/v), chloroform / water, chloroform / acetic acid / water (2:2:1, v/v), n-butanol / water, n-butanol / acetic acid / water (4:1:5, v/v) and sec-butanol / water. Left-handed coils retained more stationary phase than did right-handed ones. When the mobile phase was lighter, the best settings were P_I-T-I or P_{II}-H-I, while a heavier mobile phase requires P_I-H-O or P_{II}-T-O (*2*).

The optimized settings were the same for the fifth prototype (*5*) of type X-LLL and the polymer based system poly(ethyleneglycol)-8000 4.4% (w/w) / Dextran T500 7.0% (w/w).

The sixth prototype (*6*) has not produced the same precise results. For the three polymer based systems, the best values of stationary phase retention are obtained when the upper mobile phase is pumped in the Inward introduction mode or the lower phase in the Outward mode, whatever the coil position may be. The butanol-based system depends on the same settings with the L-position. However, the X-1.5L position requires P_I-T-I with a lighter mobile phase and P_{II}-T-O with a heavier one (*1*). For this prototype, the graphical method did not provide precise settings, which consequently cannot be considered as optimal.

Experimental Design Methodology

The study applied to the sixth cross-axis prototype can be restated using the classical Experimental Design layout. As each factor was fixed at two levels, the most convenient design is a factorial design. A mechanical constraint did not permit all the possible combinations of the levels of the seven factors studied. We were unable to rearrange the data in a complete factorial design and were thus obliged to chose a fractional factorial design.

Factors and Domain. Each of the seven factors is identified by a number, and can have a level +1 or −1 as allocated in Table I.

Table I. Experimental Domain

	Factor number	Level -	Level +
Coiling up	1	Right-handed	Left-handed
Mobile phase	2	Upper	Lower
Introduction mode	3	Inward	Outward
Planetary motion direction	4	P_{II}	P_I
Coil position	5	L	X-1.5 L
Helical coil diameter	6	5.5 cm	10 cm
Elution mode	7	Tail-to-Head (T)	Head-to-Tail (H)

Response. The response is the percentage of stationary phase retained in the chromatographic column at hydrodynamic equilibrium.

Solvents studied. The four solvent systems previously described were studied. One contained butanol and water, while the other three were composed of one or two aqueous polymer phases.

Downloaded by OHIO STATE UNIV LIBRARIES on June 29, 2012 | http://pubs.acs.org
Publication Date: May 15, 1995 | doi: 10.1021/bk-1995-0593.ch004

Solvent A: n-butanol / 0.13M $NaCl_{aq}$ (1:1, v/v) + 1.5% (w/v) of hexadecylpyridinium chloride (HPC).
Solvent B: poly(ethyleneglycol)-1000 / $K_2HPO_{4\ aq}$
Solvent C: poly(ethyleneglycol)-8000 4.4% (w/w) / Dextran T500 7.0% (w/w).
Solvent D: poly(ethyleneglycol)-8000 4.0% (w/w) / Dextran T500 5.0% (w/w).

Experimental Design. The trials are shown in the experimental matrix (Table II). While a complete factorial design with seven factors at two levels contains 128 trials, a mechanical constraint in the system prevented all possible combinations being run and only 64 trials were performed. The elution mode (factor 7) can be determined from the coiling up (factor **1**), the planetary motion (factor **4**) and the introduction mode (factor **3**). There is thus a relationship between these four factors. Factor **7** is aliased with interaction **134** (notation for the interaction between factors **1**, **3** and **4**) and the experimental design has an alias generator: **I** = **1347**. Readers interested in Experimental Design Methodology will find a detailed explanation of "alias" and "alias generator" in (*3*). Stated simply, "alias" means that two or more effects are grouped and that it is mathematically impossible to obtain each of them separately. Two or more effects are associated in an "alias". With knowledge of Experimental Design Theory it is possible to known how effects are merged and with a good understanding of the phenomenon, experimenters can correctly interpret the results. "Alias" is the price paid for reducing the number of experiments.

Calculation of Effects and Interactions by Experimental Design Method. These calculations were performed using specific software based on an algorithm described in (*3*) and (*7*). The results are shown in Table III. The numbers indicated in the cells are the values obtained from the calculations. All the results are not shown in Table III. The higher the value, the greater the effect. We have just indicated the most significant effects. As there was a mechanical constraint aliasing **7** with interaction **134**, it is impossible to completely separate the effects of a given factor or interaction from ancillary interactions. For instance, the effect of the choice of mobile phase (factor **2**) cannot be separated from the effect of interaction **12347**, hence the notation **2+12347**.

Overall Interpretation

Five points are immediately clear:

1. The four solvents behave differently:
    - The composition of solvent D is unstable and could be reduced to one phase by slight changing of temperature. The retention was very low in all the trials and there are no good settings.
    - Solvents A and B behave similarly.
    - The behavior of solvent C is different from solvents A and B, we have therefore analyzed each solvent separately.
2. Interaction **23** is very high for all four solvents:

   This interaction is positive, so factors **2** and **3** must be set at the same levels:
    - Introduction mode "Inward" (factor **3** at level –) for the upper mobile phase (factor **2** at level –)
    - Introduction mode "Outward" (factor **3** at level +) for the lower mobile phase (factor **2** at level +)

Downloaded by OHIO STATE UNIV LIBRARIES on June 29, 2012 | http://pubs.acs.org
Publication Date: May 15, 1995 | doi: 10.1021/bk-1995-0593.ch004

Table II. Results presented as 2^{7-1} experimental design with 7=134

Trial n°	Factor n°							Solvent System			
	1	2	3	4	5	6	7= 134	A	B	C	D
	level							stationary phase retention (%)			
1	–	–	–	–	–	–	–	74.2	55.6	43.4	3.6
2	+	–	–	–	–	–	+	63.3	40.9	42.3	8.8
3	–	+	–	–	–	–	–	3.0	3.0	0	0
4	+	+	–	–	–	–	+	1.9	3.7	1.9	0
5	–	–	+	–	–	–	+	0	2.0	9.3	0
6	+	–	+	–	–	–	–	0	0	0	0
7	–	+	+	–	–	–	+	74.2	62.1	8.0	1.0
8	+	+	+	–	–	–	–	72.6	52.1	0	0
9	–	–	–	+	–	–	+	74.7	53.0	46.0	0
10	+	–	–	+	–	–	–	72.6	52.1	40.0	9.3
11	–	+	–	+	–	–	+	1.5	1.5	0	0
12	+	+	–	+	–	–	–	4.2	7.4	0	0
13	–	–	+	+	–	–	–	0	0	0	0
14	+	–	+	+	–	–	+	6.0	0	10.0	0
15	–	+	+	+	–	–	–	75.8	61.1	0	1.9
16	+	+	+	+	–	–	+	72.1	55.8	0	6.8
17	–	–	–	–	+	–	–	74.7	43.9	32.3	0
18	+	–	–	–	+	–	+	45.7	38.1	32.6	6.5
19	–	+	–	–	+	–	–	2.0	0	0	0
20	+	+	–	–	+	–	+	27.0	12.1	0	0.5
21	–	–	+	–	+	–	+	28.0	0	14.1	0
22	+	–	+	–	+	–	–	0	0	11.6	0
23	–	+	+	–	+	–	+	55.0	44.4	8.0	2.0
24	+	+	+	–	+	–	–	28.5	35.3	2.8	4.7
25	–	–	–	+	+	–	+	48.9	46.0	44.4	0
26	+	–	–	+	+	–	–	85.0	63.3	35.3	2.8
27	–	+	–	+	+	–	+	40.0	7.1	0	0
28	+	+	–	+	+	–	–	0	1.9	0	0
29	–	–	+	+	+	–	–	0	0	0	0
30	+	–	+	+	+	–	+	29.5	4.7	20.0	0
31	–	+	+	+	+	–	–	5.0	33.3	0	0
32	+	+	+	+	+	–	+	60.8	53.0	6.0	0.9

–	right	up	I	P2	L	5.5	T
+	left	low	O	P1	X-15L	10	H

Continued on next page

Downloaded by OHIO STATE UNIV LIBRARIES on June 29, 2012 | http://pubs.acs.org
Publication Date: May 15, 1995 | doi: 10.1021/bk-1995-0593.ch004

Table II (Continued). Results presented as 2^{7-1} experimental design with 7=134

Trial n°	Factor n°							Solvent System			
	1	2	3	4	5	6	7= 134	A	B	C	D
	level							stationary phase retention (%)			
33	–	–	–	–	–	+	–	53.7	40.0	35.1	0
34	+	–	–	–	–	+	+	56.1	29.8	34.1	0
35	–	+	–	–	–	+	–	13.2	6.1	0	0
36	+	+	–	–	–	+	+	3.7	7.3	0	0
37	–	–	+	–	–	+	+	13.9	4.9	12.2	0
38	+	–	+	–	–	+	–	0	2.4	20.7	0
39	–	+	+	–	–	+	+	48.3	39.0	0	0
40	+	+	+	–	–	+	–	59.8	38.3	0	0
41	–	–	–	+	–	+	+	50.0	35.6	29.8	0
42	+	–	–	+	–	+	–	61.0	45.4	37.1	0
43	–	+	–	+	–	+	+	7.3	9.8	0.7	0
44	+	+	–	+	–	+	–	9.0	8.5	0	0
45	–	–	+	+	–	+	–	6.3	11.7	21.5	0
46	+	–	+	+	–	+	+	7.8	0	14.6	0
47	–	+	+	+	–	+	–	48.8	36.6	1.5	0
48	+	+	+	+	–	+	+	61.0	46.8	0	0
49	–	–	–	–	+	+	–	57.1	21.5	20.5	0
50	+	–	–	–	+	+	+	40.2	4.9	8.5	0
51	–	+	–	–	+	+	–	3.7	3.9	0	0
52	+	+	–	–	+	+	+	20.7	8.8	0	0
53	–	–	+	–	+	+	+	26.8	14.1	2.4	0
54	+	–	+	–	+	+	–	0	0	14.1	0
55	–	+	+	–	+	+	+	46.8	41.5	3.4	0
56	+	+	+	–	+	+	–	30.5	3.4	0	0
57	–	–	–	+	+	+	+	37.1	12.2	30.2	0
58	+	–	–	+	+	+	–	81.7	37.3	34.1	0
59	–	+	–	+	+	+	+	44.9	28.3	0	0
60	+	+	–	+	+	+	–	2.4	0	0	0
61	–	–	+	+	+	+	–	4.9	11.7	19.8	0
62	+	–	+	+	+	+	+	18.3	0	9.8	0
63	–	+	+	+	+	+	–	6.3	19.5	0	0
64	+	+	+	+	+	+	+	60.5	31.2	0	0

–	right	up	I	P2	L	5.5	T
+	left	low	O	P1	X-15L	10	H

Downloaded by OHIO STATE UNIV LIBRARIES on June 29, 2012 | http://pubs.acs.org
Publication Date: May 15, 1995 | doi: 10.1021/bk-1995-0593.ch004

Downloaded by OHIO STATE UNIV LIBRARIES on June 29, 2012 | http://pubs.acs.org
Publication Date: May 15, 1995 | doi: 10.1021/bk-1995-0593.ch004

Table III. Table of effects

	Solvent Systems			
	A	B	C	D
I + 1347	33	22.4	11.8	0.76
1 + 347				
2 + 12347	-2		-10.8	
3 + 147	-3.3		-5.3	
4 + 137				
5 + 13457		-3		
6 + 13467	-2.3	-3.6		-0.76
7 + 134	3.7			
12 + 2347				
13 + 47				
14 + 37	4.8	2.3		
15 + 3457				
16 + 3467				
17 + 34				
23 + 1247	22.7	17.4	6.1	0.75
24 + 1237				
25 + 123457				
26+123467				
27 + 1234	4.5	3.8		
35 + 1457	-3.2			
36+1467				
45 + 1357				
46+1367				
56+134567				
57 + 1345	4.1			
67+1346			-2.1	
123 + 247	2.9			
124 + 237	-3.5			
125 + 23457				
126+23467				
127 + 234				
135 + 457				
136 + 467				
145 + 357	3.1			
146 + 367				
156 + 34567				
157 + 345				
167 + 346				
235 + 12457	-6.6	-3.7		
236 + 12467	-3.5	-5.9	-2.4	-0.74
245 + 12357				
246 + 12367				
256+ 1234567				
257 + 12345	5.1	2.1		
267 + 12346				
356 + 14567				
456 + 13567				
567 + 13456				
1235 + 2457				
1236 + 2467	2.1			
1245 + 2357	-2.7			
1246 + 2367				
1256 + 234567				
1257 + 2345				
1267 + 2346				
1356 + 4567				
1456 + 3567				
1567 + 3456				
2356 + 124567	2.3			
2456 + 123567				
2567 + 123456				
12356 + 24567				
12456 + 23567				
12567 + 23456				

Downloaded by OHIO STATE UNIV LIBRARIES on June 29, 2012 | http://pubs.acs.org
Publication Date: May 15, 1995 | doi: 10.1021/bk-1995-0593.ch004

Figure 2 shows an example of interaction 23 for the solvent A. The first eight trials in Table II can be presented in a two-dimensional diagram with factor **2** and factor **3**. It is clear from this diagram that these two factors act together on the retention and that only two combinations are interesting.

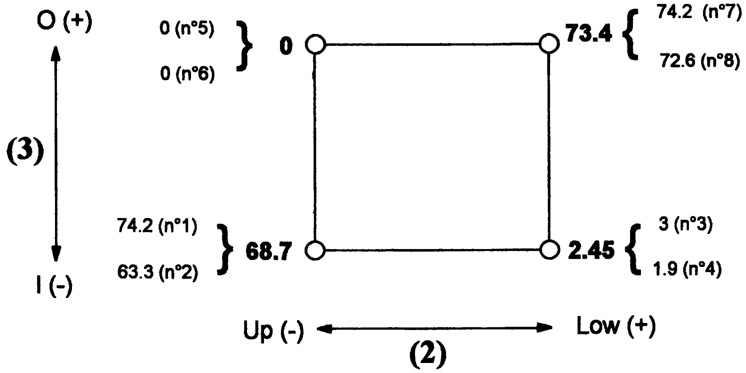

Figure 2: diagram showing the interaction 23 between the density of the mobile phase and the introduction mode for the solvent A.

3. The main factors have little or no direct influence. They act through interactions. This means that they work together and that we were obliged to take into account the combinations of two, three, four or more factors.
4. Some interactions are large, larger than the main factors: interactions **23**, **27**, **37**, **57**, **235** and **237** are larger than the effects of the main factors. The interpretation must take this into account.
5. Confusion between factor **1**, **3**, **4** and **7** lead to contrasts which cannot be interpreted:
   - **3 = 147** We cannot say whether –3.3 (for solvent A) and –5.3 (for solvent C) is due to factor **3** or to interaction **147**.
   - **7 = 134** We cannot say whether +3.7 (for solvent A) is due to factor **7** or to interaction **134**.
   - **14 = 37** We cannot say whether +4.8 (for solvent A) and +2.3 (for solvent B) is due to interaction **14** or to interaction **37**.

Interpretation by Solvent. The main factor **1** (right-handed or left-handed coil) and main factor **4** (rotation P_I or P_{II}) have no influence. Five factors can explain the results. The 64 trials can be used to construct a duplicated 2^5 design. The retention is greater for the small coil diameter and this small coil must be used for the best retention: Factor **6** at level "–".This factor introduces no important interaction. Factors **2**, **3**, **5** and 7 have been studied and particularly their interactions **23**, **27**, **35**, **37**, **57**, **235**, **237** and **257** (Tables IV, V and VI). This Table contains the 64 results as a duplicated 2^4 design for each diameter. This technique, named collapsing, or reconstructing an experimental design by leaving out one or more factors is not always accepted by some theoretical statisticians but when it is used with care it is of great use to the

Downloaded by OHIO STATE UNIV LIBRARIES on June 29, 2012 | http://pubs.acs.org
Publication Date: May 15, 1995 | doi: 10.1021/bk-1995-0593.ch004

experimenter. It can be used to detect experimental mistakes, and to be sure that a factor is of little influence.

The illustrations show the five factors **2**, **3**, **5**, **6** and **7**.

Solvent A. Table IV contains the 64 results as a duplicated 2^4 design for each coil diameter.

Table IV. Rearranged design with four influencing factors. Solvent A

Ordinal	Trial number				Factors				Responses			
number	Ø 5.5 (cm)		Ø 10 (cm)		2	3	5	7	Ø 5.5 (cm)		Ø 10 (cm)	
1	1	10	33	42	–	–	–	–	74	73	54	61
2	3	12	35	44	+	–	–	–	3	4	13	9
3	6	13	38	45	–	+	–	–	0	0	0	6
4	8	15	40	47	+	+	–	–	73	76	60	49
5	17	26	49	58	–	–	+	–	75	85	57	82
6	19	28	51	60	+	–	+	–	2	0	4	2
7	22	29	54	61	–	+	+	–	0	0	0	5
8	24	31	56	63	+	+	+	–	28	5	30	6
9	2	9	34	41	–	–	–	+	63	75	56	50
10	4	11	36	43	+	–	–	+	2	1	4	7
11	5	14	37	46	–	+	–	+	0	6	14	8
12	7	16	39	48	+	+	–	+	74	72	48	61
13	18	25	50	57	–	–	+	+	46	49	40	37
14	20	27	52	59	+	–	+	+	27	40	21	45
15	21	30	53	62	–	+	+	+	28	29	27	18
16	23	32	55	64	+	+	+	+	55	61	47	60

Figure 3 provides a more complete analysis of the results. When the mobile phase is lighter (upper), the "Inward" introduction mode must be used, with the "X–1.5 L" coil position combined with the "Tail-to-Head" elution mode:

$$2^- \; 3^- \; 5^+ \; 7^-$$

For a heavier (lower) mobile phase, the "Outward" introduction mode must be used with the "L" coil position, but the elution mode (factor 7) has no influence:

$$2^- \; 3^- \; 5^-$$

Solvent B. Table V contains the 64 results as a duplicated 2^4 design for each coil diameter. Under the same experimental conditions, the high retention values are generally smaller for solvent B than for solvent A, while the low retention values are often greater for B than for A. Optimization of the retention depends on the density of the mobile phase. Figure 4 shows that the "Inward" introduction mode must be used with a "Tail-to-Head" elution mode when using an upper mobile phase, but that the coil position may be "X–1.5 L" or "L":

Downloaded by OHIO STATE UNIV LIBRARIES on June 29, 2012 | http://pubs.acs.org
Publication Date: May 15, 1995 | doi: 10.1021/bk-1995-0593.ch004

$$2^- \; 3^- \; 7^-$$

The "Outward" introduction mode must be used for the lower mobile phase, with the "L" coil position. The elution mode is not influential:

$$2^- \; 3^+ \; 5^-$$

Table V. Rearranged design with four influencing factors. Solvent B

Ordinal	Trial number				Factors				Responses			
number	Ø 5.5 (cm)		Ø 10 (cm)		2	3	5	7	Ø 5.5 (cm)		Ø 10 (cm)	
1	1	10	33	42	–	–	–	–	56	52	40	45
2	3	12	35	44	+	–	–	–	3	7	6	8
3	6	13	38	45	–	+	–	–	0	0	2	12
4	8	15	40	47	+	+	–	–	52	61	38	37
5	17	26	49	58	–	–	+	–	44	63	21	37
6	19	28	51	60	+	–	+	–	0	2	4	0
7	22	29	54	61	–	+	+	–	0	0	0	12
8	24	31	56	63	+	+	+	–	35	33	3	20
9	2	9	34	41	–	–	–	+	41	53	30	36
10	4	11	36	43	+	–	–	+	4	2	7	10
11	5	14	37	46	–	+	–	+	2	0	5	0
12	7	16	39	48	+	+	–	+	62	56	39	47
13	18	25	50	57	–	–	+	+	38	46	5	12
14	20	27	52	59	+	–	+	+	12	7	9	28
15	21	30	53	62	–	+	+	+	0	5	14	0
16	23	32	55	64	+	+	+	+	44	53	41	31

Solvent C. Table VI contains the 64 results as a duplicated 2^4 design for each coil diameter. The coil diameter has no significant influence as shown in Figure 5.

The "Inward" introduction mode must be used plus the L coil position when the mobile phase is the upper one. The elution mode can be "Tail-to-Head" or "Head-to-Tail" for the small coil diameter:

$$2^- \; 3^- \; 5^-$$

There are no good settings with this solvent for the lower mobile phase.

Our analysis shows that factors **1** (left- or right-handed coil) and **4** (planetary motion direction) need not be considered, because they are not influential and they are not involved in significant interactions. Factor **6** must be fixed at level "–" because the retention is greater with a small coil diameter. Table VII indicates the final optimized settings in a condensed form.

Comparison of the two interpretation methods

The advantage of using experimental design can be appreciated by comparing the data analysis with that obtained using the graphical method. We used the best settings determined from the experiments carried out on the fourth cross-axis prototype

Downloaded by OHIO STATE UNIV LIBRARIES on June 29, 2012 | http://pubs.acs.org
Publication Date: May 15, 1995 | doi: 10.1021/bk-1995-0593.ch004

Table VI. Rearranged design with four influencing factors. Solvent C

Ordinal	Trial number				Factors				Responses			
number	Ø 5.5 (cm)		Ø 10 (cm)		2	3	5	7	Ø 5.5 (cm)		Ø 10 (cm)	
1	1	10	33	42	−	−	−	−	43	40	35	37
2	3	12	35	44	+	−	−	−	0	0	0	0
3	6	13	38	45	−	+	−	−	0	0	21	21
4	8	15	40	47	+	+	−	−	0	0	0	1
5	17	26	49	58	−	−	+	−	32	35	21	34
6	19	28	51	60	+	−	+	−	0	0	0	0
7	22	29	54	61	−	+	+	−	12	0	14	20
8	24	31	56	63	+	+	+	−	3	0	0	0
9	2	9	34	41	−	−	−	+	42	46	34	30
10	4	11	36	43	+	−	−	+	2	0	0	1
11	5	14	37	46	−	+	−	+	9	10	12	15
12	7	16	39	48	+	+	−	+	8	0	0	0
13	18	25	50	57	−	−	+	+	33	44	8	30
14	20	27	52	59	+	−	+	+	0	0	0	0
15	21	30	53	62	−	+	+	+	14	20	2	10
16	23	32	55	64	+	+	+	+	8	6	3	0

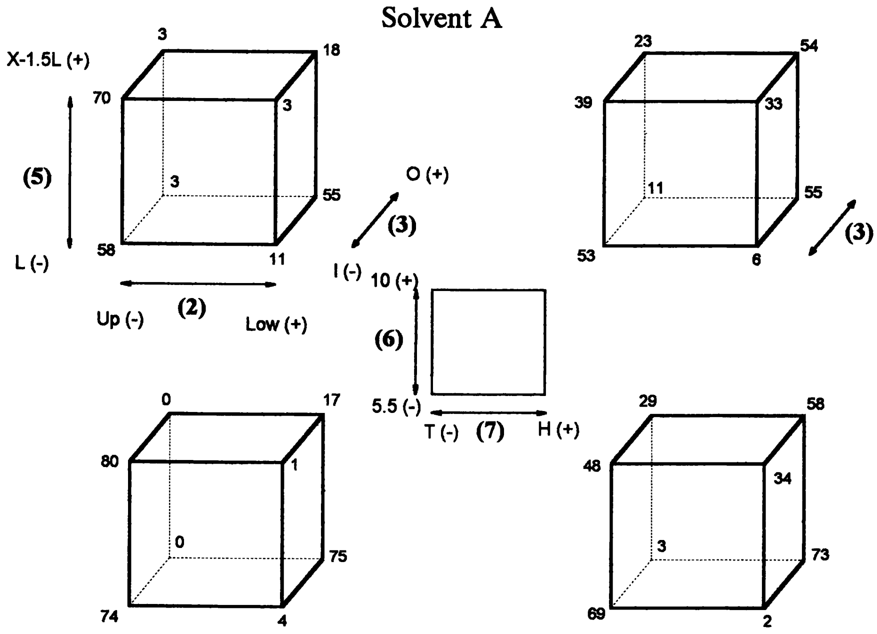
Solvent A
X-1.5L (+)
(5)
L (-)
3
18
70
3
3
55
58
11
Up (-)
(2)
Low (+)
O (+)
(3)
I (-)
10 (+)
(6)
5.5 (-)
T (-)
(7)
H (+)
23
54
39
33
11
55
53
6
(3)
0
17
80
1
0
75
74
4
29
58
48
34
3
73
69
2

Figure 3: Results for solvent A presented in a five dimension-space diagram.

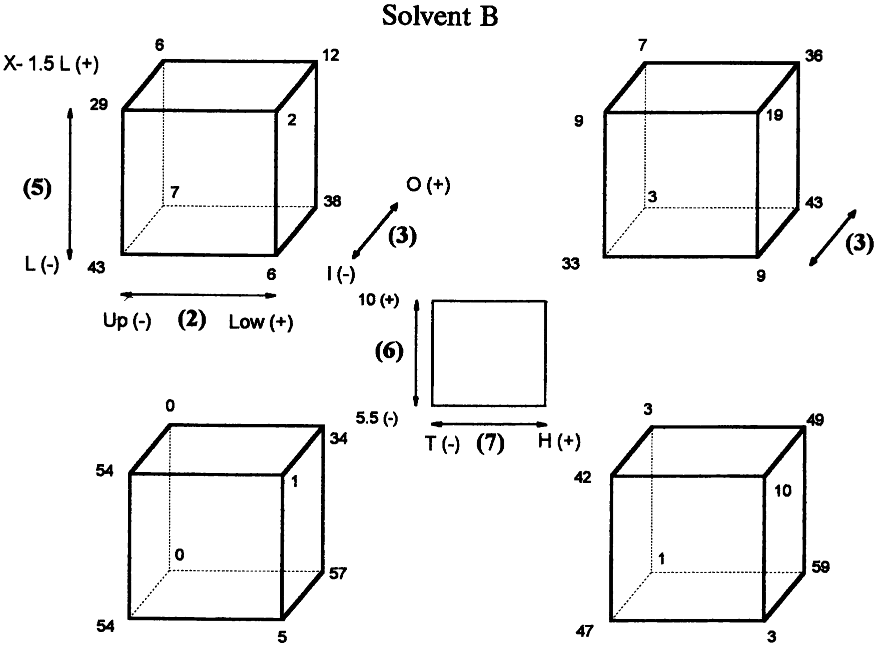
Solvent B
X- 1.5 L (+)
(5)
L (-)
6
12
29
2
7
38
43
6
Up (-)
(2)
Low (+)
O (+)
(3)
I (-)
10 (+)
(6)
5.5 (-)
T (-)
(7)
H (+)
7
36
9
19
3
43
33
9
(3)
0
34
54
1
0
57
54
5
3
49
42
10
1
59
47
3

Figure 4: Results for solvent B presented in a five dimension-space diagram.

Downloaded by OHIO STATE UNIV LIBRARIES on June 29, 2012 | http://pubs.acs.org
Publication Date: May 15, 1995 | doi: 10.1021/bk-1995-0593.ch004

Downloaded by OHIO STATE UNIV LIBRARIES on June 29, 2012 | http://pubs.acs.org
Publication Date: May 15, 1995 | doi: 10.1021/bk-1995-0593.ch004

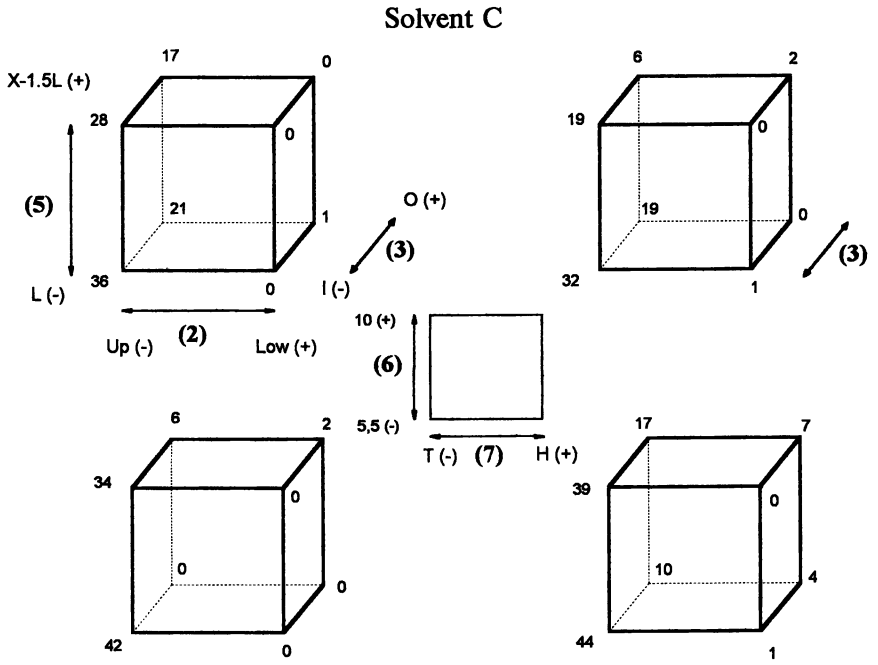
Solvent C
X-1.5L (+)
(5)
L (-)
17
0
28
0
21
1
36
0
Up (-)
(2)
Low (+)
O (+)
(3)
I (-)
10 (+)
(6)
5,5 (-)
T (-)
(7)
H (+)
6
2
19
0
19
0
32
1
(3)
6
2
34
0
0
0
42
0
17
7
39
0
10
4
44
1

Figure 5: Results for solvent C presented in a five dimension-space diagram

Table VII. Best settings for each solvent using experimental design methodology

Mobile Phase	Solvent A	Solvent B	Solvent C
Upper phase 2^-	3^- 5^+ 6^- 7^-	3^- 7^- 6^-	3^- 5^- 6^-
Lower phase 2^+	3^+ 5^- 6^-	3^+ 5^- 6^-	6^-

Downloaded by OHIO STATE UNIV LIBRARIES on June 29, 2012 | http://pubs.acs.org
Publication Date: May 15, 1995 | doi: 10.1021/bk-1995-0593.ch004

(*4*). Factor **6** does not intervene as only one diameter was available on the fourth prototype. The best settings are, for a upper mobile phase ($\mathbf{2^-}$), $\mathbf{1^+}$ $\mathbf{3^-}$ $\mathbf{4^-}$ $\mathbf{7^+}$ or $\mathbf{1^+}$ $\mathbf{3^-}$ $\mathbf{4^+}$ $\mathbf{7^-}$, and for a heavier mobile phase ($\mathbf{2^+}$), $\mathbf{1^+}$ $\mathbf{3^+}$ $\mathbf{4^-}$ $\mathbf{7^-}$ or $\mathbf{1^+}$ $\mathbf{3^+}$ $\mathbf{4^+}$ $\mathbf{7^+}$.

To make a comparison, we set factor **6** at level "-" for both methods, using solvent A. All the results are gathered in Table VIII.

Table VIII. Comparison of the two interpretation methods

Method	Factors							Trial n°	Response
	1	**2**	**3**	**4**	**5**	**6**	**7**		
	level								(%)
Graphical	+	-	-	-	-/+	-	+	2, 18	63.3, 45.7
	+	-	-	+	-/+	-	-	10, 26	72.6, 85.0
	+	+	+	-	-/+	-	-	8, 24	72.6, 28.5
	+	+	+	+	-/+	-	+	16, 32	72.1, 60.8
Experimental design	-/+	-	-	-/+	+	-	-	17, 26	74.7, 85.0
	-/+	+	+	-/+	-	-	-/+	7, 16, 15, 8	74.2, 72.1, 75.8, 72.6

When factors have no influence, their two possible levels are indicated by -/+. For the graphical method, factor **5** can have the "-" or the "+" levels, hence two trial numbers for each line. The two lines for the experimental design method lead to only one half of the predicted number of corresponding trials as factor 7 is aliased with interaction **134**: **7=134**.

The results displayed in Table VIII show that experimental design method makes it possible to find many of the best retentions of stationary phase, all above 74%. In contrast, the graphical method provides some of the best results, but also low values (*e.g.*, 28.5%).

Conclusion

Interpretation was difficult because the interactions were greater than the effects of the main factors. This is very unusual, but seems to be more frequent in cross-axis chromatography.

The best settings depend on the density of the mobile phase. The optimized settings for an upper mobile phase are an "Inward" introduction mode, a "Tail-to-Head" elution mode and a coil in the "L" position for solvents A and B. The coil needs to be in the "X–1.5 L" position for solvent C. For a lower mobile phase (for solvents A and B), the best settings are an "Outward" introduction mode and a coil in "L" position. No good settings have been found for solvent C.

Experimental design gives simple choices which are always the best settings, because it takes into account all the interactions. In the present experiment, it is impossible to interpret the results correctly if the interactions are ignored.

References

(*1*) MENET J.-M., SHINOMYIA K. and ITO Y. *J. Chromatogr.* **644** (1993) 239-252.
(*2*) ITO Y. *J. Chromatogr.* **538** (1991) 67-80.
(*3*) GOUPY J. *Methods for Experimental Design. Principles and Applications for Physicists and Chemists.* Elsevier. Amsterdam. (1993).
(*4*) ITO Y., KITAZUME E., BHATNAGAR M. and TRIMBLE F. D. *J. Chromatogr.* **538** (1991) 59-66.
(*5*) SHIBUSAWA Y. and ITO Y., *J. Liq. Chromatogr.* 15 (1992) 2787-2800.
(*6*) SHINOMYIA K., MENET J.-M. and ITO Y. *J. Chromatogr.* **644** (1993) 215-229.
(*7*) GOUPY J. *La Méthode des Plans d'Expériences.* Dunod. Paris. (1988).

RECEIVED December 22, 1994

Downloaded by OHIO STATE UNIV LIBRARIES on June 29, 2012 | http://pubs.acs.org
Publication Date: May 15, 1995 | doi: 10.1021/bk-1995-0593.ch004

Downloaded by CORNELL UNIV on June 28, 2012 | http://pubs.acs.org
Publication Date: May 15, 1995 | doi: 10.1021/bk-1995-0593.ch005

Chapter 5

Model Based on Stokes' Law as a Simple Way To Describe the Flow Pattern of the Mobile Phase in Centrifugal Partition Chromatography

A. P. Foucault, E. Camacho Frias, C. G. Bordier, and F. Le Goffic

Laboratoire de Bioorganique et Biotechnologies, ERS 71, Centre National de la Recherche Scientifique 16, Rue Pierre et Marie Curie, 75005 Paris, France

Stokes' law for small liquid droplets flowing like rigid spheres in a liquid continuous phase was used as a very simple model to describe the hydrodynamics of the flow in the channels of a centrifugal partition chromatographic column. We experimentally showed that the linear velocity of the mobile phase in the channels is not dependent upon both the flow rate and the centrifugal field, in the range ordinarily used by the chromatographer (1-10 ml/min, 700-2000 rpm). The simple model based on Stokes' law and these two experimental results lead to the conclusion that there is a linear relationship between the efficiency and the square root of "g", the centrifugal field, which is experimentally verified.

We reported recently *(1)* that the ratio of the mobile phase volume to that of the column volume was a very important parameter, acting strongly on the efficiency in all kinds of countercurrent chromatography. We also studied the dependence of the stability of the stationary phase for various biphasic systems upon their physical parameters *(2)* and we demonstrated the main influence of $\frac{\gamma}{\Delta\rho}$, where γ is the interfacial tension between the two phases, and $\Delta\rho$ their density difference.

A very simple model, which treats the mobile phase as droplets with a radius, "a", flowing in the stationary phase, seems to be compatible with all our results. Furthermore, it allows the prediction of the variation of the efficiency with the centrifugal field, which is experimentally verified.

Experimental

Apparatus. A high performance centrifugal partition chromatograph (HPCPC) (Sanki Laboratories, Kyoto, Japan) was used *(3)*. It is a bench top CPC (30 x 45 x 45 cm, ≈ 60 Kg); the column is a stacked circular partition disk rotor which contains 2136 channels with a total internal volume of 240 ml. The column is connected to the injector and the detector through two high pressure rotary seals containing a drilled sapphire rod passing through two toroidal seals similar to those used with HPLC pump pistons. The partition disks are engraved with 1.5 x 0.28 x 0.21 cm channels

0097–6156/95/0593–0062$12.00/0

In Modern Countercurrent Chromatography; Conway, W., et al.;
ACS Symposium Series; American Chemical Society: Washington, DC, 1995.

connected in series by 1.5 x 0.1 x 0.1 cm ducts. A 4-port valve included in the Series 1000 allows the HPCPC to be operated in either the descending or ascending mode. The HPCPC was connected to an HPLC System Gold (Beckman, San Ramon, CA, USA), including a solvent delivery pump Model 126, a diode array detector Model 168 with a semi-prep scale flow cell, and a manual sample injector. Approximately one meter of a 1/16" steel tubing, immersed in a warm water bath (≈40°C), was connected between the outlet of the HPCPC and the inlet of the detector, acting as a noise suppressor. Some experiments were performed with a CPC model LLN (Sanki Laboratories, Kyoto, Japan), previously described *(4)*.

Chemicals. The following solvents came from Prolabo (Paris, France) : dimethylsulfoxide, tetrahydrofuran, n-butanol, chloroform, methanol, n-propanol, heptane, acetone. The sec-butanol, methyl isobutyl ketone, and n-octanol came from Aldrich (Milwaukee, Wisconsin, USA). Water was de-ionized.

Procedure. Stability of the biphasic systems was estimated by varying the flow rate from 0 to 10 ml/min, or less if the backpressure in the HPCPC was reaching 6 MPa (≈0.86 kPSI), and measuring the volume occupied by the mobile phase at the equilibrium, noted V_m; the rotational speed was generally 1000 or 1200 rpm, and some experiments were performed at different rotational speeds, to evaluate the influence of this parameter upon the stability of the stationary phase. All the systems were evaluated in ascending and descending mode except the system octanol / water, for which the ascending mode was not explored, because our pump was unable to pump octanol at high flow rates. The experiment related to the efficiency was performed with 4-hydroxybenzoic acid as a marker of the void volume and diethyl phthalate as the analyte, in the descending mode using the heptane / methanol biphasic system.

Results and Discussion

As already stated *(2)*, the mobile phase will be envisioned as droplets with an average radius, "a", flowing in the stationary phase at a constant linear velocity, "ū", given by the Stokes law :

$$\bar{u} = \frac{2\,a^2\,\Delta\rho\ g}{9\,\eta_{SP}} \qquad [1]$$

where $g = \omega^2 R$, R being the average radius of the HPCPC centrifuge, and ω the rotational speed, $\Delta\rho$ the density difference between the two phases and η_{SP} the viscosity of the stationary phase.

$\Delta\rho$ and η_{SP} depend on the biphasic system, while "a" is dependent upon both the biphasic system and the apparatus; particularly important is the shape of the part of the channel where the continuous mobile phase coming from the ducts breaks into a discontinuous phase (if it does) flowing into the stationary phase in the channels.

With our model, we can easily obtain a relationship between the volume of the mobile phase which is in the column at steady state equilibrium, and the flow rate, F. Figure 1 is a schematic of the situation in a channel in a steady state equilibrium, when there is no accumulation of mobile phase in the channel *(1)*. During the elapsed time dt, an elementary volume of mobile phase, $dV_m = F\,dt$, is introduced at the inlet of the channel. The same volume, $dV_m = F\,dt$, is leaving the channel through the outlet. Also

Downloaded by CORNELL UNIV on June 28, 2012 | http://pubs.acs.org
Publication Date: May 15, 1995 | doi: 10.1021/bk-1995-0593.ch005

the same volume, $d\mathcal{V}_m = F\ dt$, goes through the elementary volume of the channel, $d\mathcal{V}_c = S\ dh = S\ \bar{u}\ dt$, $\bar{u}\ dt$ being the distance covered by a droplet during the elapsed time dt, and S the cross sectional area of the channel. The ratio of the volume of mobile phase, $\mathcal{V}_m$, to the volume of all the channels, $\mathcal{V}_c$, (excluding the ducts, which are filled with mobile phase only), is then :

$$\frac{\mathcal{V}_m}{\mathcal{V}_c} = \frac{1}{\bar{u}}\ \frac{F}{S} \qquad [2]$$

Adding the volume of the ducts, filled with mobile phase only ($V_{ducts} = d\ .\ V_c$, so that $\mathcal{V}_m = V_m - d\ .\ V_c$, and $\mathcal{V}_c = V_c\ (1-d)$), equation 2 becomes :

$$\frac{V_m}{V_c} = \frac{(1-d)}{\bar{u}}\ \frac{F}{S} + d \qquad [3]$$

"d" is the ratio of the volume of the column occupied by the ducts and connections with respect of the volume of the column; it includes the limit boundaries where the continuous mobile phase coming from the ducts breaks into droplets, and the boundaries where the inverse phenomenon occurs.

A first important experimental result gives to equation 3 a great potential; there is a linear relationship between the volume we can get at a given flow rate and that flow rate. This has been verified for twelve solvent systems in both descending and ascending mode using the HPCPC *(2)*. These twelve systems represent a wide range of physical and chemical properties (see Table I for abbreviations and physical data). EtOAc/Water and $CHCl_3$/Water are not very useful for purification purposes, but they have a large interfacial tension. Oct/Water is used for partition coefficient (hydrophobicity parameter) determination, and its upper phase is rather viscous. HEP/MeOH is widely used as a non polar system. WDT2, 4 and 5 are a new class of medium polarity biphasic systems we introduced recently *(5)*, containing water, dimethylsulfoxide and tetrahydrofuran, and which show very good solvating properties. MIBK/AcO/W and $CHCl_3$/MeOH/PrOH/W are medium polarity systems too, while the three butanol-containing systems are polar systems, widely used for purification of polar compounds, such as peptides. Regression analysis for the twelve systems have been published *(2)*, and Table II gives the calculated values of the linear velocities for the various mobile phases in the channel, in the descending mode, and the diameter of the corresponding Stokes droplets when working at a rotational speed of 1500 rpm (*i.e.* $g \approx 200$ G, with $G = 981$ cm sec^{-2}). The Reynolds number ($Re = \bar{u}\ a\ \rho_{SP} / \eta_{SP}$), calculated with the same conditions, is in the range 1 to 30, which validates the use of the Stokes' law, since if theoretically, with solid spheres, a laminar motion of the continuous phase around the spheres is observed for $Re \leq 1$, this laminar motion persists for a liquid droplet until $Re < 50$, due to the internal flow in the droplet itself. Some minor corrections for the calculation of the linear velocity have been omitted here for clarity, since we want to propose a simple model, and not a full hydrodynamic study.

The slopes of the lines corresponding to equation 3 provide an easy way to estimate the stability of the stationary phase in the CPC column *(2)*. The smaller the slope, the better the stability, since we can increase the flow rate while keeping a lot of stationary phase in the column.

This first result leads to the following significant conclusion : if we adopt the Stokes model to describe the flow pattern, then the linear velocity, ū, of the droplets in

Downloaded by CORNELL UNIV on June 28, 2012 | http://pubs.acs.org
Publication Date: May 15, 1995 | doi: 10.1021/bk-1995-0593.ch005

the channels does not depend upon the flow rate, in the range studied. The same result occurs using the former CPC type LLN, although this system has not been systematically studied *(1)*.

Table I. Abbreviations used in this paper, and physical data of the biphasic systems

Abbreviations	*Solvents and their volume ratio*		
EtOAc/Water	Ethyl acetate Water, 50/50		
$CHCl_3$/Water	Chloroform Water, 50/50		
n-BuOH/Water	n-Butanol Water, 50/50		
sec-BuOH/Water	sec-Butanol Water, 50/50		
HEP/MeOH	Heptane Methanol, 50/50		
Oct/Water	Octanol Water, 50/50		
	Water	Dimethylsulfoxide	Tetrahydrofuran
WDT2 (see ref. 5)	11.7	26.3	62
WDT4	21.5	21.2	57.3
WDT5	24.5	16.2	59.3
BAW	n-Butanol Acetic acid Water, 40/10/50		
MIBK/AcO/W	Methylisobutyl ketone Acetone Water, 25/50/25		
$CHCl_3$/MeOH/PrOH/W	Chloroform Methanol n-Propanol Water, 29/38.7/6.5/25.8		

Physical data of the Biphasic Systems (data from ref. 2)

System[a]	$\Delta\rho$	γ	η cP	
	g/cm³	Dyne/cm	Upper	Lower
EtOAc/Water	0.097	13.2	0.47	1.10
$CHCl_3$/Water	0.478	32.8	0.98	0.55
HEP/MeOH	0.073	1.16	0.41	0.57
WDT2	0.102	0.59	0.72	2.37
WDT4	0.130	2.15	0.62	2.88
WDT5	0.115	1.26	0.72	2.60
MIBK/AcO/W	0.084	0.25	0.70	1.42
$CHCl_3$/MeOH/PrOH/W	0.213	0.42	1.78	0.97
Oct/Water	0.137	8.5[b]	7.10	0.80
n-BuOH/Water	0.144	2.91	3.05	1.33
BAW	0.101	1.21	2.89	1.51
sec-BuOH/Water	0.093	0.53	3.64	2.02

$\Delta\rho$ = density difference; γ = interfacial tension; η = viscosity

(a) The solvent systems are roughly sorted according to the Ito Classification in hydrophobic, intermediate and hydrophilic groups.

(b) from Handbook of Chemistry and Physics

Adapted from ref. 2

Downloaded by CORNELL UNIV on June 28, 2012 | http://pubs.acs.org
Publication Date: May 15, 1995 | doi: 10.1021/bk-1995-0593.ch005

Downloaded by CORNELL UNIV on June 28, 2012 | http://pubs.acs.org
Publication Date: May 15, 1995 | doi: 10.1021/bk-1995-0593.ch005

Table II. Calculated linear velocities, and diameter of the corresponding Stokes' droplets when working at 1500 rpm (descending mode). Data from ref. 2

System	$\bar{u}$	*Stokes' diameter*
(For WDT systems, see ref. 5)	*(cm/sec)*	*μm*
$CHCl_3$/Water	28.8	73
Oct/Water	24.8	342
EtOAc/Water	19.0	92
n-BuOH/Water	13.6	166
WDT5	11.7	86
WDT4	11.9	72
HEP/MeOH	9.6	70
BAW	9.8	160
WDT2	4.9	57
sec-BuOH/Water	5.1	135
MIBK/AcO/W	4.3	57
$CHCl_3$/MeOH/PrOH/W	4.3	57

A second important experimental result is as follows : for a given biphasic system, and at a given flow rate, the volume of the mobile phase in the column is not dependent upon the rotational speed, in the range ordinarily used by the chromatographer ($\omega > 700$ rpm). Two examples are given on Figures 2 and 3, and other data can be found in reference 2.

With our simple model, this means that the linear velocity, $\bar{u}$, is not dependent upon "g", the centrifugal field, with an immediate consequence :

$$a^2 g = A \qquad [4]$$

A being a constant for a specific system and mode; this means that the higher the acceleration field, the smaller will be the radius of the droplets of mobile phase in a channel. Comparing various biphasic systems, A will characterize the dispersion of the mobile phase in the stationary phase, since a smaller value of A means that, for a given acceleration field, the continuous mobile phase coming from the duct will break into many smaller droplets, while a larger value of A means it will break into few larger droplets. "A" may be called the dispersion term; its dimension is $L^3\,T^{-2}$. From equations. 1 and 4, we get :

$$A = \frac{9}{2}\frac{\bar{u}\,\eta_{SP}}{\Delta\rho} \qquad [5]$$

As the dimension of A is the same as that of the ratio $\frac{\gamma}{\Delta\rho}$ (*i.e.* L^3T^{-2}) where γ is the interfacial tension, we can then write the following equation :

In Modern Countercurrent Chromatography; Conway, W., et al.;
ACS Symposium Series; American Chemical Society: Washington, DC, 1995.

Downloaded by CORNELL UNIV on June 28, 2012 | http://pubs.acs.org
Publication Date: May 15, 1995 | doi: 10.1021/bk-1995-0593.ch005

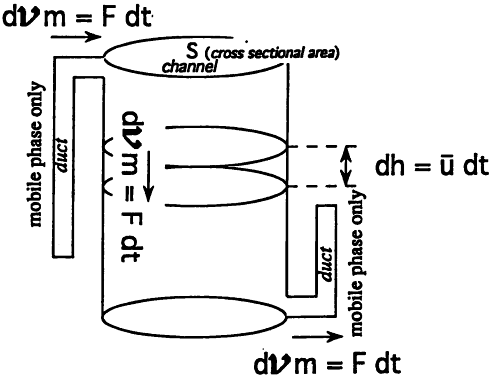
dVm = F dt
S (cross sectional area)
channel
mobile phase only
duct
dVm = F dt
dh = ū dt
duct
mobile phase only
dVm = F dt

Figure 1. Steady state equilibrium in a channel.
(Reproduced with permission from reference 1. Copyright 1992 Marcel Dekker.)

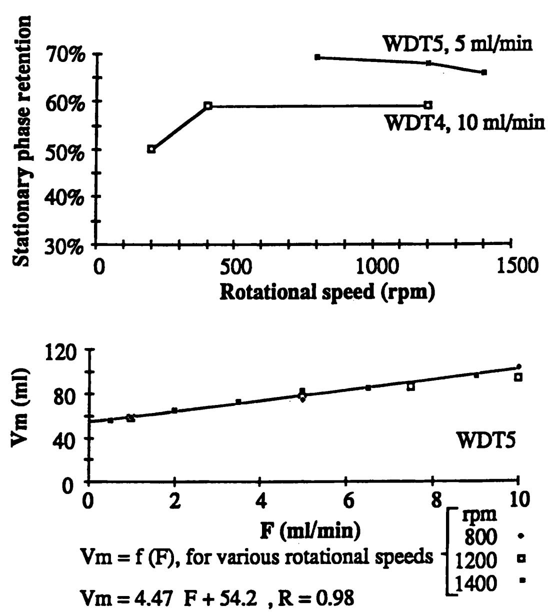

Figure 2. Independance of the stationary phase retention at higher rotational speed. Apparatus : HPCPC (2136 channels), V_C = 240 ml
Biphasic system : WDT 5 : Water / DMSO / THF, 25 / 16 / 59 v/v/v
WDT 4 : Water / DMSO / THF, 22 / 21 / 57 v/v/v
Descending mode, F as figured.

Downloaded by CORNELL UNIV on June 28, 2012 | http://pubs.acs.org
Publication Date: May 15, 1995 | doi: 10.1021/bk-1995-0593.ch005

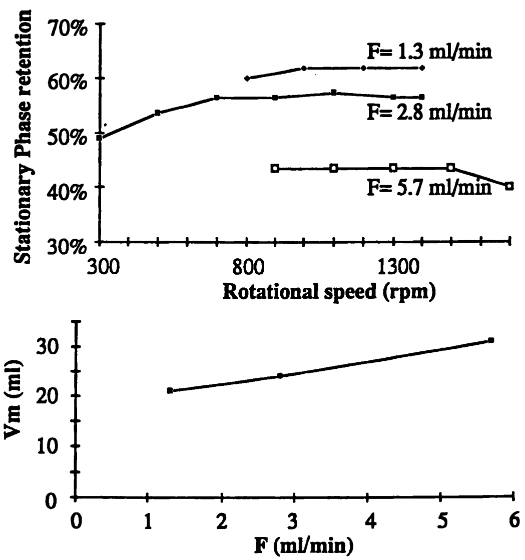

Vm = f(F) , for ω > 800 rpm
Vm = 2.29 F + 17.8 , R = 0.99

Figure 3. Independance of the stationary phase retention at higher rotational speed. Apparatus : CPC-LLN, with 3 cartridges (1200 channels), V_C = 55 ml Biphasic system : $CHCl_3$ / EtOAc / MeOH / Water, 2 / 2 / 3 / 2 v/v/v/v Descending mode, F as figured.

$$A = B\frac{\gamma}{\Delta\rho} \qquad [6]$$

where B is a dimensionless number. From equations 4 and 6 it becomes :

$$B = \frac{a^2\, g\, \Delta\rho}{\gamma} \qquad [7]$$

Equation 7 can be used to compare B to the numerous dimensionless numbers we can find in the literature, and thus find out if it has already been described : B was defined in 1928 by W.N. Bond *et al.* *(6)*, and is called the Bond number *(7)*. It characterizes the relative importance of gravitational (*i.e.* centrifugal) to surface-tension forces, and accounts for the fragility of a droplet. "A droplet of liquid in motion through another liquid differs in its behavior from a solid sphere in that it may (a) be deformed, (b) have a circulation set up within itself by the shearing effect of the relative motion of the two fluids. These effects upset the stability of the drop, causing it to oscillate about the spherical shape and eventually to burst into fragments or, at least, into smaller drops"*(7)*. From equations. 5 and 6 we get :

$$B = \frac{9}{2}\frac{\bar{u}\,\eta_{SP}}{\gamma} \qquad [8]$$

Like A, B is not dependent upon the acceleration field. Table III gives the values of A and B calculated with equations 5 and 8, for the twelve solvent systems, in the descending and ascending modes.

Table III. The dispersion term, A, and the Bond number, B

	Descending mode		*Ascending mode*	
System	A	B	A	B
EtOAc/Water	4.14	0.03	7.28	0.05
CHCl3/Water	2.66	0.04	1.46	0.02
Heptane/MeOH	2.42	0.15	3.18	0.2
WDT4	2.56	0.15	7.15	0.43
WDT2	1.58	0.27	2.9	0.5
WDT5	3.67	0.33	7.62	0.69
MIBK/AcO/W	1.61	0.53	3.27	1.08
n-BuOH/Water	13.54	0.67	4.7	0.23
CHCl3/MeOH/PrOH/W	1.61	0.82	0.88	0.45
Octanol/Water	57.87	0.93	•	•
BAW	12.64	1.06	3.69	0.31
sec-BuOH/Water	9.04	1.57	5.14	0.9

The systems are sorted according to their increasing Bond number in the descending mode. A in $cm^3 sec^{-2}$, B dimensionless
Adapted from ref. 2

Downloaded by CORNELL UNIV on June 28, 2012 | http://pubs.acs.org
Publication Date: May 15, 1995 | doi: 10.1021/bk-1995-0593.ch005

Downloaded by CORNELL UNIV on June 28, 2012 | http://pubs.acs.org
Publication Date: May 15, 1995 | doi: 10.1021/bk-1995-0593.ch005

Systems are sorted in order of increasing Bond numbers in the descending mode. Figure 4 shows the plots of ū, the linear velocity of the Stokes droplets, versus B, the Bond number. From Figure 4, we can conclude that B does not account for the stability of the systems in centrifugal partition chromatography, but (see Table III) it corresponds roughly to the Ito classification of the so-called "hydrophobic and hydrophilic systems" *(8)*; this accounts for the hydrodynamic behavior of solvents systems in the coil planet centrifuge apparatus.

Figure 5 shows the correlation between the parameter $\frac{A}{B} = \frac{\gamma}{\Delta\rho}$, a parameter which accounts both for the dispersion of the mobile phase and for the fragility of the droplets, and the average linear velocities of the mobile phases in the channels. It can be seen from these data that $\frac{\gamma}{\Delta\rho}$ varies in the same way as the average linear velocities we experimentally determined.

This correlation could be interpreted as follows :

$\frac{\gamma}{\Delta\rho}$ small ≡ **A small and B large.** Small and unstable droplets moving slowly, and easily broken into smaller ones, leading to some possible emulsification, dragging the stationary phase out of the column. These systems can be used at low flow rate, in order to minimize emulsification and keep a sufficient amount of stationary phase in the column.

$\frac{\gamma}{\Delta\rho}$ large ≡ **A large and B small.** Large and very stable droplets moving fast; if so, rapid mass transfer between mobile and stationary phase is not favored for these systems, which should display poor chromatographic efficiencies.

$\frac{\gamma}{\Delta\rho}$ medium ≡ **A and B medium.** This is the common case, and is the best suited for chromatographic applications; the droplets are small enough to allow for a reasonable rate of mass transfer between the two phases, and fast enough to keep a large amount of stationary phase in the column. Some emulsified layer may be present in the channels, as described by D. Armstrong *et al.* *(9)*, but this has no negative repercussion upon the stability of the stationary phase.

Consequence of the "Stokes model". In centrifugal partition chromatography, improvement of the efficiency by increasing the flow rate *(9)*, and that of the resolution by increasing the rotational speed *(10)*, have already been reported. Using our very simple model to describe the flow pattern of the mobile phase, we can express the interfacial area between the two phases in the channels of the CPC column. From equation 3, the volume of mobile phase in the channel (not in ducts and connections) is :

$$\nu_m = V_m - d \cdot V_c = \frac{(1-d)}{\bar{u}} \frac{F}{S} V_c \qquad [9]$$

Since the droplets have a surface $s = 4\,\pi\,a^2$, a volume $v = 4/3\,\pi\,a^3$, then the number of droplets in the channels is $n = \nu_m / v$, and the interfacial area between the two phases in the channels is :

Downloaded by CORNELL UNIV on June 28, 2012 | http://pubs.acs.org
Publication Date: May 15, 1995 | doi: 10.1021/bk-1995-0593.ch005

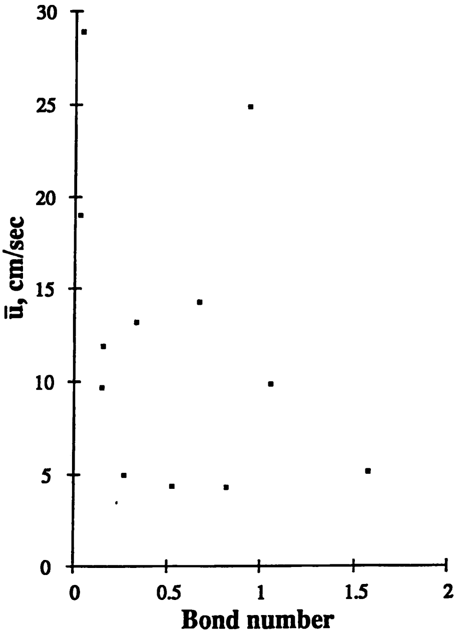

Figure 4. Plots of ū, the linear velocity of the Stokes droplets, versus B, the Bond number, showing the non-dependence of these two variables.

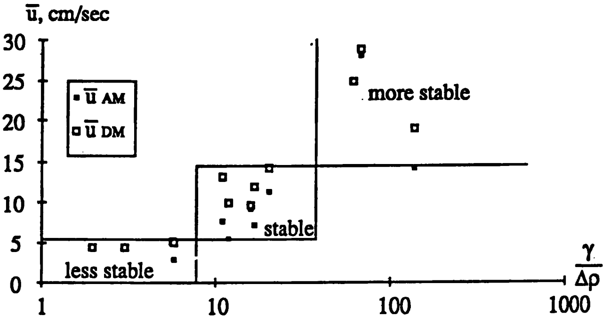

Figure 5. Correlation between the average linear velocity, ū, of the mobile phase in the channels of the HPCPC, and the parameter $\frac{\gamma}{\Delta\rho}$.

$\bar{u}_{AM}$ = average linear velocity in the ascending mode.
$\bar{u}_{DM}$ = average linear velocity in the descending mode.

(Reproduced with permission from reference 2. Copyright 1994 Marcel Dekker.)

Downloaded by CORNELL UNIV on June 28, 2012 | http://pubs.acs.org
Publication Date: May 15, 1995 | doi: 10.1021/bk-1995-0593.ch005

$$I = n\,s = \nu_m \frac{3}{a} \qquad [10]$$

From equations 4, 5, 9, and 10, we obtain :

$$I = (1\text{-}d)\,V_c \frac{F}{S} \frac{27}{2} \frac{\eta_{SP}}{\Delta\rho} A^{-3/2} g^{1/2} \qquad [11]$$

where all terms are constant for a given system and mode, except F and g.

Assuming that the efficiency is linearly related to the interfacial area, then equation 11 can be tested by independently varying F and g, then plotting the measured efficiency versus F x $g^{1/2}$, or by varying one parameter while keeping the other constant. We previously reported that the efficiency, in centrifugal partition chromatography, is much more dependent upon the volume of the mobile phase in the column than upon the flow rate *(1)*. For the HPCPC and the CPC type LLN, there exists a relationship between N, the number of theoretical plates, and $\frac{V_m}{V_c}$, which appears to be roughly linear. This partly confirms the adequacy of equation 11 since, when experiments are restricted to the steady state equilibrium corresponding to equation 3, V_m and F are linearly dependent.

Verification of equation 11 toward g has been done using the HPCPC. We used the system n–Heptane/Methanol in the descending mode, the rotational speed being varied between 700 and 2000 rpm. The flow rate was kept constant at 7 ml/min. The volume of mobile phase, V_m, was 120 ± 4 ml, which is 27 ml more than the calculated V_m (equation. 3), in order to keep this volume strictly constant throughout the experiments, because this parameter strongly influences the efficiency *(1)*. V_m was determined using 4-hydroxybenzoic acid (non retained solute), and diethyl phthalate was the analyte, with a partition coefficient of 0.27 ± 0.01. The number of plates has been estimated by using both the width at half height and at the base of the peak. Runs where the two values were not in close agreement, and runs where V_m was not constant were rejected (59 out of 77 injections were taken into consideration).

Figure 6 shows the results of this investigation. As predicted by equation 11, based on the "Stokes model", N is proportional to $g^{1/2}$, *i.e.* N is proportional to the rotational speed ω, in the range ordinarily used by the chromatographer (700 to 2000 rpm).

Regression analysis leads to the equation :

$$N = 0.98\,\omega - 175 \qquad [12]$$

Equation 12 is valid in the range studied (the intercept has no meaning), the correlation coefficient being equal to 0.97. The upper limit of this relationship should be reached when N approximates the number of physical plates, *i.e.* the number of channels, 2136 with our instrument. Figure 7 allows the comparison of two chromatograms obtained at 700 and 2000 rpm, all other parameters being kept constant.

Conclusion

Model based on Stokes' law, which is very simple and simulates the mobile phase to droplets, gives us a simple parameter ($\frac{\gamma}{\Delta\rho}$) to estimate the stability of a biphasic

Downloaded by CORNELL UNIV on June 28, 2012 | http://pubs.acs.org
Publication Date: May 15, 1995 | doi: 10.1021/bk-1995-0593.ch005

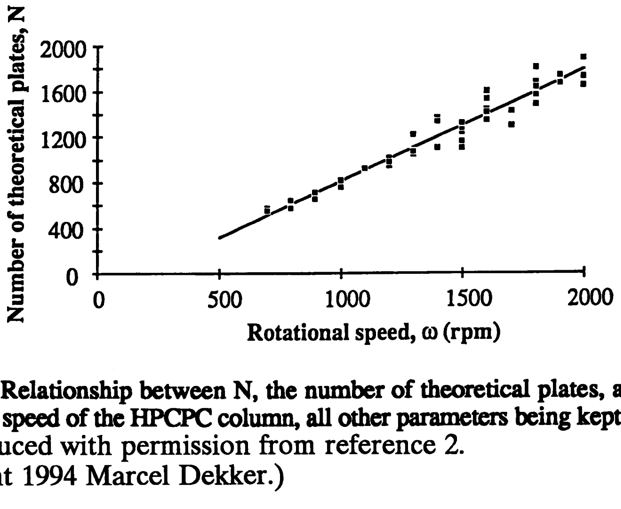

Figure 6. Relationship between N, the number of theoretical plates, and ω, the rotational speed of the HPCPC column, all other parameters being kept constant. (Reproduced with permission from reference 2. Copyright 1994 Marcel Dekker.)

Downloaded by CORNELL UNIV on June 28, 2012 | http://pubs.acs.org
Publication Date: May 15, 1995 | doi: 10.1021/bk-1995-0593.ch005

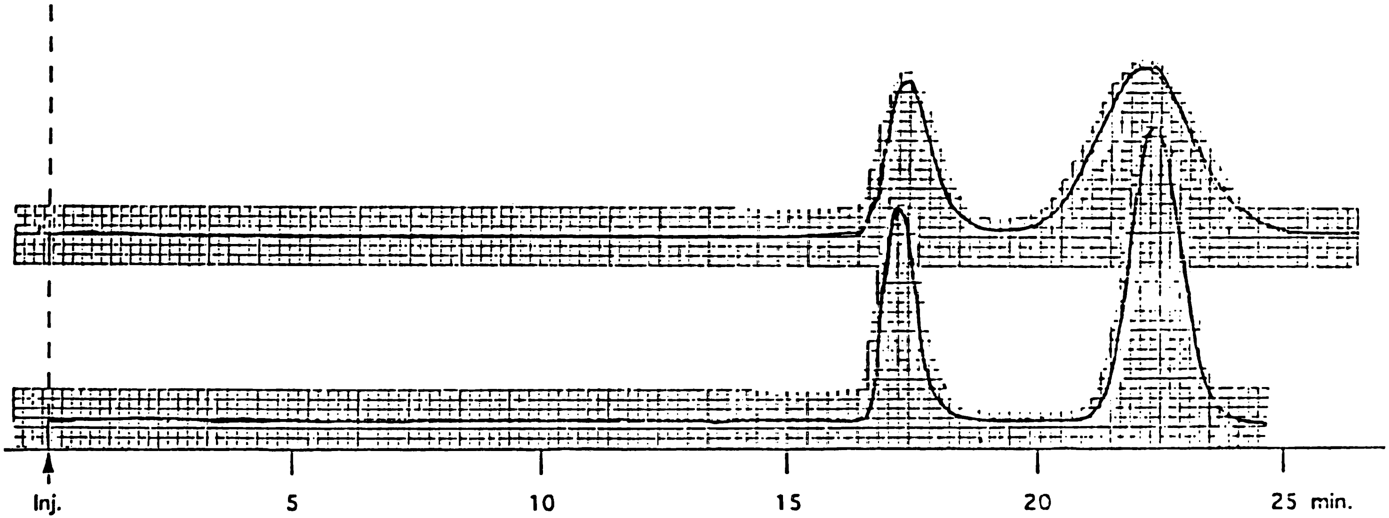

Figure 7. Comparison of HPCPC chromatograms obtained at 700 and 2000 rpm, all other parameters being kept constant.
Solvent system : Heptane / Methanol, descending mode.

Unweighted but identical quantities injected. Flow rate : 7 ml/min; $\frac{Vm}{Vc} = 0.5$

Upper : 700 rpm; lower : 2000 rpm.
(Reproduced with permission from reference 2.
Copyright 1994 Marcel Dekker.)

system in centrifugal partition chromatography, and is fully compatible with the evolution of the efficiency of the CPC column with the acceleration field. The best results will be obtained for higher rotational speed, whatever the system is, not because the retention of the stationary phase is higher, but because the dispersion of the mobile phase in the stationary phase is better.

One non-chromatographic parameter, the back pressure mainly due to hydrostatic pressure ($\Delta P \approx \Delta\rho$ g, g being the centrifugal field) *(9)* will be the major obstacle to achieve the best performance of a CPC apparatus. Instruments must be able to work at high pressure, in order to use them with any biphasic system at higher rotational speeds to obtain as many theoretical plates as the column can yield.

Literature Cited

1. Foucault, A.P., Bousquet, O., Le Goffic, F., *J. Liq. Chromatogr.*, **1992**, *15*, 2691.
2. Foucault, A.P., Camacho-Frias, E., Bordier, C.G.., Le Goffic, F., *J. Liq. Chromatogr.*, **1994**, *17*, 1
3. Foucault, A.P., Bousquet, O., Le Goffic, F., Cazes, J. *J. Liq. Chromatogr.*, **1992**, *15*, 2721
4. Berthod, A., Armstrong, D.W., *J. Liq. Chromatogr.*, **1988**, *11*, 547.
5. Foucault A. P., Durand P., Camacho Frias E., Le Goffic F., *Anal. Chem.*, **1993**, *65*, 2150
6. Bond, W.N., Newton, D.A., *Phil. Mag.*, **1928**, *5*, 794.
7. Richardson, E.G., in Hermans, J.J.,*"Flow properties of Disperse Systems"*, New York, Interscience, **1953**, Chapter VI.
8. Ito, Y., *J. Liq. Chromatogr.*, **1992**, *15*, 2639.
9. Armstrong, D.W., Bertrand, G.L., Berthod, a., *Anal. Chem.*, **1988**, *60*, 2513
10. Murayama, W., Kobayashi, T., Kosuge, Y., Yano, H., Nunogaki, Y., Nunogaki, K., *J. Chromatogr.*, **1982**, *239*, 643

RECEIVED November 28, 1994

Downloaded by CORNELL UNIV on June 28, 2012 | http://pubs.acs.org
Publication Date: May 15, 1995 | doi: 10.1021/bk-1995-0593.ch005

Downloaded by COLUMBIA UNIV on June 29, 2012 | http://pubs.acs.org
Publication Date: May 15, 1995 | doi: 10.1021/bk-1995-0593.ch006

Chapter 6

Optimization of Countercurrent Chromatography Solvent Systems

D. G. Martin

Upjohn Laboratories, Upjohn Company, Kalamazoo, MI 49007

Countercurrent chromatography (CCC) provides a high resolution, complementary technique to adsorption chromatography for the preparative separation of complex mixtures. The capacity of CCC to achieve a desired separation is greatly enhanced by the use of a solvent system which adequately retains the components of interest but allows their elution without excessive amounts of mobile phase. The most direct approach for selecting such a solvent system involves finding and modifying an appropriate system until the components of interest display partition coefficients (PC's) between 0.67 and 1.5. PC's are readily estimated by partitioning aliquots in small but equal volumes of the pre-equilibrated phases of biphasic systems of differing polarities and then estimating the amount of the components in each phase by such techniques as TLC densitometry or HPLC. Suggestions and examples of finding appropriate solvent systems are discussed.

The convenient operation and resolving power of CCC (*1, 2*) has impressed me in the decade since I acquired an Ito multilayer coil (P.C. Inc., Potomac, Maryland). CCC gave an added dimension to a variety of natural product isolation problems allowing a successful conclusion to a number of such problems where adsorption chromatography alone was apparently inadequate (*3*). The apparent reluctance of many colleagues to utilize CCC as a complementary technique to adsorption chromatography is surprizing. The resolution of most complex mixtures of natural products would benefit from successive application of all appropriate adsorption and solvent partition methodologies. Some colleagues have attempted CCC with an inappropriate system and concluded that the method is no good. Such considerations prompt this discussion on optimization of countercurrent solvent systems. This discussion is not intended as a comprehensive review but simply a presentation of some methods that have worked for me.

0097–6156/95/0593–0078$12.00/0

Downloaded by COLUMBIA UNIV on June 29, 2012 | http://pubs.acs.org
Publication Date: May 15, 1995 | doi: 10.1021/bk-1995-0593.ch006

Finding and Optimizing a Suitable Solvent System

Initial Need for a Semiquantitative Monitoring System. Development of an appropriate semiquantitative monitoring system for the components of interest is the essential first step in determining a suitable solvent system. Any monitor that allows estimation of the concentration of such components in the upper and lower layers of pre-equilibrated biphasic systems can be used. Suitable monitors include semiquantitative biological activities, HPLC, and TLC peaks estimated by densitometry. After some efforts to determine which TLC peaks correlate with biological activities of interest (*4*), TLC densitometry is an excellent monitor and will be the method discussed in subsequent remarks.

Empirical Partitioning in Systems of Varying Polarity. A suitable monitor allows initiation of the search for a biphasic system that will relatively evenly distribute the components of interest. An evenly distributed component is retained sufficiently for adequate resolution but eluted with a convenient volume of mobile phase. Components strongly prefering the mobile phase would elute close to the solvent front with limited resolution. Components strongly preferring the stationary phase would elute as broadened peaks after an inconveniently large volume of mobile phase. Alternatively, components remaining in the stationary phase could be eluted by terminating rotation with continued pumping of solvent to displace and fractionate the stationary phase. However, eluting interesting components with the more organic, less polar phase facilitates solvent evaporation and recovery of these components. If the more organic phase is mobile, the partition coefficient would be the ratio of the concentration of a component in the aqueous phase over the concentration of the component in the organic phase. For convenience and efficiency, a system in which the components of interest display partition coefficients between 0.67 and 1.50 is sought. This search is empirically carried out by partitioning small aliquots between the pre-equilibrated phases of several biphasic solvent systems of varying polarities and estimating the amount of the component or components of interest in the upper and lower phases by TLC densitometry. The lower phases of these systems should be at least 0.1 g/ml heavier than the corresponding upper phases to ensure adequate retention of the stationary phase during CCC.

Aliquot Preparation. Small samples for these determinations are conveniently prepared from a volatile solvent solution of the unknown mixture at a concentration such that 2 or 5 ul is adequate for TLC densitometry. One ml aliquots of this solution are dispensed into vials and evaporated under nitrogen.

Approximate PC's in Four Empirical Systems of Varying Polarity. Initially, such residues from a neutral unkown might be partitioned between 0.5 ml of each phase from hexane-methanol-water (10:9:1), ethyl acetate-hexane-methanol-water (1:1:1:1), chloroform-methanol-water (5:8:5), and butanol-water (1:1). Partitions on acidic or basic components might benefit from appropriate pH adjustments. The upper layer is readily accessible for spotting the appropriate 2 or 5 ul on a channeled TLC plate with a disposable micro-pipette. The sample is then drawn up into a pasteur pipet with a device which allows one to hold a liquid and slowly release it back into the vial making the lower phase accesible for spotting the same volume on an adjacent channel. After development, the dried plate is scanned by densitometry. The ratio of the peak heights or peak areas of the components of interest in the stationary phase over these components in the mobile phase directly affords an estimate of the PC in that solvent system. If one of the four systems fortuitously distributed the sample with a suitable PC, that system is utilized for CCC.

Optimization of Appropriate Solvent System. More likely, one or two of the systems will afford measurable PC's <0.67 or >1.50. Such systems require optimization by changing the relative amounts of the solvents, substituting a different solvent for one of the solvents, or including an additional modifying solvent. Ususally, the system affording the most favorable PC can be modified to an optimized system.

Modification of Hexane, Aqueous Methanol Systems. If the component in hexane aqueous methanol systems favors the upper phase, substitute acetonitrile for some of the water to pull components toward the lower phase. If the component favors the lower phase, incrementally decrease the methanol/water ratio while adding increments of ethyl acetate or diethyl ether. Increments of 5-10% usually afford significant changes in the PC. Keep in mind the dual role of solvents. They contribute to the density of the phases as well as affect the PC's of dissolved components. For this reason, diethyl ether is a particularly effective modifier for organic upper phase systems and carbon tetrachloride an effective modifier for organic lower phase systems, especially those with relatively high methanol/water ratios.

Modification of Ethyl Acetate, Hexane, Aqueous Methanol Systems. If the component in ethyl acetate-hexane-methanol-water systems favors the upper phase, incrementally decrease the ethyl acetate/hexane ratio while increasing the methanol/water ratio. Alternatively, substitute diethyl ether for a portion or all of the ethyl acetate. If the component favors the lower phase, incrementally increase the ethyl acetate/hexane ratio and decrease the methanol/water ratio.

Modification of Halocarbon, Aqueous Methanol Systems. Chloroform-methanol-water systems are susceptible to a great deal of modification and can handle a wide range of polarities, especially if the component favors the lower phase of the 5:8:5 system. Incremental substitutions or additions of methylene chloride, carbon tetrachloride, toluene, or cyclohexane while increasing the methanol/water ratio will drive components toward the upper phase. If the component favors the upper phase of the 5:8:5 system, incrementally decrease the methanol/water ratio.

Modification of Aqueous Butanol Systems. If the component favors the upper phase in aqueous butanol systems, incremental additions of diethyl ether may push components toward the aqueous phase. If the lower phase is favored, the addition of a volatile salt such as triethylammonium acetate will drive components toward the upper phase.

Downloaded by COLUMBIA UNIV on June 29, 2012 | http://pubs.acs.org
Publication Date: May 15, 1995 | doi: 10.1021/bk-1995-0593.ch006

Downloaded by COLUMBIA UNIV on June 29, 2012 | http://pubs.acs.org
Publication Date: May 15, 1995 | doi: 10.1021/bk-1995-0593.ch006

Isolation and Purification of Tylophorosides by CCC

The contributions of CCC to the isolation and purification of tylophoroside and acetyltylophoroside from the African plant Tylophora sylvatica will be used to illustrate these methods. Collaborators from the University of Arizona, the Upjohn Company, and Johns Hopkins University determined the structures (*5*) of the purified glycosides (Figure 1). The attachment of the 3 sugar unit by a vinyl ether linkage on the aglycone was unprecedented in a natural product. It is interesting that plant material collected during the dry season in the seacoast region of Ivory Coast yielded mainly the free alcohol while plant material collected during the rainy season from the mid-eastern region of Ivory Coast afforded mainly the acetate of the same alcohol. Dr. Jean-Noel Gnabre received his PhD in pharmacology and toxicology in 1991 from the University of Arizona . His dissertation (*6*) was on the antiallergic activity of Tylophora sylvatica. In 1988 Jean-Noel was a graduate student at the University of Arizona using a basophil dependent serotonin release (BDSR) assay to investigate the antiallergic properties in T. sylvatica plant material from his native Ivory Coast. That September, he came to my lab at Upjohn for help in fractionating this plant material.

Semiquantitative Monitor Development. After solvent extraction and silica gel chromatography, he had obtained 2 fractions that appeared as relatively simple mixtures on silica gel TLC plates developed with chloroform-aqueous methanol and visualized by charring but which were apparently not susceptible to further purification by silica gel chromatography. Silica gel TLC's on these fractions were repeated with the same solvent system. The plates were initially scanned by densitometry with 220 nm UV light and then charred. A facile comparison (Figure 2) of the two methods of visualization was achieved by placing the densitometric tracings directly above reproductions of the corresponding charred plates at the same scale. Three obvious conclusions were drawn. The sample on the left contained a minor component very susceptible to charring, both samples contained components insensitive to charring, and silica gel TLC with this system afforded inadequate resolution. These same 2 samples were then chromatographed on reverse phase (C18) plates with 70% methanol and visualized with both 220 nm UV light and charring (Figure 3). TLC on C18 plates scanned by densitometery with 220 nm UV light afforded much better resolution and provided an adequate monitoring system.

Empirical Partitioning. Aliquots of the 2 fractions were partitioned between the pre-equilibrated phases of 1:1:1:1, 2:1:2:1, and 3:1:3:1 toluene-chloroform-methanol-water systems. TLC densitometry indicated that the higher methanol/water and toluene/chloroform ratios left the bulk of these components in the upper phase but equal amounts of the solvents distributed approximately 60% of the major component into the lower phase (PC about 0.67). Evaluating these same partitions with the BDSR assay suggested that the 3:1:3:1 system afforded the most even distribution of the biological activity. The most obvious explanation of this discrepancy would be the presence of biologically active lipophilic components not readily detected by this C18 assay.

Downloaded by COLUMBIA UNIV on June 29, 2012 | http://pubs.acs.org
Publication Date: May 15, 1995 | doi: 10.1021/bk-1995-0593.ch006

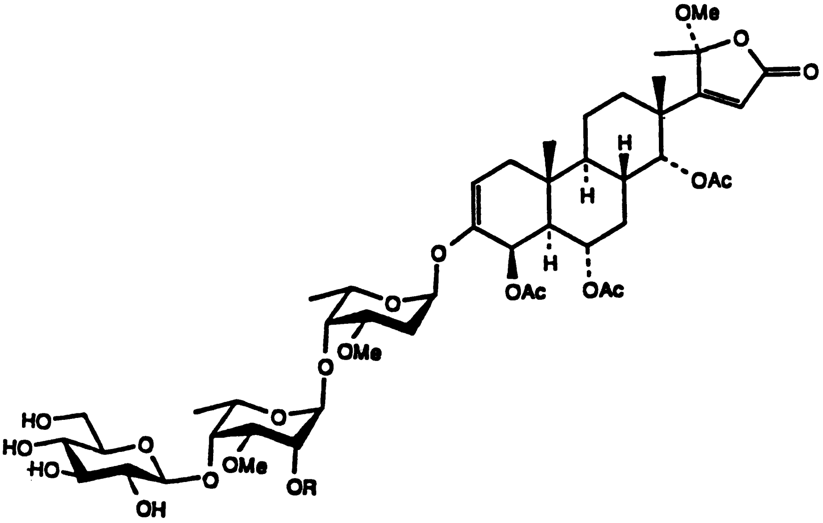
OMe
O
O
H
OAc
H
O
H
OAc
OAc
O
OMe
O
HO
O
HO
O
HO
OMe
O
OR
OH

Tylophoroside, R = H
Acetyltylophoroside, R = Ac

Figure 1. Tylophoroside Structures.

Downloaded by COLUMBIA UNIV on June 29, 2012 | http://pubs.acs.org
Publication Date: May 15, 1995 | doi: 10.1021/bk-1995-0593.ch006

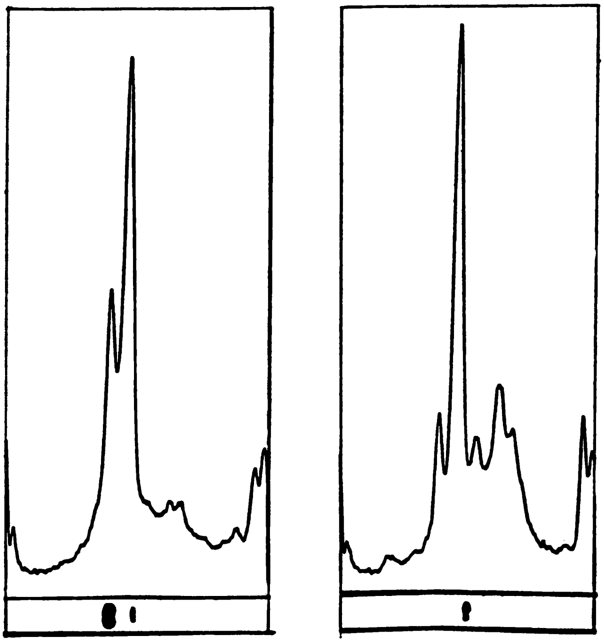

Figure 2. Silica Gel TLC of 2 Samples.

Top: Densitometric Visualization with 220 nm UV
Bottom: Visualization by Charring

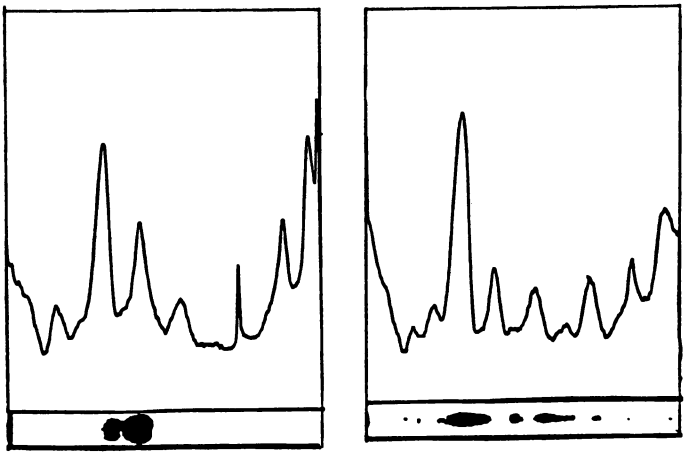

Figure 3. C18 TLC of 2 Samples.

Top: Densitometric Visualization with 220 nm UV
Bottom: Visualization by Charring

Initial Isolation by CCC. Preliminary fractionations on 200 mg samples of the 2 fractions were carried out in an Ito Coil (335 ml volume) with the system from equal parts of the 4 solvents. Upper phase was utilized as stationary phase and about 50% was retained when mobile phase appeared in the effluent. Collected fractions of the mobile phase were monitored by TLC densitometry and the Arizona BDSR assay. As suspected, fractions near the solvent front displayed significant BDSR activity but lacked TLC peaks. After 114 ml of mobile phase had been eluted, eluate contained the major TLC component (Rf 0.3) which also displayed BDSR activity. These fractions from the two 200 mg samples held 21 and 47 mg of fairly homogeneous Rf 0.3 component which was selected as the primary isolation target and ultimately identified as tylophoroside.

Downloaded by COLUMBIA UNIV on June 29, 2012 | http://pubs.acs.org
Publication Date: May 15, 1995 | doi: 10.1021/bk-1995-0593.ch006

Initial Enrichment and Separation from Lipophilic Activity. The sample size of the 2 available crude fractions (over 3.5 g) would require multiple runs in the Ito coil or significant enrichment by other means. Small scale C18 chromatography afforded a good recovery of nicely enriched tylophoroside but irreversibly bound most of the lipophilic activity. To preserve the possibility of fractionating this lipophilic activity as a secondary target, separation of lipophilic components from the tylophoroside was necessary before enriching the tylophoroside by C18 chromatography. The crude samples were initially partitioned in a separatory funnel in the pre-equilibrated phases of the system used for CCC. The lower layer was separated and the spent upper layer extracted with 2 fresh portions of lower phase. The combined lower layers, containing all of the tylophoroside as well as the lipophilic activity, was then evaporated to a residue and extracted with a limited volume of acetone. The acetone soluble residue, containing the tylophoroside in 2.27 g of residue, was divided into 4 equal portions and submitted to overloaded CCC in the same solvent system to crudely separate the lipophilic activity from the tylophoroside. It wasn't pretty but it worked! The relatively crude sample, heavy loading, and nature of the components present caused initial emulsions and less than ideal behavior. At a flow rate of 3 ml/minute only 40% of the stationary phase was retained when mobile phase appeared in the eluate. Mobile phase fractions were monitored and pooled. Fractions preceding tylophoroside contained 1.00 g of the lipophilic BDSR activity from the 4 runs. Fractions containing significant tylophoroside totalled 0.84 g. The tylophoroside in these fractions was further upgraded by chromatography on C18 which afforded 0.39 g of the strongly enriched targeted compound.

Final Purification by CCC in Optimized Systems. Plans to achieve final purification by CCC in an optimized system developed by slightly increasing the toluene/chloroform and methanol/water ratios over their values in the 1:1:1:1 system were modified when attempted partitions of the enriched sample produced heavy emulsions. Partitioning a sample in ethyl acetate-hexane-methanol-water (3:2:2:3) left most of the tylophoroside in the lower aqueous phase. Replacing hexane with diethyl ether and decreasing the methanol/water ratio proved fruitful. The PC was 1.27 in 3:2:2:5 ethyl acetate-ether-methanol-water and 1.08 when the ethyl acetate/ether ratio was increased to 7/3. The densities of the upper and lower phases of the 7:3:2:5 system were 0.86 and 0.96, respectively, and that system was selected for CCC.

Tylophoroside. The Ito coil (335 ml volume) was loaded with lower phase as stationary and 325 mg of enriched tylophoroside in 8 ml of a mixture of the phases was injected through a loop valve. Rotation at 800 rpm's and mobile phase flow at 2.5 ml/minute were initiated. After the initial loss of 78 ml of stationary phase, 257 ml of stationary phase was retained. Then somewhat anomalous behavior was observed; fractions of mobile phase containing significant stationary phase were collected until the tylophoroside had been eluted. The initial 212 ml of mixed phase elute contained 20 mg of contaminating components. Tylophoroside appeared in the eluate 290 ml after the initiation of mobile phase flow. This volume is slightly greater than the original retention volume of stationary phase in reasonable agreement with the PC estimated by solvent partitioning. The next 22 ml of eluate contained 8 mg of slightly impure tylophoroside followed by 241 mg of homogeneous tylophoroside in 92 ml of eluate. The following two 20 ml fractions of eluate held 12, and 2 mg, respectively, residues of impure tylophoroside.

Downloaded by COLUMBIA UNIV on June 29, 2012 | http://pubs.acs.org
Publication Date: May 15, 1995 | doi: 10.1021/bk-1995-0593.ch006

Acetyltylophoroside. J. Gnabre obtained a second batch of Tylophora sylvatica, collected during the rainy season in the mid-eastern region of Ivory Coast. In the course of extracting and enriching the glycoside from this collection, he astutely observed that the major glycoside appeared to be slightly more lipophilic than tylophoroside on TLC analysis. Solvent partitioning confirmed this increased lipophilicity. The new glycoside had a PC of 0.67 in the 7:3:2:5 ethyl acetate-ether-methanol-water system in which tylophoroside had a PC of 1.08.

Final purification of this new glycoside, subsequently established to be acetyltylophoroside, was readily accomplished by CCC with this solvent system. An Ito coil with a 365 ml volume was loaded with lower phase as stationary and 250 mg of enriched acetyltylophoroside in a mixture of the phases was injected through the loop valve. Rotation and mobile phase flow were initiated. Initially, 70 ml stationary phase were lost for a stationary phase retention of 295 ml. The initial 126 ml of mixed phase eluate contained 43 mg of contaminating components. Acetyltylophoroside appeared in the eluate 196 ml after the initiation of mobile phase flow. Again this volume of mobile phase is in good agreement with the volume expected from the 0.67 PC estimated by solvent partitioning. The next 42 ml of eluate contained 24 mg of impure acetyltylophoroside followed by 97 mg of homogeneous acetyltylophoroside in 105 ml of eluate. The following 21 ml fraction held only 4 mg of an apparent mixture of tylophoroside, acetyltylophoroside, and other contaminants.

Decreasing the ethyl acetate/ether ratio from 7/3 to 3/2 and increasing the methanol/water ratio from 2/5 to 2/4 should delay the elution of acetyltylophoroside. In the interest of exploring the effect this delay might have on the quality of the acetyltylohoroside eluted, CCC was also carried out in 3:2:2:4 ethyl acetate-ether-methanol-water. The Ito coil (365 ml volume) was loaded with lower phase as stationary and a solution of 340 mg of enriched acetyltylophoroside was injected. Rotation and mobile phase flow were initiated. After the initial loss of 88 ml of stationary phase, 277 ml were retained. Acetyltylophoroside appeared in the eluate 278 ml after the initiation of mobile phase flow consistent with a PC of 1.0 in this system. The next 38 ml of eluate contained 24 mg of impure acetyltylophoroside followed by 151 mg of homogeneous acetyltylophoroside in 114 ml of eluate. The following 19 ml fraction held only 6 mg of impure acetyltylophoroside. The 2 solvent systems both efficiently delivered homogenous acetyltylophoroside.

Acknowledgments. The author is grateful for the excellent facilties and resources provided by the Upjohn Company, the many contributions and support of coworkers, the extensive pioneering and development efforts of Dr. Yoichiro Ito and his colleagues on CCC, and the planet coil centrifuge manufactured by the late Peter Carmeci.

Downloaded by COLUMBIA UNIV on June 29, 2012 | http://pubs.acs.org
Publication Date: May 15, 1995 | doi: 10.1021/bk-1995-0593.ch006

Literature Cited.

1. Ito, Y.*J. Chromatogr.* **1991,** *538,* pp 3-25.
2. Conway, W. D. *Countercurrent Chromatography: apparatus, theory, and applications;* VCH Publishers, Inc.: New York, NY, 1990; pp 3-468.
3. Martin, D. G.; Biles, C.; Peltonen, R. E.*Am. Laboratory* **1986,** *18,* pp 21-26.
4. Martin, D. G. In *Countercurrent Chromatography: theory and practice;* Mandava, N. B.; Ito, Y., Eds.; Chromatographic Science Series; Marcel Dekker, Inc.: New York, NY, 1988, Vol.44; pp 565-580.
5. Gnabre, J. N.; Pinnas, J. L.; Martin, D. G.; Mizsak, S. A.; Kloosterman, D. A.; Baczynskyj, L. B.; Nielsen, J. W.; Bates, R. B.; Hoffman, J. J.; Kane, V. V. *Tetrahedron* **1991,** *47,* 3545- 3554.
6. Gnabre, J. N. *Antiallergic Activity of Tylophora Sylvatica;* PhD dissertation, University of Arizona, 1991.

RECEIVED November 28, 1994

Downloaded by STANFORD UNIV GREEN LIBR on June 28, 2012 | http://pubs.acs.org
Publication Date: May 15, 1995 | doi: 10.1021/bk-1995-0593.ch007

Chapter 7

Separation of Three Alkaloids from *Senecio fuberi* Hemsl by High-Speed Countercurrent Chromatography

D.-G. Cai[1], M.-J. Gu[1], G.-P. Zhu[1], J.-D. Zhang[1], T. Jin[1], T.-Y. Zhang[2], and Yoichiro Ito[3]

[1]Research Center of Pharmacy of People's Liberation Army's Navy, Shanghai 200083, China
[2]Beijing Institute of New Technology Application, Beijing 100035, China
[3]Laboratory of Biophysical Chemistry, National Heart, Lung, and Blood Institute, National Institutes of Health, Building 10, Room 7N322, Bethesda, MD 20892

Three alkaloids, squalidine, platyphylline, and neoplatyphylline from *Senecio fuberi Hemsl*, were completely separated by high-speed counter-current chromatography (CCC). Separation was performed with a two-phase solvent system composed of chloroform/0.07M sodium phosphate-0.04M citrate buffer (pH 6.20-6.45) (1:1) in which the upper aqueous phase served as the stationary phase, and the lower chloroform phase as the mobile phase. Each alkaloid was identified by the physical and chemical constants as well as TLC and mass spectral data. Platyphylline and neoplatyphylline are cis-trans isomers which are difficult to separate by other means on a preparative scale.

Senecio fuberi Hemsl (Composite) is a perennial herb growing in Emei Mountain areas in Sichuan province and in the provinces of Yunnan and Guizhou in southwest China. It is used as a folk remedy for treating injuries resulting from falls, fractures, contusions and strains as well as for reducing swelling due to injury. It is reported (*1*) that the herb contains three alkaloids: squalidine, neoplatyphylline, and platyphylline. Squalidine and platyphylline show antitumor (*1*) and anticholinergic (*2*) effects, respectively. The structures of squalidine, platyphylline and neoplatyphylline are shown in Figure 1. The latter two are cis-trans isomers which could not be separated by conventional preparative methods or even by countercurrent chromatography (CCC) using the horizontal flow-through coil planet centrifuge (*3*).

In recent years, we have applied a new high-efficiency liquid-liquid chromatography without solid support, high-speed CCC, to separate some alkaloids from traditional Chinese herbal medicines (*4-6*). This paper describes the separation of these alkaloids from *Senecio fuberi Hemsl* by this technique. All three were completely resolved within 1 hour. Platyphylline and neoplatyphylline were identified by melting point, optical rotation, MS, and ^{1}HNMR.

0097-6156/95/0593-0087$12.00/0

Downloaded by STANFORD UNIV GREEN LIBR on June 28, 2012 | http://pubs.acs.org
Publication Date: May 15, 1995 | doi: 10.1021/bk-1995-0593.ch007

Materials and Methods

CCC Apparatus and Separation Procedure. The multilayer coil high-speed CCC used in our experiments was obtained from the Beijing Institute of New Technology Application, Beijing, China. The operation and efficiency of the apparatus were previously described (*5*). The coil planet centrifuge was rotated at 750 rpm during the separation. The mobile phase flowed from the internal terminal to the external terminal of the multilayer coil at 2ml/min. The effluent was monitored by a uv detector at 254 nm and collected by an automatic fraction collector.

Preparation of Solvent System. The two-phase solvent system for the CCC separation was composed of chloroform and a mixture of 0.07M sodium phosphate and 0.04M citrate buffer (1:1, v/v). Three buffer mixtures at 6.21, 6.38 and 6.45 in pH were used. The upper aqueous phase was used as the stationary phase and the lower organic phase as the mobile phase. The retention of the stationary phase, measured after the separation, was 80.4% of the total column capacity.

Preparation of Sample Solutions. The crude alkaloid fractions were obtained from *Senecio fuberi Hemsl* using a conventional pH gradient extraction as summarized in Figure 2. From fractions A and B thus obtained, two sample solutions were prepared as follows: Solution 1 was made by dissolving a 5mg quantity of alkaloid fraction A and a 10mg quantity of alkaloid fraction B in 1 ml of mobile phase, and Solution 2 was made by adding 10-12 mg of alkaloid fraction B to 1 ml of the mobile phase. These two sample solutions were chromatographed separately by the high-speed CCC centrifuge.

Analyses of Separated Fractions. Melting points of the purified fraction were determined by a Yanaco MD-53 apparatus. Optical rotations were measured by a DRT optical meter. The EI mass spectra were obtained by a JMS-300 spectrometer and HNMR spectra by a Brucker MSL-300 instrument operated at 300 MHz. TLC plates were prepared in a conventional way with silica-gel-G. The plates were developed in a solvent composed of chloroform/methanol/ ammonium hydroxide (85:14:10, v/v) followed by spraying with a Dragendorf reagent after drying.

Results and Discussion

The sample solution 1 above was well separated by high-speed CCC into 5 peaks in about 1 hour (Figure 3). The retention times of peaks 2 and 5 were the same as those of the authentic squalidine and platyphylline standards, respectively. Among all peaks resolved, peaks 2 and 5 were identified as squalidine and platyphylline, respectively, by co-TLC with pure standard samples: The peak 4 had an Rf value of 0.55 (Figure 4). Peaks 1 and 3 have yet to be assayed.

To identify the chemical structure of the peak 4 fraction, sample solution 2 was chromatographed. The ratio of the solute contents between peaks 4 and 5 was estimated as about 2:3 measured by the peak areas, in which traces of peaks 1, 2, and 3 were also present. About 30mg of pure alkaloids of the peak 4 fraction were obtained from 6 experiments and subjected to further analysis. The melting point was 135.5-137.5°C, $[\alpha]^{18}_{D}$, +3.47 (0.006627. $CHCl_3$). The ^{1}HNMR spectrum of peak 4 closely resembled that of platyphylline, except that the chemical shift of CH_3-CH=C(-CO) proton was 6.59 which is identical to that of neoplatyphylline. The mass spectrum of the peak 4 fraction showed that the molecular weight of the component was 337. The m/z values of the important fragments were as follows: 337(M^+), 332(M-15), 320(M-17), 252, 221, 140, 138, 123, 122, 108, 96, 95 and 82(M^+), etc. All data above indicated that the compound is identical to neoplatyphylline reported elsewhere (*7*).

In order to speed up the separation, the effect of the buffer pH of the solvent system on the separation was examined. Raising the

Downloaded by STANFORD UNIV GREEN LIBR on June 28, 2012 | http://pubs.acs.org
Publication Date: May 15, 1995 | doi: 10.1021/bk-1995-0593.ch007

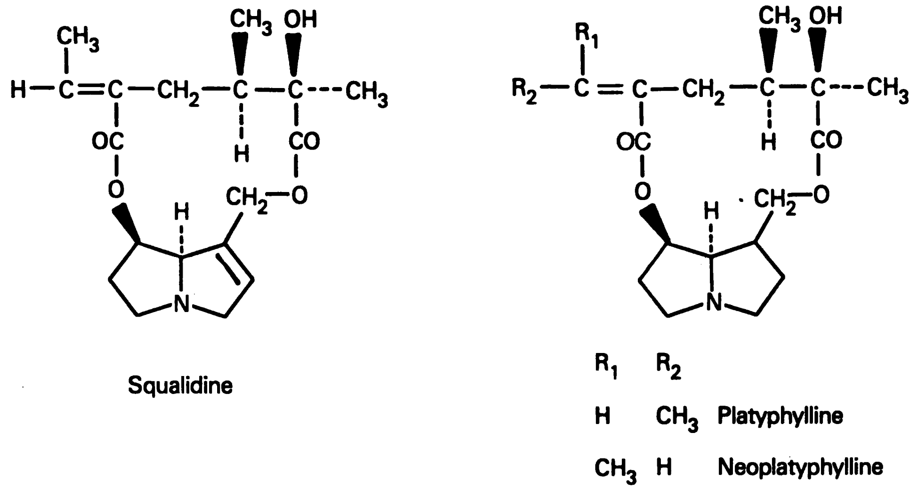
Squalidine
R1 R2
H CH3 Platyphylline
CH3 H Neoplatyphylline

Figure 1. Chemical structures of squalidine, platyphylline, and neoplatyphylline.

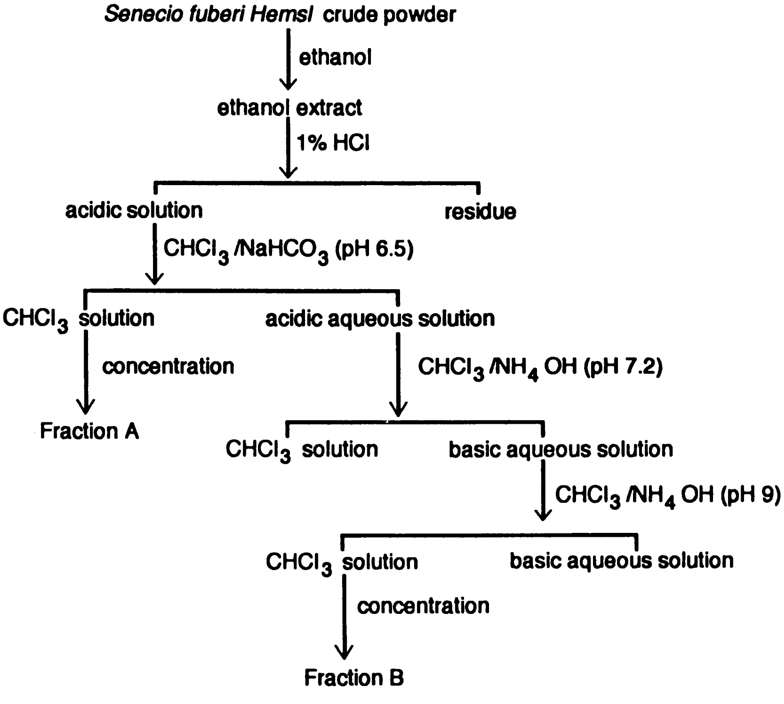
Senecio fuberi Hemsl crude powder
ethanol
ethanol extract
1% HCl
acidic solution
residue
CHCl3 /NaHCO3 (pH 6.5)
CHCl3 solution
acidic aqueous solution
concentration
CHCl3 /NH4 OH (pH 7.2)
Fraction A
CHCl3 solution
basic aqueous solution
CHCl3 /NH4 OH (pH 9)
CHCl3 solution
basic aqueous solution
concentration
Fraction B

Figure 2. Conventional pH gradient extraction of alkaloids from *Senecio fuberi Hemsl.*

Downloaded by STANFORD UNIV GREEN LIBR on June 28, 2012 | http://pubs.acs.org
Publication Date: May 15, 1995 | doi: 10.1021/bk-1995-0593.ch007

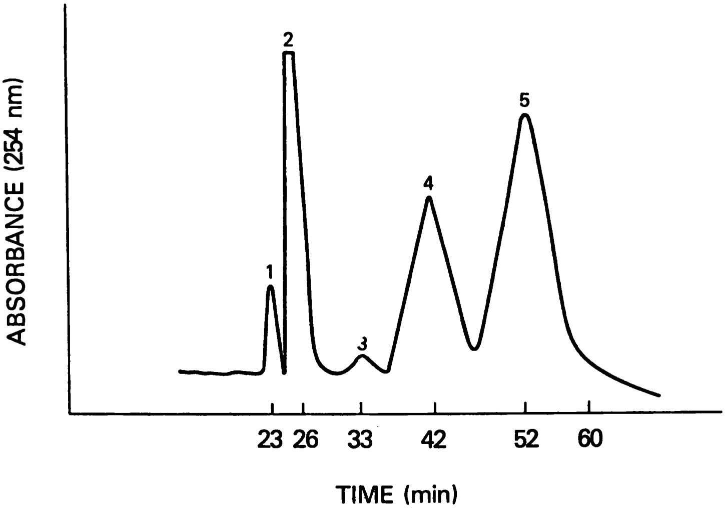

Figure 3. High-speed CCC chromatogram of squalidine (peak 2), platyphylline (peak 5) and neoplatyphylline (peak 4) from *Senecio fuberi Hemsl.* Minor peaks 1 and 3 have not been identified.

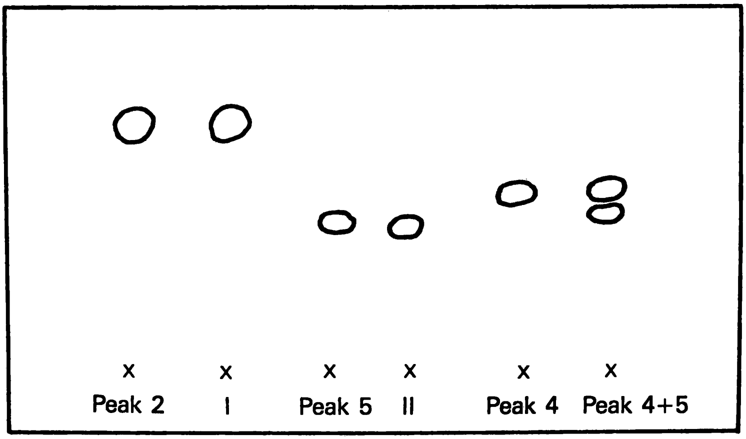

Figure 4. TLC analysis of high-speed CCC fractions from *Senecio fuberi Hemsl.* I and II are pure standards of squalidine and platyphylline, respectively.

Downloaded by STANFORD UNIV GREEN LIBR on June 28, 2012 | http://pubs.acs.org
Publication Date: May 15, 1995 | doi: 10.1021/bk-1995-0593.ch007

Table I EFFECTS OF BUFFER pH ON SEPARATION

Buffer (pH)	R_t (min)		R_v (min)	
	peak 4	peak 5	peak 4	peak 5
6.21	70	92	104	184
6.38	56	70	112	140
6.45	42	52	84	104

R_t : retention time; R_v : retention volume

buffer pH from 6.21 to 6.45 shortened the retention times from 70 to 42 min for peak 4 and from 90 to 52 min for peak 5 as shown in Table I. Accordingly, the retention volume of these two peaks were reduced from 140 to 85 ml for peak 4 and 185 to 104ml for peak 5. Under these conditions, peaks 4 and 5 were still completely resolved.

The results of the present studies demonstrated that high-speed CCC yields an efficient preparative separation of platyphylline and neoplatyphylline, cis-trans isomers of alkaloids, from *Senecio fuberi Hemsl*. The method may also be applied to the separation of various other alkaloids.

Literature Cited

1. Wu, S.-R.; Cai, D.-G; Lu, Y.-Q. *Chinese Traditional Herbal and Drugs* **1983**, 14 (5), 45.

2. Gan, S.-D.; Wang, J.-H. *Bulletin of the Academy of Military Medical Sciences* **1882**, 1, 61.

3. Cai, D.-G.; Gou, J.-X.; Zhou, W.-W.; Zhang, T.-Y.; Hau, X. *Bulletin of Chinese Materia Medica* **1985**, 10 (12), 29.

4. Zhang, T.-Y.; Pannell, L.K.; Cai, D.-G.; Ito, Y. *J. Liq. Chromatogr.* **1988**, 11 (8), 661-1971.

5. Cai, D.-G.; Gu, M.-J.; Zhang, J.-D.; Zhu, G.-P.; Zhang, T.-Y.; Li, N.; Ito, Y. *J. Liq. Chromatogr.* **1990**, 13 (12), 2399-2408.

6. Cai, D.-G.; Gu, M.-J.; Zhu, G.-P.; Zhang, T.-Y.; Ito, Y. *J. Liq. Chromatogr.* **1992**, 15 (15 & 16), 2873-2881.

7. Culvenor, C.C.C.; Koretskaya, N.I.; Smith, L.W.; Utkin, L.M. *Aust. J. Chem.* **1968**, 21, 1671-1673.

RECEIVED March 10, 1995

Downloaded by YORK UNIV on June 29, 2012 | http://pubs.acs.org
Publication Date: May 15, 1995 | doi: 10.1021/bk-1995-0593.ch008

Chapter 8

Separation of Gardenia Yellow Components by High-Speed Countercurrent Chromatography

H. Oka[1], Y. Ikai[1], S. Yamada[1], J. Hayakawa[1], K.-I. Harada[2], M. Suzuki[2], H. Nakazawa[3], and Yoichiro Ito[4]

[1]Aichi Prefectural Institute of Public Health, Nagare 7–6, Tsuji-machi, Kita-ku, Nagoya 462, Japan
[2]Faculty of Pharmacy, Meijo University, Yagotoyama 150, Tenpaku-ku, Nagoya 468, Japan
[3]National Institute of Public Health, 4–6–1, Shirokanedai, Minato-ku, Tokyo 108, Japan
[4]Laboratory of Biophysical Chemistry, National Heart, Lung, and Blood Institute, Building 10, Room 7N–322, National Institutes of Health, Bethesda, MD 20892

High-speed countercurrent chromatography (HSCCC) has been successfully applied to preparative separation of gardenia yellow components. Three components, geniposide, *trans*-crocin, and 13-*cis*-crocin, were isolated from 25mg of the sample using a two-phase solvent system composed of ethyl acetate-*n*-butanol-water (2:3:5). Due to the exposure to uv light emitted from the fluorescent room lamp, *trans*-crocin and 13-*cis*-crocin were photoisomerized to 13-*cis*- and *trans*-forms, respectively. It is also the first time that the presence of 13-*cis*-crocin and two glycosyl esters of crocetin in gardenia yellow is demonstrated by frit fast atom bombardment liquid chromatography/mass spectrometry and HPLC with photodiode array detection.

Gardenia yellow is a natural food additive extracted from gardenia fruit (*Gardenia jasminoides* ELLIS) and widely used for coloring Japanese food. It is known that the yellow color is derived from a water soluble pigment including *trans*-crocin (Fig. 1 **1a**) and *trans*-crocetin (**1b**) as major components while gardenia yellow also contains geniposide (**2**) as a colorless major component (*1-4*). Various minor components such as 13-*cis*-crocin (**3a**), 13-*cis*-crocetin (**3b**), and other glycosyl esters of *trans*- and 13-*cis*-crocetins (**1c**, **1d**, **3c**, and **3d**) may also be present in the gardenia yellow, since they have been identified as minor yellow pigments in saffron (*Crocus stativs* L.) extract which contains *trans*-crocin as a major component (*5*). The quantities of these components vary according to locality and season. For food sanitation and safe manufacturing practice, therefore, the development of a simple and precise method for identifying the minor components is required. Although high performance liquid chromatography (HPLC) is considered to be a powerful technique for the analysis of the components in commercial preparations and foods, pure compounds from

0097–6156/95/0593–0092$12.00/0

Downloaded by YORK UNIV on June 29, 2012 | http://pubs.acs.org
Publication Date: May 15, 1995 | doi: 10.1021/bk-1995-0593.ch008

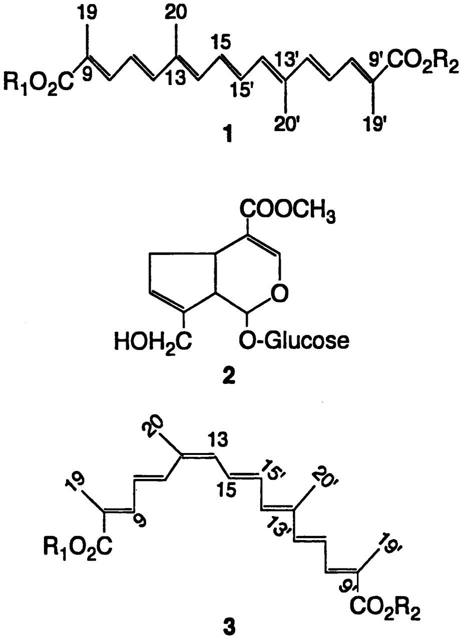

a: R1=R2=ß-D-gentiobiosyl
b: R1=R2=H
c: R1=ß-D-gentiobiosyl; R2=H
d: R1=R2=ß-D-glucosyl

Figure 1. Structures of gardenia yellow components.
1a: *trans*-crocin, 2: geniposide, 3a: 13-*cis*-crocin

gardenia yellow for use as the reference standards are not commercially available. In addition, no effective method for isolation of these components has been reported.

Recently, HSCCC, an advanced liquid-liquid partition method that does not require solid support (*6*), has been reported for the separation of synthetic dyes (*7,8*) and antibiotics (*9,10*). In these studies, HSCCC was used to provide useful amounts of standards. We report below the identification of the components of gardenia yellow using frit fast atom bombardment (FAB) liquid chromatography/mass spectrometry (LC/MS) and HPLC with photodiode array (PDA) detection.

Experimental

Reagents. Acetonitrile, *n*-butanol, ethyl acetate, and glycerol were of analytical grade and purchased from Wako (Osaka, Japan). Gardenia yellow of food additive grade was purchased from Wako.

HPLC analysis. A chromatograph equipped with constant flow pumps (LC-100P, Yokogawa, Tokyo, Japan) was used with variable wavelength UV/VIS detectors (LC-100U, Yokogawa) operated at 254 nm for the detection of geniposide and at 435 nm for the detection of crocin. The separation was performed on LiChrosorb RP-18 (5 μm, 125 x 4.0 mm, I.D., E. Merck, Darmstadt, Germany) under the following conditions: mobile phase: acetonitrile-water; gradient rate: acetonitrile 5-45%, linear 20 min; flow rate: 1 mL/min.

For photodiode array detection, a UV/VIS diode array detector (991J, Waters, Milford, USA) was used. Mobile phase: acetonitrile-water containing 1.0 % glycerol and 3 mM potassium chloride; gradient rate: acetonitrile 5-45 %, linear 40 min; flow rate: 0.5 mL/min; scan range: 210-500 nm.

Frit FAB LC/MS. The separation was performed on LiChrosorb RP-18 (5 μm, 125 x 4.0 mm, I.D., E. Merck, Darmstadt, Germany) under the following conditions: mobile phase: acetonitrile-water containing 1.0 % glycerol and 3 mM potassium chloride: gradient rate: acetonitrile 5-45 %, linear 40 min; flow rate: 0.5 mL/min.

The mass spectrometer and the data system used were a JMS-AX505W (Jeol, Tokyo, Japan) and a JMA-DA5000 (Jeol), respectively. The temperature of ion source was kept at 60°C and a neutral xenon beam was used as a primary beam for the ionization by FAB. The acceleration voltages of the primary and secondary beams were adjusted to 3 and 5 kV, respectively. The LC/MS data were obtained by scanning from *m/z* 100 to *m/z* 1500 with a cycle time of 6.5 seconds. The TIC range was set to scan *m/z* 300-1500.

The HPLC and mass spectrometer were interfaced by a laboratory-made flow splitter, connection tubing (fused silica 100 cm x 0.06 mm, i.d.), and a frit-FAB probe. The effluent from HPLC was split at the ratio of 4 : 500 and the smaller portion of the effluent was introduced into the mass spectrometer through the connection tubing at a flow rate of 4 μL/min.

Measurement of Partition Coefficient. Approximately 1 mg of the test sample was weighed in a 10 mL test tube to which 2 mL of each phase of preequilibrated two-phase solvent system was added. The test tube was stoppered and shaken vigorously for 1 min to equilibrate the sample thoroughly with the two phases. Then, equal volumes of the upper and lower phases were analyzed by HPLC to get the partition coefficient.

HSCCC Separation. The apparatus used was a HSCCC-1A prototype multi-layer coil planet centrifuge (Shimadzu, Kyoto, Japan) with a 10 cm orbital radius which produces a synchronous planetary motion at 800 rpm. The multi-layer coil was prepared by winding a *ca*. 160 m length of PTFE tubing onto the column holder with a 10 cm hub diameter and a 15 cm hub length, making six coiled layers with a total capacity of about 300 mL. The two-phase solvent system composed of ethyl acetate-*n*-butanol-water solution (2:3:5) was thoroughly equilibrated in a separatory funnel by repeated vigorous shaking and degassing at room temperature. The column was first entirely filled with the upper non-aqueous stationary phase, then 25 mg of the sample dissolved in 2 mL of both phases was loaded. The centrifuge was rotated at 800 rpm, while the lower aqueous mobile phase was pumped into the head of the column (the heat-tail relationship of the rotating coil is conventionally defined by the Archimedean screw force, where all objects of different densities are driven toward the head of the coil) at a flow rate of 2 mL/min by HPLC pump (LC-6A, Shimadzu). The effluent from the outlet of the column was fractionated into test tubes at 2 mL per tube with a fraction collector (DF-2000, Tokyo Rikakikai,

Downloaded by YORK UNIV on June 29, 2012 | http://pubs.acs.org
Publication Date: May 15, 1995 | doi: 10.1021/bk-1995-0593.ch008

Tokyo, Japan). When separation was completed, retention of the stationary phase was measured by collecting the column contents by forcing them out of the column with pressurized nitrogen gas combined with slow rotation of the coil in the tail-to-head elution mode. A 0.2 mL volume of the contents of each test tube was diluted with distilled water and the absorbance was determined with a UV/VIS spectrophotometer (Ubest-50, Japan Spectroscopic, Tokyo, Japan) at 254 and 435 nm.

FABMS Analysis. The FAB mass spectra were obtained in a JMS-AX505W double-focusing mass spectrometer. A xenon ion gun was operated at 3 kV. The matrix used was glycerol+1M potassium chloride (1+1).

Results and Discussion

Identification of Gardenia Yellow Components Using HPLC with Frit-FABMS and PDA Detection. The gardenia yellow components were analyzed using HPLC with a frit FABMS and a PDA detector. Fig. 2 shows HPLC chromatograms monitored at 254, 325, and 435 nm, and the UV-VIS spectra at the tops of each peak on the chromatogram are shown in Fig. 3. Total ion current (TIC) and mass chromatograms monitored at *m/z* 427, 691, and 1015 for potassium adduct ions of geniposide, crocin, and diglycosil ester of crocetin, respectively, are shown in Fig. 4. Mass spectra at the tops of each peak on the mass chromatograms are given in Fig. 5. Peak 1 showed an absorption maximum at 238 nm (Fig. 3A) that originates from its α, ß-unsaturated ester carbonyl moiety. The FAB mass spectrum suggested that the molecular weight of the compound corresponding to peak 1 is 388. These spectral data agree completely with those of geniposide (**2**)(*11,12*).

The molecular weights of the compounds corresponding to peaks 2 and 3 were estimated to be 976 from their FAB mass spectra (Fig. 5B and C). The UV-VIS spectrum of peak 2 showed the absorbance maxima at 410 (sh), 444, and 463 nm (Fig. 3B) and these spectral data correspond with those of *trans*-crocin (**1a**)(*5*). The UV-VIS spectrum of peak 3 was quite similar to that of peak 2 in the range of 350-500 nm (Fig. 3C), but in addition it showed a strong absorption maximum at 328 nm, suggesting the presence of a *cis* double bond in the polyene molecule (*5,13*). Consequently, these spectral data were consistent with those of 13-*cis*-crocin which has been isolated from the saffron extract (*5*). This is the first time that 13-*cis*-crocin (2a) was found in gardenia yellow.

Peaks 4 and 5 showed almost the same UV-VIS spectra as those of peaks 2 and 3 (Fig. 3D and E), indicating that these compounds have the same polylene chromophore. Since molecular weights of both compounds are estimated to be 652, the compounds from peaks 4 and 5 were considered to be glycosyl esters of crocetins where two glucose molecules have been eliminated from *trans*- (**1c** or **1d**) and 13-*cis*-crocins (**3c** or **3d**), respectively. This is also the first time that these glycosyl esters have been found in gardenia yellow, although they were present in the saffron extract (*5*). Crocetins were not detected in the gardenia yellow used in the present study as previously reported by Kamikura (*4*).

Selection of two-phase solvent system. In order to select a suitable solvent system for HSCCC, the following three requirements should be satisfied (*14,15*): 1) For satisfactory retention of the stationary phase, settling time of the solvent systems should be shorter than 30 seconds; 2) to avoid excessive waste of one solvent, the mixture should provide nearly equal volumes of each phase; and 3) for efficient separations, the partition coefficient (*K*) of the target compound should be close to 1. In general small *K* values may result in a loss of peak resolution, while large *K* values tend to excessively broaden the sample band. The *K* value of a pure compound is determined simply by measuring UV absorbance of the solute in both phases after

Downloaded by YORK UNIV on June 29, 2012 | http://pubs.acs.org
Publication Date: May 15, 1995 | doi: 10.1021/bk-1995-0593.ch008

Downloaded by YORK UNIV on June 29, 2012 | http://pubs.acs.org
Publication Date: May 15, 1995 | doi: 10.1021/bk-1995-0593.ch008

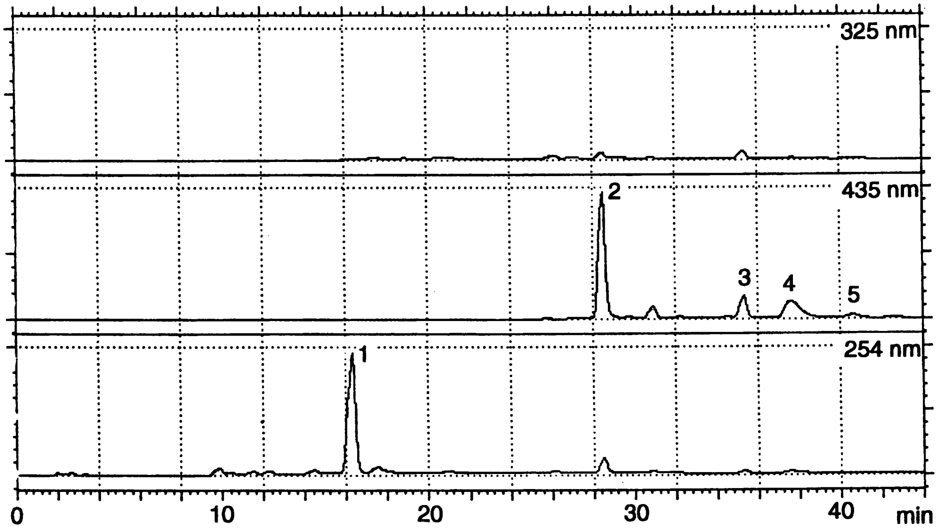

Figure 2. HPLC chromatograms of gardenia yellow components with photodiode array detection.
HPLC conditions: See Experimental.

Downloaded by YORK UNIV on June 29, 2012 | http://pubs.acs.org
Publication Date: May 15, 1995 | doi: 10.1021/bk-1995-0593.ch008

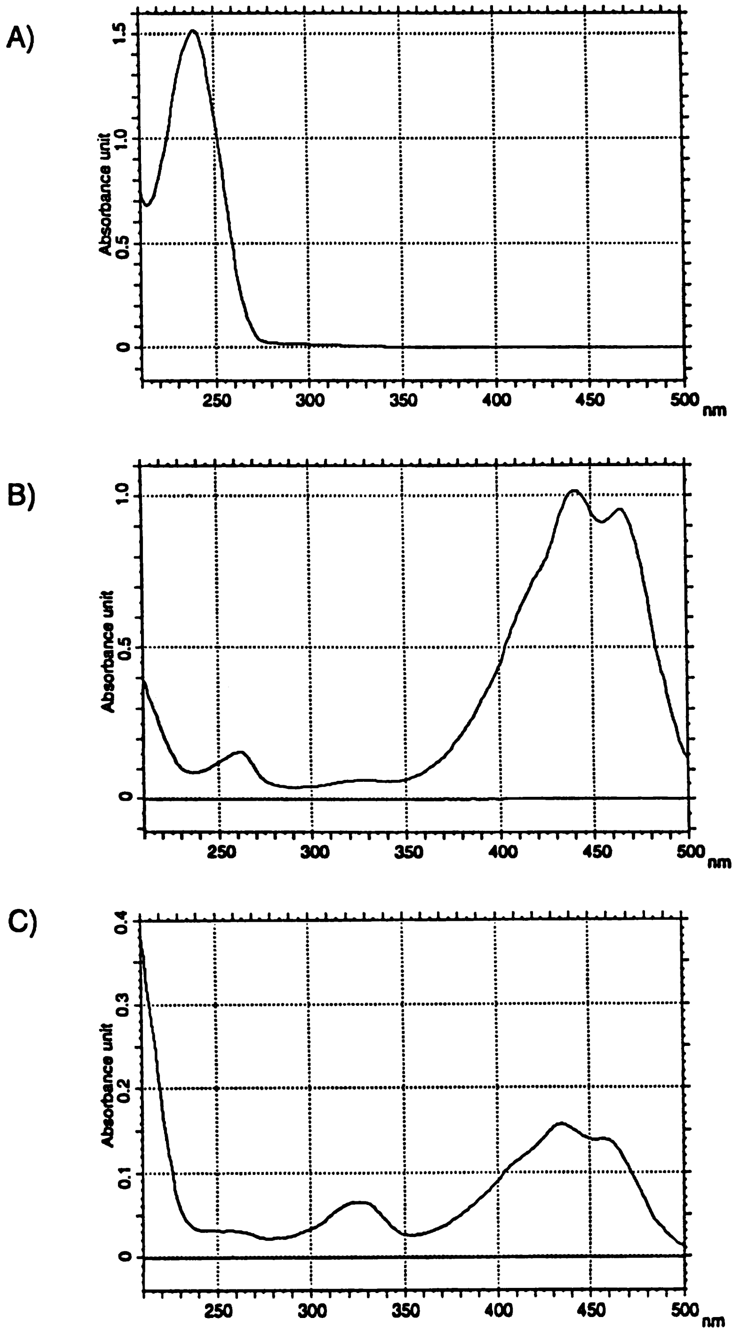

Figure 3. UV/VIS-spectra of gardenia yellow components, A) peak 1, B) peak 2, C) peak 3, D) peak 4, E) peak 5 HPLC conditions: See Experimental.

Continued on next page

Downloaded by YORK UNIV on June 29, 2012 | http://pubs.acs.org
Publication Date: May 15, 1995 | doi: 10.1021/bk-1995-0593.ch008

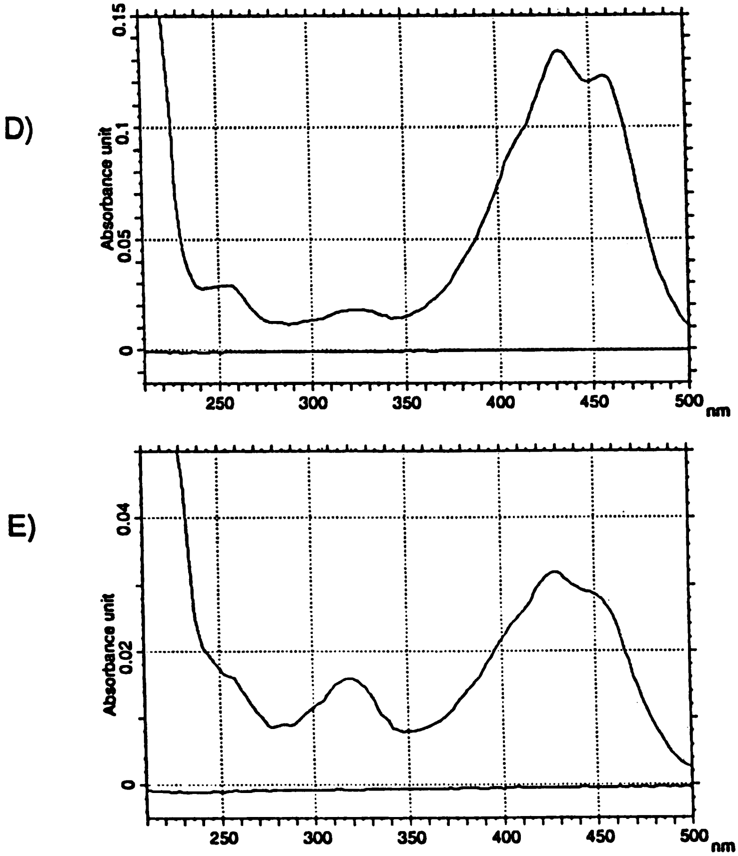

Figure 3. *Continued.*

In Modern Countercurrent Chromatography; Conway, W., et al.;
ACS Symposium Series; American Chemical Society: Washington, DC, 1995.

Downloaded by YORK UNIV on June 29, 2012 | http://pubs.acs.org
Publication Date: May 15, 1995 | doi: 10.1021/bk-1995-0593.ch008

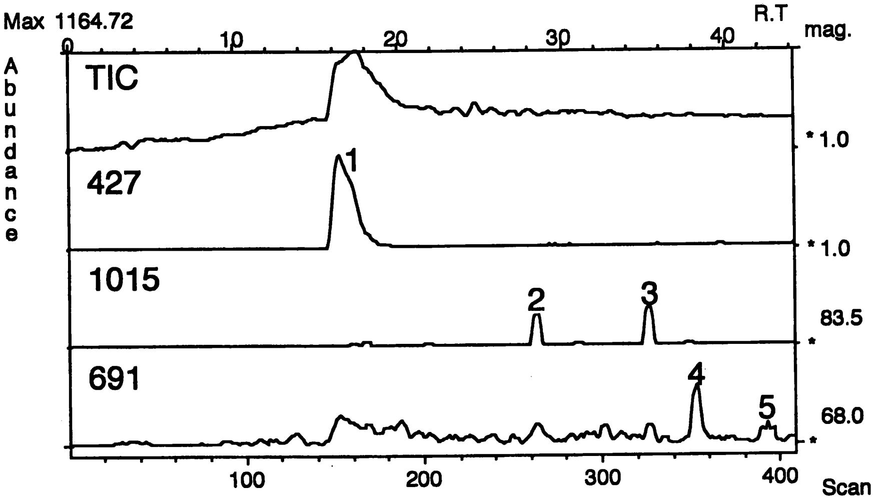

Figure 4. Mass chromatograms of gardenia yellow components under frit-FAB LC/MS conditions.
LC/MS conditions: See Experimental.

Downloaded by YORK UNIV on June 29, 2012 | http://pubs.acs.org
Publication Date: May 15, 1995 | doi: 10.1021/bk-1995-0593.ch008

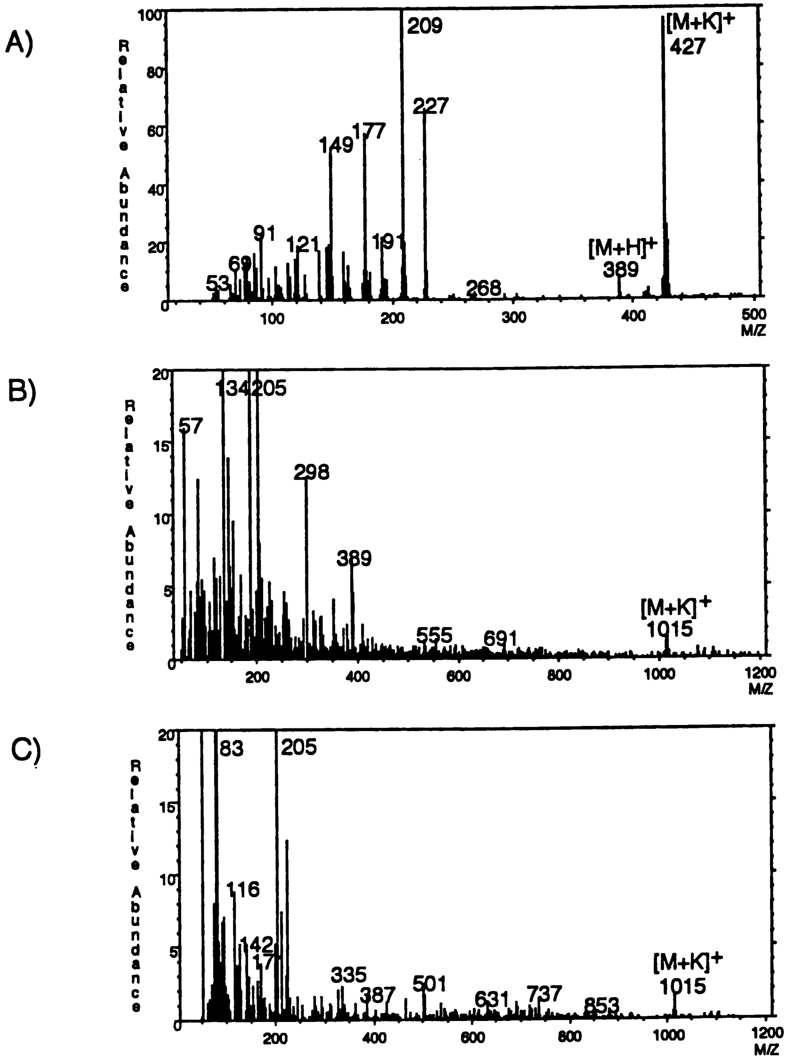

Figure 5. FAB mass spectra of gardenia yellow components. A) peak 1, B) peak 2, C) peak 3, D) peak 4, E) peak 5. LC/MS conditions: See Experimental.

Downloaded by YORK UNIV on June 29, 2012 | http://pubs.acs.org
Publication Date: May 15, 1995 | doi: 10.1021/bk-1995-0593.ch008

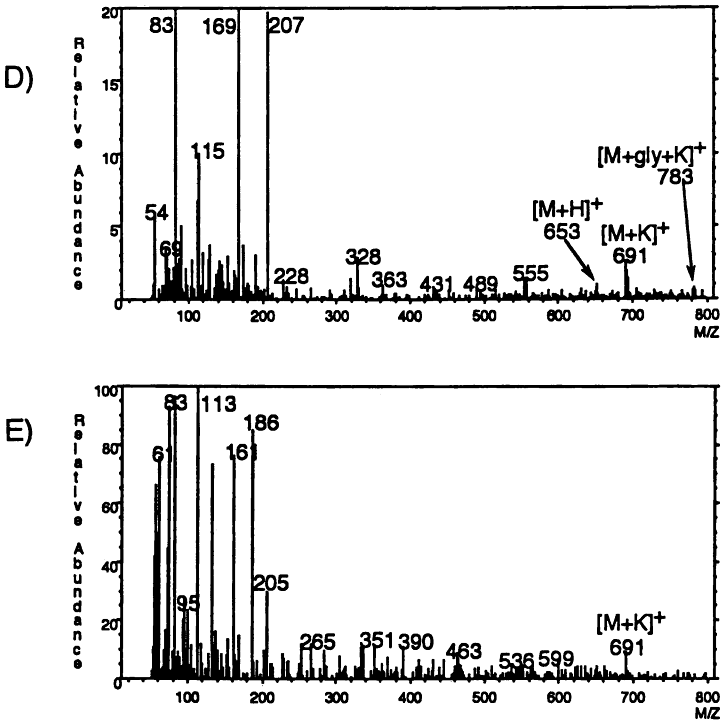

Figure 5. *Continued.*

partitioning in the two-phase solvent system. However, when a sample is a mixture of various components such as gardenia yellow, a precise *K* value of each component cannot be determined by the above method. However, this problem may be solved by the HPLC method. As shown in Fig. 6A, HPLC can separate gardenia yellow components into fourteen peaks. After partitioning the sample with the two-phase solvent system, the resulting upper and lower phases were analyzed by HPLC and the *K* values of each component were determined.

We have selected a two-phase solvent system composed of ethyl acetate, *n*-butanol, and water because it is useful for separation of components with a broad range of hydrophobicity by modifying the volume ratio of the three solventsl (*4*). In the ethyl acetate-*n*-butanol-water (3-2-5) system first examined, the *K* values of the components corresponding to peaks 1 (**2**), 2 (**1a**), and 3 (**3a**) were 0.5, 0.4, and 0.9, respectively. This indicated that the components of peaks 1 and 2 are mostly partitioned in the lower aqueous phase (Table I). Although the ethyl acetate-*n*-butanol-water (2-2-5) and (4.5-5.5-10) systems gave improved *K* values for peaks 1 and 2, their *K* values were too close to each other. Finally, a slightly more polar solvent mixture of ethyl acetate-*n*-butanol-water (2-3-5) yielded the best *K* values as shown in Table I. In this solvent system, peaks a, b, c, and d are eluted together near the solvent front, and peaks f, h, 4, i, and 5 remain in the column contents. The other peaks are eluted in the order of peaks 1, e, 2, and 3 where peaks 1, 2, and 3 will be completely separated. The settling time of this solvent system was 12 seconds and volume ratio of the upper and lower phases was 1.09. Therefore, this solvent system was selected for the purification of the gardenia yellow components.

Purification of Gardenia Yellow Components Using HSCCC. Using the above solvent system, a 25mg amount of gardenia yellow was separated by HSCCC. The retention of the stationary phase was 65.8 % and the separation was completed in 4.5 h with the total elution volume 540 mL. The elution curves of the gardenia yellow monitored at 254 and 435 nm are shown in Fig. 7. The components were resolved into four main peaks (A-D). The fractions corresponding to each peak maximum and the column contents were analyzed by HPLC. These chromatograms were referred to the chromatograms obtained from the original sample (in Fig. 6A) to identify each component eluted in peaks A - D. The results indicated the following: Peak A contained the components corresponding to the peaks a, b, c, and d; Peak B contained geniposide **2** (peak 2) with a minute amount of peak e; peaks C and D contained *trans*-crocin **1a** (peak 2) and 13-*cis*-crocin **3A** (peak 3), respectively, while the rest including peaks f, h, 4, i, and 5 remained in the column contents. Peak g was not detected apparently due to its low concentration.

On the basis of the elution curves and the results of HPLC analysis, fractions corresponding to peaks 1 (geniposide, **2**), 2 (all *trans*-crocin, **1a**), and 3 (13-*cis*-crocin, **3a**) were each combined and analyzed by HPLC. Figs. 6B - D show the chromatograms of the combined fractions. As shown in Fig. 6B, the component corresponding to peak 1 (geniposide, **2**) in the first fraction (fraction 89 - 108) is almost isolated from other components. On the basis of the molecular weight of 388 determined by its FAB mass spectrum, this compound is identified as geniposide. In the HPLC analysis, geniposide (**2**) constituted about 74 % of the total peak area at 254 nm in the original sample, but its purity was increased to over 99% after a single step purification by HSCCC, yielding 6.8 mg of pure geniposide (**2**). As shown in Fig. 6C and D, the HPLC chromatograms of the second (fractions 122 - 138, 1.3 mg) and the third (fractions 190 -208, 0.3mg) combined fractions showed the identical elution profile both containing peak 2 (*trans*-crocin, **1a**) and peak 3 (13-*cis*-crocin, **3a**), in spite of the fact that the *cis*- and *trans*-crocins were completely separated by HSCCC according to the HPLC analysis performed shortly after the elution. This strange finding led us to investigate photoisomerization of crocin as described below.

Downloaded by YORK UNIV on June 29, 2012 | http://pubs.acs.org
Publication Date: May 15, 1995 | doi: 10.1021/bk-1995-0593.ch008

Downloaded by YORK UNIV on June 29, 2012 | http://pubs.acs.org
Publication Date: May 15, 1995 | doi: 10.1021/bk-1995-0593.ch008

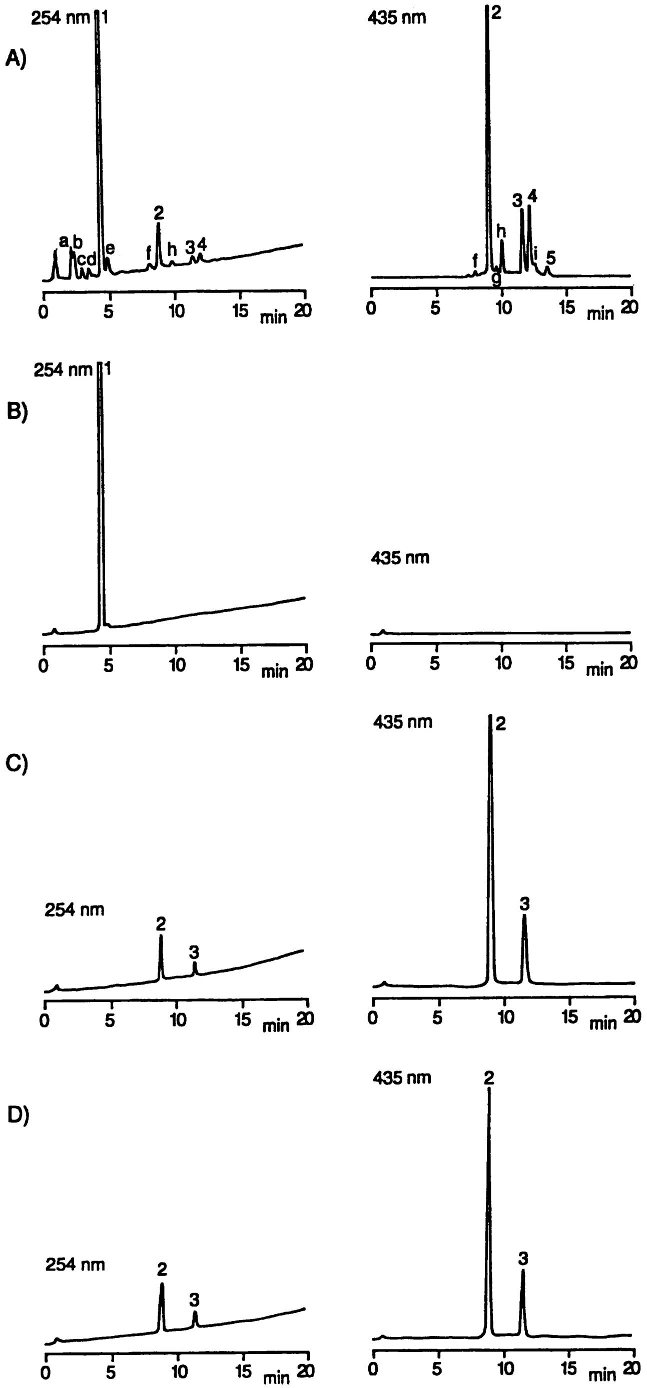

Figure 6. 6HPLC separation of gardenia yellow components. A) original gardenia yellow, B) fraction 1, C) fraction 2, D) fraction 3. HPLC conditions: See Experimental.

Downloaded by YORK UNIV on June 29, 2012 | http://pubs.acs.org
Publication Date: May 15, 1995 | doi: 10.1021/bk-1995-0593.ch008

TABLE I

PARTITION COEFFICIENTS OF GARDENIA YELLOW COMPONENTS

**K*=Peak area of upper phase divided by paek area of lower phase.

**EA: ethyl acetate, B: n-butanol, W: water

Solvent systems**	Partition coefficients*													
	Peak No.													
	a	b	c	d	1	e	f	2	g	h	3	4	i	5
EA : B : W														
3 : 2 : 5	0.1	0.1	0	0	0.5	0.5	3.0	0.4	0.9	4.0	0.9	∞	∞	∞
2 : 2 : 5	0.1	0.1	0	0	0.7	0.6	∞	0.8	1.0	5.2	0.9	∞	∞	∞
4.5 : 5.5 : 10	0.1	0.2	0.2	0	0.8	0.8	∞	1.0	1.5	6.3	2.1	∞	∞	∞
2 : 3 : 5	0.1	0.2	0.2	0	0.9	1.0	∞	1.4	2.2	8.2	3.3	∞	∞	∞

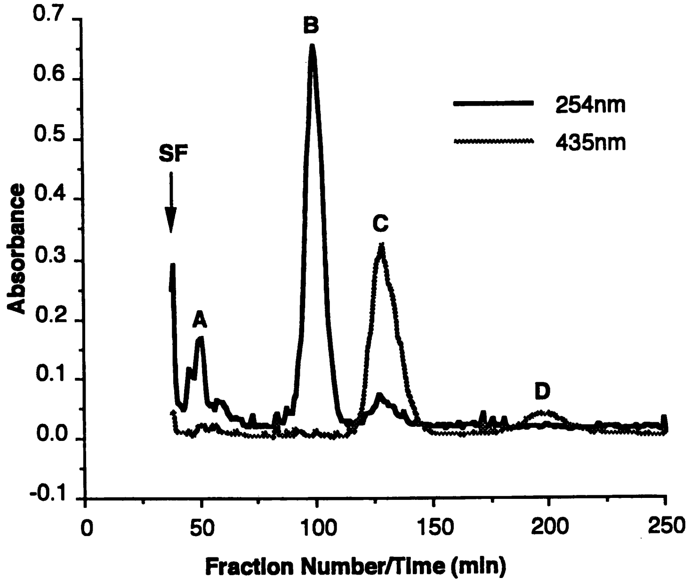

Figure 7. Separation of gardenia yellow components by HSCCC. HSCCC conditions: See Experimental.
SF=solvent front

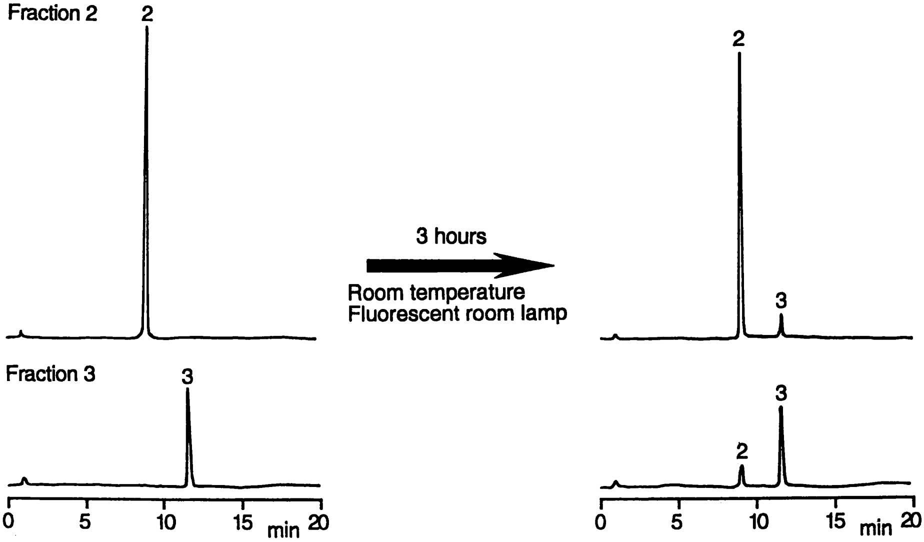

Figure 8. Photoisomerization of crocin.
HPLC conditions: See Experimental.

Downloaded by YORK UNIV on June 29, 2012 | http://pubs.acs.org
Publication Date: May 15, 1995 | doi: 10.1021/bk-1995-0593.ch008

Photoisomerization of Crocin. It was found that *trans*- and *cis*-crocins were photoisomerized to *cis*- and *trans*-forms, respectively. In order to confirm this phenomenon, the following experiments were carried out: HSCCC fractions containing peaks 2 and 3 were analyzed by HPLC, immediately after the separation and again after standing for 3h at room temperature under fluorescent room light. As shown in Fig. 8 (left), the first HPLC analysis of the fractions corresponding to peaks 2 and 3 each produced a single peak, indicating that the two components are completely separated by HSCCC. However, in the second HPLC analysis after standing for 3h, 13-*cis*-crocin appeared in the peak 2 fraction and *trans*-crocin, in the peak 3 fraction (Fig. 9, right). Furthermore, after standing under the same conditions for 24 h, the HPLC analysis produced the chromatograms identical to those in Fig. 6 C and D. Based on the above findings, we conclude that *trans*- and 13-*cis*-crocins were completely separated by HSCCC but after isolation *trans*-crocin and 13-*cis*-crocin were photoisomerized to 13-*cis*- and *trans*-forms, respectively, under the fluorescent lamp illumination at room temperature.

Conclusion

HSCCC was successfully applied to the preparative separation of gardenia yellow components, yielding the following results: 1) The two-phase solvent system composed of ethyl acetate-*n*-butanol-water (2:3:5) is most suitable for the separation of gardenia yellow components; 2) Three components, geniposide, *trans*-crocin, and 13-*cis*-crocin can be isolated; 3) *trans*-crocin and 13-*cis*-crocin are gradually photoisomerized to 13-*cis*- and *trans*-forms, respectively, at room temperature under fluorescent room lamp illumination; and 4) 13-*cis*-crocin and glycosyl esters of crocetin (missing two glucose molecules from *trans*-crocin and 13-*cis*-crocin) were detected for the first time in gardenia yellow by HPLC-FABMS and PDA.

Acknowledgment

The authors thank Dr. Henry M. Fales for editing the manuscript.

Literature Cited

1. Kuhn, R.; Winterstein, A.; Wiegand, W. *Helv. Chem. Acta* **1928**, *11*, 716-724.
2. Umetani, Y.; Fukui, H; Tabata, M. *Yakugaku Zasshi* **1980**, *100*, 920-924.
3. Noda, N.; Yamada, S; Hayakawa, J; Uno, K. *Eisei Kagaku* **1983**, *29*, 7-12.
4. Kamikura, M.; Nakazato, K. *J. Food Hyg. Soc. Jpn.* **1985**, *26*, 150-159.
5. Speranza, G.; Dadà, G; Manitto, P; Monti, D; Gramatica, P. *Gazzetta Chimica Italiana* **1984**, *114*, 189-192.
6. Ito, Y. in *Countercurrent Chromatography, Theory and Practice*, Mandava, N.B. and Ito, Y., Eds.; Marcel Dekker, New York, NY, 1988, Ch. 3, pp. 79-442.
7. Fales, H.M.; Pannell, L.K.; Sokoloski, E.A.; Carmeci, P. *Anal. Chem.* **1985**, *57*, 376-378.
8. Oka, H.; Ikai, Y.; Kawamura, N.; Hayakawa, J.; Yamada, M.; Harada, K.-I.; Murata, H.; Suzuki, M.; Nakazawa, H.; Suzuki, S.; Sakita, T.; Fujita, M.; Maeda, Y.; Ito, Y. *J. Chromatogr.* **1991**, *538*, 149-156.
9. Harada, K.-I.; Kimura, I.; Yoshikawa, A.; Suzuki, M.; Nakazawa, H.; Hattori, S.; Komori, K.; Ito, Y. *J. Liq. Chromatogr.* **1990**, *13*, 2373-2388.
10 Harada, K.-I.; Ikai, Y.; Yamazaki, Y.; Oka, H.; Suzuki, M.; Nakazawa, H.; Ito, Y. *J. Chromatogr.* **1991**, *538*, 203-212.
11. Kamikura, M.; Nakazato, K. *J. Food Hyg. Soc. Jpn.* **1984**, *25*, 517-524.
12. Inoue, H.; Takeda, Y.; Saito, S.; Sakai, H.; Sakuragi, R. *Yakugaku Zasshi* **1974**, *94*, 577-586.
13. Scott, A.I. *Interpretation of the Ultraviolet Spectra of Natural Products*, Pergamon Press, New York, 1964, Ch. 8, pp. 228-312.
14. Oka, F.; Oka, H.; Ito, Y. *J. Chromatogr.* **1991**, *538*, 99-108.
15. Roscher, R.; Winterhalter, P. *J. Agric. Food Chem.* **1993**, *41*, 1452-1457.

RECEIVED December 30, 1994

Downloaded by YORK UNIV on June 29, 2012 | http://pubs.acs.org
Publication Date: May 15, 1995 | doi: 10.1021/bk-1995-0593.ch008

Downloaded by PENNSYLVANIA STATE UNIV on June 29, 2012 | http://pubs.acs.org
Publication Date: May 15, 1995 | doi: 10.1021/bk-1995-0593.ch009

Chapter 9

Separation of Cucurbitacin B and Cucurbitacin E from Fruit Base of *Cucumis melo* L. by High-Speed Countercurrent Chromatography

Q. Z. Du[1], X. P. Xiong[1], and Yoichiro Ito[2]

[1]Tea Research Institute, Chinese Academy of Agricultural Sciences, Hangzhou, Zhejiang 310008, China
[2]Laboratory of Biophysical Chemistry, National Heart, Lung, and Blood Institute, National Institutes of Health, Building 10, Room 7N322, Bethesda, MD 20892

Cucurbitacin B (CuB) and cucurbitacin E (CuE) were separated from the fruit base of *Cucumis melo L.* by high-speed countercurrent chromatography (CCC) using a two-phase solvent system composed of hexane/ethyl acetate/methanol/water (12:24:16:9 by volume). Three successive 300mg injections of sample, indicated by HPLC assay to contain 61.4% CuB and 35.1% CuE, were made at leap-frog intervals, prior to emergence of the second peak, thereby greatly reducing the overall separation time. Measurement of the stationary phase retention indicated that many more sample injections can be made without renewing the column contents.

Guadi, the fruit base of *Cucumis melo L.*, is a Chinese traditional herbal drug used for treating chronic hepatitis (*1*). Recent studies (*2,3*) have shown that cucurbitacin B (CuB) and cucurbitacin E (CuE) (Fig. 1) are the main bioactive components in Guadi, and Cucurbitacin Tablet containing a mixture of CuB and CuE extracted from the fruit base of *Cucumis melo L.* is currently substituted for Guadi in China. However, it has been found that the curative effect of CuB is different from that of CuE (*4*), hence the separation of these two compounds is desired. In this paper, we report isolation of CuB and CuE from a crude fruit extract of *Cucumis melo L.* by high-speed CCC (*5*).

Experimental

Apparatus. High-speed CCC experiments were performed using a coil planet centrifuge equipped with a multilayer coil column that was designed and fabricated at the Beijing Institute of New Technology Application, Beijing, China. The multilayer coil was prepared by winding a 1.6mm ID PTFE (polytetrafluoroethylene) tube coaxially onto the column holder hub. The total column capacity measured 230 ml. The high-speed CCC centrifuge was rotated at 800 rpm with an 8-cm revolution radius. The system was equipped with an FMI pump (Zhejiang Instrument Factory, Hangzhou, China), a variable UV detector (UV-752, Shanghai Analytical Instrument Factory, Shanghai, China), a recorder, an injection valve and a fraction collector.

0097–6156/95/0593–0107$12.00/0

Reagents. All organic solvents were of analytical grade and purchased from Shanghai Chemical Factory, Shanghai, China. Standards for cucurbitacin B (CuB) and cucurbitacin E (CuE) were purchased from Tianjin Institute of Pharmaceutical Research, State Pharmaceutical Administration of China, Tianjin, China.

Extraction of CuB and CuE from *C. melo* Fruit. The extraction was initiated by refluxing 1 Kg of *C. melo* fruit powder in 10 liters of 95% ethanol at 80°C for 2 hours. The ethanol extract was concentrated to a syrup in a rotary evaporator. The syrup was extracted with ether. The ether extract was evaporated to dryness, defatted with petroleum ether, then redissolved in ethanol and decolorized with active carbon. The ethanol solution was evaporated to dryness to obtain a crude CuB and CuE mixture. The crude mixture was recrystallized from methanol to yield 2.2 g of white powder containing CuB and CuE.

High-Speed CCC Separation Procedure. The experiment was performed with a two-phase solvent system composed of hexane/ethyl acetate/methanol/water (12:24:16:9, v/v). The solvent mixture was thoroughly equilibrated in a separatory funnel at room temperature and the two phases separated shortly before use. In each separation the multilayer coil was first entirely filled with the lower aqueous stationary phase. Then the upper organic mobile phase was pumped into the inlet of the column at a flow rate of 1.5 ml/min, while the apparatus was rotated at 800 rpm. After the mobile phase front emerged and the two phases had established hydrodynamic equilibrium throughout the column, three successive injections of the sample solution (300mg of a CuB and CuE mixture in 20ml of mobile phase) was made through the injection valve in 100 minute intervals. The effluent from the outlet of the column was continuously monitored with a UV detector at 234 nm and the fractions were collected with a fraction collector.

HPLC Analysis. The original sample solution and CCC fractions were analyzed by reversed-phase HPLC using Shimadzu HPLC equipment (Shimadzu Corporation, Kyoto, Japan) consisting of an LC-10AD pump, an SPD-10A UV-VIS detector, a manual injector and a C-R10A recording processor. HPLC separations were performed on a Shim-pack CLC-ODS-C18 column, 15 X 0.60 cm ID (Shimadzu Corporation). The mobile phase composed of methanol-ethyl acetate-water (3:1:1, v/v) was eluted isocratically at a flow-rate of 1 ml/min and the effluent was monitored at 234 nm.

Results and Discussion

HPLC analysis of the original sample shown in Fig. 2 indicates that the sample contained 35.1% CuE (retention time: 4.56 min) and 61.4% CuB (retention time: 5.75 min). The high-speed CCC separation consisted of three successive injections of the sample at 100 minute intervals. This interval was chosen to leap-frog the second peak, so that the overall separation time for the three injections was significantly shorter than three times the time required for separation of a single sample. After the separation was completed, the column contents were expelled into a graduated cylinder to estimate the retention of the stationary phase. It was found that 161 ml (70% of the total column capacity) of the stationary phase still remained in the column, suggesting that many more sample injections could be made without replenishing the stationary phase.

Fig. 3 shows the chromatogram resulting from three successive sample injections. The fractions corresponding to peak 1 and peak 2 contained CuE and CuB, respectively, as confirmed by the HPLC analysis using the CuE and CuB standards. Peak fractions corresponding to each component were combined and evaporated to dryness in vacuum to yield 307 mg of CuE from peak 1 and 501 mg of CuB from peak 2, a recovery of 89.8% of total sample weight. The recovered amounts correspond to a sample composition of 37.9% CuE and 61.2% CuB, in good agreement with the HPLC assay.

Downloaded by PENNSYLVANIA STATE UNIV on June 29, 2012 | http://pubs.acs.org
Publication Date: May 15, 1995 | doi: 10.1021/bk-1995-0593.ch009

Downloaded by PENNSYLVANIA STATE UNIV on June 29, 2012 | http://pubs.acs.org
Publication Date: May 15, 1995 | doi: 10.1021/bk-1995-0593.ch009

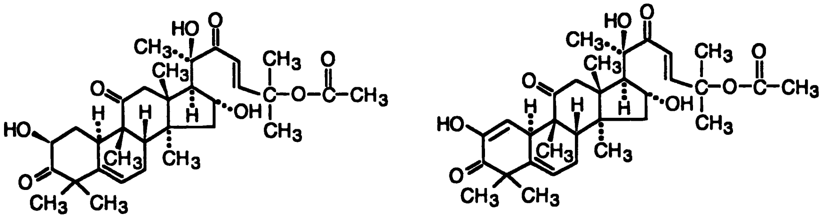

Cucurbitacin B **Cucurbitacin E**

Figure 1. Structures of cucurbitacin B (CuB) and cucurbitacin E (CuE).

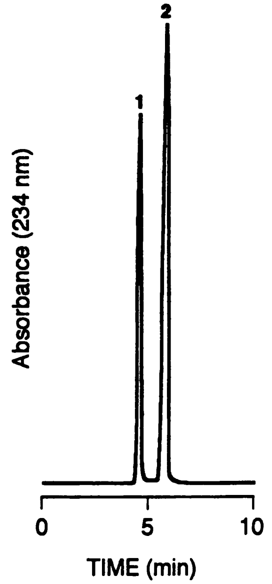

Figure 2. HPLC analysis of CuB and CuE in the original sample solution obtained from the fruit base of *Cucumis melo L.* Mobile phase: methanol-ethyl acetate-water (3:1:1, v/v); flow-rate: 1 ml/min; detection: 234 nm. Peak 1: CuE; peak 2: CuB.

Downloaded by PENNSYLVANIA STATE UNIV on June 29, 2012 | http://pubs.acs.org
Publication Date: May 15, 1995 | doi: 10.1021/bk-1995-0593.ch009

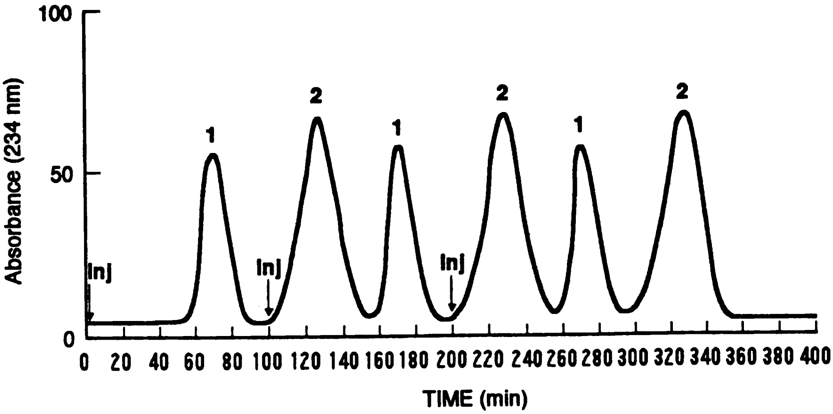

Figure 3. High-speed CCC separation of CuB and CuE by three successive injections of the sample solution. Solvent system: hexane/ethyl acetate/methanol/water (12:24:16:9); flow-rate: 1.5 ml/min; detection: 234 nm. Peak 1: CuB; peak 2: CuE.

The above results were obtained from a 230ml capacity column. We believe that increased production of CuB and CuE may be feasible by the use of a larger capacity column.

Literature Cited

1. Hu, R.S.; Peng; Y.G.; Chen, B.Y.; Chen, Y.X. *Chinese Traditional and Herbal Drugs* **1982**, 13 (10), 13.
2. Han, D.W. *Chinese Journal of Medicine* **1979**, 59, 206.
3. Liu, Y.J.; Liu, W.Q. *Chinese Traditional and Herbal Drugs* **1992**, 23(11), 605.
4. Huang, X.D.; Gou, J.X. *Chinese Foreign Medicine-Pharmaceutical Division* **1985**, 3, 132.
5. Ito, Y. *CRC Crit. Rev. Anal. Chem.* **1986**, 17, 65.

RECEIVED January 24, 1995

Downloaded by CORNELL UNIV on June 29, 2012 | http://pubs.acs.org
Publication Date: May 15, 1995 | doi: 10.1021/bk-1995-0593.ch010

Chapter 10

Purification of the Human Immunodeficiency Virus-1 Aspartyl Proteinase Substrate Peptide

Martha Knight[1], Yoichiro Ito[2], Bhaskar Chandrasekhar[1], Kazuyuki Takahashi[1], and Anil B. Mukherjee[3]

[1]Peptide Technologies Corporation, 8401 Helgerman Court, Gaithersburg, MD 20877
[2]Laboratory of Biophysical Chemistry, National Heart, Lung, and Blood Institute, National Institutes of Health, Building 10, Room 7N322, Bethesda, MD 20892
[3]Human Genetics Branch, National Institute of Child Health and Human Development, National Institutes of Health, Bethesda, MD 20892

A rapid and sensitive assay for the aspartyl protease enzyme of the HIV-1 virus is being developed for detecting potential inhibitors. A tritiated peptide serves as the substrate and after the reaction, the radiolabeled product is counted in solution while the substrate is removed from solution by adsorption onto charcoal added to the tube as a tablet. The labeled substrate was synthesized with an unsaturated proline in the sequence. After tritiation the radiolabeled substrate peptide was isolated by rapid countercurrent chromatography. The tritiation reaction was loaded on a multi-layer coil planet centrifuge in the solvent system t-butyl methyl ether, acetonitrile and 1% aq. trifluoroacetic acid (2:2:3 by volume) and chromatographed at a flow of 120 ml/hr and a centrifugation rate of 800 rpm. The excess radioactive side products were eluted after the solvent front followed by the peptide. The peptide was separated within 1 hr and could be directly used in the experiments.

The retroviral-caused acquired immunodefficiency syndrome (AIDS) is a serious, threatening public health problem today. It is of great importance to develop a cure for this disease. The most successful drugs developed to date are those directed to the reverse transcriptase enzyme that synthesizes the retroviral DNA in infected cells and permits the growth of viral particles. Reverse transcriptase inhibitor drugs such as AZT and DDI ameliorate the symptoms and delay the onset of the disease but do not cure it. Presently, another enzyme present in the HIV-1 virus that has been studied is the aspartyl proteinase which functions to process the viral translated polypeptide into the individual protein components (*1-2*). A potent and specific inhibitor of this enzyme may serve as a therapeutic drug for AIDS, possibly in combination with other drugs. The aspartyl protease is an 11 KDa, 99-residue protein that functions as a homodimer with a 2-fold

0097–6156/95/0593–0111$12.00/0

axis of symmetry. The active site has the sequence Asp-Thr(Ser)-Gly which identifies it with the aspartyl proteinase family of proteolytic enzymes (*3-5*). Its peptide bond cleavage specificity resembles, generally, that of chymotrypsin (*6-7*).

A convenient and sensitive radiopeptidase assay for the HIV-1 aspartyl proteinase is proposed as a screen for potential inhibitors of this enzyme. The rapid procedure eliminates the need for time consuming HPLC separations presently used to measure products formed by the action of the enzyme on a peptide substrate. Thus, potential anti-AIDS therapeutics will be identified more rapidly.

Downloaded by CORNELL UNIV on June 29, 2012 | http://pubs.acs.org
Publication Date: May 15, 1995 | doi: 10.1021/bk-1995-0593.ch010

Design of Assay. While there are some assays developed to date that are based on colorimetric and fluorimetric detection or ion-exchange separations (*8-10*), we have adapted a previously used scheme of separation based on the use of an amphiphilic substrate peptide with part of its sequence hydrophobic and the other part highly polar. Such a peptide when cleaved generates fragments, one of which is relatively polar and can easily be separated from the substrate which remains bound to hydrophobic surfaces (*11-12*). The substrate is radiolabeled in its polar segment. After the proteolytic reaction, a dextran charcoal pellet is added into the reaction and the remaining substrate binds to the charcoal. The radiolabeled product can be prevented from binding by addition of cold peptide and the radioactivity due to the product can be counted in solution. A suitable peptide that can serve as a substrate in an assay for the aspartyl protease was designed from the following analysis.

The sites in the *gag-pol* polypeptide which are hydrolyzed by the retroviral aspartyl protease have been identified and peptides whose sequences span these sites were tested for susceptibility to cleavage by this enzyme. The results taken from this study are in Table I (*13*). The K_m and V_{max} measured for each peptide are listed. Among these peptides the best candidate that could serve as an amphiphilic substrate in this assay is the peptide V of the *pol*59-72 sequence which has a relatively hydrophobic sequence on the amino side of the scissile bond and no aromatic amino acids on the carboxyl side. Moreover, the peptide substrate has the highest V_{max} and one of the lowest values of the K_m. Thus, it was hypothesized a useful substrate could be designed from this peptide. Other peptides with modifications could be used. Most assays have been developed from peptides I,II and III (*9-10*) and an analogue of III has been used as an inhibitor complex with the enzyme that allowed the crystal structure to be determined (*14*). Thus, any of the peptides with appropriate modification could serve in this assay, but the sequence selected here requires the least modification and has the best kinetic parameters.

Therefore, Pca-Gly-Thr-Val-Ser-Phe-Asn-Phe-dehydroPro-Gln-Ile-Thr-NH_2, which corresponds to the *pol* 61-72 sequence, was synthesized with dehydro Pro in place of Pro^{69}. Pyroglutamic acid substituted for Gln and the carboxyl end was amidated to reduce susceptibility to exopeptidases. The peptide was labeled by catalytic tritiation placing 2 atoms on the Pro. After various experiments, it was decided to improve the solubility of the substrate while still preserving the amphiphilicity, by adding a Lys to the carboxyl end. The assay is diagrammed using this peptide as shown in Fig. 1.

Downloaded by CORNELL UNIV on June 29, 2012 | http://pubs.acs.org
Publication Date: May 15, 1995 | doi: 10.1021/bk-1995-0593.ch010

Table I. Hydrolysis of peptides corresponding to peptide cleavage sites by the HIV-1 Aspartyl Protease (*13*)

Peptides Hydrolyzed		*Sequence*	K_m	V_{max}
			mM	*nmol/ min/mg*
		HIV-1 Site		
I	GAG 124-138	HSSQVSQNY↓PIVQNI	N.D.	>275
II	GAG 357-370	GHKARVL↓AEAMSQV	2.3	100
III	GAG 370-383	VTNTATIM↓MQRGNF	0.16	682
IV	GAG 440-453	SYKGRPGNF↓LQSRP	13.9	382
V	POL 59-72	DRQGTVSFNF↓PQIT	0.70	954
VI	POL 162-174	GCTLNF↓PISPIET	N.D.	>120
VII	POL 721-734	AGIRKIL↓FLDGIDK	6.1	145

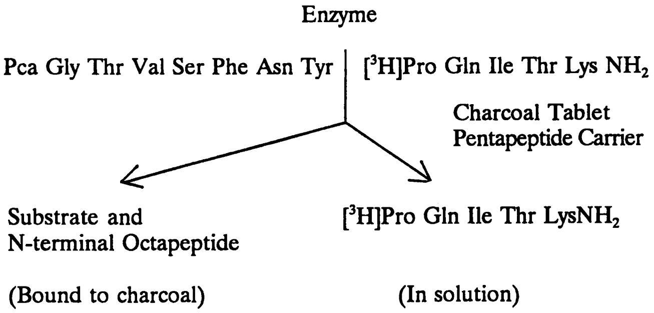
Enzyme
Pca Gly Thr Val Ser Phe Asn Tyr
[^{3}H]Pro Gln Ile Thr Lys NH_2
Charcoal Tablet
Pentapeptide Carrier
Substrate and
N-terminal Octapeptide
[^{3}H]Pro Gln Ile Thr LysNH_2
(Bound to charcoal)
(In solution)

Figure 1. Diagram of the HIV protease radiometric assay.

The initial experiments of the assay are herein described, followed by the introduction of an improved substrate. Countercurrent chromatography was used in the preparation of the new radiolabeled substrate.

Experimental

Preparation of labeled substrate peptide. The peptides in Table II were synthesized by solid phase methods, analyzed by amino acid analysis and HPLC as previously described (*15-16*) and were greater than 95% pure. The dehydro Pro peptides (#623 and #623C) were radiolabeled and used in the assays. The peptides with Pro (#623A and #623B) are concentration standards for HPLC experiments and kinetic measurements.

Table II. *POL* 61-72 Substrate Peptides

No.	*Structure*	*Experimental use*
623	Pca-GTVSFNF▲PQIT-amide	for tritiation
623A	Pca-GTVSFNFPQIT-amide	HPLC standard, K_m determination
623B	Pca-GTVSFNYPQITK-amide	HPLC standard, K_m determination
623C	Pca-GTVSFNY▲PQITK-amide	for tritiation

Pca = pyrrolidone carboxylic acid or pyroglutamic acid
▲Pro = dehydro Proline

The dehydro Pro peptides were sent to New England Nuclear (Boston, MA) for catalytic tritiation. In the case of peptide 623, an amount of 10 mCi was received and purified by adsorption to polystyrene (SM-2 resin, Bio-Rad Laboratories, Hercules, CA). The specific activity was measured to be 1.8 X 10^{14} cpm/mmole which is close to 120 mCi/mg. An analytical separation was run by reverse phase HPLC. The specific activity was determined from the peak height of the peptide and the radioactivity eluting at the same retention time of 15 min.

Peptide, #623C, with Lys at the carboxyl end was radiolabeled as above for experiments but was purified by high-speed countercurrent chromatography. This preparation of substrate was also used in the biochemical experiments.

Countercurrent chromatographic purification. An amount of 10 mCi of the tritiation reaction of the dehydro-Pro tridecapeptide, #623C, was purified. 10 mg was catalytically tritiated to a specific activity of 132.3 mCi/mg. A sample of 10 mCi was loaded on a multi-layer coil planet centrifuge (P.C. Inc, Potomac, MD), 325 ml coil of 1.6 mm I.D. tubing 165 m long (*17*). The apparatus has a

Downloaded by CORNELL UNIV on June 29, 2012 | http://pubs.acs.org
Publication Date: May 15, 1995 | doi: 10.1021/bk-1995-0593.ch010

In Modern Countercurrent Chromatography; Conway, W., et al.;
ACS Symposium Series; American Chemical Society: Washington, DC, 1995.

10 cm orbital radius and the ß value of the tubing coil ranges from 0.5 at the internal terminal to 0.85 at the external end. The tubing is coiled in 16 layers. The coil was filled with the upper phase of the solvent system, t-butyl methyl ether/acetonitrile/1% aq. trifluoroacetic acid in a volume ratio of 2:2:3. The instrument was rotated at 800 rpm and the lower aq. phase used as the mobile phase eluted at 120 ml/hr. A Beckman Accu-Flo pump (Fullerton, CA) and an LKB Ultrorac fraction collector (Piscataway, NJ) were used. The separation was conducted at room temperature. Fractions of 3 ml were collected every min. Aliquots of 25 µl of each fraction were counted in a liquid scintillation counter. The fractions determined to contain radioactive peptide were pooled and the solvent evaporated. The sample was dissolved in 50% methanol and stored at -40°C.

Downloaded by CORNELL UNIV on June 29, 2012 | http://pubs.acs.org
Publication Date: May 15, 1995 | doi: 10.1021/bk-1995-0593.ch010

Charcoal Pellet Radiometric Enzymatic Assay. The enzyme, HIV-1 aspartyl protease, 1 µg or less, (Bachem Bioscience, Inc. Philadelphia, PA or American Bio-Technologies, Cambridge, MA) is reacted with 1 pM [^{3}H] substrate (approximately 10,000 cpm) in a suitable buffer such as 0.05 M NaH_2PO_4, pH 5.7, 0.05 M Tris, pH 7.5, or 1.3 M Na acetate, pH 5.2, in a total volume of 1 ml at 37°C for 15 min. At the end of the incubation, the duplicate sample tubes are placed in ice and 20 µl of 2.5 N HCl and a high concentration of carrier peptide, Pro-Gln-Ile-Thr-Lys-amide, 20 µl of 10 mg/ml solution, are added to each tube. A sample acidified at time 0 is also made. A charcoal pellet (dextran-coated charcoal, 2 mg, West Chem Products) is added, the tubes are vortexed and left to stand at room temperature for 20 min. The tubes are centrifuged at 1000 x g for 10 min and 700 µl of the supernatant is counted by scintillimetry. The concentration of product formed is calculated from the cpm at the end of the incubation period minus the cpm at time 0. The amount of enzyme and period of incubation are adjusted to generate 10 to 20% product under initial velocity conditions.

Results and Discussion

Recombinant HIV-1 aspartyl protease was reacted with the ^{3}H-dodecapeptide substrate, #623, in 0.05 M Tris, pH 7.5, in a reaction containing 1 µg enzyme, 12,015 cpm or 0.065 nM ^{3}H peptide, in 1 ml reaction volume. The same amount of substrate with 100 µg chymotrypsin (Sigma, St. Louis, MO) was reacted and another reaction of the HIV enzyme in 0.15M NaCl in phosphate was run as well. The reactions were done in duplicate and incubated at 37°C for 15 min. At 0 and 15 min, reactions were terminated by the addition of 20 µl of 2.5 N HCl and placed in ice. Then to all tubes, 20 µl of 10^{-2}M Pro-Gln-Ile-Thr- amide and a tablet of dextran coated charcoal were added. The tubes were mixed and left to stand at room temperature for 20 min. The samples were centrifuged at 4000 rpm for 15 min and 700 µl of the supernatant were counted. The following results were obtained after subtracting the cpm at 0 min from the cpm at 15 min. See Table III.

Downloaded by CORNELL UNIV on June 29, 2012 | http://pubs.acs.org
Publication Date: May 15, 1995 | doi: 10.1021/bk-1995-0593.ch010

Table III. Hydrolysis of 65 pM [^{3}H] Pro^{69}*POL*61-72

Enzyme	*Amount*	*CPM*	*pM/15 min*	*% Product*
Chymotrypsin	100 µg	3123	16.9	26
rec HIV protease	1 µg	0	0	0
rec HIV protease plus NaCl	1 µg	604	3.3	5

The results show the generation of product by the two enzymes. The reaction with chymotrypsin is to show the validity of the assay in case the retroviral enzyme was not active. The activity of the aspartyl protease is stimulated by the presence of NaCl as is reported by others (*18*). This convenient assay is shown to work and can be used in experiments to screen for inhibitory compounds.

It was decided to modify the structure of the peptide by adding positively charged Lys to the carboxyl end to improve the water solubility. Also, if necessary, the peptide could be labeled at that site on the ϵ amino group. (The Lys can be labeled with ^{14}C-O-methyl-isourea to ^{14}C-Homoarg, for example, which will preserve the positive charge, maintain the water solubility and be a more stable compound). The Phe^{68} at the scissile bond was changed to Tyr for easier analytical determination of specific activity (by absorbance) and to make the peptide more water soluble by its increased polarity. Studies of specificity of the enzyme have indicated Tyr-Pro to be an optimal site of cleavage (*7*). Thus, the peptide substrate Pca-Gly-Thr-Val-Ser-Phe-Asn-Tyr-Pro-Gln-Ile-Thr-Lys-NH_2 (#623B) was synthesized for preliminary studies by HPLC to determine if it is a substrate and has the site of cleavage. The HPLC separation did show the expected proteolysis. The corresponding dehydroPro peptide (#623C) was then synthesized and tritiated.

The countercurrent chromatographic separation of tritiated peptide #623C is shown in Figure 2. The counts per min are plotted per fraction. The stationary phase emerged at the 29th fraction which is the solvent front. Thus the stationary phase retained in the run was 69.3% The tritiated peptide was recovered in the peak of fractions 50-56. The peptide was eluted in less than an hour in these conditions. From the elution volume of the peak the partition coefficient is 3.4 (lower phase to upper phase). Most of the radioactivity or side products was eluted in the solvent front. About 15% of the total radioactivity was in the peptide peak. The peptide could be used directly in the biochemical experiments.

The use of this solvent system consisting of almost equal parts of ether, acetonitrile and an aqueous solution (*19*) enables the separation of the more polar peptides at room temperature under rapid flow rates and centrifugation rates. Previously, most peptides could not be chromatographed easily in the high-speed conditions due to carryover of the stationary phase. Certain hydrophobic peptides were separated at elevated temperatures (*17*). In this

Downloaded by CORNELL UNIV on June 29, 2012 | http://pubs.acs.org
Publication Date: May 15, 1995 | doi: 10.1021/bk-1995-0593.ch010

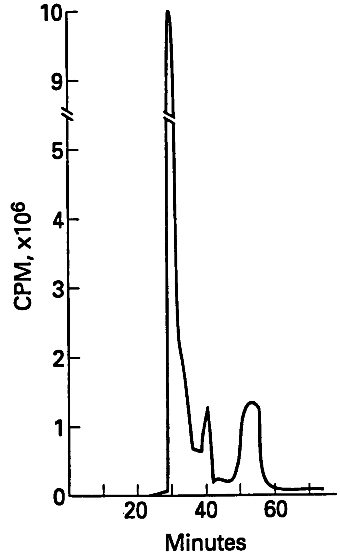

Figure 2. Separation of [^{3}H-Pro^{69},Tyr^{68},Lys^{73}]*pol*(61-72) from the tritiation reaction of # 623C by high speed countercurrent chromatography. Radioactivity indicated is of the elution fractions collected every minute. Radiolabeled peptide was contained in fractions 50-56. Conditions of the experiment are described in the text.

stable 2-phase solvent system, the high density difference between the phases diminishes carryover. Thus, it is now possible that all peptides can be purified by high-speed countercurrent chromatography.

Acknowledgments

This work was supported in part by a Small Business Innovation Research grant no. AI 33255 from the Public Health Service. This research was conducted in part under a Cooperative Research and Development agreement (CRADA) with the National Institutes of Health.

Literature Cited

1. Ratner, L.; Haseltine, W.; Patarca, R.; Livak, K.J.; Starcich, B.; Josephs, S.F.; Doran, E.R.; Rafalski, J.A.; Whitehorn, E.A.; Baumeister, K.; Ivanoff, L.; Petteway, S.R., Jr.; Pearson, M.L.; Lautenberger, J.A.; Papas, T.S.; Ghrayeb, J.; Chang, N.T.; Gallo, R.C.; Wong-Staal, F., *Nature* **1985,** *313,* 277-284.
2. Toh, H.; Ono, M.; Saigo, K.; Miyata, T., *Nature* **1985,** *315,* 691-692.
3. Pearl, L.H., Taylor, W.R., *Nature* 1987, *329,* 351-354.

4. Kohl, N.E.; Emini, E.A.; Schlief, W.A.; Davis, L.; Heimbach, J.C.; Dixon, R.A.; Scholnick, E.M.; Sigal, I.S., *Proc. Natl. Acad. Sci. USA* **1988,** *85*, 4686-4690.
5. Navia, M.A.; Fitzgerald, P.M.D.; McKeever, B.M.; Leu, C.T.; Heimbach, J.C.; Herber, W.K.; Sigal, I.S.; Drake, P.L.; Springer, J.P., *Nature* **1989,** *337*, 615-620.
6. Wlodawer, A.; Miller, M.; Jaskólski, M.; Sathyanarayana, B.K.; Baldwin, E.; Weber, I.T.; Selk, L.M.; Clawson, L.; Schneider, J.; Kent, S.B.H., *Science* **1989,** *245*, 616-621.
7. Henderson, L.E.; Benveniste, R.E.; Sowder, R.; Copeland, T.D.; Schultz, A.M.; Oroszlan, S., *J. Virol.* **1988,** *62*, 2587-2595.
8. Broadhurst, A.V.; Roberts, N.A.; Ritchie, A.J.; Handa, B.K.; Day, C., *Anal. Biochem.* **1991,** *193*, 280-286.
9. Billich, A.; Winkler, G., *Peptide Res.* **1990,** *3*, 274-276.
10. Geoghegan, K.F.; Spencer, R.W.; Danley, D.E.; Contillo, L.G.,Jr.; Andrews, G.C.; *FEBS Lett.* **1990,** *62*, 119-122.
11. Knight, M.; Klee, W.A., *J. Biol. Chem.* **1979,** *254*, 10426-10430.
12. Knight, M.; Klee, W.A., *J. Biol. Chem.* **1978,** *253*, 3843-3847.
13. Darke, P.L.; Nutt, R.F.; Brady, S.F.; Garsky, V.M.; Ciccarone, T.M.; Leu, C.T.; Lumma, P.K.; Freidinger, R.M.; Veber, D.F.; Sigal, I.S., *Biochem. Biophys. Res. Commun.* **1988,** *156*, 297-303.
14. Miller, M.; Schneider, J.; Sathyanarayana, B.K.; Toth, M.V.; Marshall, G.R.; Clawson, L.; Selk, L.; Kent, S.B.H.; Wlodawer, A., *Science* **1989,** *246*, 1149-1152.
15. Stewart, J.M.; Young, J.D. *Solid Phase Peptide Synthesis*; Pierce Chem. Co.: Rockland, IL, 1983.
16. Knight, M.; Gluch, S.; Meyer, R.; Cooley, R.S., *J. Chromatog.* **1989,** *484*, 299-305.
17. Knight, M; Ito, Y.; Peters, P.; diBello, C., *J. Liq. Chromatog.* **1985,** *8*, 2281-2291.
18. Richards, A.D.; Roberts, R.F.; Durin, B.M.; Graves, M.C.; Kay, J., *FEBS Lett.* **1989,** *247*, 113-117.
19. Knight, M.; Takahashi, K., *J. Liq. Chromatog.* **1992,** *15*, 2819-2829.

RECEIVED November 28, 1994

Downloaded by CORNELL UNIV on June 29, 2012 | http://pubs.acs.org
Publication Date: May 15, 1995 | doi: 10.1021/bk-1995-0593.ch010

Downloaded by STANFORD UNIV GREEN LIBR on June 29, 2012 | http://pubs.acs.org
Publication Date: May 15, 1995 | doi: 10.1021/bk-1995-0593.ch011

Chapter 11

Countercurrent Chromatographic Isolation of High- and Low-Density Lipoprotein Fractions from Human Serum

Y. Shibusawa[1], T. Chiba[1], U. Matsumoto[1], and Yoichiro Ito[2]

[1]Division of Analytical Chemistry, Tokyo College of Pharmacy, 1432–1 Horinouchi, Hachioji, Tokyo 192–03, Japan
[2]Laboratory of Biophysical Chemistry, National Heart, Lung, and Blood Institute, National Institutes of Health, Building 10, Room 7N322, Bethesda, MD 20892

High- and low-density lipoproteins (HDLs, LDLs) were fractionated by countercurrent chromatography using the type-XL cross-axis coil planet centrifuge using two-phase aqueous polymer systems. The best separations were achieved with a polymer phase system composed of 16%(w/w) polyethylene glycol 1000 and 12.5%(w/w) dibasic potassium phosphate at pH 9.4 by eluting the lower phase at 2.0 ml/min. HDL-LDL fractions containing 1.26, 1.27 and 0.42 mg/ml of phospholipids, cholesterols and triglycerides, respectively, were collected from 4 ml of human serum within 3 h. The presence of HDLs and LDLs were confirmed by gel electrophoresis with Sudan Black B staining. The HDL-LDL fractions were found to be free of serum proteins in SDS polyacrylamide slab gel electrophoresis.

Serum lipoproteins are molecular assemblies of lipids and proteins. They consist of hydrophobic core molecules, such as triglycerides and esterified cholesterols, and surface amphophilic molecules composed of apoproteins, phospholipids and free cholesterols.

Chromatographic separations of lipoproteins have been reported using several types of column packings (*1-6*). Countercurrent chromatography (CCC) refers to liquid-liquid partition chromatography which is carried out without the aid of a solid support matrix. Consequently the system eliminates all complications arising from this source.

Recently, we have succeeded in separating high-density (HDLs) and low-density (LDLs) lipoproteins with an aqueous polymer phase system using a type-XLL cross-axis coil planet centrifuge (CPC) (*7*). In this work the human serum was first processed by ultracentrifugation to eliminate serum proteins such as albumins and globulins from the sample. In the present study, this step was also done by CCC using a type-XL cross-axis CPC with a polymer phase system composed of polyethylene glycol (PEG) and potassium phosphate buffers over a broad range of pH.

Experimental

Apparatus. The detailed design of the cross-axis CPC has been described earlier (*8,9*). The apparatus holds a symmetrically placed pair of horizontal rotary shafts, one on each side of the rotary frame,

0097–6156/95/0593–0119$12.00/0

Downloaded by STANFORD UNIV GREEN LIBR on June 29, 2012 | http://pubs.acs.org
Publication Date: May 15, 1995 | doi: 10.1021/bk-1995-0593.ch011

at a distance of 10cm from the centrifuge axis. A spool-shaped column holder is mounted on each rotary shaft at an off-center position 10cm from the midpoint.

Each multilayer coil separation column was prepared from 2.6 mm ID polytetrafluoroethylene (PTFE) tubing (Zeus Industrial Products, Raritan, NJ, USA) by winding it onto a 15.2 cm diameter holder, forming multiple layers of left-handed coils between a pair of flanges spaced 5 cm apart. The column consisted of 4 layers of coil with a 170-ml capacity. A pair of columns mounted on the rotary frame was connected in series to make up a total capacity of 340 ml. Both inflow and outflow tubes exit together at the center of the top plate of the centrifuge case where they are tightly supported with silicon-rubber-padded clamps. The speed of the apparatus is regulated at 500 rpm with a speed control unit (Bodine Electric Company, Chicago, IL, USA).

Reagents. Polyethylene glycol 600 (PEG 600)(number average molecular weight[Mn]=570-630), PEG 1000 (Mn=950-1050), PEG 2000 (Mn=1800-2200), PEG 4000 (Mn=2700-3400) and potassium phosphates were obtained from Kanto Chemicals (Tokyo, Japan). Test reagents for phospholipids (Phospholipid B test Wako), cholesterols (Cholesterol C test Wako), and triglycerides (Triglyceride G test Wako) were purchased from Wako Pure Chemical Industries (Osaka, Japan). Other chemicals were reagent grade.

Preparation of PEG-Potassium Phosphate Aqueous Two-Phase Systems. Two-phase solvent systems composed of 16%(w/w) PEG (600, 1000, 2000 or 4000) and 12.5%(w/w) potassium phosphate (KPi) aqueous solutions were prepared by dissolving 320 g of PEG and 250 g of KPi (mixture of anhydrous KH_2PO_4 and K_2HPO_4) in 1430 g of distilled water, and the solvent systems containing 25% PEG and 12.5% KPi were similarly prepared by dissolving 500 g of PEG and 250 g of KPi in 1250 g of distilled water.

Fig. 1 shows the composition of eight different polymer phase systems composed of PEG 1000 and KPi buffer. The pH values of the solvent systems were adjusted to 6.8, 7.3, 8.0 and 9.4 by changing the ratio between monobasic and dibasic potassium phosphates in the two-phase system. When the concentration of monobasic to dibasic potassium phosphate slightly exceeds a one to one ratio, the solvent mixture forms a single phase.

Preparation of Standard HDL, LDL and VLDL Fractions from Human Serum. Each main class of lipoproteins was collected by ultracentrifugation using a multiple discontinuous density gradient, as proposed by Sclavons et al. (*10*).

Human blood was collected from fasting normolipidemic healthy males in tubes containing 0.15% EDTA. The plasma was separated by centrifugation (7°C, 700 g, 20 min) and its density was adjusted to 1.30 g/ml by adding solid KBr. A discontinuous density gradient (total volume 18.5ml) was formed by layering adjusted plasma salt (NaCl/KBr) solutions with densities of 1.240, 1.063, 1.019 and 1.006 g/ml, and distilled water (0.5 ml) sequentially over the sample plasma. The tubes were placed in an RPV 50T vertical rotor and subjected to ultracentrifugation at 313500 g at 7°C for 80 min.

Measurement of Partition Coefficient (K) Values of Lipoproteins and Serum Proteins. The partition coefficient of each protein sample was determined spectrophotometrically by a simple test tube procedure. About 1.0 ml of each phase of the equilibrated two-phase solvent system was delivered in a test tube to which about 1 mg of the serum protein or 0.1 ml of the standard lipoprotein fraction was added. The contents were thoroughly mixed and allowed to settle at room temperature. After two clear layers were formed, an aliquot (usually 0.5 ml) of each phase was pipetted and diluted with 1.0 ml of distilled water to determine the absorbance at 280 nm using a Shimadzu UV-1200

Downloaded by STANFORD UNIV GREEN LIBR on June 29, 2012 | http://pubs.acs.org
Publication Date: May 15, 1995 | doi: 10.1021/bk-1995-0593.ch011

Solvent System (w/w %)	Composition (w/w %)			pH	Volume Ratio (UP/LP)***
	PEG 1000	KH_2PO_4	K_2HPO_4		
PEG*1000 25%	25%	0	12.5	9.4	1.31
KPi** 12.5%		2.1	10.4	8.0	1.40
		4.2	8.3	7.3	1.61
		6.25	6.25	6.8	1.73
PEG 1000 16%	16%	0	12.5	9.4	0.82
KPi 12.5%		2.1	10.4	8.0	0.88
		4.2	8.3	7.3	1.00
		6.25	6.25	6.8	1.22

PEG* : polyethylene glycol; KPi**: potassium phosphate; UP/LP***: volume of upper phase divided by that of lower phase

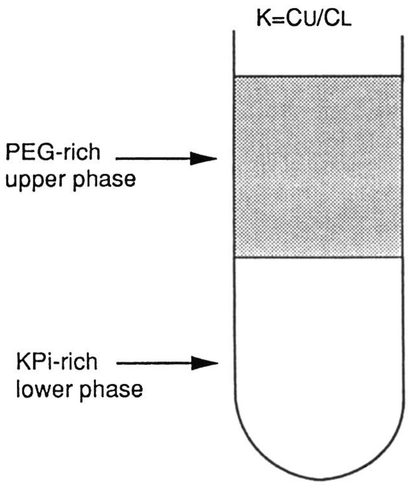

Figure 1. Composition of various aqueous polymer phase systems used for countercurrent chromatography of human serum lipoproteins.

Downloaded by STANFORD UNIV GREEN LIBR on June 29, 2012 | http://pubs.acs.org
Publication Date: May 15, 1995 | doi: 10.1021/bk-1995-0593.ch011

spectrophotometer (Shimadzu Corp., Kyoto, Japan). The partition coefficient values ($K=C_U/C_L$) were obtained by dividing the absorbance value of the upper phase by that of the lower phase.

Preparation of Human Serum from Peripheral Blood. Human blood (ca. 10 ml) was collected from normolipidemic males by venipuncture after 12-16 h of fasting. The blood was allowed to stand at room temperature until agglutination was completed. The serum was collected after centrifugation at 1000 g at 15°C for 15 min.

CCC Fractionation of Lipoproteins from Human Serum. In each experiment, the CCC column was first entirely filled with the PEG-rich upper stationary phase and the sample solution [a mixture of 4 ml human serum and 2 ml each of upper and lower phases to which proper amounts of PEG and inorganic phosphate (KPi) were added to adjust the two-phase composition] was injected through the sample port. Then the KPi-rich lower mobile phase was eluted through the column at various flow rates ranging from 0.5 to 2.0 ml/min while the apparatus was rotated at 500 rpm. The effluent from the outlet of the column was continuously monitored with an ISCO UA-5 absorbance monitor (Instrumentation Specialties, Lincoln, NE, USA) at 280 nm and fractionated into a fraction collector (Instrumentation Specialties). After the desired peak(s) were collected, the column was eluted with the PEG-rich upper phase (initially used as the stationary phase) in the opposite direction without stopping the centrifuge run. This reversed elution mode was continued until all retained analytes were eluted from the column.

Analysis of CCC Fractions. An aliquot of each fraction was diluted in distilled water three time its volume, and the absorbance was measured at 280 nm with a Shimadzu UV-1200 spectrophotometer. Phospholipids, cholesterols, and triglycerides in the CCC fractions were determined by enzymatic analyses (*11-13*). Phospholipids, such as phosphatidyl cholines, were hydrolyzed by phospholipase D and liberated choline was subsequently oxidized by choline oxidase. Cholesterols were oxidized by cholesterol oxidase. Triglycerides were hydrolysed by lipase to form glycerol which was then phosphorylated by adenosine triphosphate in the presence of glycerol kinase, and then the glycerophosphate thus produced was subsequently oxidized by peroxidase. The hydrogen peroxides produced from phospholipids, cholesterols and triglycerides were oxidatively coupled with 4-aminoantipyrine and phenol in the presence of peroxidase to yield a red color which was measured by absorbance at 505 nm. Concentrations of the phospholipids, cholesterols and triglycerides in the CCC fractions were determined by calibration curves constructed from the standard solutions.

Characterization of Human Lipoproteins and Serum Proteins by Polyacrylamide Gel Electrophoresis. The lipoproteins in the CCC fractions were characterized using polyacrylamide gel disk electrophoresis (disk PAGE) with a method modified from that of Frings et al. (*14*). The eluate (ca. 50-60 ml) consisting of KPi-rich lower phase (normal elution mode) or PEG-rich upper phase (reversed elution mode) was placed in dialysis bags (molecular mass cut-off values: 3500) and dialyzed overnight. Then the bags were immersed into aqueous 30%(w/v) PEG 8000 until the contents were concentrated to 1 ml. Disk PAGE was performed in a 3.1%(w/v) separation gel and a 2.5%(w/v) sample gel in glass tubes (10 x 0.5 cm ID gel bed) as follows: A 30 μl aliquot of the concentrated eluate was mixed with 15 μl of 0.25%(w/v) Sudan Black B in 30%(w/v) ethanol, and 450 μl of the sample gel solution was added. The mixture was placed on the polymerized gel, and allowed to stand under a daylight fluorescent lamp for about 30 min. When photopolymerization was complete, the gel tubes were inserted into the electrophoretic cell. Bromophenol Blue (BPB), 0.01 %(w/v), was added to the upper running buffer as a marker. The run was completed at 3mA per gel in about 1 h, at which time the marker had migrated 5 mm from the end of the tube.

Serum proteins in the CCC fractions were also characterized by SDS slab gel electrophoresis (SDS-PAGE) according to the method of Laemmli (*15*). Gels containing 3%(w/v) (stacking gel) and 10% (w/v) (separation gel) acrylamide were prepared from a stock solution of 30% (w/v) acrylamide and 0.8% (w/v) N, N'-methylene-bis acrylamide. A 5.5 x 10 cm separation gel and a 1.0 x 10 cm stacking gel each 0.75 mm thick were prepared between glass plates. A 5 μl-volume of concentrated eluate was mixed with 95 μl of sample solution [a mixture of 0.025M tris(hydroxymethyl)aminomethane, 2%(w/v) sodium dodecyl sulphate (SDS), 5%(w/v) 2-mercaptoethanol, 4%(w/v) glycerol and 0.01%(w/v) Bromophenol Blue (BPB)] and 10-20 μl of the sample solution was loaded over the stacking gel. Electrophoresis proceeded at a current of 10 mA until the BPB marker reached the stacking gel. Thereafter, the current of the apparatus was increased to 20 mA and the electrophoresis continued until the BPB marker reached the bottom of the separation gel. The migrated proteins were stained for 5 minutes at room temperature with the staining solution composed of 0.25%(w/v) Coomassie Brilliant Blue, 50%(v/v) methanol and 10%(v/v) acetic acid. The gel was destained by washing in a mixture of 7.5%(v/v) acetic acid and 2.5%(v/v) methanol.

Results and Discussion

Partition Coefficient of Lipoproteins and Serum Proteins. CCC is a two-phase procedure where the separation is based on the difference in partition coefficient of solutes within the phases. To achieve efficient separation of lipoproteins from human serum, it is essential to optimize the partition coefficient of each component by selecting a proper pH of the polymer phase system.

Fig. 2 shows the partition coefficients of three lipoproteins and three serum proteins plotted on a logarithmic scale against pH of two different polymer phase systems: 16% PEG 1000-12.5% KPi and 25% PEG 1000-12.5% KPi. In the 16% PEG 1000 systems (Fig. 2 left), serum proteins and VLDL show an increase of their partition coefficients with pH from 6.8 to 9.4, while the partition coefficients of HDL and LDL display quite different trends. At the highest pH of 9.4, the partition coefficients of both HDLs and LDLs are less than 1.0 indicating that these lipoproteins are mainly distributed to the KPi-rich lower phase. On the other hand, VLDL is not expected to separate from α-globulin at any pH.

In the 25% PEG 1000 system (Fig. 2, right), all proteins except γ-globulin show similar trends for their K-pH curves indicating that the system is unsuitable for the desired separation.

CCC of Human Serum. The effect of the molecular weight of the PEG was studied with the 16%(w/w) PEG-12.5%(w/w) KPi system. Figs. 3A-D show chromatograms of human serum (4 ml) obtained from four solvent systems each containing different molecular weight PEGs (M_n = 600, 1000, 2000, and 4000).

In the PEG 600 system, all proteins including HDLs, LDLs and serum proteins were strongly retained in the PEG-rich upper stationary phase and eluted together when the column was eluted in a reversed elution mode with the PEG-rich upper phase.

Similarly, when PEGs with molecular weights higher than 2000 were used in the solvent system, all proteins including HDLs, LDLs and serum proteins were distributed to the KPi-rich lower phase and eluted together at the solvent front (SF) of the chromatogram (Figs. 3C and 3D).

Successful separation of the combined HDL and LDL fraction was achieved with the 16% PEG 1000-12.5% KPi solvent system at pH 9.4 where both HDL and LDL were eluted together near the solvent front while other proteins were retained in the column for a much longer

Downloaded by STANFORD UNIV GREEN LIBR on June 29, 2012 | http://pubs.acs.org
Publication Date: May 15, 1995 | doi: 10.1021/bk-1995-0593.ch011

Downloaded by STANFORD UNIV GREEN LIBR on June 29, 2012 | http://pubs.acs.org
Publication Date: May 15, 1995 | doi: 10.1021/bk-1995-0593.ch011

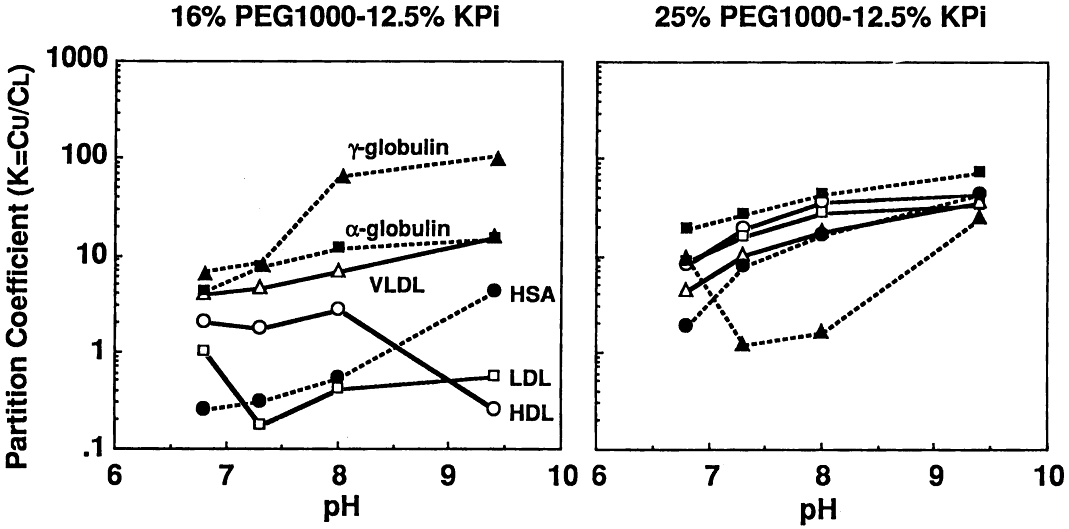

Figure 2. Partition coefficients (K) of HDLs (○), LDLs (□), VLDLs (△), HSA (•), α-globulin (■) and γ-globulin (▲) in various polymer phase systems composed of PEG 1000 and potassium phosphate. K is solute concentration in the upper phase divided by that in the lower phase.

Downloaded by STANFORD UNIV GREEN LIBR on June 29, 2012 | http://pubs.acs.org
Publication Date: May 15, 1995 | doi: 10.1021/bk-1995-0593.ch011

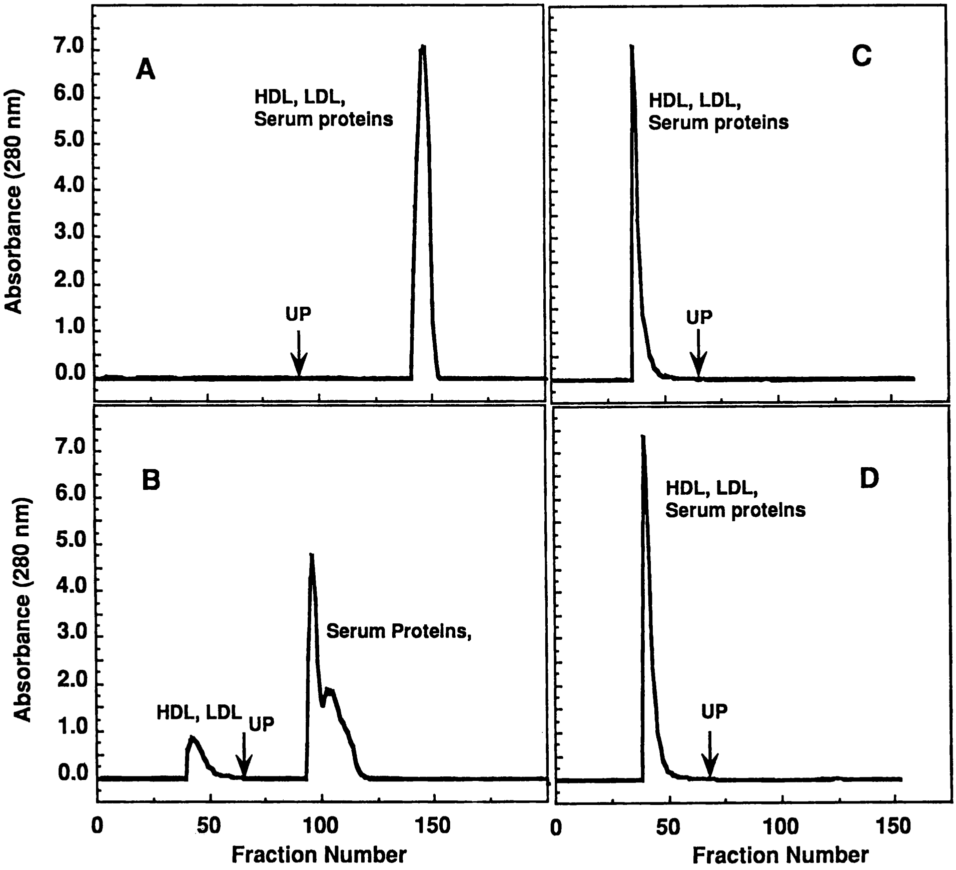

Figure 3. CCC fractionation of HDL-LDL fractions from human serum with four different aqueous polymer phase systems containing PEG 600 (A), PEG 1000 (B), PEG 2000 (C) and PEG 4000 (D). Experimental conditions: Column: 2.6 mm ID PTFE multilayer coils (x 2) with 340ml capacity; Sample: mixture of 4ml-volume of human serum, 2ml upper phase and 2ml lower phase in which 0.9 g of PEG 1000 and 0.7 g of dibasic potassium phosphate were dissolved; Solvent systems: 16%(w/w) PEG 1000-12.5%(w/w) K_2HPO_4 at pH 9.4; Mobile phase: Lower phase; Flow rate: 2.0 ml/min; Revolution: 500 rpm; SF = solvent front; UP = starting point of reversed elution mode with the upper phase mobile.

period of time. The separation time of these two lipoproteins was 3 h. From the partition behavior of the VLDLs (Fig. 2, left), we assume that these lipoproteins are eluted by the PEG-rich upper phase in the second peak or its shoulder.

The effect of the flow-rate of the mobile phase on the lipoprotein fractionation was next investigated using the 16% PEG 1000-12.5% KPi (pH 9.4) polymer phase system by eluting the KPi-rich lower phase. Figs. 4A-C show chromatograms of human serum at a flow-rate of 2.0 (A), 1.0 (B), and 0.5 ml/min (C). The HDL-LDL fractions were eluted in 3 h (A), 6 h (B) and 7.5 h (C) according to the applied flow-rates. It was evident from these chromatograms that HDL and LDL were not resolved even at the lowest flow-rate of 0.5 ml/min.

Fig. 5 shows both the disk and slab polyacrylamide gel electrophoresis of the CCC fractions (Fig. 3B). The first peak corresponding to fractions 40-55 contained both HDLs and LDLs. The second peak, which was produced by eluting with the PEG-rich upper phase, consisted mostly of human serum proteins such as HSA, α- and γ-globulins. The 3.1% disk-PAGE (Fig. 5 B, left) shows that CCC

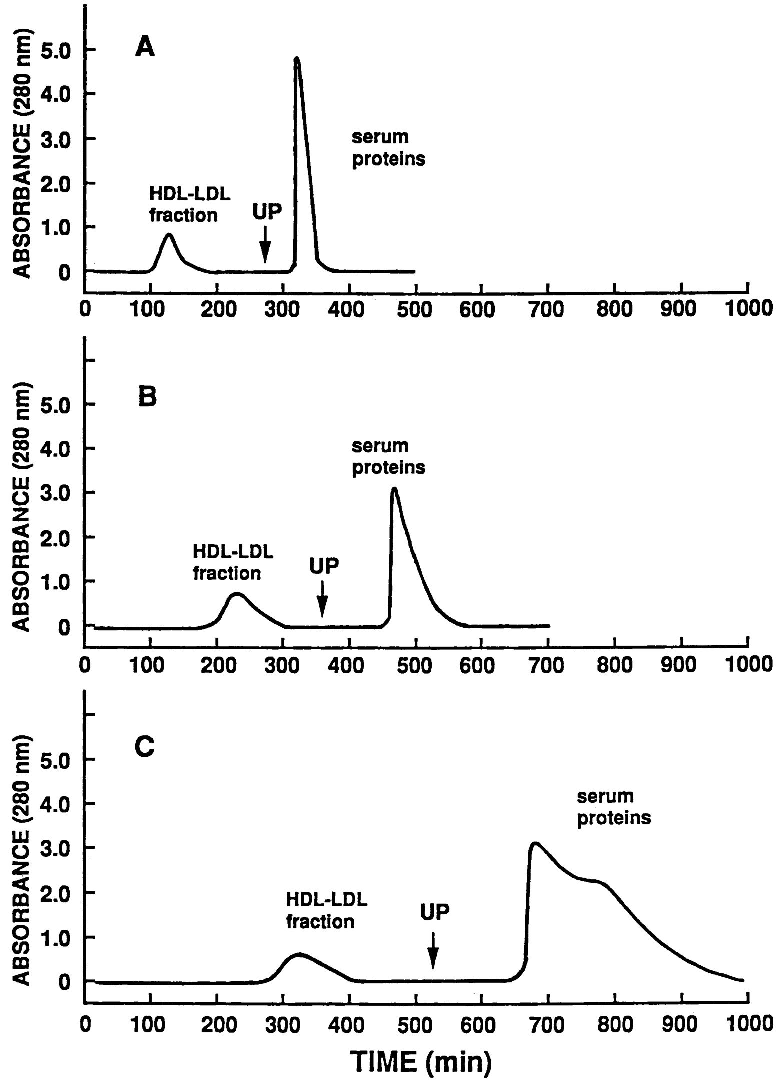

Figure 4. CCC fractionation of HDL-LDL from human serum at different flow-rate of the lower phase. Experimental conditions are same as those described in Fig. 3B except the following: Flow-rate: 0.5 ml/min (A), 1.0 ml/min (B) and 2.0 ml/min (C). SF = solvent front; UP = the starting point of the reversed elution mode with the upper phase mobile.

Downloaded by STANFORD UNIV GREEN LIBR on June 29, 2012 | http://pubs.acs.org
Publication Date: May 15, 1995 | doi: 10.1021/bk-1995-0593.ch011

fractions 40-55 contained both HDLs and LDLs while other fractions (92-100, 101-110 and 111-120) show only BPB bands used as a marker. The 12% SDS PAGE (Fig. 5B, right) revealed that the serum proteins including HSA were eluted in fractions 92-120. The HDL-LDL fractions corresponding to CCC fractions 40-55 were free of serum proteins, but contained ApoA and ApoB proteins, which are the apolipoproteins of HDLs and LDLs, respectively.

The results of our studies show that the HDL-LDL fractions were fractionated within 3 h by CCC with a polymer phase system composed of 16% PEG 1000 and 12.5% dibasic potassium phosphate at a relatively high flow-rate of 2.0 ml/min.

Downloaded by STANFORD UNIV GREEN LIBR on June 29, 2012 | http://pubs.acs.org
Publication Date: May 15, 1995 | doi: 10.1021/bk-1995-0593.ch011

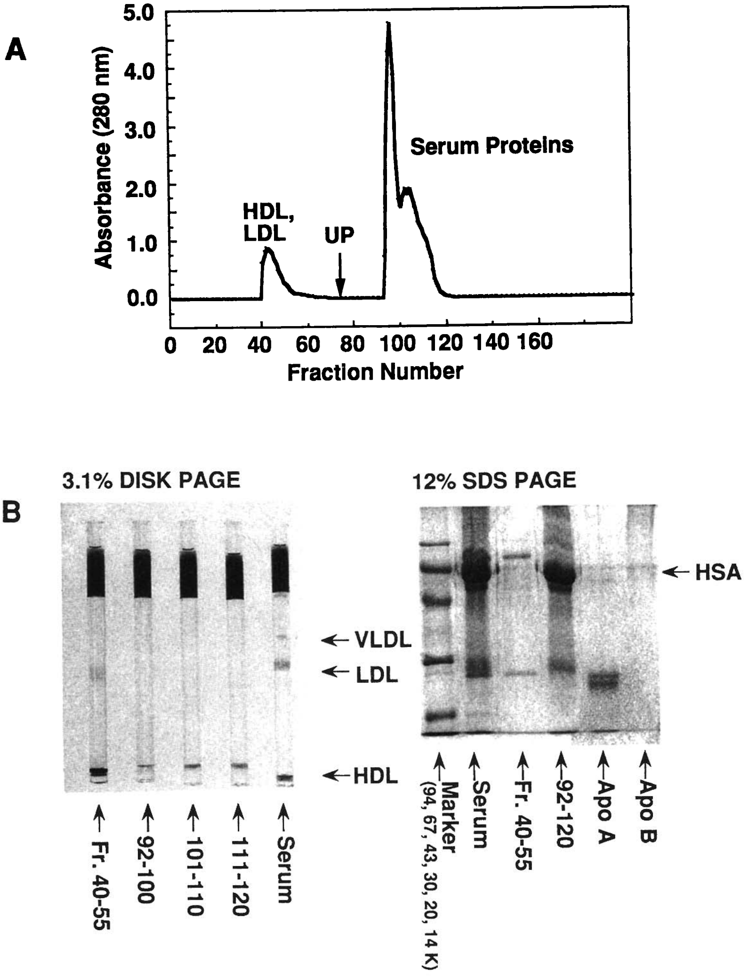

Figure 5. CCC fractionation of HDL-LDL (A) and polyacrylamide gel electrophoresis of lipoproteins and serum proteins (B). Experimental conditions are same as those described in Fig. 3B; SF = solvent front; UP = the starting point of the reversed elution mode with the upper phase mobile.

The amounts of phospholipids, cholesterols and triglycerides in the CCC fractions, 44-55 and 92-120, were determined by enzymatic analysis. The triglycerides in the serum protein fractions (92-120) eluted with the PEG-rich upper phase were as high as 0.74 mg/ml. It is most likely that the VLDLs were eluted in the same fractions, because they contain more triglycerides than other lipoproteins.

Conclusion

The CCC fractionation of the HDL-LDL fractions by the cross-axis CCC is greatly influenced by the molecular weight of PEG in the solvent systems. A polymer system composed of 16% PEG 1000 and 12.5% dibasic potassium phosphate (pH 9.4) was found to be most suitable since it provides a large difference in K values between the serum proteins and major lipoproteins (HDLs and LDLs). This solvent system allows CCC fractionation of these two lipoproteins directly from the human serum in 3 h. Since the partition system (with PEGs) is very mild, there may be less breakdown of the lipoproteins than with column or centrifugation in high salt media. Direct comparison of the samples with the above mentioned techniques would be interesting. With further refinement we hope to fractionate HDLs and LDLs.

Acknowledgment

The authors wish to thank Dr. Henry M. Fales for his helpful advice and editing of the manuscript. This project has been funded at least in part with Grant-in-Aid for General Scientific Research from the Ministry of Education, Science and Culture in Japan under contract number 05671792.

Literature Cited

1. Sata, T.; Estrich, D.L.; Wood, P.P.S.; Kinsell, L.W. *J. Lipid Res.* **1970**, 11, 331.
2. Rudel, L.L.; Lee, J.A.; Morris, M.D.; Felts, J.M. *Biochem. J.* **1974**, 139, 89.
3. Clifton, P.M.; Mackinnon, A.M.; Barter, P. *J. Chromatogr.* **1987**, 414, 25.
4. Hara, I.; Okazaki, M.; Ohno, Y. *J. Biochem.* **1980**, 87, 1863.
5. Okazaki, M.; Shiraishi, K.; Ohno, Y.; Hara, I. *J. Chromatogr.* **1981**, 223, 285.
6. Okazaki, M.; Ohno, Y.; Hara, I. *J. Biochem.* **1981**, 89, 871.
7. Shibusawa, Y.; Ito, Y.; Ikewaki, K.; Rader, D.J.; Brewer, H.B.Jr. *J. Chromatogr.* **1992**, 596, 188.
8. Ito, Y.; Oka, H.; Slemp, J.L. *J. Chromatogr.* **1989**, 463, 305.
9. Bhatnagar, M; Oka, H.; Ito, Y. *J. Chromatogr.* **1989**, 463, 317.
10. Sclavons, M.M.; Cordonnier, C.M.; Mailleux, P.M.; Heller, F.R.; Desager, J.-P.; Harvengt, C.M. *Clin. Chim. Acta* **1985**, 153, 125.
11. Takayama, M.; Itoh, S.; Nagasaki, T.; Tanimizu, I. *Clin. Chim. Acta* **1977**, 79, 93.
12. Allain, C.; Poon, L.S.; Chan, C.S.G.; Richmond, W.; Fu, P.C. *Clin. Chem.* **1974**, 20, 470.
13. Spayd, R.W.; Bruschi, B.; Burdick, B.A.; Dappen, G.M.; Eikenbery, J.N.; Esders, T.W.; Figureras, J.; Goodhue, C.T.; LaRossa, D.D.; Nelson, R.W.; Rand, R.N.; Wu, T.-W. *Clin. Chem.* **1978**, 24, 1343.
14. Frings, C.S.; Foster, L.B.; Cohen, P.S. *Clin. Chem.* **1971**, 17, 111.
15. Laemmli, U.K. *Nature* **1970**, 227, 680.

RECEIVED December 30, 1994

Downloaded by STANFORD UNIV GREEN LIBR on June 29, 2012 | http://pubs.acs.org
Publication Date: May 15, 1995 | doi: 10.1021/bk-1995-0593.ch011

Downloaded by PENNSYLVANIA STATE UNIV on June 29, 2012 | http://pubs.acs.org
Publication Date: May 15, 1995 | doi: 10.1021/bk-1995-0593.ch012

Chapter 12

On-Line Fast Atom Bombardment Mass Spectrometric Detection in High-Speed Countercurrent Chromatography Through a Moving Belt Interface

James N. McGuire[1], Mark L. Proefke[1], Walter D. Conway[2], and Kenneth L. Rinehart[1,3]

[1]Department of Chemistry, University of Illinois at Urbana-Champaign, 1209 West California Street, Urbana, IL 61820
[2]Department of Pharmaceutics, School of Pharmacy, State University of New York at Buffalo, 565 Hochstetter Hall, Buffalo, NY 14260

A high-speed countercurrent chromatograph with on-line fast atom bombardment (FAB) mass spectrometric detection through a moving belt interface (MBI) was employed in the separation of two model systems. The relatively high flow-rate compatibility of the MBI allowed the use of a commercially-available multi-layer coil planet centrifuge with a specially designed, small-volume (16.8 mL) analytical coil. Flow rates of up to 800 μL/min were successfully deposited onto the belt using an organic-rich mobile phase. The MBI ran without generating any noticeable back-pressure on the chromatographic system and produced matrix-free FAB spectra.

Countercurrent chromatography (CCC) was pioneered by Ito and evolved from liquid-liquid partition chromatography, which was introduced by Martin and Synge in 1941, and the older equilibrium countercurrent distribution (CCD) instruments. Countercurrent technology has spawned a rather large family of loosely related instruments, whose history and emergence is well documented (*1*). On a preparative scale, high-speed CCC (HSCCC) has been used extensively in the separation of natural products (*1,2*). On an analytical scale, researchers are building smaller, faster instruments in an effort to decrease run times and increase resolution (*3*). Unfortunately, while speed and resolution are improving, HSCCC is still largely incompatible with standard, optics-based on-line detectors that are common to high-performance liquid chromatography (HPLC). Stationary phase bleed produces tremendous amounts of noise in both refractive index and ultraviolet/visible (UV/Vis) detectors due to a chaotic reference stream and emulsification in the flow cell, respectively. While emulsification can be minimized by post-column addition of a third solvent to coalesce the two liquid phases (*4*), the added solvent decreases sensitivity by dilution.

On-line mass spectrometric detection avoids the solvent problems associated with common optical detectors and is an almost universal detector with high sensitivity. Accordingly, the following mass spectrometric techniques have been successfully coupled with countercurrent chromatography: thermospray (TSP), frit fast atom bombardment (frit FAB, or continuous-flow FAB, CF-FAB), electron ionization (EI), chemical

---

[3]Corresponding author

0097–6156/95/0593–0129$12.00/0

ionization (CI), and electrospray ionization (*3*). The two most common HSCCC/MS interfaces, TSP and frit FAB, suffer from either flow rate or back-pressure problems. Thermospray accepts flow rates up to 700 µL/min from the CCC but generates pressures that can rupture the poly(tetrafluoroethylene) (PTFE) tubing in the CCC column (*5*). An HPLC pump must therefore be placed between the coil and the TSP interface to regulate the back-pressure on the countercurrent instrument. Frit FAB does not produce deleterious pressures but can only tolerate flows of 1-5 µL/min (*3*). The sample has to be split at least 1:200 at 1 mL/min, which is the desired flow rate for our CCC instrument.

The moving belt interface (MBI) seems ideal for HSCCC because it can accept high flow rates (up to 1 mL/min for organic-rich mobile phases) without generating large back-pressures. In the MBI (Figure 1), the sample is deposited onto a continuously circulating polyimide belt through the Δ-depositor (*6*), which is heated at the tip to prevent freezing. The design of the Δ-depositor allows for a relatively even coat of the eluent on the belt. Solvent is initially removed in the first stage by a roughing pump. As the belt travels toward the source it passes through two additional stages, which are at higher vacuum, and then into the source. Unlike most MBI experiments (*7*), which rely on flash evaporation by infrared heating followed by ionization, our system uses a xenon beam for direct desorption of the analytes from the belt (*6,8*). Using FAB and the moving belt interface represents a departure from CF-FAB or frit FAB, which still rely on an added matrix to hold the sample on the target. Consequently, HSCCC/MBI/FAB mass spectra are free of matrix peaks that complicate most FAB spectra.

Downloaded by PENNSYLVANIA STATE UNIV on June 29, 2012 | http://pubs.acs.org
Publication Date: May 15, 1995 | doi: 10.1021/bk-1995-0593.ch012

Experimental

Materials. Organic solvents were Burdick and Jackson HPLC grade (Baxter, McGaw Park, IL) used directly without further purification. The water used was purified using a Milli-Q water purification system (Millipore Corp., Marlborough, MA). The solvent systems were allowed to equilibrate overnight before being filtered and degassed with a 0.45-µm nylon filter apparatus, then separated. The erythromycins were purchased from Sigma (St. Louis, MO) and used without purification.

Analytical High-Speed CCC. All HSCCC separations were performed on a P.C., Inc. (P.C., Inc., Potomac, MD) High-Speed Countercurrent Chromatograph equipped with an experimental, small-volume analytical coil. The coil was wound with 30.0 m of 0.85 mm i.d. PTFE tubing in two layers on a core of 8.59 cm radius (b = 0.85). Column volume was measured as 16.8 mL. The mobile phase was pumped through the column at the desired flow rate until equilibrated with the stationary phase. Stationary phase retention for the solvent systems used varied from 50 to 80% as measured by the amount of stationary phase eluted in the mobile phase during equilibration.

Moving Belt Interface. A VG Instruments (Manchester, UK) moving belt interface was used in the following studies with a few modifications. The spray nebulizer was replaced by a heated, direct liquid depositor of our own design (*6*). This eliminated the need for the infrared solvent evaporation heater. Temperature was regulated at the depositor tip by a modified Omega model # 4001KC temperature controller (Omega, Stamford, CT). The clean-up heater of the interface was also removed and replaced with a methanol washer operating at 1 mL/min. The polyimide belt used (Pacific Belting Industries, Inc., Los Angeles, CA) was conditioned by roughing with #600 sandpaper followed by sonication in a dilute sodium dodecyl sulfate solution.

Mass Spectrometry. Measurements were performed on a VG ZAB-SE mass spectrometer operating at 8 kV and 1000 resolution. Ions were produced from the belt by fast atom bombardment using xenon atoms accelerated at 8 kV with 1 mA current. The ion source was operated at ambient temperature.

Downloaded by PENNSYLVANIA STATE UNIV on June 29, 2012 | http://pubs.acs.org
Publication Date: May 15, 1995 | doi: 10.1021/bk-1995-0593.ch012

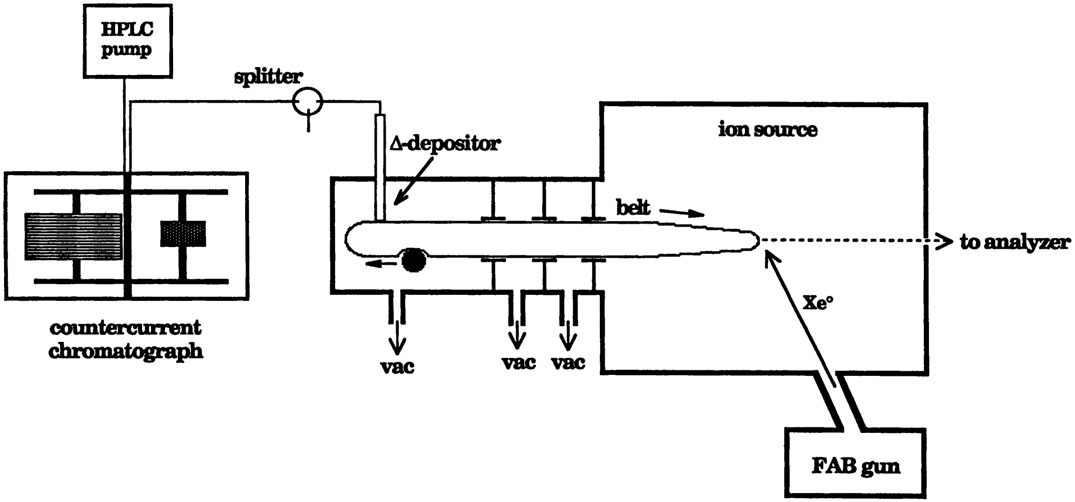
HPLC pump
splitter
Δ-depositor
ion source
belt
to analyzer
Xe°
countercurrent chromatograph
vac
vac
vac
FAB gun

Figure 1. Schematic of high-speed countercurrent chromatograph/moving belt interface set-up.

Protected Dipeptides. Boc-Ala-Tyr(O-2,6-Cl_2-Bn)-OMe (AY) and Boc-Ala-Leu-OMe (AL) (see Figure 3 for structures) were separated in all cases with 1-1-1-1 hexane-EtOAc-MeOH-H_2O (upper phase = mobile phase) at a flow rate of 500 µL/min and rotation speed of 1200 rpm. The example shown is for an injection of 300 µg of each compound in a concentrated methanolic solution. Two Waters 510 HPLC pumps regulated by a model 680 automated controller (Waters Assoc., Milford, MA) were used for HSCCC and HPLC analyses. Initial countercurrent runs were done with on-line photodiode array (PDA, Waters model 990) detection. HSCCC runs performed with PDA detection required post-column addition of methanol to minimize emulsification in the flow cell. Methanol was mixed into the flow stream through an interface of our own design but similar to one previously described by Schaufelberger (*4*). HSCCC runs performed with the moving belt interface required a split so that only 80% of the flow stream was deposited onto the belt. The partition coefficients (K = [up]/[low]), as measured by integration of HPLC peaks, were K = 2.8 for AY and K = 0.7 for AL as determined by HPLC analysis on a diamino column (Varian AX-5, 4.0 x 300 mm; Varian Assoc., Sunnyvale, CA). Assuming a stationary phase retention of 61%, which is derived from the reconstructed ion chromatogram, the partition coefficients estimated from CCC were 3.6 and 0.5 for AY and AL, respectively.

Erythromycins. Erythromycin A (ErA), erythromycin estolate (ErEst) and erythromycin ethyl succinate (ErSucc) were chromatographed at 1 mL/min and rotation speed of 1200 rpm using 4-7-4-3 hexane-EtOAc-MeOH-H_2O (upper phase = mobile phase). The example shown in Figure 4 is for a 500-µg injection of a mixture containing equal amounts by weight of the three components in methanol. The CCC flow stream was split so that 800 µL/min reached the belt. A Beckman 114M HPLC pump (Beckman, Fullerton, CA) was used for solvent delivery in the CCC experiments. Attempts at determining the partition coefficients of the erythromycins by HPLC were unsuccessful.

Downloaded by PENNSYLVANIA STATE UNIV on June 29, 2012 | http://pubs.acs.org
Publication Date: May 15, 1995 | doi: 10.1021/bk-1995-0593.ch012

Results And Discussion

HSCCC/MBI. A prototype, small-volume analytical coil (16.8 mL) was installed on a commercially-available multi-layer coil planet centrifuge. Although it was feared that the 0.85-mm i.d. PTFE tubing in the column might be too narrow to provide sufficient stationary phase retention at the available rotation speeds (< 1400 rpm), the system performed well (50-80% stationary phase retention) and was stable for up to several hours with a variety of solvent systems including those with 1-butanol. We found a flow rate of 1 mL/min to be optimum with respect to band broadening and stationary phase retention. In both of our experiments the flow stream from the chromatograph was reduced by 20% to avoid overloading the mass spectrometer with solvent. The moving belt interface did not produce any added back-pressures or other problems at 800 µL/min with an organic-rich mobile phase. These higher flow rates were only tolerated in the absence of water, whose presence necessitated a flow rate of 200 - 400 µL/min onto the belt to avoid freezing in the depositor tip (*6,8*).

Dipeptides. Peptides are logical choices as analytes for the initial moving belt experiment because they demonstrate the ability of FAB to produce recognizable molecular ions from polar compounds. Additionally, the generality of mass spectrometric detection is demonstrated with the peptides, which have weak chromophores and are not ideal for UV/Vis detection. In fact, aside from the aromatic groups in tyrosine, phenylalanine, histidine, and tryptophan, the only appreciable absorbance arises from the amide functionality.

Downloaded by PENNSYLVANIA STATE UNIV on June 29, 2012 | http://pubs.acs.org
Publication Date: May 15, 1995 | doi: 10.1021/bk-1995-0593.ch012

Two protected dipeptides, Boc-Ala-Tyr(O-2,6-Cl_2-Bn)-OMe (AY, MW = 524 Da) and Boc-Ala-Leu-OMe (AL, MW = 316 Da), were separated with baseline resolution using 1-1-1-1 hexane-EtOAc-MeOH-H_2O (upper phase = mobile phase). The first peak in the reconstructed ion chromatogram (RIC, Figure 2) is AY as evidenced by its mass spectrum (Figure 3). The pseudo-molecular ion (M + Na) appears at *m/z* 547. Sodium adducts are commonly seen with the moving belt due to the presence of sodium dodecyl sulfate (SDS), which is used to inhibit droplet formation on the polyimide belt material. The large peak at *m/z* 159 arises from the dichlorobenzyl protecting group on the phenolic oxygen of tyrosine. The peak at *m/z* 354 is the Y" fragment expected from cleavage of the peptide amide bond (*9*). The other major peak, *m/z* 294, arises from α,β-bond cleavage of the Tyr unit. A second Y" fragment accounts for *m/z* 425. The sodium adduct of AL (M + Na) is clearly visible at *m/z* 339 in the mass spectrum (fig 3) for the second peak in the RIC (fig 2), but most of the fragment ions are from M + H. Again, the Y" fragments are relatively intense at *m/z* 217 (plus a Na analog at *m/z* 239) and 146. Loss of the *tert*-butyl group from the Boc protecting group on the amino terminus gives *m/z* 261.

Erythromycins. The erythromycins are an important class of macrolide antibiotics used in the treatment of gram-positive bacterial infections. Like the peptides, the erythromycins have weak chromophores and are commonly detected in HPLC analyses by electrochemical methods. A mixture of erythromycin A (ErA, MW = 733 Da), erythromycin estolate (ErEst, MW = 789 Da) and erythromycin ethyl succinate (ErSucc, MW = 861 Da) was separated with 4-7-4-3 hexane-EtOAc-MeOH-H_2O (upper phase = mobile phase). The identity of each of the peaks in the RIC (Figure 4) was deduced by characteristic fragment ions (Figure 5) from cleavage of the differing desosamine sugar groups. Each antibiotic should give the following, distinctive signals: ErA *m/z* 158 (desosaminyl), ErEst *m/z* 214 (desosaminyl propionate ester) and ErSucc *m/z* 286 (desosaminyl ethyl succinate ester). The fastest eluting erythromycin is the estolate, which is identified by signals at *m/z* 214 and 772 (M + H - H_2O) (Figure 5). Both of these ions appeared in the shoulder of the second peak. This shoulder is probably due to remaining ErEst on the belt that has rolled around and is presented for ionization again. The estolate, which is actually sold as the sodium dodecyl sulfate salt, must have a relatively high affinity for the SDS used in conditioning the belt and is not completely removed by the methanol wash. The second major peak in the RIC gives the expected desosaminyl fragment ion at *m/z* 286 from ErSucc as well as *m/z* 862 (M + H). Erythromycin A is relatively polar and is retained in the stationary phase. The large peak near the end of the RIC corresponds to ErA and gives primarily *m/z* 756 (M + Na) and 158 in its mass spectrum. The small peaks in the elution of the stationary phase arise from minor amounts of ErA, which ionizes very well by FAB.

Conclusions

The moving belt interface of FAB with high-speed countercurrent chromatography works well. Analytes which are normally difficult to see by optical methods can be detected easily by the mass spectrometer and identified using the resulting structural information. The MBI has advantages over thermospray and frit FAB (also CF-FAB) with respect to back-pressure and flow-rate compatibility, respectively. Furthermore, the MBI does not require addition of FAB matrix, which can sometimes adversely affect chromatographic separations. It is also possible to use this system as a predictor for a preparative-scale separation. For example, an unknown mixture could be run on the analytical coil and its major peaks identified by FAB. The experiment could then be repeated on the same countercurrent chromatograph with a larger column and the identities

Downloaded by PENNSYLVANIA STATE UNIV on June 29, 2012 | http://pubs.acs.org
Publication Date: May 15, 1995 | doi: 10.1021/bk-1995-0593.ch012

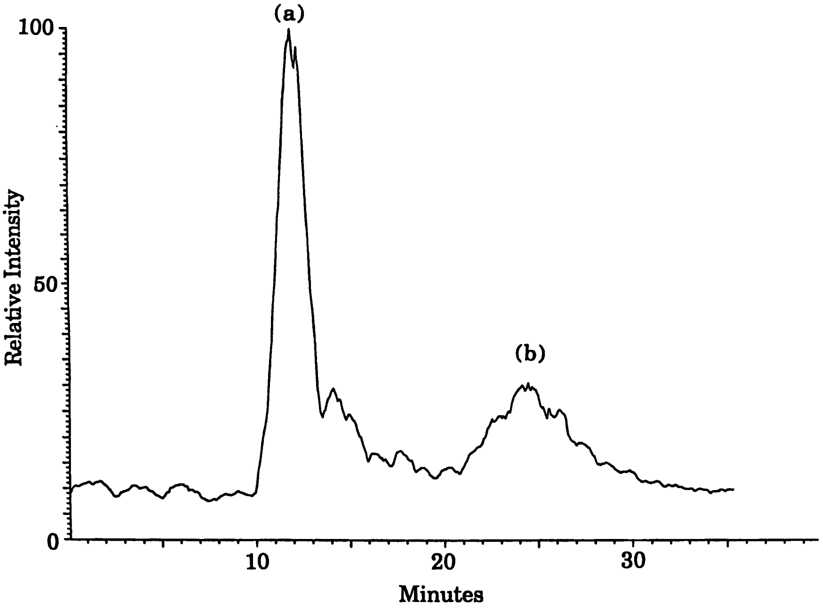

Figure 2. Reconstructed ion chromatogram for the separation of two protected dipeptides, AY and AL. See Figure 3 for data on (a) and (b).

Downloaded by PENNSYLVANIA STATE UNIV on June 29, 2012 | http://pubs.acs.org
Publication Date: May 15, 1995 | doi: 10.1021/bk-1995-0593.ch012

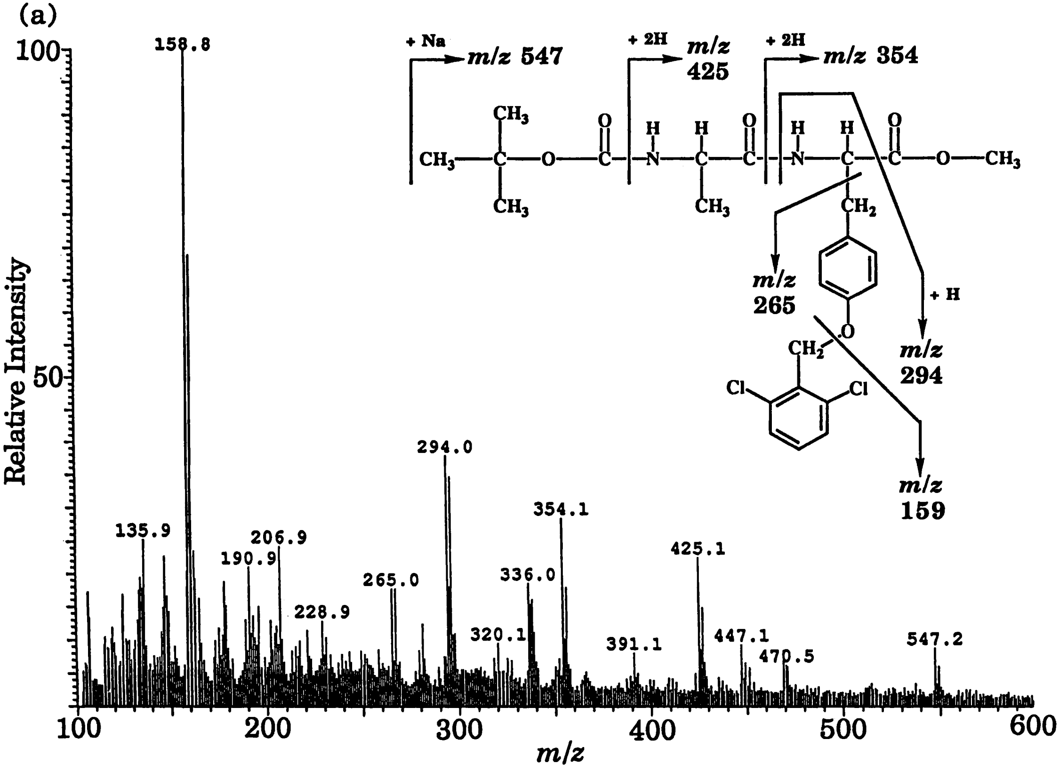

Figure 3. Averaged mass spectra corresponding to peaks in RIC for the protected dipeptides. The labels correspond to the peaks in Figure 2, (a) Boc-Ala-Tyr(O-2,6-Cl_2-Bn)-OMe (AY, MW = 524 Da) and (b) Boc-Ala-Leu-OMe (AL, MW = 316 Da).

Continued on next page

Downloaded by PENNSYLVANIA STATE UNIV on June 29, 2012 | http://pubs.acs.org
Publication Date: May 15, 1995 | doi: 10.1021/bk-1995-0593.ch012

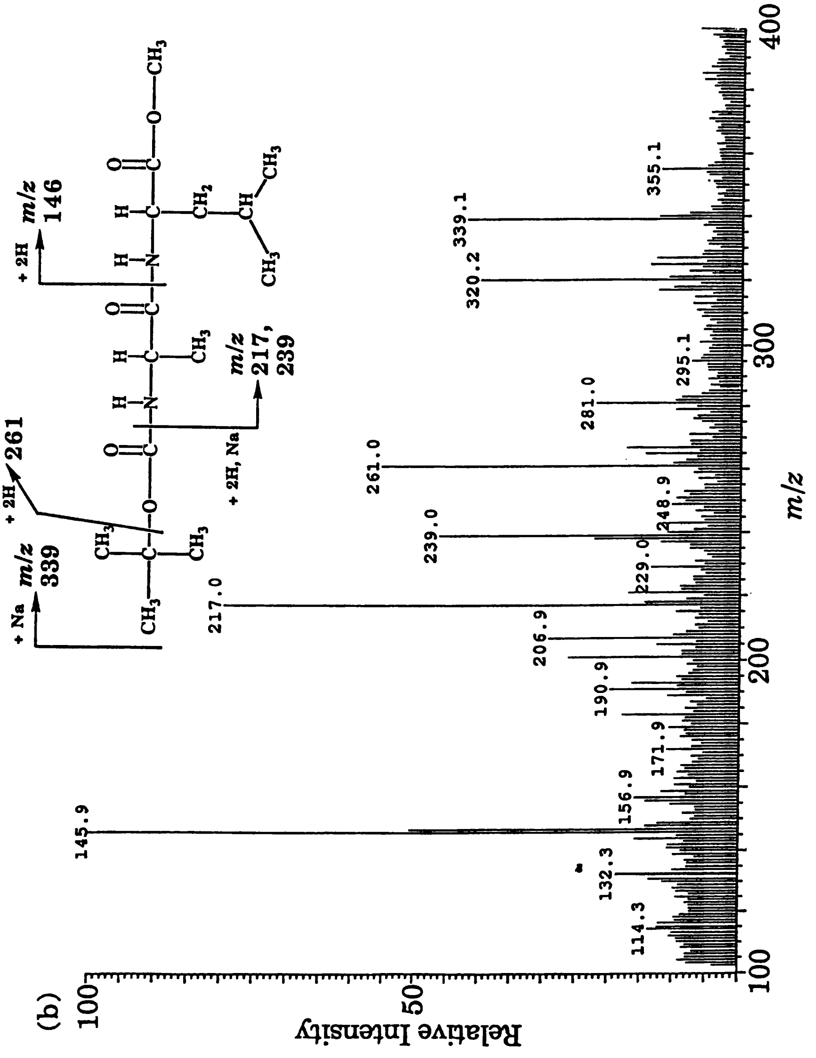

Figure 3. *Continued.*

Downloaded by PENNSYLVANIA STATE UNIV on June 29, 2012 | http://pubs.acs.org
Publication Date: May 15, 1995 | doi: 10.1021/bk-1995-0593.ch012

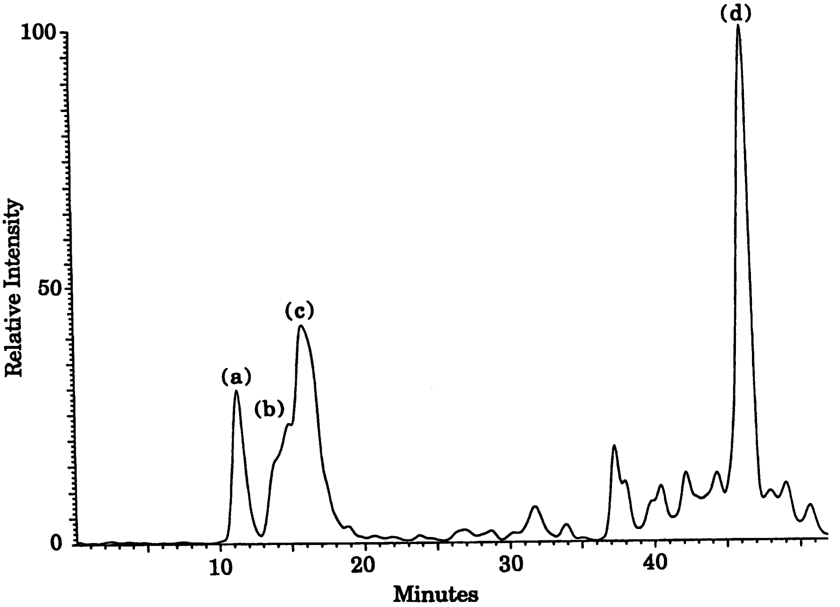

Figure 4. Reconstructed ion chromatogram for the erythromycins.

Downloaded by PENNSYLVANIA STATE UNIV on June 29, 2012 | http://pubs.acs.org
Publication Date: May 15, 1995 | doi: 10.1021/bk-1995-0593.ch012

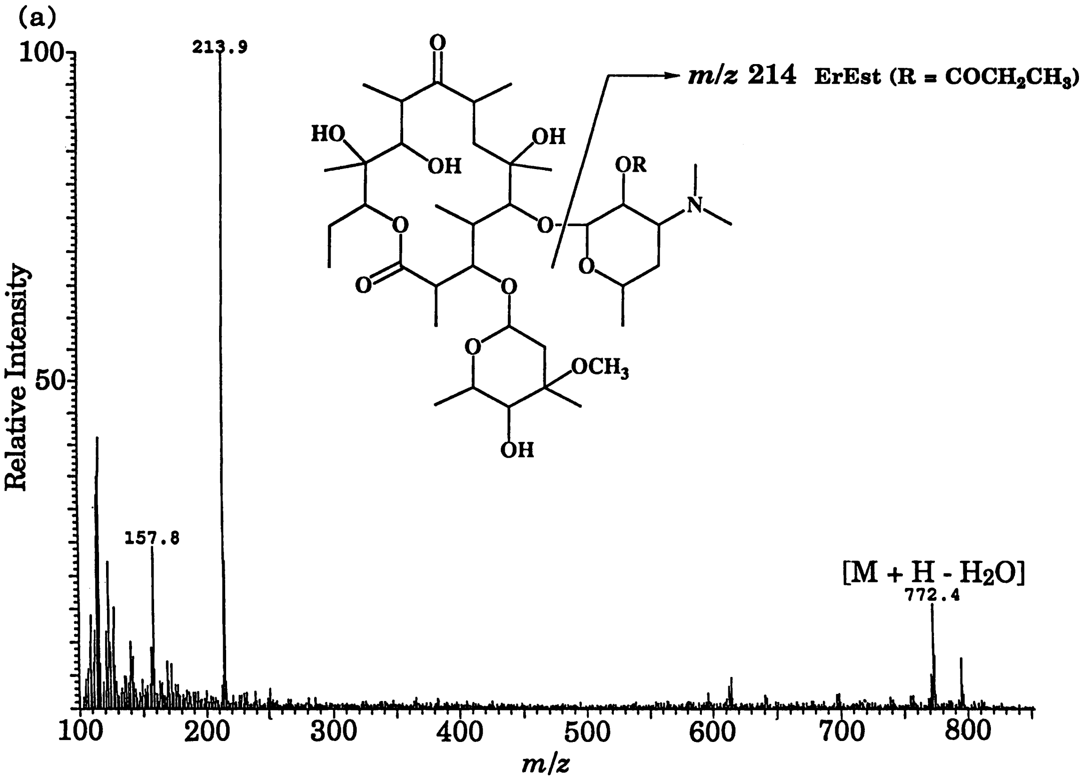

Figure 5. Averaged mass spectra corresponding to peaks in RIC for the erythromycins: (a) & (b) erythromycin estolate (ErEst, MW = 789 Da), (c) erythromycin succinate (ErSucc, MW = 861 Da), (d) erythromycin A (ErA, MW = 733 Da).

Downloaded by PENNSYLVANIA STATE UNIV on June 29, 2012 | http://pubs.acs.org
Publication Date: May 15, 1995 | doi: 10.1021/bk-1995-0593.ch012

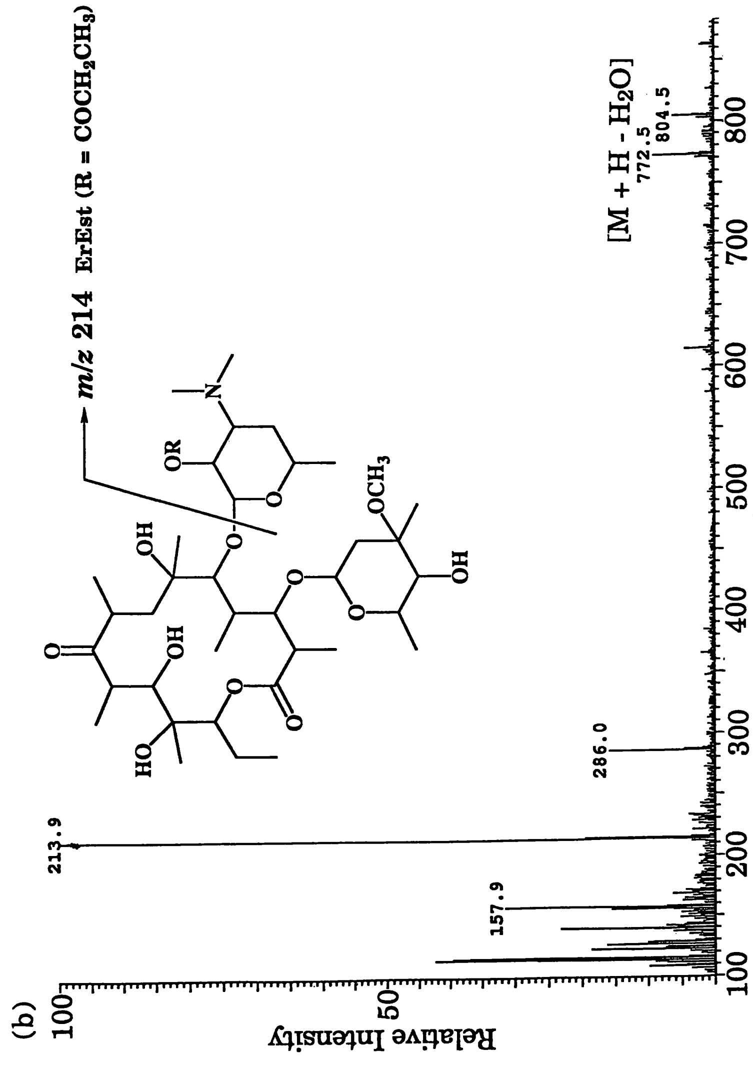

Figure 5. *Continued. Continued on next page.*

Downloaded by PENNSYLVANIA STATE UNIV on June 29, 2012 | http://pubs.acs.org
Publication Date: May 15, 1995 | doi: 10.1021/bk-1995-0593.ch012

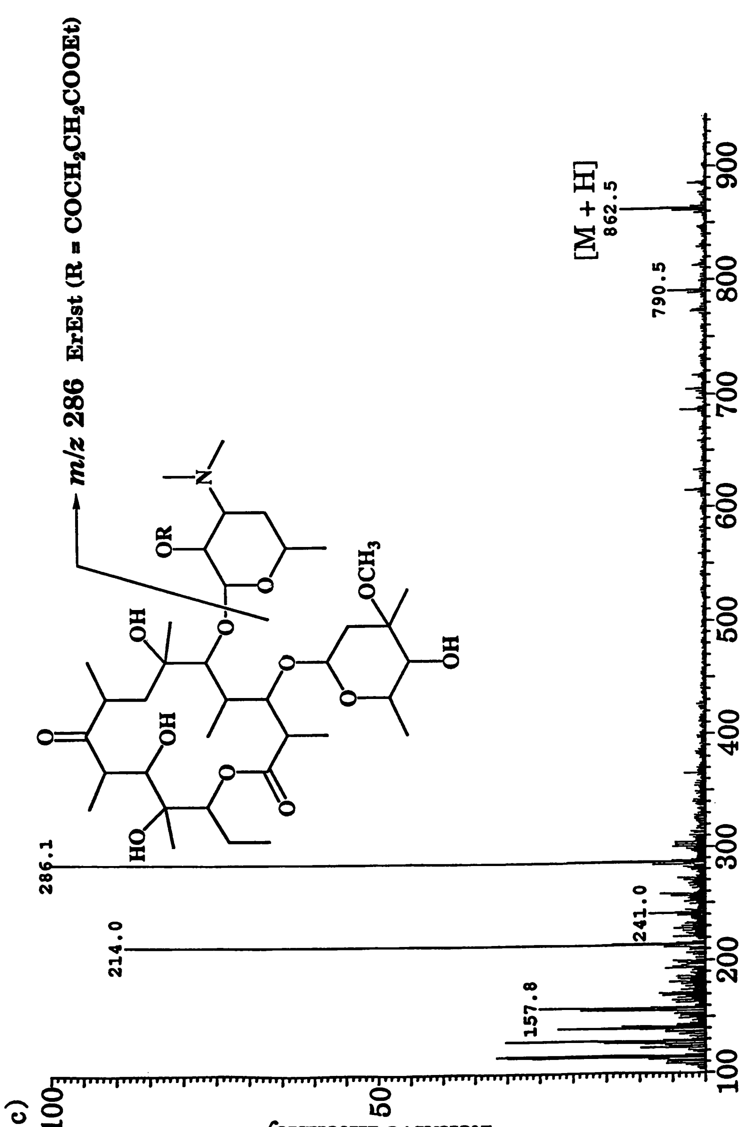

Figure 5. *Continued.*

Downloaded by PENNSYLVANIA STATE UNIV on June 29, 2012 | http://pubs.acs.org
Publication Date: May 15, 1995 | doi: 10.1021/bk-1995-0593.ch012

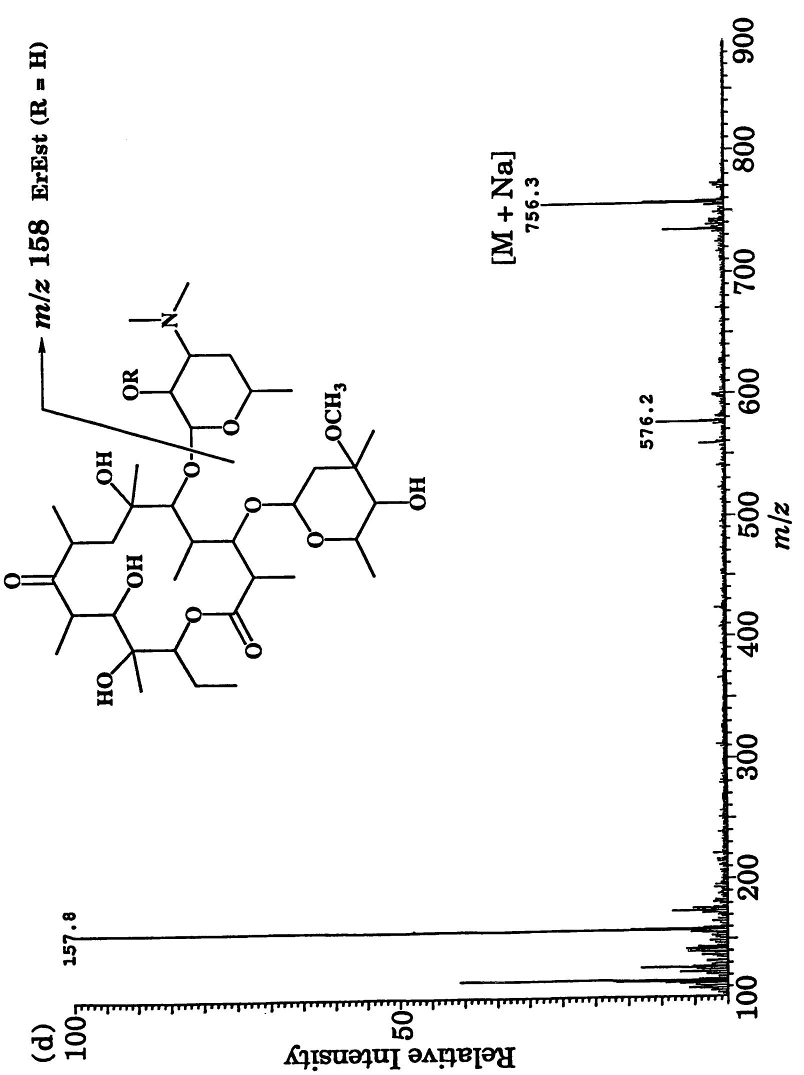

Figure 5. *Continued.*

and retention volumes of the major constituents would be known. For this reason, HSCCC/MBI/FAB is proposed as a valuable tool in the separation of natural products.

Acknowledgments

This work was supported by grants from the National Institute of Allergy and Infectious Diseases (AI 0479) and the National Institute of General Medical Sciences (GM 27029). The protected dipeptides were obtained from Dr. M. Namikoshi (University of Illinois at Urbana-Champaign).

Downloaded by PENNSYLVANIA STATE UNIV on June 29, 2012 | http://pubs.acs.org
Publication Date: May 15, 1995 | doi: 10.1021/bk-1995-0593.ch012

Literature Cited

1. (a) Mandava, N. B.; Ito, Y. *Countercurrent Chromatography: Theory and Practice*; Chromatographic Science Series, vol. 44; Dekker: New York, 1988; (b) Conway, W. D. *Countercurrent Chromatography. Apparatus, Theory, and Applications*; VCH: New York, 1990.
2. Fregeau, N. L.; Rinehart, K. L. In *High-Speed Countercurrent Chromatography*; Ito, Y.; Conway, W. D., Eds.; Wiley: New York; in press.
3. Oka, H.; Ikai, Y.; Kawamura, N.; Hayakawa, J.; Harada, K.; Murata, H.; Suzuki, M.; Ito, Y. *Anal. Chem.* **1991**, *63*, 2861-2865.
4. Schaufelberger, D. E. *J. Liq. Chrom.* **1989**, *12*, 2263-2280.
5. Lee, Y. W.; Voyksner, R. D.; Fang, Q. C.; Cook, C. E.; Ito, Y. *J. Liq. Chrom.* **1988**, *11*, 153-171.
6. Proefke, M. L. Ph.D. Dissertation, University of Illinois at Urbana-Champaign, Dec. 1991.
7. Niessen, W. M. A.; Tjaden, U. R.; Van der Greef, J. *J. Chrom.* **1991**, *554*, 3-26.
8. Stroh, J. G.; Cook, J. C.; Milberg, R. M.; Brayton, L.; Kihara, T.; Huang, Z.; Rinehart, K. L., Jr.; Lewis, I. A. S. *Anal. Chem.* **1985**, *57*, 985-991. see also ref. 6.
9. Roepstorff, P.; Fohlman, J. *Biomed. Mass. Spectrom.* **1984**, *11*, 601.

RECEIVED November 28, 1994

Downloaded by OHIO STATE UNIV LIBRARIES on June 28, 2012 | http://pubs.acs.org
Publication Date: May 15, 1995 | doi: 10.1021/bk-1995-0593.ch013

Chapter 13

Measurement of Partition Coefficient Using Centrifugal Partition Chromatography

Method Development and Application to the Determination of Solute Properties

Ruey-Shiuan Tsai, Pierre-Alain Carrupt, and Bernard Testa

Institut de Chimie Thérapeutique, Ecole de Pharmacie, BEP, Université de Lausanne, CH–1015 Lausanne, Switzerland

Measurement of partition coefficients in various solvent systems has been developed using flow-through centrifugal partition chromatography (CPC). The present paper details the experimental design, and shows that this method is able to measure compounds in a log P range of *ca.* -3.2 to 3.2 in a precise, accurate and rapid way. The usefulness of some lipophilicity-derived parameters such as Δlog $P_{oct\text{-}alk}$ (log $P_{octanol}$ minus log P_{alkane}, reflecting mainly the hydrogen bond donor acidity of solutes) was thus reinforced due to the timely development of this method. We also demonstrated the application of the Δlog P parameter both in characterizing the structural properties of drugs and in uncovering their pharmacological implications.

Lipophilicity is a molecular property of drugs and other xenobiotics of significance mainly because of its intimate relation with biological activity (*1-2*). This is particularly true when absorption, penetration or distribution is the limiting step in drug activity (*3*). Moreover, quantitative structure-activity relationship (QSAR) studies have often shown that hydrophobic interactions play an important role in the processes of molecular recognition underlying, e.g., drug-receptor interactions (*4*). Lipophilicity is conventionally expressed as the partition coefficient in an octanol/water system, while other immicible organic/aqueous systems such as chloroform/water and alkane/water have also been used to express this molecular property (*5-6*).

A conceptual analysis of lipophilicity has revealed that it can be factorised into a steric/bulk term (i.e. hydrophobicity, denoted as V) and polarity (denoted as Λ) (*7*). V expressess the hydrophobic structuration of hydration shells in water, and dispersive forces between solute and organic phase, while Λ is the sum of polar interactions between solute and the two phases (Fig. 1) (*8*). The physicochemical nature of solute partitioning in a biphasic system thus involves complex intermolecular interactions. This analysis equally implies that the rich structural information content encoded in partition coefficients can in principle be unravelled. Indeed, structure-lipophilicity relationship studies have revealed inter- and intramolecular interactions which are not always detectable by other approaches (*9-10*).

0097–6156/95/0593–0143$12.00/0

Downloaded by OHIO STATE UNIV LIBRARIES on June 28, 2012 | http://pubs.acs.org
Publication Date: May 15, 1995 | doi: 10.1021/bk-1995-0593.ch013

A number of experimental techniques have been developed to measure liquid-liquid partition coefficients, the most frequently used one being the shake-flask method (*11-12*), in which the two poorly miscible liquid phases are gently stirred until partition equilibrium is reached. This method however suffers from several pratical limitations due to various factors such as time consumption, formation of microemulsions, concentration and salt effects, solute impurities and solute solubility, volatility or instability (*13*). Other methods such as the "Filter Probe" (*14*) and octanol-coated HPLC (*15*) have also been mentioned in the literature, but they are all limited to compounds of log P > -1.3 and have not yet been extensively validated. The recently developed pH-metric method using two-phase titration techniques (*16*) has the advantage of measuring compounds without a chromophore in the UV or visible range, but it is limited to ionisable compounds.

In the past few years, our laboratory has shown a strong dedication to the measurement of partition coefficients using various centrifugal partition chromatographic (CPC) techniques (*17-20*). This liquid-liquid chromatographic method which uses two poorly miscible solvents (usually an organic solvent and water) as stationary and mobile phases provides a unique means for the measurement of partition coefficients. Our experience has shown that this method is able to measure compounds of log P values in the range between -3.2 and 3.2 and is not restricted to ionisable compounds. Its precision and accuracy have also been shown to be much superior to the shake-flask method. The first goal of this paper is to detail the optimised experimental design and procedure for this method. Furthermore, parameters derived from partition coefficients in different solvent systems will be used to characterise the structural properties of drugs and hence reveal their pharmacological implications.

Method Development

Calculation of Partition Coefficients. In the CPC system, the partition coefficient (log P) is defined as the ratio of solute concentrations in the stationary phase and in the mobile phase. When using the aqueous solution as eluent, the partiton coefficient is calculated as (*21*):

$$\log P = \log \frac{(t_R - t_0) \bullet U}{V_t - U \bullet t_0} \qquad (1)$$

where t_R is the retention time of the solute, U the flow rate of the mobile phase and V_t the total capacity of the columns. When using the organic solvent as mobile phase, the partition coefficient is then calculated as:

$$\log P = \log \frac{V_t - U \bullet t_0}{(t_R - t_0) \bullet U} \qquad (2)$$

Considerations about the Equipment. Four different types of counter-current chromatographs have been used to measure partition coeffients in our laboratory,

Downloaded by OHIO STATE UNIV LIBRARIES on June 28, 2012 | http://pubs.acs.org
Publication Date: May 15, 1995 | doi: 10.1021/bk-1995-0593.ch013

namely multichannel cartridges CPC (Sanki Engineering, Kyoto, Japan), toroidal coil planet centrifuge, flow-through multilayer coil planet centrifuge (also called Ito multilayer coil separator-extractor, P. C. Inc., Kim Place, Potomac, Maryland, USA) and horizontal flow-through multilayer CPC (model CCC-1000, Pharma-Tech Research, Baltimore, Maryland, USA). According to Ito (22), the CPC systems can be classified into two types, namely hydrostatic and hydrodynamic systems. The hydrostatic systems use stationary cartridges or coils in the multichannel cartridges CPC or the toroidal coil planet centrifuge, respectively. Thus, solutes percolate through the stationary and mobile phases, the retention of the stationary phase being mainly governed by the centrifugal force. The pressure generated in these systems is relatively high and the tubing leakage is an often encountered problem. In the hydrodynamic systems such as the flow-through multilayer coil planet centrifuge or the horizontal flow-through multilayer CPC, the rotation of the coiled column around its own axis creates an Archimedean screw force which, in combination with a revolutionary centrifugal force away from the centre of the centrifuge, allows a continuous mixing of the two phases while retaining a high proportion of the stationary phase and producing a low pressure in the system. All these features assure a high solute partition efficiency and a high retention of the stationary phase in the hydrodynamic systems as compared with the hydrostatic systems. For more details about the mechanisms of the systems, the reader is referred to an excellent review by Ito (22).

For a number of reasons, we have given preference to horizontal flow-through multilayer CPC consisting of three columns. Its centrifuge does not need to be counterbalanced when the volume ratio of stationary versus mobile phase is changed. In addition, when filling a vertical coiled column with volatile organic solvents such as chloroform, some air is likely to accumulate in the tubing and will perturb the measurement. This problem is easier to overcome when using an horizontal coiled column.

It is apparent that the length of tubing must also influence the partitioning equilibrium of solutes. In our experience, a length of 50-60 m of tubing is sufficient to ensure a partitioning equilibrium of solutes between the two phases. For the purpose of measuring the partition coefficients of very lipophilic or hydrophilic compounds, it is important to have a maximal retention of the stationary phase. In this respect, the tubing diameter becomes one of the important factors controlling the retention volume of stationary phase. Increasing the internal diameter of tubing generally results in a greater retention volume of the stationary phase, but the use of tubing with i.d. > 2.6 mm does not improve further the retention. The polytetrafluoroethylene (PTFE) tubing with an i.d. 2.6 mm and o.d. 3.4 mm (#10, Zeus Industrial Products, Orangeburg, Southern California, USA) has thus become our optimal choice. This internal diameter together with a length of 50-60 m yields a total volume of ca. 300-320 ml.

Experimental Design. Experimental layout for the measurement of partition coefficients using CPC is similar to that of capacity factors using HPLC, except that CPC uses a centrifuge mounted with coiled columns rather a solid-phase column. We use a Kontron model 420 HPLC pump (Kontron Instrument, Zürich, Switzerland) between 0.05-10 ml/min, to propel the mobile phase and a Kontron model 432 UV-vis detector (variable wavelength) coupled with a Hewlett-Packard 3392A integrator (Hewlett-Packard, Avondale, Pennsylvania, USA) to detect the eluate. A flowmeter (Phase Separations, Queensferry, UK) is used to measure precisely the flow rate. It must be noted that a stable flow rate is of critical importance for the measurements.

It is important to estimate in advance the partition coefficient of the investigated compounds in order to set up optimal conditions. We have used the

Downloaded by OHIO STATE UNIV LIBRARIES on June 28, 2012 | http://pubs.acs.org
Publication Date: May 15, 1995 | doi: 10.1021/bk-1995-0593.ch013

CLOGP program of Hansch and Leo to estimate partition coefficients in octanol/water systems (*23*). For compounds of log P values > 0, it is appropriate to use the organic phase as mobile phase. For compounds of log P values < 0, the aqueous phase should be used as mobile phase. Measurements begin by filling the columns at a flow rate of 5 ml/min with the stationary phase presaturated with the mobile phase. When filling the columns with volatile solvents such as alkanes, the flow rate should be reduced to prevent the accumulation of air bubbles in the columns. When the columns are full, the centrifuge is rotated at a speed of ca. 800-1000 rpm and the mobile phase is propelled into the columns. For different log P ranges, the flow rate of mobile phase should be accordingly adjusted in order to elute the solute at an appropriate retention time. Here we recommend an approximate scheme for the use of flow rate at different log P ranges (see also Fig. 2):

for $\log P > 2.5$ or $\log P < -2.5$	$U = 0.5$ ml/min
for $1.5 < \log P < 2.5$ or $-2.5 < \log P < -1.5$	$U = 1$ ml/min
for $0.5 < \log P < 1.5$ or $-1.5 < \log P < -0.5$	$U = 3$ ml/min
for $0 < \log P < 0.5$ or $-0.5 < \log P < 0$	$U = 6$ ml/min

Under flow rates of 0.5, 1, 3 and 6 ml/min, *ca.* 310, 305, 290 and 270 ml of the stationary phase of an octanol/water system can be retained.

After the system has reached its equilibrium, i.e. no more stationary phase exudes from the columns, a Merck injector is used to inject 200 μl samples containing 0.1-5 mM of solutes dissolved in the mobile phase.

A precise measurement of the dead volume or retention time of non-retained solutes (t_0) is of primordial importance for the accurate measurement of partition coefficients, particularly for compounds with log P > 2.5 or < -2.5. In the past, we used either anthracene or biphenyl as the non-retained solute when the organic phase was the eluent. However, anthracene is easily oxidized in solution, while biphenyl is more stable and is thus our preferred standard of t_0 determination. As for non-retained hydrophilic compounds when water is the eluent, potassium dichromate, sodium nitrate and cobalt chloride are used satisfactorily in our laboratory.

In principle, UV-vis spectrometry is not the only mode of detection of eluates, and refractometry should allow to detect compounds lacking a chromophore. Admittedly, we have not yet investigated UV-inactive compounds.

As compared to the shake-flask method, the measurement of partition coefficients using CPC is much less perturbed by small amounts of impurities in the sample. Furthermore, the simultaneous determination of several compounds is feasible if their eluted chromatograms are well separated (see Fig. 3 as an example). The effects of concentration appear negligible, as exemplified in Fig. 4 where the retention times of 5-fluorouracil at three concentrations show only negligible differences.

It is not necessary to empty and refill the columns each day provided that the same solvent system is used. Note that the organic solvents can be reused after distillation and saturation with aqueous solution. Before changing the solvent system, it is advisable to wash the coils with methol and dry them with a flow of nitrogen.

Validation of the Method in Different Solvent Systems

The octanol/water partition coefficients measured by the CPC method were validated by comparison with the shake-flask method (*20*). Note that each compound was measured at least in triplicate and three measurements usually took no more than 2 hours. Among the compounds examined (which include alcohols, benzenes, phenols, anilines, benzamides, acetanilides, benzoic acids, benzenesulfonamides, amino acids,

Downloaded by OHIO STATE UNIV LIBRARIES on June 28, 2012 | http://pubs.acs.org
Publication Date: May 15, 1995 | doi: 10.1021/bk-1995-0593.ch013

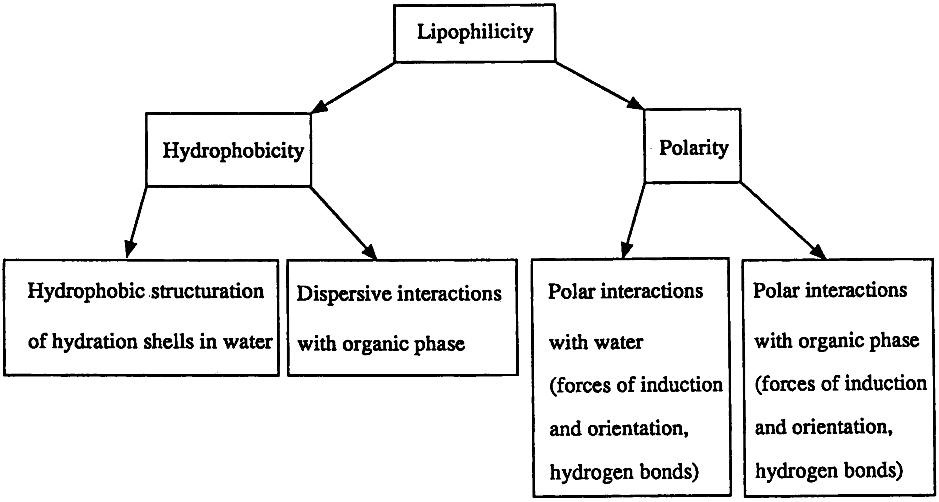
Lipophilicity
Hydrophobicity
Polarity
Hydrophobic structuration of hydration shells in water
Dispersive interactions with organic phase
Polar interactions with water (forces of induction and orientation, hydrogen bonds)
Polar interactions with organic phase (forces of induction and orientation, hydrogen bonds)

Figure 1. Conceptual factorization of lipophilicity.

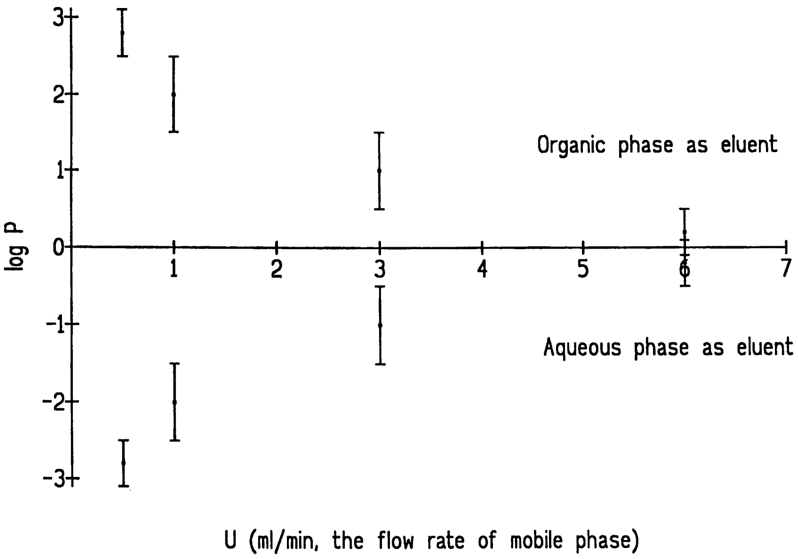

Figure 2. A proposed scheme for the flow rates of mobile phase in different log P ranges.

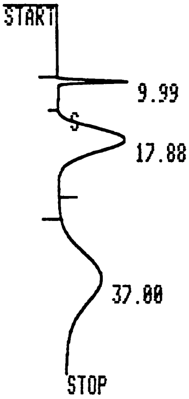

Figure 3. A chromatogram of a mixture of three compounds demonstrating their simultaneous log P measurements. The indicated values are the retention times of eluted compounds. (Reproduced with permission from reference 20. Copyright 1991 Elsevier.)

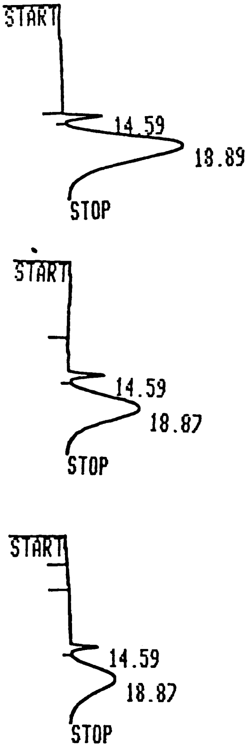

Figure 4. Three chromatograms showing the reproducibility of measurements at different solute concentrations. (Reproduced with permission from reference 20. Copyright 1991 Elsevier.)

Downloaded by OHIO STATE UNIV LIBRARIES on June 28, 2012 | http://pubs.acs.org
Publication Date: May 15, 1995 | doi: 10.1021/bk-1995-0593.ch013

nucleosides etc.), excellent correlations between the partition coefficients measured by the two methods were found (Fig. 5). These results have demonstrated the applicability of CPC for measuring partition coefficients. However, our experience has shown that the CPC method is limited to compounds with log P values between -3.2 and 3.2. Beyond this range, the solute elutes some seconds later than the non-retained compound, resulting in large errors in the calculation of partition coefficients. While different modes of operation such as the interchange of ascending and descending mode could enlarge the range of measurable log P values, these methods are rather tedious and likely to bear additional errors. To date, we find no solution to this limitation. For the measurement of log P beyond this range, it is thus recommended to consider other indirect methods, e.g. RP-HPLC for very lipophilic compounds (*24*).

We have also measured partition coefficients in heptane/water systems (P_{hep}) and compared the results with published values obtained by the shake-flask method (*20*). Again, an excellent correlation was found between the results of the two methods (Fig. 6). While a greater volume of stationary phase can be retained in the heptane/water system than in the octanol/water system, the range of log P values cannot be significantly enlarged as indicated in Fig. 6. It should also be noted that air bubbles may co-elute with the solutes when using heptane as mobile phase, thus perturbing the detection of eluates. To circumvent this problem, we have recently replaced heptane by the less volatile dodecane, with no influence on the values of the partition coefficients thus measured.

Downloaded by OHIO STATE UNIV LIBRARIES on June 28, 2012 | http://pubs.acs.org
Publication Date: May 15, 1995 | doi: 10.1021/bk-1995-0593.ch013

Structural Information Encoded in Lipophilicity

In recent years, Taft, Kamlet, Abraham and co-workers have factorized partition coefficients by the solvatochromic method using structural parameters such as dipolarity/polarisability (π^*), hydrogen bond donor acidity (α) and hydrogen bond acceptor basicity (β) (*25*). These structural parameters of solutes together with calculated van der Waals volume (V_w) have proven their usefulness in characterising the structural determinants of solubility-related molecular properties of neutral organic solutes in solution (S_p) (*26*). This is usually described in a linear free-energy relationship:

$$S_p = m\,(V_w/100) + s\,\pi^* + a\,\alpha + b\,\beta + S_{p0} \qquad (3)$$

where m, s, a and b are the regression coefficients which reflect the relative contribution of each parameter to S_p, and S_{p0} is the intercept of the multivariate regression. The tentative solvation model behind Eqn. 3 is the endoergic creation of a cavity in the solvent as reflected by the V_w term and then introduction of the solute in the cavity which leads to exoergic polar solute-water interactions as reflected by the π^*, α and β terms (see also Fig. 1).

We have applied this approach to evaluate and identify the intermolecular forces underlying the partitioning mechanisms of solutes in various organic/aqueous biphasic systems (*27*). For example, the partition coefficients in an octanol/water system were found to be mainly accounted for by a positive V_w term and negative β and π^* terms, while the contribution of α term is negligible (Eqn. 4). Here n is the number of compounds, r the correlation coefficient and s the standard deviation of the regression. Values in parentheses are the 95 % confidence limits.

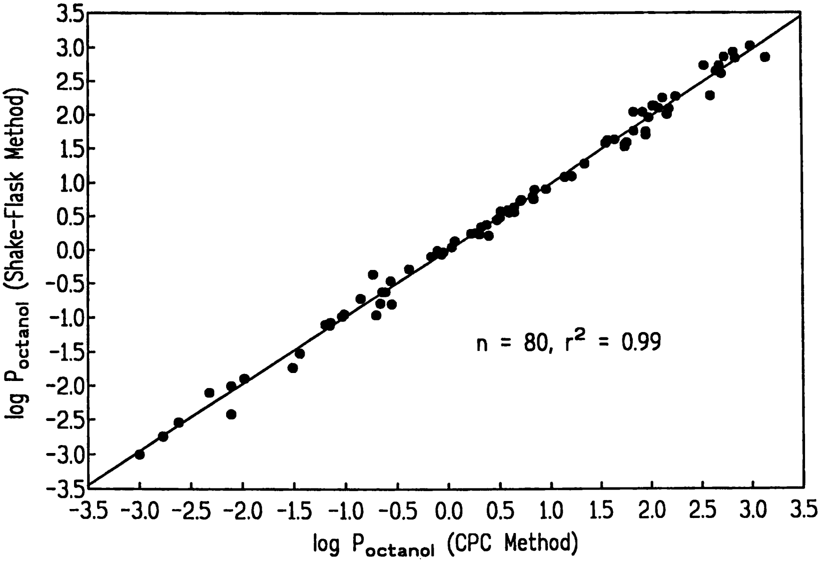

Figure 5. Linear relationship between octanol/water partition coefficients measured by the CPC and shake-flask methods. (Reproduced with permission from reference 20. Copyright 1991 Elsevier.)

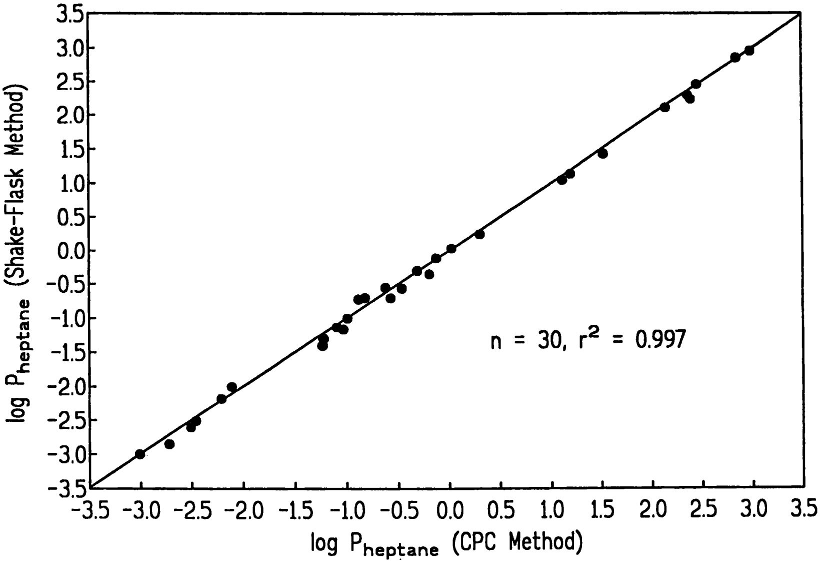

Figure 6. Linear relationship between heptane/water partition coefficients measured by the CPC and shake-flask methods. (Reproduced with permission from reference 20. Copyright 1991 Elsevier.)

Downloaded by OHIO STATE UNIV LIBRARIES on June 28, 2012 | http://pubs.acs.org
Publication Date: May 15, 1995 | doi: 10.1021/bk-1995-0593.ch013

Downloaded by OHIO STATE UNIV LIBRARIES on June 28, 2012 | http://pubs.acs.org
Publication Date: May 15, 1995 | doi: 10.1021/bk-1995-0593.ch013

$$\log P_{oct} = 5.83(\pm 0.53)\,(V_w/100) - 0.74\,(\pm 0.31)\,\pi^* - 0.15\,(\pm 0.23)\,\alpha - 3.51(\pm 0.38)\,\beta - 0.02(\pm 0.34) \quad (4)$$

$n = 78;\ r = 0.960;\ s = 0.296$

Eqn. 4 thus implies that the octanol phase is as good a hydrogen bond acceptor as the aqueous phase. In heptane/water systems, the α term contributes significantly and negatively to the partition coefficients, revealing another solvation/hydration balance:

$$\log P_{hep} = 6.78(\pm 0.69)\,(V_w/100) - 1.02\,(\pm 0.39)\,\pi^* - 3.54\,(\pm 0.30)\,\alpha - 5.35(\pm 0.50)\,\beta - 0.06(\pm 0.43) \quad (5)$$

$n = 75;\ r = 0.977;\ s = 0.360$

Interestingly, the different structural features of the two solvent systems lead to the finding that the parameter $\Delta\log P_{oct\text{-}alk}$ ($\log P_{octanol} - \log P_{alkane}$) reflects primarily the hydrogen bond donor acidity of solutes and secondarily their hydrogen bond acceptor basicity:[27]

$$\Delta\log P_{oct\text{-}alk} = 0.12(\pm 0.30)\,\pi^* + 3.40(\pm 0.25)\,\alpha + 1.96(\pm 0.42)\,\beta - 0.43(\pm 0.27) \quad (6)$$

$n = 75;\ r = 0.962;\ s = 0.31$

$$\Delta\log P_{oct\text{-}alk} = 3.54(\pm 0.36)\,\alpha + 0.37(\pm 0.15) \quad (7)$$

$n = 75;\ r = 0.915;\ s = 0.45$

Thus the $\Delta\log P_{oct\text{-}alk}$ parameter can be used to assess the hydrogen bond donor capacity of solutes, provided that the log P values in the two solvent systems are measured with high precision and accuracy. The timely development of the CPC method to measure partition coefficients can thus reinforce the usefulness of this $\Delta\log P_{oct\text{-}alk}$ parameter in structure-activity relationship studies.

Application of Lipophilicity-Derived Structural Parameters to Quantitative Structure-Activity Relationships

The $\Delta\log P_{oct\text{-}alk}$ parameter has been shown to be correlated with brain penetration of centrally acting H_2 histamine antagonists. A good correlation was found between the brain/blood concentration ratios at equilibrium in the rat and the Δlog P parameter (*28*):

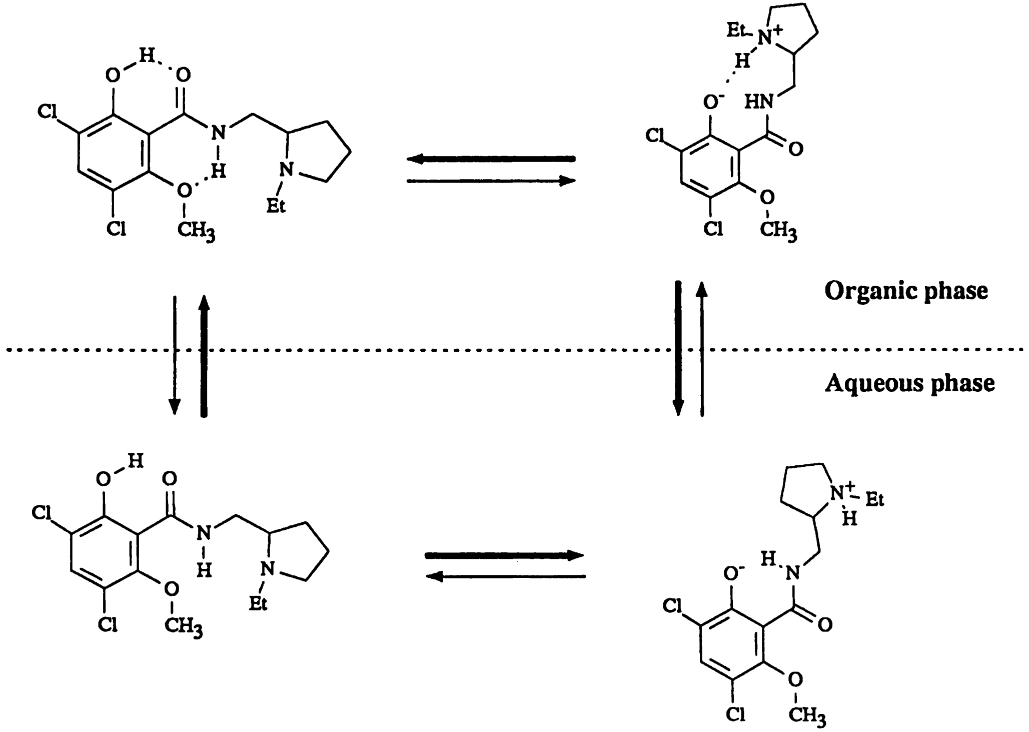

Figure 7. The interconversion, predominance, and conformational behaviour of neutral and zwitterionic raclopride in a biphasic system (*31*).

Downloaded by OHIO STATE UNIV LIBRARIES on June 28, 2012 | http://pubs.acs.org
Publication Date: May 15, 1995 | doi: 10.1021/bk-1995-0593.ch013

$$\log (C_{brain}/C_{blood}) = -\,0.49(\pm 0.16)\ \Delta\log P_{oct\text{-}alk} + 0.89(\pm 0.50) \qquad (8)$$

$n = 20$; $r = 0.831$; $s = 0.44$

In addition, the human skin permeation (K_p) of alcohols and steroid hormones has been shown to be determined mainly by their hydrogen bond donor acidity and to some extent also by their lipophilicity (*29*):

$$\log K_p = -\,1.46(\pm 0.23)\ \Delta\log P_{oct\text{-}alk} + 0.29(\pm 0.14) \log P_{oct} - 3.75(\pm 0.61) \qquad (9)$$

$n = 21$; $r = 0.954$; $s = 0.35$

These two examples strongly suggest that the passive transport of strong hydrogen bond donor solutes across membranes such as the skin or the blood-brain barrier will be hindered by hydrogen bonding to acceptor groups in membrane constituents (e.g., lipids and phospholipids).

Another interesting example comes from the physicochemical and structural investigation of antidopaminergic 6-methoxysalicylamides such as raclopride (*30-31*). This compound has been shown by us to exist in water at pH 7.4 as a zwitterion with stereoelectronic features completely different from those of other classes of dopamine antagonists such as substituted benzamides (*30*). Using first-derivative UV spectroscopy, the neutral rather than zwitterionic form of raclopride was found to partition predominantly into the octanol or heptane phase (*31*). Furthermore, the low $\Delta\log P_{oct\text{-}alk}$ value of raclopride (0.5) indicates the existence of strong internal hydrogen bonds OH•••O=C and CH_3O•••HNC=O in biological lipophilic media. A simplified scheme showing the interconversion, predominance and conformational behaviour of neutral and zwitterionic raclopride in a biphasic system is presented in Fig. 7. The $\Delta\log P_{oct\text{-}alk}$ parameter thus helps in revealing the true pharmacophoric features of 6-methoxysalicylamides which are therefore stereoelectronically similar to those of other substituted benzamides.

Conclusion

The factorization of lipophilicity represents a major advance in understanding the intermolecular forces it encodes and interpreting lipophilicity-activity relationships. The counterpoint to these theoretical advances is the development of centrifugal partition chromatography (CPC) as a highly effective and precise experimental technique for measuring partition coefficients.

Acknowledgments

The authors are indebted to the Swiss National Science Foundation for financial support.

Literature Cited

(1) Hansch, C.; Leo, A. *Substituent Constants for Correlation Analysis in Chemistry and Biology*; Wiely: New York, 1979.

Downloaded by OHIO STATE UNIV LIBRARIES on June 28, 2012 | http://pubs.acs.org
Publication Date: May 15, 1995 | doi: 10.1021/bk-1995-0593.ch013

(2) Rekker, R. F. *The Hydrophobic Fragmental Constant*; Elsevier: Amsterdam, 1977.

(3) See for example, Hansch, C.; Vittoria, A.; Silipo, C.; Jow, P. Y. C. *J. Med. Chem.* **1975**, *18*, 546.

(4) See for example, El Tayar, N.; Klipatrick, G. J.; van de Waterbeemd, H.; Testa, B.; Jenner, P.; Marsden, C. D. *Eur. J. Med. Chem.* **1988**, *23*, 173.

(5) Stein, W. D. *The Movement of Molecules Across Cell Membranes*; Academic Press: New York, 1967.

(6) Wright, L. L.; Painter, G. R. *Mol. Pharmacol.* **1992**, *41*, 957.

(7) Testa, B.; Seiler, P. *Arzneim.-Forsch.* **1981**, *31*, 1053.

(8) Tsai, R.-S. Ph.D. Thesis, Université de Lausanne, 1992.

(9) Tsai, R.-S.; Testa, B.; El Tayar, N.; Carrupt, P.-A. *J. Chem. Soc. Perkin Trans. 2* **1991**, 1797.

(10) Altomare, C.; Tsai, R.-S.; El Tayar, N.; Testa, B.; Carotti, A.; Cellamare, S.; De Benedetti, P. G. *J. Pharm. Pharmacol.* **1991**, *43*, 191.

(11) Leo, A.; Hansch, C.; Elkins, D. *Chem. Rev.* **1971**, *71*, 525.

(12) Dearden, J. C.; O'Hara, J. H. *Eur. J. Med. Chem.* **1978**, *13*, 415.

(13) Dearden, J. C.; Bresnen, G. M. *Quant. Struct.-Act. Relat.* **1988**, *7*, 133.

(14) Tomlinson, E. *J. Pharm. Sci.* **1982**, *71*, 602.

(15) Mirrlees, M. S.; Moulton, S. J.; Murphy, C. T.; Taylor, P. J. *J. Med. Chem.* **1976**, *19*, 615,

(16) Avdeef, A. *J. Pharm. Sci.* **1993**, *82*, 183.

(17) Tsai, R.-S.; El Tayar, N.; Testa, B.; Ito, Y. *J. Chromatogr.* **1991**, *538*, 119.

(18) El Tayar, N.; Marston, A.; Bechalany, A.; Hostettmann, K.; Testa, B. *J. Chromatogr.* **1989**, *469*, 91.

(19) Vallat, P.; El Tayar, N.; Testa, B.; Slacanin, I.; Marston, A.; Hostettmann, K. *J. Chromatogr.* **1990**, *504*, 411.

(20) El Tayar, N.; Tsai, R.-S.; Vallat, P.; Altomare, C.; Testa, B. *J. Chromatogr.* **1991**, *556*, 181.

(21) Berthod, A.; Armstrong, D. W. *J. Liq. Chromatogr.* **1988**, *11*, 567.

(22) Ito, Y. *CRC Crit. Rev. Anal. Chem.* **1986**, *17*, 65.

(23) Hansch, C.; Leo, A. MEDCHEM Project, Pomona College, Claremont, CA 91711, version 3.54, 1989.

(24) Minick, D. J.; Sabatka, J. J.; Brent, D. A. *J. Liq. Chromatogr.* **1987**, *10*, 2565.

(25) Kamlet, M. J.; Doherty, R. M.; Abraham, M. J.; Marcus, Y.; Taft, R. W. *J. Phys. Chem.* **1988**, *92*, 5244.

(26) Taft, R. W.; Abraham, M. H.; Doherty, R. M.; Kamlet, M. J. *Nature* **1985**, *313*, 384.

(27) El Tayar, N.; Tsai, R.-S.; Testa, B.; Carrupt, P.-A.; Leo, A. *J. Pharm. Sci.* **1991**, *80*, 590.

(28) Young, R. C.; Mitchell, R. C.; Brown, T. H.; Ganellin, C. R.; Griffiths, R.; Jones, M.; Rana, K. K.; Saunders, D.; Smith, I. R.; Nerina, E. S.; Wilks, T. J. *J. Med. Chem.* **1988**, *31*, 656.

(29) El Tayar, N.; Tsai, R.-S.; Testa, B.; Carrupt, P.-A.; Hansch, C.; Leo, A. *J. Pharm. Sci.* **1991**, *80*, 744.

(30) Carrupt, P.-A.; Tsai, R.-S.; El Tayar, N.; Testa, B.; de Paulis, T.; Höberg, T. *Helv. Chim. Acta* **1991**, *74*, 956.

(31) Tsai, R.-S.; Carrupt, P.-A.; Testa, B.; Gaillard, P.; El Tayar, N.; Höberg, T. *J. Med. Chem.* **1993**, *36*, 196.

RECEIVED January 19, 1995

Downloaded by OHIO STATE UNIV LIBRARIES on June 28, 2012 | http://pubs.acs.org
Publication Date: May 15, 1995 | doi: 10.1021/bk-1995-0593.ch013

Downloaded by UNIV OF GUELPH LIBRARY on June 29, 2012 | http://pubs.acs.org
Publication Date: May 15, 1995 | doi: 10.1021/bk-1995-0593.ch014

Chapter 14

pH-Zone-Refining Countercurrent Chromatography

A New Technique for Preparative Separation

Yoichiro Ito[1], Kazufusa Shinomiya[1,3], H. M. Fales[1], Adrian Weisz[2,4], and Alan L. Scher[2]

[1]Laboratory of Biophysical Chemistry, National Heart, Lung, and Blood Institute, National Institutes of Health, Building 10, Room 7N322, Bethesda, MD 20892
[2]Office of Cosmetics and Colors, Center for Food Safety and Applied Nutrition, U.S. Food and Drug Administration, Washington, DC 20204

pH-Zone-refining countercurrent chromatography (CCC) separates organic acids and bases into a succession of highly concentrated rectangular peaks that elute according to their pK_as and hydrophobicities. The hydrodynamic mechanism of the present method is illustrated along with a simple mathematical analysis. Examples of the application of the present method are described to demonstrate its advantage over conventional CCC. Similarities and differences between pH-zone-refining CCC, displacement chromatography, and isotachophoresis are discussed.

Conventional liquid partition chromatography employs a solid support, which may introduce complications due to adsorptive sample loss or solute deactivation. Furthermore, the amount of stationary phase available to the solute is limited by the requirement of maintaining a stable layer adhering to the support. When attempts are made to scale up the technique to a preparative level, this limitation results in a sharp decrease in efficiency (peak distortion) as the process moves into nonlinear regions of the partition isotherm of one or more of the solutes.

These difficulties are overcome by the use of countercurrent chromatography (CCC) (*1-3*), because no support is required and the stationary phase occupies 60 to 80% of the column volume. The tubular chromatography column is rotated so that centrifugal force and the helical column configuration separate and retain the two liquid phases. The superimposed planetary motion provides efficient mixing of the stationary and mobile phases, thereby speeding the mass transfer of the solutes.

---

[3] Current address: College of Pharmacy, Nihon University, 7–7–1, Narashinodai, Funabashi-shi, Chiba 274, Japan

[4] Guest researcher at Laboratory of Biophysical Chemistry, National Heart, Lung, and Blood Institute, National Institutes of Health, Bethesda, MD 20892

This chapter not subject to U.S. copyright
Published 1995 American Chemical Society

Among various models of the CCC instruments so far developed, the high-speed CCC centrifuge produces the most efficient separations in a short period of time (*4,5*). However, even with this technique the sample loading capacity is ultimately limited by the column size—a standard column with 300-mL capacity can be used for no more than several hundred milligrams of solute.

A new purification technique called pH-zone-refining CCC [because of its similarity to the zone-refining technique (*6*)] increases the sample capacity at least tenfold over conventional CCC and produces highly concentrated purified fractions. The method stemmed from discovery that addition of an organic acid either to the sample solution or to the stationary phase produced an abnormally sharp elution peak in the separation of certain acidic thyroxine derivatives (*7*). Increasing the size of the sample resulted in formation of a train of rectangular elution peaks comparable to those observed in displacement chromatography (*8*) and isotachophoresis (*9*).

The present article describes the general principle of pH-zone-refining CCC and includes a simple mathematical treatment of the technique, followed by applications to various ionizable compounds.

Principle

The pH-Zone-refining CCC technology uses a retainer acid (or base) in the stationary phase and an eluent base (or acid) in the mobile phase. This combination, acting in concert with the planetary motion of the CCC column, causes multiple solute transfers to occur between the two phases, resulting in separation of the solutes according to their acidity and hydrophobicity.

The experimental process is outlined in Figures 1 and 2A-C for the separation of acidic solutes. The preparation of the solvent phases initiates the experiment (Figure 1). A two-phase solvent system composed of water and either diethyl ether or methyl *tert*-butyl ether is thoroughly equilibrated in a separatory funnel at room temperature, and the two phases are separated. Either phase can be used as the stationary or mobile phase. In this case, the upper organic phase is acidified with a small amount of the retainer acid (trifluoroacetic acid, TFA) and used as the stationary phase (shaded). An eluent base (aqueous NH_3) is added to the lower aqueous phase, which is then used as the mobile component. The solute mixture is dissolved (or even suspended, see below) in a portion of the acidified stationary phase, and this is introduced at the column inlet. The mobile phase is then pumped into the column inlet while the apparatus rotates at an optimum speed selected for each pair of phases. At first some of the stationary phase is displaced from the column, but finally both phases are retained because of the centrifugal forces acting within the system.

Figure 2A-C illustrates the results of model experiments using three different samples: (A) a small amount of sample containing one major component (RCOOH), (B) a large amount of the same sample, and (C) a sample containing three different components (R_1COOH, R_2COOH, and R_3COOH), each in large quantity. In each figure, the upper diagram shows the action of the solutes as they undergo transfer between the phases within the column, and the lower diagram depicts the resulting elution profile.

In Figure 2A, as the ammoniacal mobile phase progresses through the column (after displacing its equilibrium volume of stationary phase, as mentioned above),

Downloaded by UNIV OF GUELPH LIBRARY on June 29, 2012 | http://pubs.acs.org
Publication Date: May 15, 1995 | doi: 10.1021/bk-1995-0593.ch014

Downloaded by UNIV OF GUELPH LIBRARY on June 29, 2012 | http://pubs.acs.org
Publication Date: May 15, 1995 | doi: 10.1021/bk-1995-0593.ch014

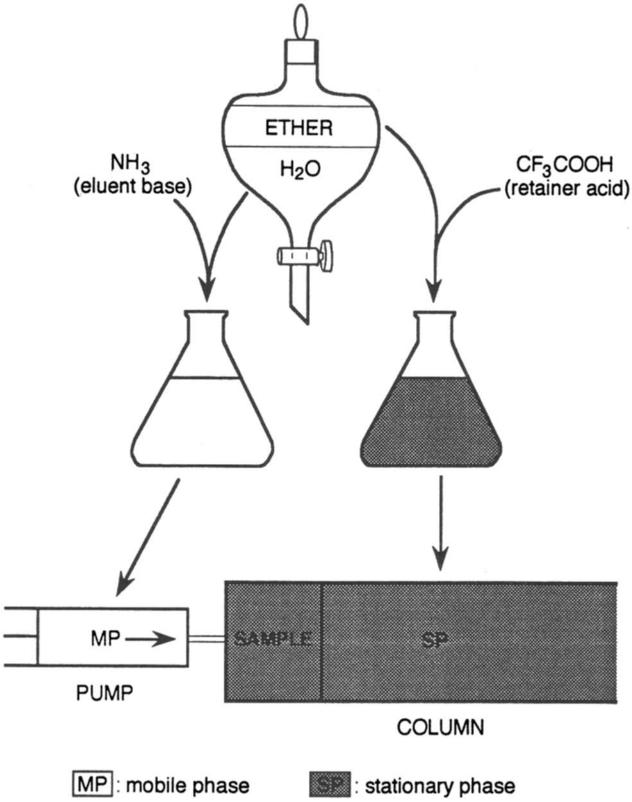
ETHER
H_2O
NH_3
(eluent base)
CF_3COOH
(retainer acid)
MP →
PUMP
SAMPLE
SP
COLUMN
MP : mobile phase
SP : stationary phase

Figure 1. Preparation of solvent phases to initiate the model experiments.

Downloaded by UNIV OF GUELPH LIBRARY on June 29, 2012 | http://pubs.acs.org
Publication Date: May 15, 1995 | doi: 10.1021/bk-1995-0593.ch014

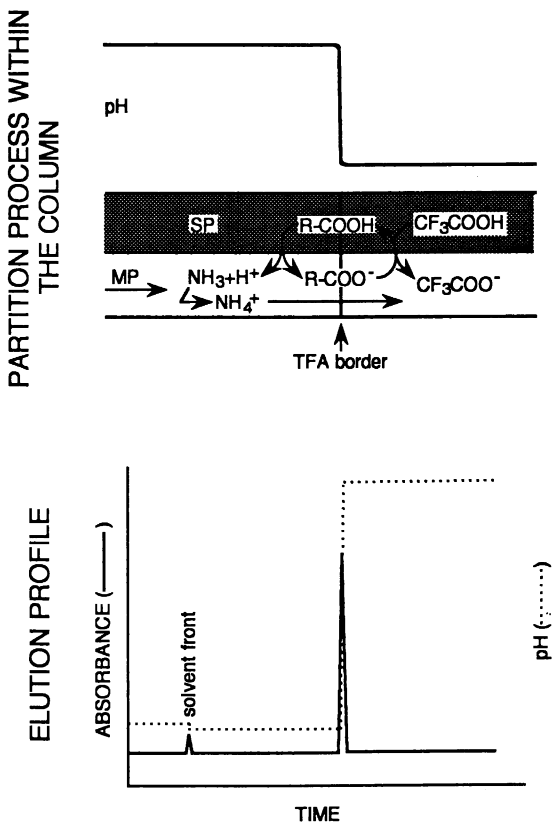
PARTITION PROCESS WITHIN THE COLUMN
pH
SP
R-COOH
CF3COOH
MP
NH3+H+
NH4+
R-COO-
CF3COO-
TFA border
ELUTION PROFILE
ABSORBANCE (——)
solvent front
pH (........)
TIME

Figure 2A. Chromatography of a small amount of sample mixture containing one major component.

Downloaded by UNIV OF GUELPH LIBRARY on June 29, 2012 | http://pubs.acs.org
Publication Date: May 15, 1995 | doi: 10.1021/bk-1995-0593.ch014

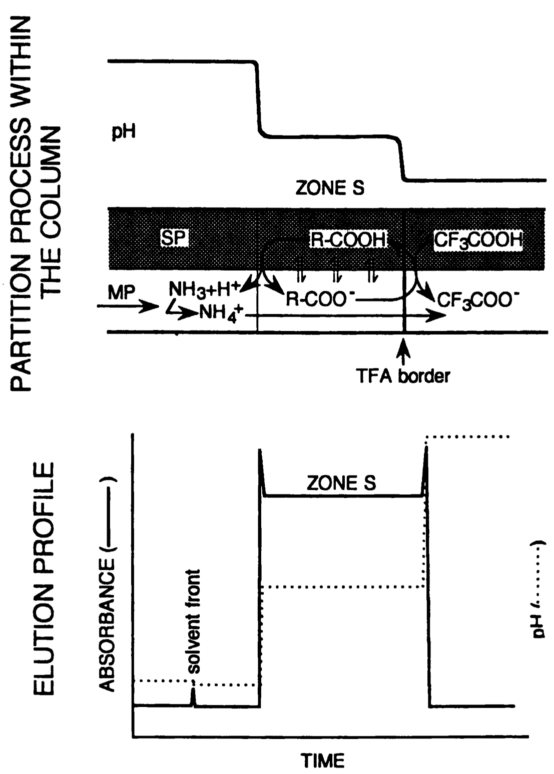

PARTITION PROCESS WITHIN THE COLUMN

ELUTION PROFILE

pH
ZONE S
SP
R-COOH
CF3COOH
MP
NH3+H+
NH4+
R-COO-
CF3COO-
TFA border
ABSORBANCE (——)
solvent front
ZONE S
pH (........)
TIME

Figure 2B. Chromatography of a large amount of sample mixture containing one major component.

Downloaded by UNIV OF GUELPH LIBRARY on June 29, 2012 | http://pubs.acs.org
Publication Date: May 15, 1995 | doi: 10.1021/bk-1995-0593.ch014

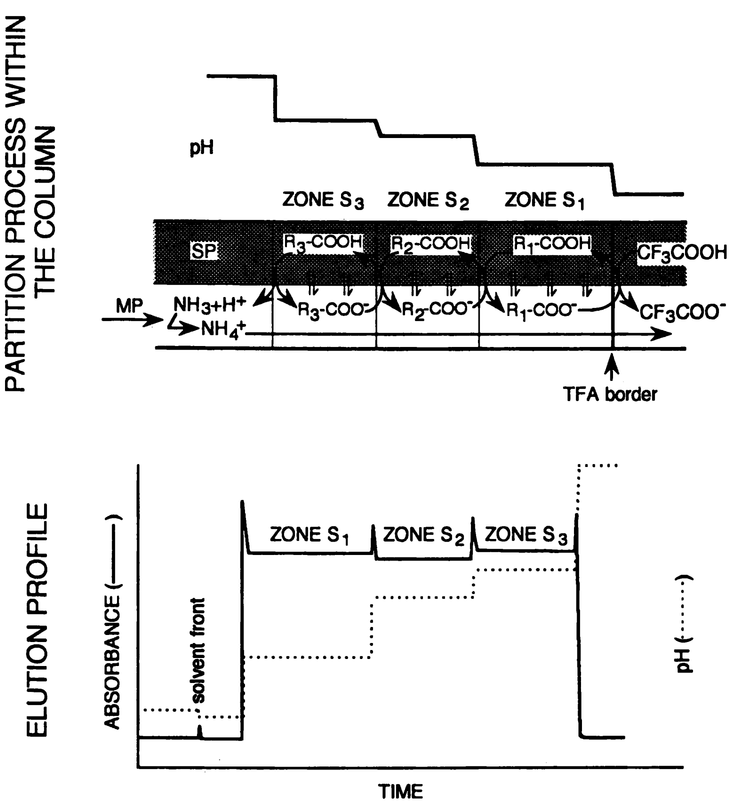
PARTITION PROCESS WITHIN THE COLUMN
pH
ZONE S3
ZONE S2
ZONE S1
SP
R3-COOH
R2-COOH
R1-COOH
CF3COOH
MP
NH3+H+
NH4+
R3-COO-
R2-COO-
R1-COO-
CF3COO-
TFA border
ELUTION PROFILE
ABSORBANCE (——)
solvent front
ZONE S1
ZONE S2
ZONE S3
pH (·······)
TIME

Figure 2C. Chromatography of a large amount of sample mixture containing three major components.

it extracts TFA from the stationary phase by converting it to the ammonium salt. The front of the mobile phase gradually becomes less basic as the ammonia in this zone is consumed and finally it becomes very acidic because of the partitioning and dissociation of TFA in the aqueous phase at this pH. The mobile phase front (solvent front, Figure 2A) now continues through the column and elutes with this acidic pH. The concentration of the free and dissociated TFA in the eluate remains constant because a partition steady state is reached with the initial concentration of TFA in the organic phase. This situation persists until the stationary phase at the outlet of the column is abruptly depleted of its TFA and the eluent pH rises sharply. More precisely, the apparent partition coefficient of TFA (total TFA in organic phase/total TFA in aqueous phase) in this system depends on its concentration—at higher concentrations relatively more TFA partitions into the organic stationary phase. The band-sharpening effect of this nonlinear isotherm dominates the sum of all band-broadening effects including the nonequilibrium partition process and longitudinal mixing. This sharp border marks the rear edge of the TFA peak as it moves through the column at a uniform rate that is less than that of the mobile phase. It thus plays an essential role in establishing the elution time of the front of the peak of the first acidic solute to elute and in defining the sharp leading edge of that peak.

If only a small amount of that weaker acid is present, as in Figure 2A, its own partition isotherm remains in the linear region and it elutes as a "normally shaped" peak. Significantly, however, it elutes as a much sharper peak than would a neutral compound with the same retention time because the acid is concentrated and elutes in the sharp peak transition between the TFA and the eluting base (*7*).

If a larger amount of RCOOH is present (Figure 2B), it in turn enters a region of isotherm nonlinearity, eluting like the TFA as a broad, flat-topped peak. Acids with still higher pK_as and hydrophobicities are retained by the stationary phase until RCOOH has also completely eluted. Loss of solute from the mobile phase at the front end of the solute zone (zone S) is compensated for by its return to the same phase at the trailing edge, where it encounters unbuffered ammonia. Consequently, once a steady-state hydrodynamic equilibrium is established, the solute zones maintain their width and specific pH levels. All fronts move at a constant rate determined by the TFA border, while the NH_4^+ counter ions are steadily passing through the zone while in the mobile phase. Meanwhile, small amounts of impurities present within zone S are subjected to continuous partitioning between the two phases, and they migrate either forward or backward toward the zone boundaries. As a result, the main body of the solute is eluted as a rectangular peak associated with sharp impurity peaks at both edges as shown in the lower diagram (Figure 2B).

Introduction of large equimolar amounts of three different solutes ($R_{1-3}COOH$) with very similar molar absorptivities (Figure 2C) results in mutual competition to occupy the column space immediately behind the sharp TFA retainer border. Because solute R_1COOH has the lowest pK_a value and hydrophobicity, it provides the lowest pH within its zone S_1 by protonating other components, forcing them into the stationary phase, and delaying their movement. Solute R_1COOH forms a second sharp trailing border for the next zone in the same manner as the TFA retainer acid. Competition for the available protons now continues between the

Downloaded by UNIV OF GUELPH LIBRARY on June 29, 2012 | http://pubs.acs.org
Publication Date: May 15, 1995 | doi: 10.1021/bk-1995-0593.ch014

other two solutes, and solute R_2COOH with a lower pK_a value and hydrophobicity drives out R_3COOH to establish the second zone. Finally solute R_3COOH occupies the end of the zone train to form a sharp trailing border. As indicated by curved arrows, proton transfer takes place at each zone boundary from the solute in the preceding zone (stationary phase) to those in the following zone (mobile phase), as governed by the difference in pH between these two neighboring zones, while the NH_4^+ counter ions continuously move with the mobile phase. After equilibrium is reached within the column, all solute zones move at the same rate as that of the trailing TFA border while constantly maintaining their own widths and pH levels. The nearly equal height of the flat-topped peaks in Figure 2C is merely a reflection of the nearly equal molar absorptivities and concentrations of the solutes in the effluent.

Downloaded by UNIV OF GUELPH LIBRARY on June 29, 2012 | http://pubs.acs.org
Publication Date: May 15, 1995 | doi: 10.1021/bk-1995-0593.ch014

Simple Mathematical Model of pH-Zone-Refining CCC

Figure 3 schematically illustrates the longitudinal cross section through a portion of the coiled column. The eluent is aqueous ammonia, and the stationary organic phase initially contains TFA. As discussed earlier, when the leading edge of the ammonia-containing mobile phase encounters the stationary phase, the TFA within that phase is extracted into the mobile phase until all of the ammonia is protonated. This results in formation of a sharp trailing boundary of the retainer acid. The elution rate of this retainer boundary through the column becomes constant when the concentration of the retainer acid in the mobile phase front (C_r) reaches partition equilibrium with the initial concentration of the retainer acid in the stationary phase (C_R). At this point, C_r and C_R are related by

$$\frac{C_R}{C_r} = K_r \qquad (1)$$

where K_r is the apparent partition coefficient of the retainer acid at this equilibrium state.

Retention Volume and Elution Rate of the Trailing Border of the Retainer Acid. The retention volume of the retainer acid (V_r) (the volume of the mobile phase required to elute the retainer acid completely through and from the column) and the elution rate (u) of the sharp retainer border through the column space occupied by the mobile phase are related by the following equations:

$$C_R V_s = C_r (V_r - V_m) \qquad (2)$$

$$V_m / u = V_r / u_m \qquad (3)$$

where V_s and V_m, respectively, indicate the volumes of stationary and mobile phases which remain in the column after the solvent front is eluted. Equation 2 shows that the net amount of the retainer acid in the stationary phase retained in the column is equal to the amount eluted from the column. In equation 3 the left term indicates the time required for the retainer acid to travel through the entire length of the column, which equals the retention time of the retainer acid in the chromatogram, indicated in the right term.

From equations 1-3, the retention volume of the retainer acid (V_r), the elution rate of the retainer border through the column (u), and the apparent partition coefficient of the retainer acid at the equilibrium state (K_r) are given in the following equations. Using equation 1 to substitute C_R/C_r in equation 2 gives:

$$V_r = K_r V_s + V_m \qquad (4)$$

Using equation 4 to substitute V_r in equation 3 gives:

$$u = \frac{u_m}{(V_s/V_m)K_r + 1} \qquad (5)$$

which is rearranged to:

$$K_r = \left(\frac{u_m}{u} - 1\right)\left(\frac{V_m}{V_s}\right) \qquad (6)$$

Apparent Partition Coefficient of Retainer Acid at Plateau. The actual value of K_r is obtained from the concentration of eluent base (C_E) and both the partition ratio (K_{D-r}) and the dissociation constant (K_{a-r}) of the retainer acid by using the following equation, provided that the concentrations of the eluent base and the anion of the retainer acid in the organic stationary phase are negligible:

$$K_r = \frac{1}{\dfrac{C_E}{2C_R} + \dfrac{1}{K_{D-r}} + \sqrt{\left(\dfrac{C_E}{2C_R}\right)^2 + \dfrac{K_{a-r}}{C_R K_{D-r}}}} \qquad (7)$$

Equation 7 is obtained from equation 1, the equations for the acid dissociation constant and the partition ratio of the retainer acid, and the charge balance equation as previously shown (Ito, Y. in *High-Speed Countercurrent Chromatography*; Ito, Y; Conway W.D., Eds.; Chemical Analysis Series, Wiley: New York, NY, in press).

Formation of Solute Zones Behind the Sharp Retainer Border. The experiment is repeated by similarly filling the column with organic stationary phase that has been acidified with the retainer acid. This is followed by injection of the sample solution containing an acidic solute with a pK_a and hydrophobicity higher than that of the retainer acid. Then the mobile phase containing an eluent base (aqueous NH_3) at concentration C_E is eluted through the column at a flow rate of u_m (L/min). This again results in the formation of the sharp retainer border which moves

Downloaded by UNIV OF GUELPH LIBRARY on June 29, 2012 | http://pubs.acs.org
Publication Date: May 15, 1995 | doi: 10.1021/bk-1995-0593.ch014

through the column volume occupied by the mobile phase at a uniform rate of u (L/min), which is lower than that of the mobile phase.

As explained earlier, analytes undergo a partition cycle around the sharp retainer border by repeated protonation and deprotonation caused by the large difference in pH between each side of the retainer border (Figure 2A). As this process takes place with a continuous supply of analyte from the mobile phase, the solute concentration around the retainer border gradually increases. The higher solute concentration, then, results in a lowered pH, which in turn raises the solute partition coefficient behind the retainer border until partition equilibrium is established between the two phases.

In order to facilitate mathematical treatment of the above hydrodynamic process, the moving trailing border of the retainer acid (Figure 3) is set stationary as indicated in Figure 4. From this modified viewpoint, both mobile and stationary phases pass through the retainer border countercurrent to each other at the relative rate of u_m - u (L/min) and $-uV_s/V_m$ (L/min), as indicated by the pair of arrows placed across the retainer front in the diagram. Now consider the partition process taking place on each side of the retainer border under a steady supply of the analyte from the mobile phase. On the right side where the pH is low, all analyte present in the flowing mobile phase is immediately protonated, forming a hydrophobic, nonionic form. It is quickly transferred into the stationary phase and sent back to the left side of the retainer border. On the left side of the retainer border (where the pH is high), the analyte is quickly transferred to the mobile phase. Because of the continuous supply of the analyte from the mobile phase, the solute concentration on the left side of the retainer border starts to rise. This causes a decrease in pH, which in turn increases the partition coefficient of the solute (due to its nonlinear isotherm) until a steady-state partition equilibrium is established between the two phases. Movements of the analyte are indicated by the thick arrows across the interface in the diagram. At this time, the rate of the analyte transfer from the mobile phase to the stationary phase on the right side of the retainer border is given by the analyte concentration in the mobile phase (C_m) multiplied by the rate of transfer of the mobile phase through the retainer border (u_m - u). The analyte transferred from the mobile phase is then uniformly distributed in the stationary phase at a concentration (C_s) that is determined by the relative flow rate of the stationary phase through the trailing border of the retainer acid (uV_s/V_m). Therefore, at a given moment

$$C_m(u_m-u) = C_s u V_s / V_m \tag{8}$$

From equation 8, the apparent solute partition coefficient (K_s) is expressed as:

$$K_s = \frac{C_s}{C_m} = \left(\frac{u_m}{u}-1\right)\left(\frac{V_m}{V_s}\right) \tag{9}$$

Downloaded by UNIV OF GUELPH LIBRARY on June 29, 2012 | http://pubs.acs.org
Publication Date: May 15, 1995 | doi: 10.1021/bk-1995-0593.ch014

Downloaded by UNIV OF GUELPH LIBRARY on June 29, 2012 | http://pubs.acs.org
Publication Date: May 15, 1995 | doi: 10.1021/bk-1995-0593.ch014

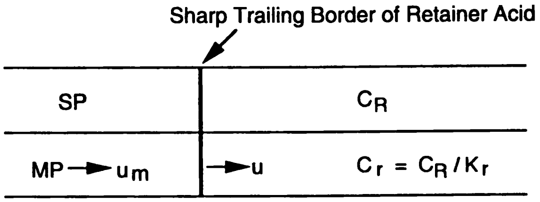
Sharp Trailing Border of Retainer Acid
SP
C_R
MP → u_m
→ u
$C_r = C_R/K_r$

Figure 3. A portion of the separation column showing a sharp trailing border of the retainer acid.

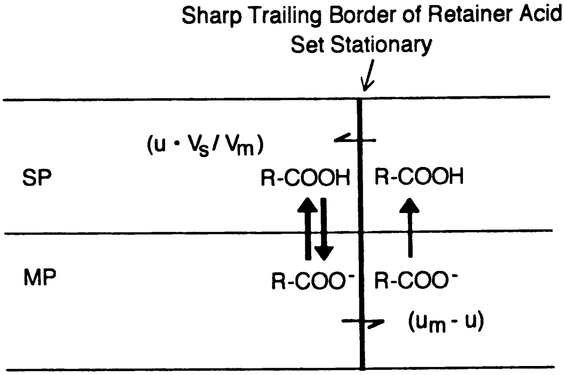
Sharp Trailing Border of Retainer Acid
Set Stationary
$(u \cdot V_s/V_m)$
SP
R-COOH
R-COOH
MP
R-COO⁻
R-COO⁻
$(u_m - u)$

Figure 4. A portion of the separation column showing analyte movement around a stationary retainer border.

Comparison of equations 6 and 9 shows that the solute partition coefficient (K_s) on the left side of the retainer border is equal to that of the retainer acid itself (K_r) on the right side of the border, i.e., $K_s = K_r$. This shows that the ratio of the solute concentrations in the stationary and mobile phases in the equilibrated solute zone is equal to and determined by that of the retainer acid. Once this partition equilibrium is reached, further supply of the solute through the mobile phase results in development of the solute zone behind the sharp border of the retainer acid. The width of the solute zone increases proportionally with the amount of the solute loaded into the column.

The pH of the mobile phase in the equilibrated solute zone (pH_z) is given by the following equation:

$$pH_z = pK_a + \log\left(\frac{K_{D-s}}{K_s} - 1\right) \tag{10}$$

where $K_{D\text{-}s}$ is the partition ratio of the analyte, i.e., $[AH_{org}]/[AH_{aq}]$ (concentration of the protonated analyte in the organic phase/concentration of the protonated analyte in the aqueous phase); this term also represents the hydrophobicity of the solute molecule. Since $K_s = K_r$, the value of pH_z can be computed from equations 7 and 10.

Multiple Solute Zones and Their Mutual Relationship. When two or more different solutes are introduced in large quantities, the solutes form a train of solute zones as illustrated in Figure 5. After the partition equilibrium is reached, each solute zone consists of a single component, equipped with self-sharpening boundaries and arranged in an increasing order of the zone pH (pH_z) determined by the solute pK_a and $K_{D\text{-}s}$ (hydrophobicity) as indicated in equation 10. All solute zones move together at the same rate, which is determined by that of the retainer acid. As described earlier, the apparent partition coefficient of the solute in each zone is equal to that of the retainer acid. Therefore,

$$K_r = \frac{C_{s\text{-}1}}{C_{m\text{-}1}} = \frac{C_{s\text{-}2}}{C_{m\text{-}2}} = \frac{C_{s\text{-}3}}{C_{m\text{-}3}} \cdots \tag{11}$$

$$pH_{z\text{-}retainer} < pH_{z\text{-}1} < pH_{z\text{-}2} < pH_{z\text{-}3} < \ldots \tag{12}$$

Consequently, the retainer acid and the following solute zones are eluted as a succession of pH zones, each corresponding to a single species with its specific pK_a and hydrophobicity.

Figure 6 shows the relationship between the pH-K plot of the solutes (left) and the elution profiles of their pH zones (right). Each pH-K curve is computed from equation 10 by using the pK_a and partition ratio ($K_{D\text{-}s}$) of the solute. If these parameters are not available, the pH-K curve can be obtained by equilibrating

Downloaded by UNIV OF GUELPH LIBRARY on June 29, 2012 | http://pubs.acs.org
Publication Date: May 15, 1995 | doi: 10.1021/bk-1995-0593.ch014

Downloaded by UNIV OF GUELPH LIBRARY on June 29, 2012 | http://pubs.acs.org
Publication Date: May 15, 1995 | doi: 10.1021/bk-1995-0593.ch014

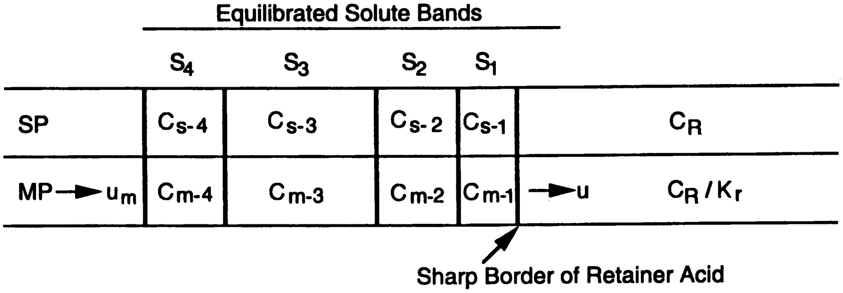
Equilibrated Solute Bands
S_4
S_3
S_2
S_1
SP
C_{s-4}
C_{s-3}
C_{s-2}
C_{s-1}
C_R
MP → u_m
C_{m-4}
C_{m-3}
C_{m-2}
C_{m-1}
→ u
C_R / K_r
Sharp Border of Retainer Acid

Figure 5. A portion of the separation column showing a train of equilibrated solute zones

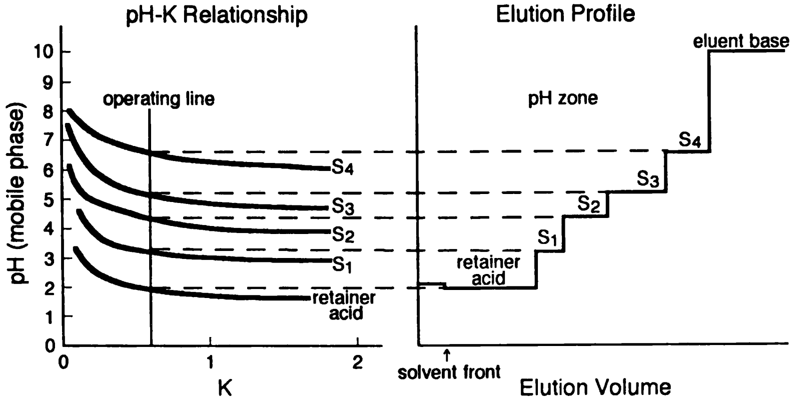

Figure 6. Relationship between pH-K curves and eluted pH zones.

Downloaded by UNIV OF GUELPH LIBRARY on June 29, 2012 | http://pubs.acs.org
Publication Date: May 15, 1995 | doi: 10.1021/bk-1995-0593.ch014

various amounts of the solute with the solvent system (containing the eluent base but no retainer acid), and measuring both the pH and the solute concentration in the upper and lower phases. A vertical line drawn through the critical K value (K_r or K_s) is the operating line which intersects each curve to determine the pH level in the corresponding solute zone as shown in the right diagram.

These curves are useful for predicting the order of elution, the pH of each solute zone, and the feasibility of a given separation. A successful separation is expected if the individual curves are evenly distributed some distance apart. Measuring the pH values of analyte zones provides an additional means to monitor the eluate, and may be the preferred way to monitor the elution of analytes without chromophores.

Experimental

Apparatus. A commercial model (Ito Multilayer Coil Separator/Extractor, P.C,. Inc., Potomac, MD) of the high-speed CCC centrifuge was used throughout the present studies. The design of the apparatus was described previously (*4*). The apparatus consisted of a multilayer coil separation column and a counterweight held symmetrically at a distance of 10 cm from the central axis of the centrifuge. The column holder was equipped with a plastic gear which was engaged to an identical stationary gear mounted around the central axis of the apparatus. This gear arrangement produced the desired planetary motion of the column holder, i.e., rotation and revolution in the same direction at the same rate. This planetary motion, besides providing the mixing action, prevented the flow tubes from twisting continuously during revolution, allowing elution of the mobile phase without the use of rotary seals.

The separation column consisted of a single piece of polytetrafluoroethylene (PTFE) tubing, 160 m × 1.6 mm i.d. (Zeus Industrial Products, Raritan, NJ), wound around the column holder hub and forming 16 layers with 320 mL total capacity. Both terminals of the column were connected to a PTFE flow tube, 0.85 mm i.d. (Zeus Industrial Products). A leak-free junction was made by inserting the end of the flow tube into the column terminals and wrapping copper wire tightly around the junction.

The speed of the apparatus was regulated at 800 rpm with a speed controller (Bodine Electric Company, North Chicago, IL).

Reagents. Methyl *tert*-butyl ether, acetonitrile, methanol, hexane, ethyl acetate, chloroform, and trifluoroacetic acid (TFA) were all glass-distilled chromatographic grade (Burdick & Jackson Laboratories, Muskegon, MI). Diethyl ether (Mallinckrodt, Inc., Paris, KY), ammonium hydroxide (aqueous ammonia), and ammonium acetate (Fisher Scientific, Pittsburgh, PA) were all reagent grade. Samples used in the present studies included dinitrophenyl (DNP) amino acids, indole auxins (Sigma Chemical Company, St. Louis, MO), and L-proline benzylester (Travenol Laboratories, Los Angels, CA). D&C Orange No. 5 (a mixture of hydroxyxanthene dyes) was obtained from the US Food and Drug Administration (Washington, DC).

Preparation of the Two-Phase Solvent System and Sample Solutions. The two-phase solvent systems used in the present study are listed in Table I. Each was prepared by thoroughly equilibrating the solvent mixture in a separatory funnel at room temperature and separating the two phases. Usually the upper organic phase was acidified with TFA (retainer acid), typically 0.04% (v/v) (0.005 M), while aqueous NH_3 (eluent base) was added to the lower aqueous phase, typically at a concentration of 0.1% (v/v) (0.0148 M). In some cases, the retainer acid was added to the sample solution instead of to the stationary phase.

The sample solutions were prepared by dissolving the sample in a sufficient quantity of the two-phase mixture. Volume varied according to the sample size from 4 to 200 mL. In the separation of components of hydroxyxanthene dyes (D&C Orange No. 5), retainer acid (TFA) was added to the sample solution instead of to the stationary phase. In some separations in which the solubility of the sample was limited, the suspension was thoroughly sonicated and directly loaded into the column without filtration.

Downloaded by UNIV OF GUELPH LIBRARY on June 29, 2012 | http://pubs.acs.org
Publication Date: May 15, 1995 | doi: 10.1021/bk-1995-0593.ch014

Separation Procedure. In each separation, the column was entirely filled with the stationary phase and the sample solution was injected through the sample port. Then the mobile phase was eluted through the column at a flow rate of 3 mL/min while the apparatus was rotated at 800 rpm. The effluent from the outlet of the column was continuously monitored by measuring absorbance at 206 nm with a UV detector (Uvicord S, LKB Instruments, Bromma/Stockholm, Sweden), and fractions were collected (usually 3 mL/tube or 1 min/tube) (Ultrorac, LKB Instruments). After all the desired peaks were eluted, the apparatus was stopped and the column contents were collected in a graduated cylinder by connecting the inlet of the column to an N_2 line pressured at 80 psi. The percent retention of the stationary phase relative to the total column capacity was computed from the volume of the stationary phase collected.

Analysis of the Eluate. The absorbance of the effluent was monitored at 206 nm by using an LKB Uvicord S detector, which produced successive plateaus of the main components as well as sharp peaks of impurities at the edges of each plateau. It is important to stress, however, that the absorbance traces in Figures 7-11 are at best qualitative because the interference filter used transmitted a considerable amount of light at wavelengths above 206 nm. Although the eluate transmitted virtually no light at 206 nm, the detector was responding to changes in transmittance at higher wavelengths. The flat tops of the peaks are not attributable to saturation of the detector, because the absorbance frequently increased before, between, and/or after the plateaus. The nearly equal heights of the plateaus in a chromatogram reflect decreased sensitivity at high absorbance due to the logarithmic response (transmittance) of our detector, the detection of a range of wavelengths, and the similarity of the compounds being separated. The 0-250 absorbance axis in Figure 8 represents a calibration at 206 nm obtained by diluting a fraction from within the flat-topped zone at one arbitrary point. Although the lower sensitivity at high absorbance may hide differences in absorbance, the peaks are indeed flat-topped for the reasons mentioned earlier. Different absorbances for plateaus in a chromatogram have been obtained when detectors with short

Downloaded by UNIV OF GUELPH LIBRARY on June 29, 2012 | http://pubs.acs.org
Publication Date: May 15, 1995 | doi: 10.1021/bk-1995-0593.ch014

Table I. Analytes and Two-Phase Solvent Systems Used in the Present Studies

Analytes	*Solvent System*		*Retainer in SP*[a]	*Eluent in MP*[b]
DNP[c] amino acids	MBE[d]	4	TFA[e] in sample solution	NH_3
	AcN[f]	1		
	H_2O	5		
	MBE		TFA	NH_3
	H_2O			
Indole auxins	MBE		TFA	NH_3
	H_2O			
Stereo-isomers[g]	Hexane	1	TFA + octanoic acid	NH_3
	EtOAc[h]	1		
	MeOH	1		
	H_2O	1		
D&C Orange No. 5	DEE[i]	4	TFA in sample solution	NH_3
	AcN	1		
	NH_4OAc[j] 10 mM	5		
L-Proline benzylester	MBE		TEA[k]	HCl
	H_2O			

[a] SP: stationary phase. [b] MP; mobile phase. [c] DNP: dinitrophenyl. [d] MBE: methyl *tert*-butyl ether. [e] TFA: trifluoroacetic acid. [f] AcN: acetonitrile. [g] Stereoisomers: 1-methyl-4-methoxymethylcyclohexanecarboxylic acids. [h] EtOAc: ethyl acetate. [i] DEE: diethyl ether. [j] NH_4OAc: ammonium acetate. [k] TEA: triethylamine.

pathlengths were used. Approximately half of the total response of the detector was due to absorption at 206 nm and half was due to absorption at longer wavelengths. In one respect, this lack of wavelength specificity was convenient in the present study because the detector responded to changes in transmittance at longer wavelengths, thereby detecting the sample components and certain impurities at the plateau edges.

The pH value of each fraction was manually determined with a portable pH meter (Accumet Portable Laboratory, Fisher Scientific, Pittsburgh, PA).

Amino acid derivatives were identified by their partition coefficients in a standard two-phase system composed of chloroform-acetic acid-0.1 M HCl (2:2:1, v/v) as follows: An aliquot of each fraction (0.2 mL for DNP amino acids and 1 mL for L-proline benzylester) was transferred to a test tube and evaporated under vacuum (Speed Vac Concentrator, Savant Instruments, Inc., Hicksville, NJ). Then 2 mL of the standard solvent system (1 mL of each phase) was added to each tube and the contents were vigorously shaken to equilibrate the solute between the two phases at room temperature. After two clear layers were formed, an aliquot of each phase was diluted with a known volume of methanol, and the absorbance was determined at 430 nm with a Zeiss PM6 spectrophotometer. In the indole auxin separation, each component was similarly identified by using a two-phase solvent system composed of hexane-ethyl acetate-methanol-water (1:1:1:1, v/v).

The fractions of hydroxyxanthene dyes were analyzed by reversed-phase high-performance liquid chromatography (HPLC) to evaluate purity and yields as follows: The system consisted of a Model 8800 ternary pump, Model 8500 dynamic mixer, Model 8780 autosampler, and Model 4270 integrator (all Spectra-Physics, San Jose, CA); and a Model 490 dual-wavelength UV-VIS detector set at 254 and 520 nm (Waters Associates, Milford, MA). The autosampler was equipped with a Model 7010 injector (Rheodyne, Cotati, CA) with a 20-μL sample loop. A Hypersil MOS-1 RPC-8 column, 250 x 4.6 mm i.d., with 5-μm particles (Keystone Scientific, Bellefonte, PA) was used throughout.

In the separation of the two stereoisomers of 1-methyl-4-methoxymethylcyclohexanecarboxylic acids, the eluted fractions were identified by gas chromatography-mass spectrometry (GC-MS).

Downloaded by UNIV OF GUELPH LIBRARY on June 29, 2012 | http://pubs.acs.org
Publication Date: May 15, 1995 | doi: 10.1021/bk-1995-0593.ch014

Results and Discussion

Examples of pH-Zone-Refining CCC. The countercurrent chromatograms of DNP amino acids in Figure 7 demonstrate that the technique can produce greater peak resolution with increased sample size. Each separation was performed with a solvent system of methyl *tert*-butyl ether-acetonitrile-water (4:1:5, v/v). A 200-μL quantity of TFA (retainer acid) was added to the sample solution and 0.1% (v/v) ammonium hydroxide (eluent base) was added to the aqueous mobile phase to raise the pH to 10.5. The other experimental conditions were as follows: Apparatus, high-speed CCC centrifuge with 10-cm revolution radius (j-type); column, semipreparative multilayer coil, 160 m × 1.6 mm i.d., with total capacity of 325 mL; flow rate, 3 mL/min; revolution, 800 rpm.

In the top chromatogram, a small quantity (6 mg) of the sample mixture containing six different DNP amino acids was eluted as single sharp peak showing

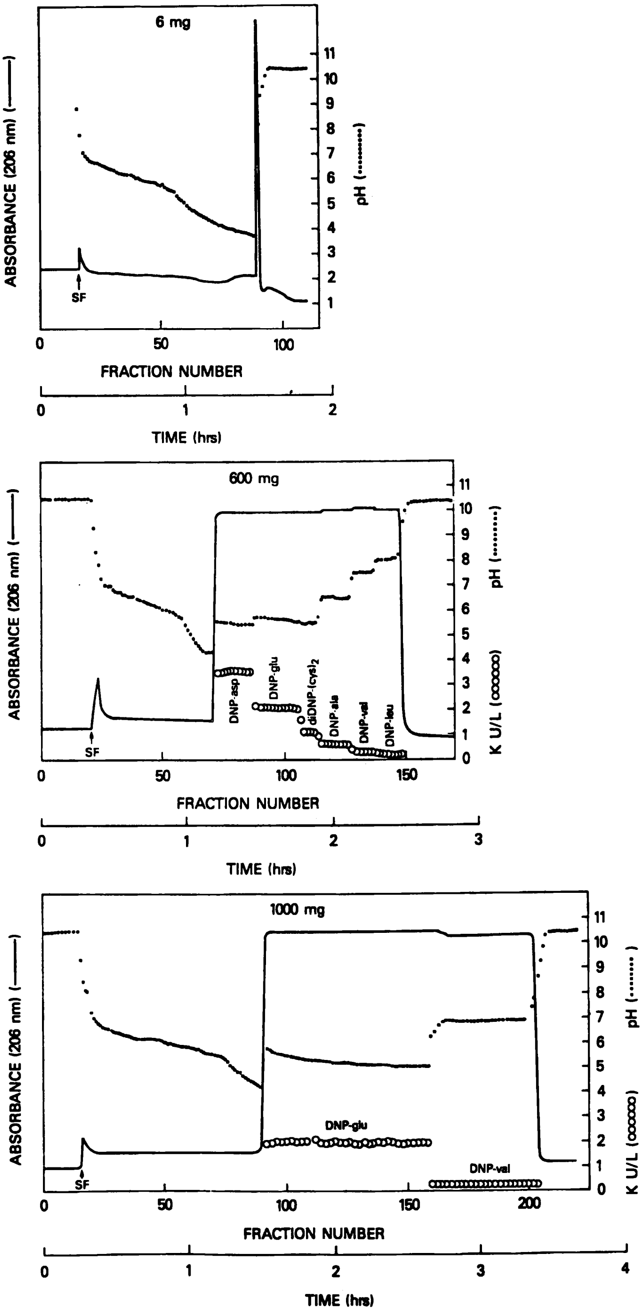

Figure 7. Chromatograms of DNP amino acids. Top: Separation of six different DNP amino acids in a small amount (6 mg) of sample mixture; Middle: Separation of six different DNP amino acids in a large amount (600 mg) of the same sample; Bottom: Separation of DNP-L-glutamic acid and DNP-L-valine (500 mg of each). SF = solvent front.

Downloaded by UNIV OF GUELPH LIBRARY on June 29, 2012 | http://pubs.acs.org
Publication Date: May 15, 1995 | doi: 10.1021/bk-1995-0593.ch014

no separation of its components. When the sample size was increased by a factor of 100 (600 mg), all components again seemed to elute together as a highly concentrated rectangular peak when detected only by measurement of absorbance (middle chromatogram, in which the flat top indicates limited sensitivity of the detector; see above). However, partition coefficient measurements of each fraction in a standard solvent system of chloroform-acetic acid-0.1 M HCl (2:2:1) revealed that the individual components were in fact well resolved as rectangular peaks, each corresponding to a specific pH zone shown by a dotted line in the chromatogram.

The bottom chromatogram illustrates the separation of 500 mg each of DNP glutamic acid and DNP valine under similar experimental conditions. Each component formed a broad plateau as detected by pH measurement or determined by partition coefficient measurement of residues from individual fractions. The plateau lengths increased in proportion to the increased sample size. The sharp transition in partition coefficient between two fractions indicates the high purity of each. A gradual decline of the pH curves in both pH zones was apparently caused by a steady increase of the elution rate of the retainer border when the retainer acid was added to the sample solution instead of to the stationary phase.

The present method has been successfully applied to the purification of various hydroxyxanthene dyes by using a two-phase solvent system of diethyl ether-acetonitrile-10 mM ammonium acetate (4:1:5, v/v). The chromatogram in Figure 8b shows a typical example in which the three major components in 5 g of D&C Orange No. 5 were separated in 12.5 h (*10*). The experimental conditions were as follows: Sample, 5 g of crude sample dissolved in 80 mL of stationary phase; retainer acid, 200 μL of TFA in sample solution; eluent base, ammonium hydroxide added to aqueous mobile phase to adjust pH to 9.0. All other experimental conditions were the same as those used for Figure 7. HPLC analyses of fractions taken from the plateaus (arrows, Figure 8b) demonstrated the high purity of each component. For comparison, the chromatogram from HPLC analysis of the original sample is shown in Figure 8a.

In the above examples, the separations were performed by adding the retainer to the sample solution. If the retainer is added to the stationary phase, it forms a flat pH zone starting immediately after the solvent front, followed by a pH plateau of each solute zone.

Figure 9 shows a chromatogram obtained from three homologous indole auxins by using a simple solvent system composed of methyl *tert*-butyl ether and water. The organic stationary phase was acidified with TFA (0.04%, v/v) (pH 2.5), and ammonium hydroxide was added to the aqueous mobile phase (0.05%, v/v) (pH 10.4). The experimental conditions were as follows: Sample, indole-3-acetic acid (500 mg), indole-3-carboxylic acid (50 mg), and indole-3-butyric acid (250 mg) in 20 mL of stationary phase; retainer acid, 200 μL of TFA in 500 mL of stationary phase. The other experimental conditions were the same as those used for Figure 7. An aliquot of each fraction was evaporated, and the residue was redissolved in the standard two-phase solvent system composed of hexane-ethyl acetate-methanol-water (1:1:1:1, v/v) to measure the partition coefficients for identification. Again, each component formed a specific pH zone and eluted as a rectangular peak as shown by the shaded area in the chromatogram. The above caveat concerning the absorbance trace applies in this case.

Downloaded by UNIV OF GUELPH LIBRARY on June 29, 2012 | http://pubs.acs.org
Publication Date: May 15, 1995 | doi: 10.1021/bk-1995-0593.ch014

Downloaded by UNIV OF GUELPH LIBRARY on June 29, 2012 | http://pubs.acs.org
Publication Date: May 15, 1995 | doi: 10.1021/bk-1995-0593.ch014

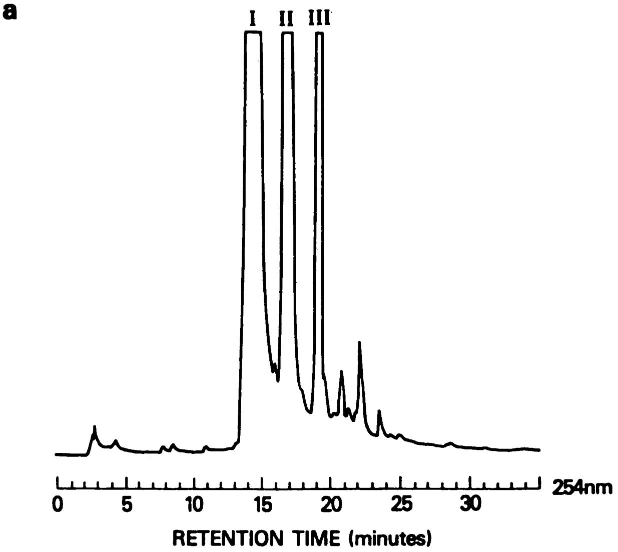

Figure 8. Separation of major components in D&C Orange No. 5 by pH-zone-refining CCC. Top: Chromatogram from HPLC analysis of original sample; Bottom: CCC separation of major components in D&C Orange No. 5, showing rectangular peak of each component and chromatograms from HPLC analyses for identification. SF = solvent front.

Continued on next page

Downloaded by UNIV OF GUELPH LIBRARY on June 29, 2012 | http://pubs.acs.org
Publication Date: May 15, 1995 | doi: 10.1021/bk-1995-0593.ch014

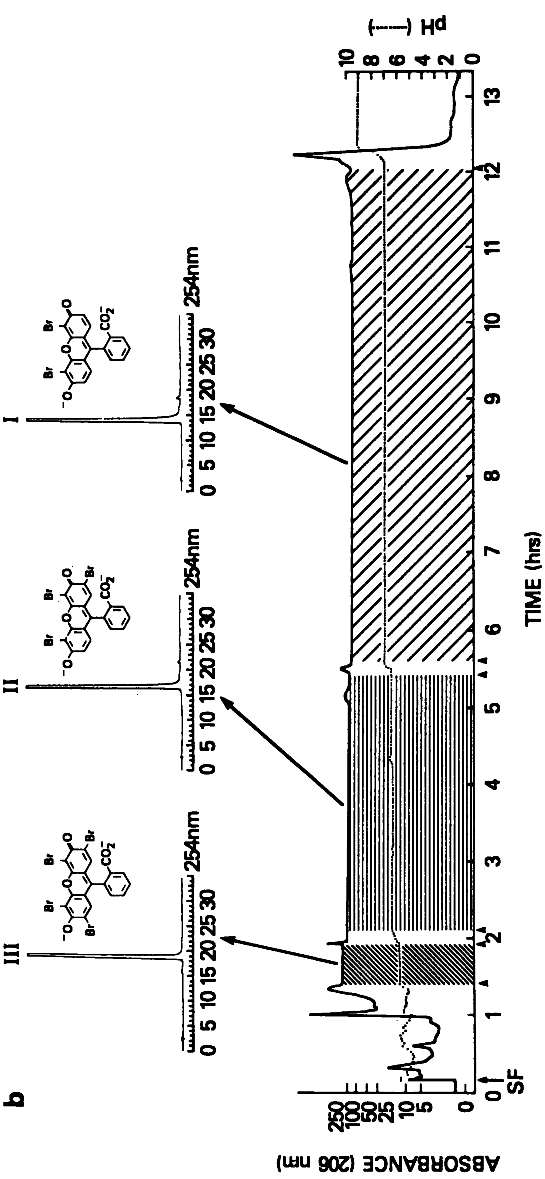

Figure 8. *Continued.*

Downloaded by UNIV OF GUELPH LIBRARY on June 29, 2012 | http://pubs.acs.org
Publication Date: May 15, 1995 | doi: 10.1021/bk-1995-0593.ch014

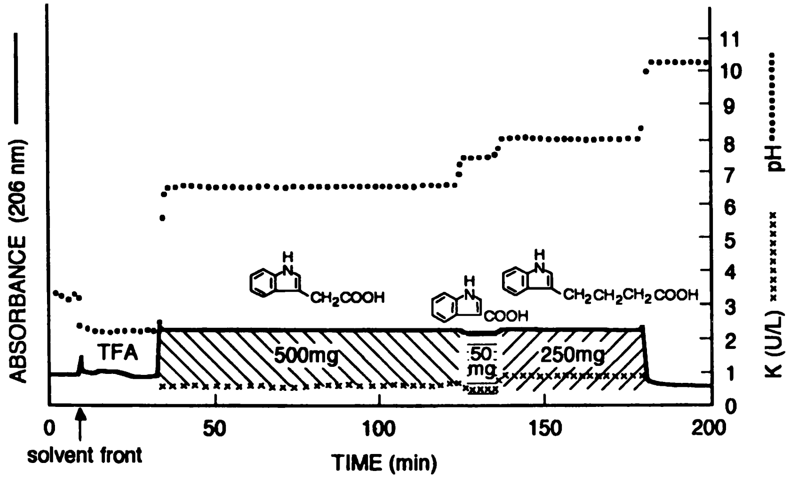

Figure 9. Separation of three indole auxins by the addition of the retainer acid to the stationary phase.

Figure 10 shows a more demanding separation. Here two stereoisomers of 1-methyl-4-methoxymethylcyclohexanecarboxylic acids were successfully separated *(11)*. The experiment was performed with a two-phase solvent system composed of hexane-ethyl acetate-methanol-water (1:1:1:1, v/v). Two retainer acids, TFA and octanoic acid (used to delay elution of the first acid until fraction 32), were added to the upper organic stationary phase, each at 0.02% (v/v) (pH 2.42) while an eluent base, ammonium hydroxide, was added to the lower aqueous phase at 0.025% (v/v) (pH 9.89). After the column was filled with the above stationary phase, a sample solution containing 400 mg of the crude mixture of the stereoisomers (MW 186) in 3 mL of solvent (2.5 mL of upper phase and 0.5 mL of lower phase) was introduced. The mobile phase was eluted at a flow rate of 3 mL/min while the column was rotated at 800 rpm. The other experimental conditions were the same as those used for Figure 7.

Because ethyl acetate in the solvent system strongly absorbs below 255 nm, it hides any response by the carboxylic acids. The chromatogram (lower diagram in Figure 10) shows responses only to impurities, not to TFA, octanoic acid, or the cyclohexanecarboxylic acids. Gas chromatographic analyses of fractions 42-63 and 69-76 revealed that the cis- and trans-isomers were well resolved as shown in the upper diagram.

Obviously, the present method can also be applied to the separation of basic compounds by using a retainer base and an eluent acid. One example is shown in Figure 11 in which 1 g of an aged sample of L-proline benzylester was purified by the present method. The experiment was performed with a two-phase solvent system composed of methyl *tert*-butyl ether and water. Triethylamine (retainer base) was added at 10 mM (pH 10.43) to the organic stationary phase, while HCl (eluent acid) was added to the aqueous mobile phase at 20 mM (pH 1.75). The sample solution was prepared by dissolving 1 g of the L-proline benzylester HCl salt in 5 mL of water, adjusting the pH of the solution to ca. 9.5 with NaOH, and then adding 10 mL of methyl *tert*-butyl ether to form two layers. The other experimental conditions were the same as those used for Figure 7.

The chromatogram (Figure 11) shows large impurity peaks, which eluted immediately after the solvent front. These are followed by the rectangular peak of L-proline benzylester (shaded) associated with sharp impurity peaks on each side. The rectangular proline ester peak eluted with a constant pH of 6.2 and a uniform partition coefficient value of around 5.

Remarks on pH-Zone-Refining CCC vs. Displacement Chromatography

The overall results described above strongly indicate that the present technique bears a remarkable resemblance to displacement chromatography (*8*). The most important common feature of these two chromatographic techniques is the rectangular elution peaks created by interaction between the solutes: One solute suppresses the affinity or ionization of its companions, affecting their apparent partition coefficients. However, pH-zone-refining CCC is also subject to a unique and well-characterized hydrodynamic action that is not available in simple column displacement chromatography. Differences between these two techniques are

Downloaded by UNIV OF GUELPH LIBRARY on June 29, 2012 | http://pubs.acs.org
Publication Date: May 15, 1995 | doi: 10.1021/bk-1995-0593.ch014

Downloaded by UNIV OF GUELPH LIBRARY on June 29, 2012 | http://pubs.acs.org
Publication Date: May 15, 1995 | doi: 10.1021/bk-1995-0593.ch014

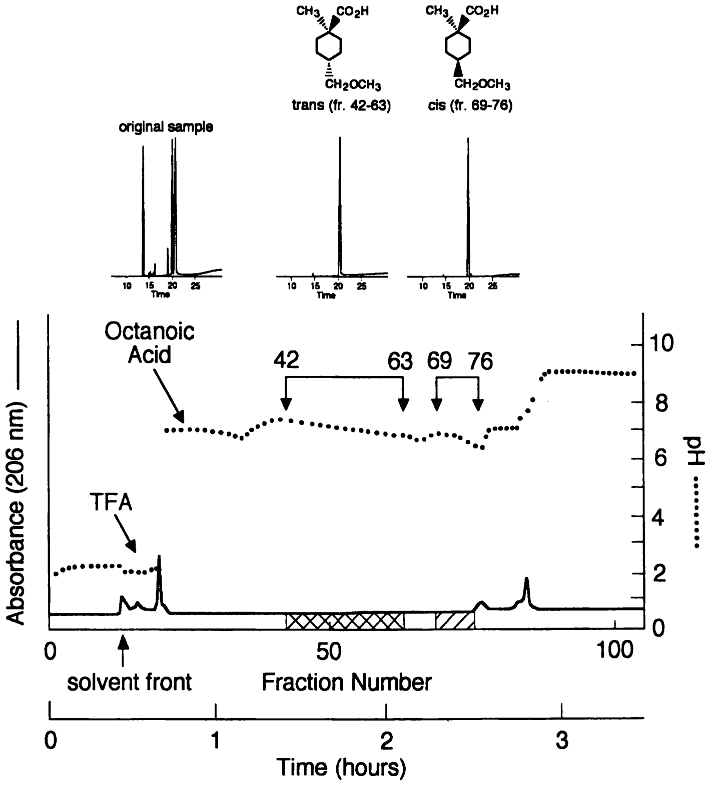

Figure 10. Separation of trans- and cis-stereoisomers of 1-methyl-4-methoxymethylcyclohexanecarboxylic acid by pH-zone-refining CCC. Gas chromatographic analysis of fractions is shown in upper segment.

summarized in Table II. Each technique uses a key reagent which acts in an entirely opposite manner in terms of both location and mode of solute transfer. In pH-zone-refining CCC, the retainer acid causes transfers of solutes from the mobile phase to the stationary phase at the front end of the solute bands to establish a sharp boundary which determines the elution rate of the succeeding solute bands. In displacement chromatography, on the other hand, the displacer acts at the back of the solute bands to displace the solute molecules adsorbed onto the stationary solid support, forming a sharp boundary which determines the elution rate of all the preceding solute bands. Surprisingly, these opposite actions of the key reagents produce almost identical results including formation of a train of analyte bands traveling through the column at a uniform rate, self-sharpening boundaries in each solute band, uniform partition coefficient values within all solute bands, distribution of impurities at zone boundaries, and the overall profile of the elution peaks.

There are some significant differences between the chromatograms produced by these two techniques: In pH-zone refining CCC, the solutes are eluted in increasing order of their pK_a values and hydrophobicities. The concentration of each solute is mainly determined by that of the counter ions in the mobile phase and the valency of the solute molecule. In displacement chromatography, on the other hand, the affinity of the solute for the stationary phase determines both the eluting order of the solutes and their concentrations in the mobile phase; hence, the solute concentration increases in the later-eluting peaks.

Despite the close similarities between these two chromatographic techniques, pH-zone-refining CCC provides some important advantages over displacement chromatography in terms of irreversible adsorption, etc. One of the major advantages, in our opinion, is that suitable chromatographic conditions can be determined easily for a given set of samples.

The function of the retainer acid is to sharpen the front of the first eluting acid and to determine the advancing rate of all of the succeeding eluates. Although there is nothing extraordinary about TFA, its strong acidity and moderate lipophilicity recommend it for the separation of a wide assortment of organic acids. If desired, common organic acids such as formic through octanoic acids may be used individually or in combination as spacers. Triethylamine is similarly convenient as the retainer base for the separation of basic compounds.

The two-phase solvent systems can be selected according to the hydrophobicity and solubility of the sample. For analytes with moderate hydrophobicities, solvent systems composed of an ether (diethyl ether or methyl *tert*-butyl ether) and water are successful in many cases. If solubility is a problem, the solvent system may be modified to a ternary system such as ether-acetonitrile-water (4:1:5). For separation of hydrophobic solutes, a series of solvent systems composed of hexane-ethyl acetate-methanol-water is convenient. The hydrophobicity is conveniently adjusted by changing the ratio of hexane to ethyl acetate from 5:5:5:5 through 6:4:5:5, 7:3:5:5, 8:2:5:5, and 9:1:5:5 to 10:0:5:5 to meet the partition coefficient of the sample (*3*). For the separation of polar compounds, a butanol-water system may be useful. The apparent partition coefficient of the solutes in the solvent system is also adjusted by changing the concentration of the retainer acid such as TFA in the stationary phase.

Downloaded by UNIV OF GUELPH LIBRARY on June 29, 2012 | http://pubs.acs.org
Publication Date: May 15, 1995 | doi: 10.1021/bk-1995-0593.ch014

Downloaded by UNIV OF GUELPH LIBRARY on June 29, 2012 | http://pubs.acs.org
Publication Date: May 15, 1995 | doi: 10.1021/bk-1995-0593.ch014

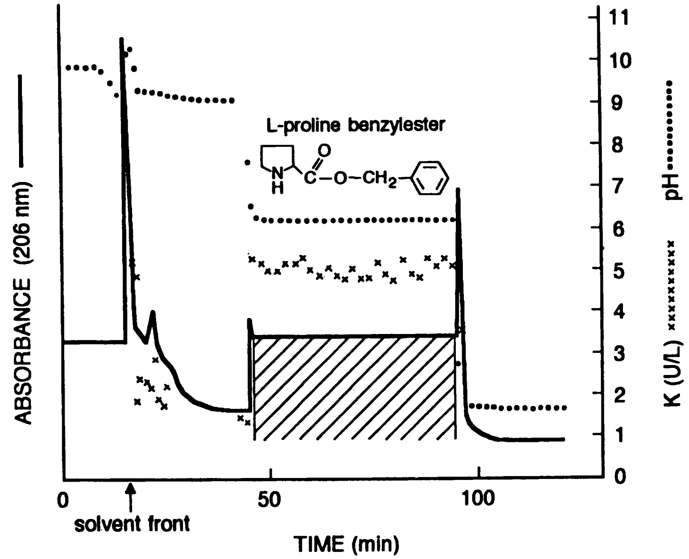

Figure 11. Purification of L-proline benzylester, using a retainer base and an eluent acid.

Table II. Comparison of pH-Zone-Refining CCC and Displacement Chromatography

	pH-Zone-Refining CCC	*Displacement Chromatography*
Key reagent	Retainer	Displacer
Acting location	Front of solute bands	Back of solute bands
Solute transfer	Mobile phase → stationary phase	Stationary phase → mobile phase
Elution order of analytes	pK_a and hydrophobicity	Affinity to SP
Analyte concn. determined by	Concn. of counter ion	Affinity to SP

Downloaded by UNIV OF GUELPH LIBRARY on June 29, 2012 | http://pubs.acs.org
Publication Date: May 15, 1995 | doi: 10.1021/bk-1995-0593.ch014

Another advantage of pH-zone-refining CCC, compared with displacement chromatography, is that the system usually retains a large volume of the stationary phase, i.e., from 60% to over 80% of the total column capacity in preparative-scale separations. Furthermore, the lack of a solid support matrix in the column space allows introduction of suspensions with minimum risk of clogging the column.

On the other hand, displacement chromatography has at least one important advantage over pH-zone-refining CCC in that the method covers a broad spectrum of samples, including both ionizable and nonionizable compounds. In the above work, our applications have been limited to ionizable compounds.

Isotachophoresis (*7*) also shares some important features with the present technique. As in pH-zone refining CCC, it forms a train of sample bands by the aid of the leading ionic component, which suppresses the ionization of other analytes at the front end. Isotachophoresis is also limited to ionizable compounds although the zone arrangement is governed by electrophoretic mobility instead of pK_a and hydrophobicity as in pH-zone refining CCC.

Conclusions

The results of our studies indicate that pH-zone-refining CCC yields efficient preparative-scale separations comparable to those obtained in displacement chromatography without the need for a support material.

The present method offers the following advantages over conventional CCC methods:

1) An over 10-fold increase in sample loading capacity for a given column,
2) high concentration of analytes in the eluate,
3) higher overall purity with larger sample size, and
4) concentration of minor components.

We believe that this simple technique will find many applications in preparative-scale separations.

Glossary

u_m : Flow rate (L/min) of MP (mobile phase)
u : Elution rate (L/min) of the retainer border through MP
V_m : Volume (L) of MP in the column
V_s : Volume (L) of SP (stationary phase) retained in the column
V_r : Volume (L) of MP required to elute the retainer acid completely from the column
K_r : Apparent partition coefficient of the retainer acid in the equilibrium zone
K_s : Apparent partition coefficient of solute S in the equilibrium zone
$K_{D\text{-}r}$: Partition ratio of the retainer acid
$K_{D\text{-}s}$: Partition ratio of solute S
$K_{a\text{-}r}$: Dissociation constant of the retainer acid
pH_z : pH of MP in the equilibrium zone of solute S
C_r : Concentration (M) of the retainer acid in MP
C_R : Initial concentration (M) of the retainer acid in SP

C_E : Initial concentration (M) of the eluent base in MP
C_m : Concentration (M) of solute S in MP in the equilibrium zone
C_s : Concentration (M) of solute S in SP in the equilibrium zone

Literature Cited

1. Ito, Y. In *Countercurrent Chromatography: Theory and Practice*; Mandava, N.B.; Ito, Y., Eds.; Marcel Dekker: New York, NY, 1988, pp 79-442.
2. Conway, W.D. *Countercurrent Chromatography*; *Principle, Apparatus and Applications*; VCH: New York, NY, 1990.
3. Ito, Y. In *Chromatography, Journal of Chromatography Library*, Part A, 5th Ed.; Heftmann, E., Ed.; Elsevier Scientific Publishing Company: Amsterdam, Netherlands, 1992, Chapter 2, pp A69-A107.
4. Ito, Y.; Sandlin, J.L.; Bowers, W.G. *J. Chromatogr.* **1982**, *244*, 247-258.
5. Ito, Y. *CRC Crit. Rev. Anal. Chem.* **1986**, *17*, 65-143.
6. Wilcox, W.R. In *Kirk-Othmer Encyclopedia of Chemical Technology*, 3rd Ed.; Wiley Interscience: New York, 1984, Vol. 24, pp 903-917.
7. Ito, Y; Shibusawa, Y.; Fales, H.M.; Cahnmann, H.J. *J. Chromatogr.* **1992**, *625*, 177-181.
8. Horváth, C.; Nahum, A.; Frenz, J.H. *J. Chromatogr.* **1981**, *218*, 365-393.
9. Boček, P.; Deml, M.; Gebauer, P.; Dolnik, V. In *Analytical Isotachophoresis*; Radola, B.J., Ed.; Electrophoresis Library; VCH: New York, NY, 1988.
10. Weisz, A.; Scher, A.L.; Shinomiya, K.; Fales, H.M.; Ito, Y. *J. Am. Chem. Soc.* **1994**, *116*, 704-708.
11. Denekamp, C.; Mandelbaum, A.; Weisz, A.; Ito, Y. *J. Chromatogr. A* **1994**, *685*, 253-257.

RECEIVED December 28, 1994

Downloaded by UNIV OF GUELPH LIBRARY on June 29, 2012 | http://pubs.acs.org
Publication Date: May 15, 1995 | doi: 10.1021/bk-1995-0593.ch014

Downloaded by YORK UNIV on June 28, 2012 | http://pubs.acs.org
Publication Date: May 15, 1995 | doi: 10.1021/bk-1995-0593.ch015

Chapter 15

Equilibrium Model for pH-Zone-Refining Countercurrent Chromatography

Alan L. Scher[1] and Yoichiro Ito[2]

[1]Office of Cosmetics and Colors, Center for Food Safety and Applied Nutrition, U.S. Food and Drug Administration, Washington, DC 20204
[2]Laboratory of Biophysical Chemistry, National Heart, Lung and Blood Institute, National Institutes of Health, Building 10, Room 7N322, Bethesda, MD 20892

Theoretical chromatograms for preparative separations of organic acids by pH-zone-refining countercurrent chromatography (CCC) were simulated using a computer program. Countercurrent distribution was used as a model. The simulated chromatograms contain flat-top peaks with steep sides and are consistent with experimental chromatograms in which organic acids in an organic stationary phase are separated by elution with aqueous base. The effects of the pK_as, partition ratios (K_Ds), concentrations of the sample acids, and concentrations of the retaining acid and eluting base were investigated. Separations depended on differences in the pK_as and K_Ds of the acids. Mixtures of acids with $\Delta p(K_a/K_D) = 1$ were theoretically separated with recoveries of 99% of each acid with ≥99% purity, even on a low-efficiency column (275 theoretical plates). These simulations are valuable for predicting and optimizing pH-zone-refining CCC separations.

pH-Zone-refining CCC has been shown to be an excellent general technique for the preparative chromatography of up to multigram quantities of organic acids and of organic bases (*1-5*). The technique, apparatus, and many examples are described in these references. The desire to characterize these separations and to optimize experimental conditions led us to develop an approach to mathematically simulate pH-zone-refining CCC chromatograms.

Description of pH-Zone-Refining CCC

In pH-zone-refining CCC, an open tubular CCC column (wound in helical layers) is filled with an organic stationary phase, and a mixture of acids in the stationary phase is injected into the column. The column is rotated at ca. 800-1000 rpm to

This chapter not subject to U.S. copyright
Published 1995 American Chemical Society

Downloaded by YORK UNIV on June 28, 2012 | http://pubs.acs.org
Publication Date: May 15, 1995 | doi: 10.1021/bk-1995-0593.ch015

develop centrifugal forces that retain the stationary phase. The column is then eluted with a basic aqueous mobile phase. Fractions are collected, and the pH and the absorbance of the effluent are monitored.

In each section of the column, acid-base and partition equilibria are approached between the solutes in the two phases as the aqueous mobile phase proceeds through the column. Mass transfer of the solutes is expected to be fast because of intense mixing of the phases by the rotating CCC column. This system of individual sections in which solutes in two phases are equilibrated describes countercurrent distribution, where the phases are mixed and equilibrium is established in individual tubes. When the number of tubes is large, countercurrent distribution approaches CCC and may be used as a model.

Countercurrent Distribution Model

A series of tubes (Figure 1, four tubes are shown) is filled with the organic stationary phase. The first tube (or tubes) contains a sample mixture of monoprotic organic acids in the stationary phase. Aqueous NaOH is added to the first tube, the mixture is shaken, and the solutes dissociate and partition into the organic and aqueous phases (Figure 2). This mixture of n monoprotic acids, HAi ($i = 1$ to n), and their sodium salts in an aqueous-organic two-phase solvent system may contain H^+_{aq}, OH^-_{aq}, Na^+_{aq}, Ai^-_{aq}, HAi_{aq}, and HAi_{org}.

It is assumed that the concentrations of other solute forms are negligible, and that the system is ideal—i.e., the partition ratios, K_Ds (Equation 1), and the acid dissociation constants, K_as (Equation 2), do not vary at the solute concentrations used.

$$HAi_{aq} \rightleftarrows HAi_{org} \qquad K_D^{HAi} = \frac{[HAi_{org}]}{[HAi_{aq}]} \tag{1}$$

$$HAi_{aq} \rightleftarrows H^+_{aq} + Ai^-_{aq} \qquad K_a^{HAi} = \frac{[H^+_{aq}] \times [Ai^-_{aq}]}{[HAi_{aq}]} \tag{2}$$

The charge-balance equation for the ionic solutes is:

$$\sum_{i=1}^{n} [Ai^-_{aq}] = [H^+_{aq}] + [Na^+_{aq}] - [OH^-_{aq}] = [H^+_{aq}] + [Na^+_{aq}] - \frac{K_W}{[H^+_{aq}]} \tag{3}$$

The mass-balance equation for TAi, the total amounts (moles) of HAi and Ai^- in a tube, is:

$$TAi = \left([Ai^-_{aq}] + [HAi_{aq}]\right) \times vol_{aq} + [HAi_{org}] \times vol_{org} \tag{4}$$

Downloaded by YORK UNIV on June 28, 2012 | http://pubs.acs.org
Publication Date: May 15, 1995 | doi: 10.1021/bk-1995-0593.ch015

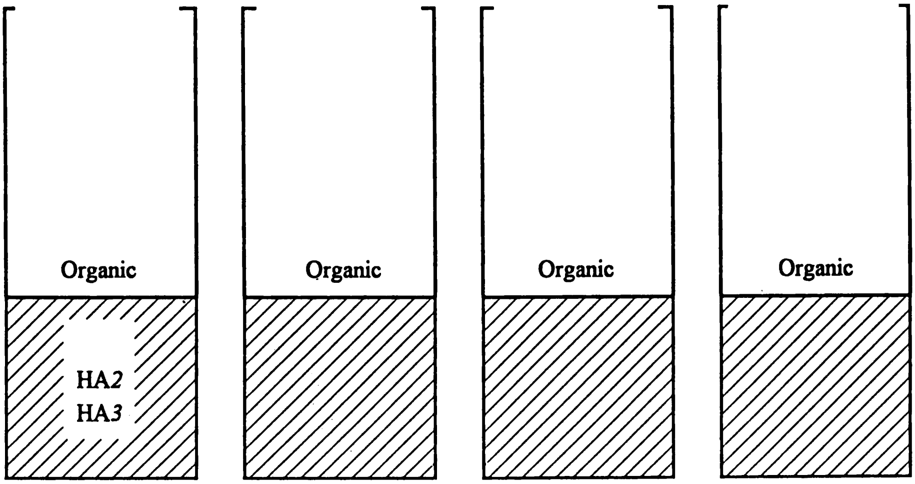
Organic
HA*2*
HA*3*
Organic
Organic
Organic

Figure 1. Countercurrent distribution model with organic stationary phase in all the tubes but without retaining acid in the sample or stationary phase. A sample of two organic acids (HA*2* and HA*3*) is in the first tube.

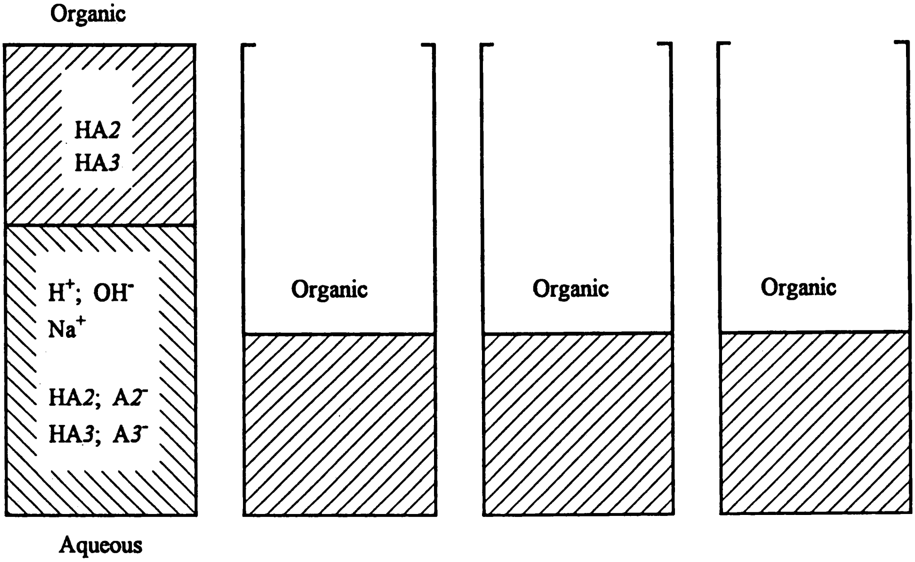
Organic
HA*2*
HA*3*
H⁺; OH⁻
Na⁺
HA*2*; A*2*⁻
HA*3*; A*3*⁻
Aqueous
Organic
Organic
Organic

Figure 2. Countercurrent distribution model with organic stationary phase in all the tubes but without retaining acid in the sample or stationary phase. A sample of two organic acids (HA*2* and HA*3*) and aqueous NaOH are in the first tube.

Downloaded by YORK UNIV on June 28, 2012 | http://pubs.acs.org
Publication Date: May 15, 1995 | doi: 10.1021/bk-1995-0593.ch015

Using Equations 1 and 2 to successively substitute $[HAi_{org}]$ and $[HAi_{aq}]$ in Equation 4 yields a modified mass balance equation:

$$\frac{TAi}{vol_{aq}} = [Ai^{-}_{aq}] \times \left(1 + \frac{[H^{+}_{aq}]}{K_a^{HAi}} + \frac{[H^{+}_{aq}] \times K_D^{HAi} \times vol_{org}}{K_a^{HAi} \times vol_{aq}} \right) \qquad (5)$$

Using Equation 5 to substitute Ai^{-}_{aq} in Equation 3 yields Equation 6, from which the $[H^{+}_{aq}]$ in an equilibrated section may be numerically solved.

$$\sum_{i=1}^{n} \frac{\dfrac{TAi}{vol_{aq}}}{1 + \dfrac{[H^{+}_{aq}]}{K_a^{HAi}} \times \left(1 + \dfrac{K_D^{HAi} \times vol_{org}}{vol_{aq}} \right)} = [H^{+}_{aq}] + [Na^{+}_{aq}] - \frac{K_W}{[H^{+}_{aq}]} \qquad (6)$$

Mathematical Solution

The computer program Mathematica (Wolfram Research, Inc., Champaign, IL) is used to expand Equation 6 into a (2 + *n*)-power polynomial equation in $[H^{+}_{aq}]$ and to numerically solve the polynomial for $[H^{+}_{aq}]$ in a tube from TAi/vol_{aq}, $[Na^{+}_{aq}]$, K_D, K_a, and vol_{org}/vol_{aq}. The concentrations of all the solutes in each phase of the tube (or column section) are calculated.

The aqueous eluting base with known vol_{aq} and $[NaOH_{aq}]$ is theoretically added to the first tube, which contains organic phase with known *TAi* and vol_{org}. The calculated $[H^{+}_{aq}]$ is the largest positive root of the polynomial derived by expanding Equation 6. The concentrations of the solutes in both phases are calculated by successively using Equations 5, 2, and 1. The aqueous phase in the first tube is transferred into succeeding tubes which contain organic phase with known *TAi* and the same vol_{org}. The TAi/vol_{aq}, the $[H^{+}_{aq}]$, and the solute concentrations are calculated for each successive tube until the aqueous mobile phase segment is removed from the last tube.

Further vol_{aq}s of aqueous eluting base are added to the first tube and transferred to successive tubes, and analogous calculations are made. The theoretical chromatograms are plots of the calculated pH and concentrations of the solutes in the aqueous phase that is removed from the last tube.

Effect of Retaining Acid

A retaining acid, either mixed with the sample or dissolved in the stationary phase, is required for the success of preparative pH-zone-refining CCC separations. The retaining acid is a moderately strong acid that will protonate salts of the sample acids. Because the retaining acid partitions preferentially into the organic phase, it is not washed from the column. Trifluoroacetic acid with a pK_a of ~0.3 (*6*) and an estimated K_D of 39 (see below) is used as a model retaining acid.

A set of theoretical chromatograms for separations (1) with no retaining acid, (2) with retaining acid that is mixed with sample acids, (3) with retaining acid that is dissolved in the stationary phase, and (4) insufficient retaining acid shows that the presence of retaining acid markedly improves the separation.

Separation of Two Acids in the Sample—No Retaining Acid. A simulated chromatogram (Figure 3) of two acids, HA*2* and HA*3*, with pK_as of 3 and 4, respectively, and K_D of 40 each shows a partial separation. The mole ratio of HA*2* to HA*3* in the sample was 1:2. In the effluent, the purity of HA*2* was at best 85 mole % and decreased steadily. Theoretical recovery of 80% pure HA*2* was 89%, and recovery of >99% pure HA*3* was 79%.

Separation of Two Acids with a Retaining Acid in the Sample. Addition of a strong organic acid, HA*1* (e.g., trifluoroacetic acid), to the sample in the first tube in the model in Figure 2 produces a new model (Figure 4). The calculated chromatogram (Figure 5) shows excellent separation of the three acids into nearly rectangular peaks with minimal overlap. The improvement in the separation when

Downloaded by YORK UNIV on June 28, 2012 | http://pubs.acs.org
Publication Date: May 15, 1995 | doi: 10.1021/bk-1995-0593.ch015

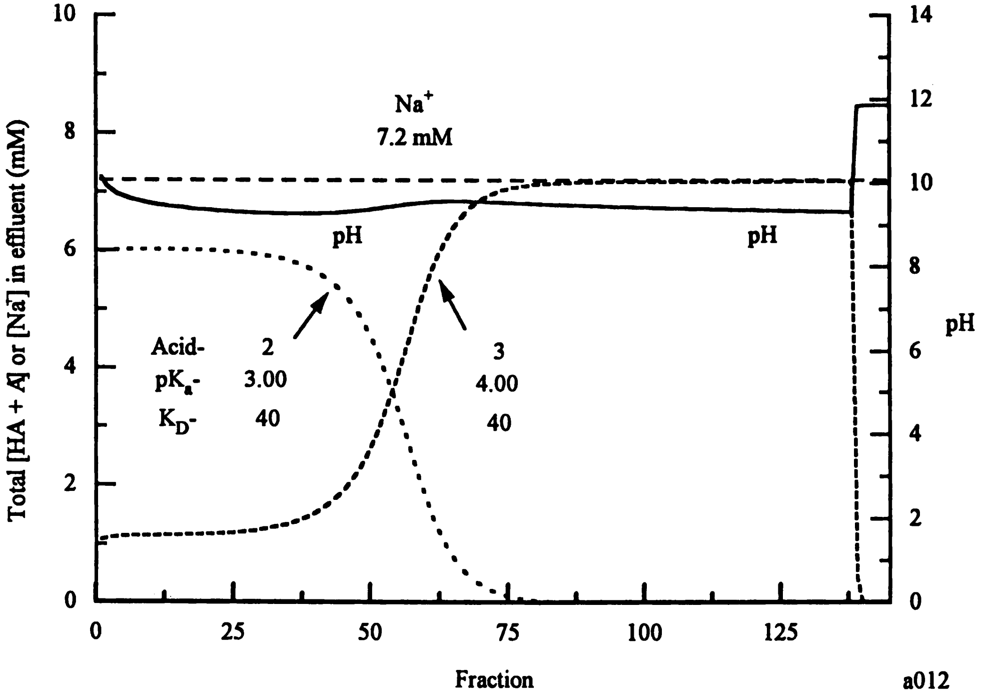

Figure 3. Simulated chromatogram of a mixture of two acids corresponding to Figures 1 and 2. No retaining acid is used. The sample with [HA*2*] = 20 mM and [HA*3*] = 40 mM in 3 mL of the stationary phase is contained in the first three plates. [$NaOH_{aq}$] = 0.72 mM, vol_{org}= 275 mL, vol_{aq}= 50 mL, column volume = 325 mL, theoretical plates = 275. A plate (tube) contains 1 mL organic phase and 0.18 mL aqueous phase.

Downloaded by YORK UNIV on June 28, 2012 | http://pubs.acs.org
Publication Date: May 15, 1995 | doi: 10.1021/bk-1995-0593.ch015

the retaining acid is added (Figure 5 vs. Figure 3) is dramatic. The pH slowly decreases during a peak and sharply increases in the transition between peaks. Theoretical recoveries of >99% pure acids were >99.5% for HA*2* and HA*3*.

Separation of Two Acids with a Retaining Acid in the Stationary Phase. If the amount of retaining acid in the first tube is instead apportioned into the stationary phase in all the tubes (Figure 6), then the calculated chromatogram (Figure 7) shows not only an excellent separation into nearly rectangular peaks, but also pH plateaus. Theoretical recoveries of >99% pure acid were >99.5% for HA*2* and HA*3*.

Separation of Three Acids with Insufficient or Sufficient Retaining Acid in the Stationary Phase. If insufficient retaining acid is added to the column, then the recoveries of pure compounds that elute at the beginning of the chromatogram decrease. pH-Zone-refining CCC separations of three acids with 0.05 and 0.2 mM of retaining acid HA*1* were simulated. HA*2*, HA*3*, and HA*4* have (1) pK_as of 3, 4, and 3, and (2) K_Ds of 40, 40, and 4000, respectively. When insufficient retaining acid is used, the chromatogram (Figure 8) shows considerable overlap of HA*2* and HA*3* but negligible overlap of HA*3* and HA*4*. Initially, the simulated separation of HA*2* and HA*3* is excellent. However, after ca. 2/3 of the HA*2* has eluted, the separation abruptly deteriorates and resembles the poor separation in Figure 3, in

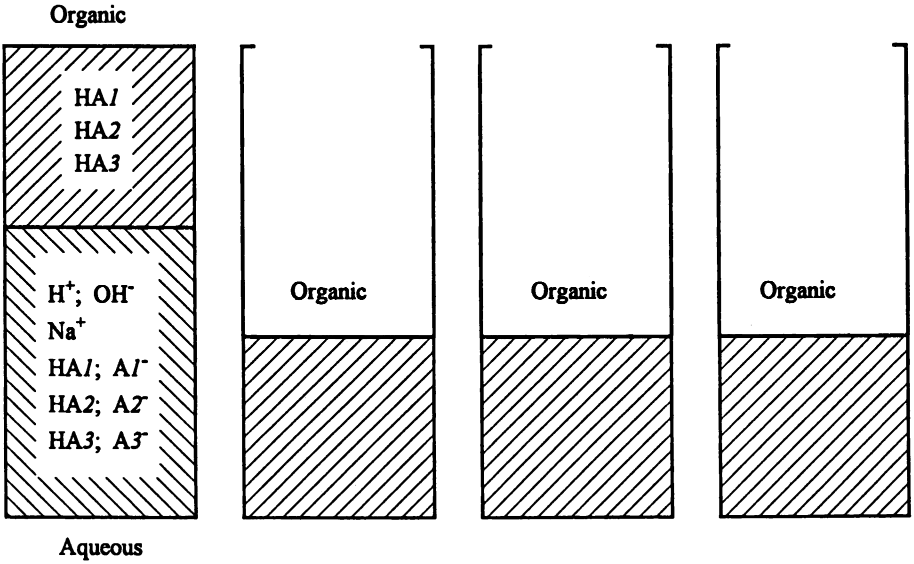

Figure 4. Countercurrent distribution model with organic stationary phase in all of the tubes and retaining acid in the sample. A retaining acid (HA*1*), a sample of two organic acids (HA*2* and HA*3*), and aqueous NaOH are in the first tube.

Downloaded by YORK UNIV on June 28, 2012 | http://pubs.acs.org
Publication Date: May 15, 1995 | doi: 10.1021/bk-1995-0593.ch015

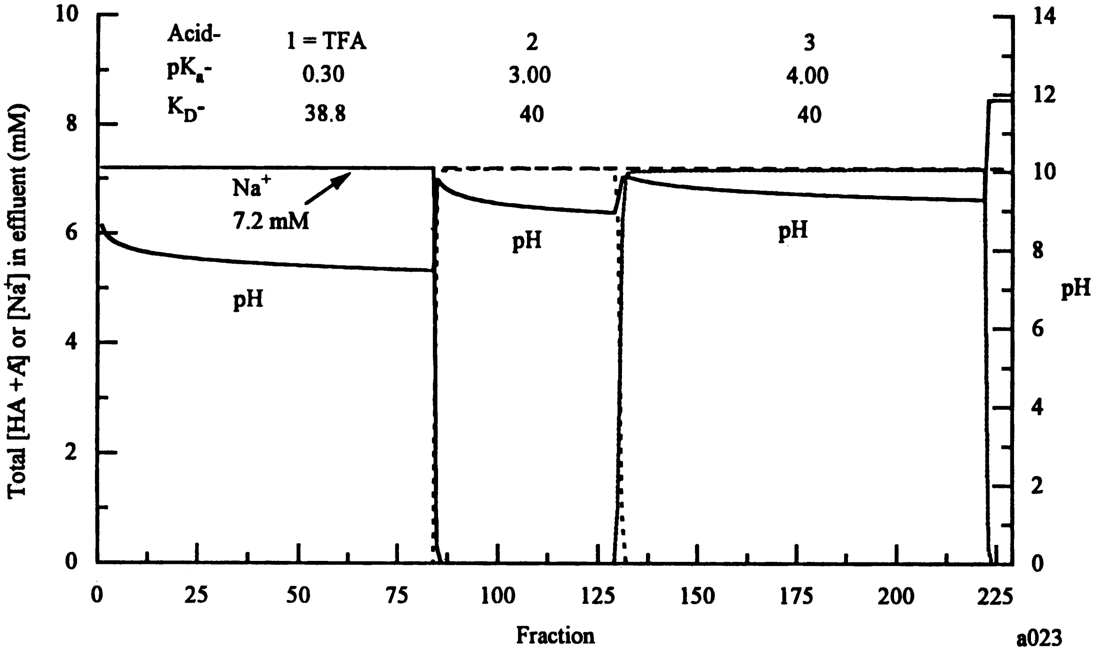

Figure 5. Simulated chromatogram of a mixture of two acids plus a retaining acid in the sample corresponding to Figure 4. The sample with [TFA] = 36.7 mM, [HA*2*] = 20 mM, and [HA*3*] = 40 mM in 3 mL of the stationary phase is contained in the first three plates. Other conditions are as described for Figure 3.

Downloaded by YORK UNIV on June 28, 2012 | http://pubs.acs.org
Publication Date: May 15, 1995 | doi: 10.1021/bk-1995-0593.ch015

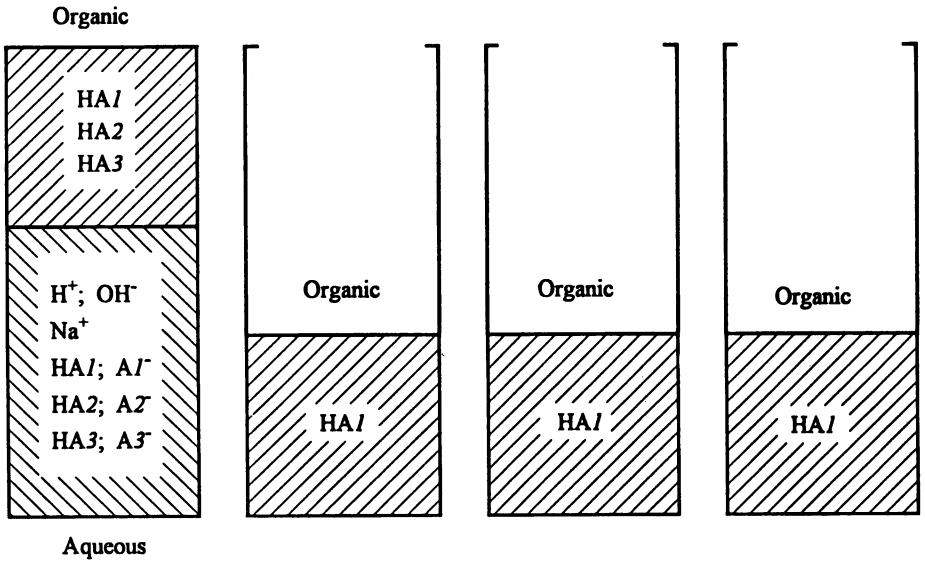
Organic
HA*1*
HA*2*
HA*3*
H^+; OH^-
Na^+
HA*1*; $A1^-$
HA*2*; $A2^-$
HA*3*; $A3^-$
Aqueous
Organic
HA*1*
Organic
HA*1*
Organic
HA*1*

Figure 6. Countercurrent distribution model with a retaining acid (HA*1*) in the organic stationary phase in all of the tubes. A sample of two organic acids (HA*2* and HA*3*) and aqueous NaOH are in the first tube.

Downloaded by YORK UNIV on June 28, 2012 | http://pubs.acs.org
Publication Date: May 15, 1995 | doi: 10.1021/bk-1995-0593.ch015

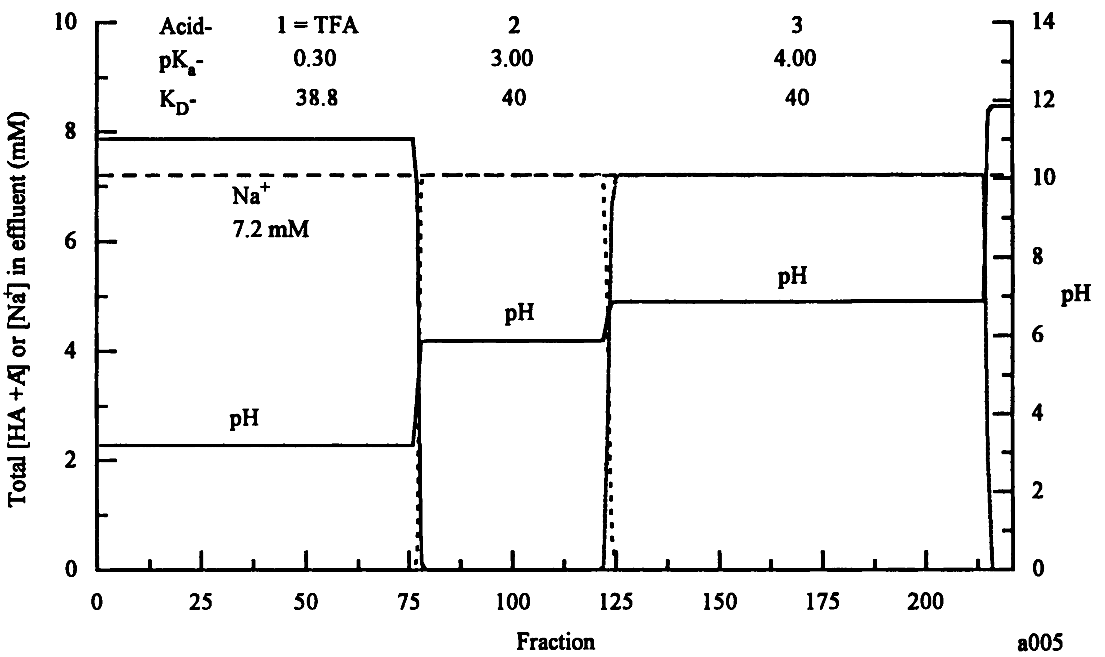

Figure 7. Simulated chromatogram of a mixture of two acids, plus retaining acid in the stationary phase corresponding to Figure 6. The sample in 3 mL of the acidified stationary phase is in the first three plates. The retaining acid with [TFA] = 0.4 mM is in the 1 mL of stationary phase in each of the 275 plates. Other conditions are as described for Figure 3.

Downloaded by YORK UNIV on June 28, 2012 | http://pubs.acs.org
Publication Date: May 15, 1995 | doi: 10.1021/bk-1995-0593.ch015

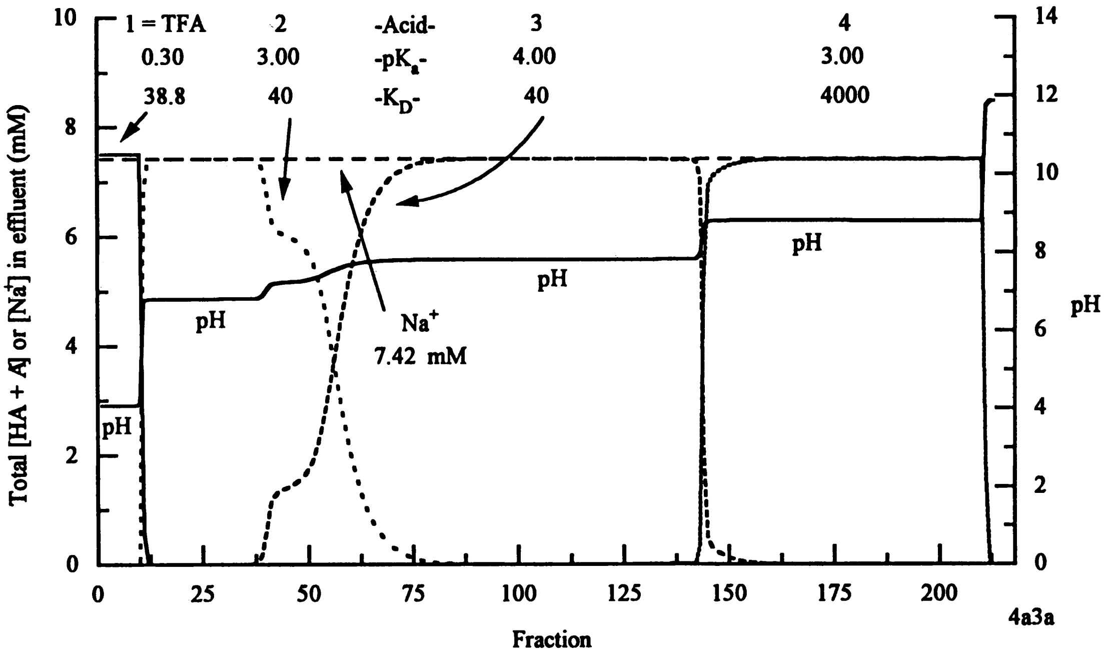

Figure 8. Simulated chromatogram of a mixture of three acids, plus insufficient retaining acid in the stationary phase for a good separation. The sample with [HA*2*] = 20 mM, [HA*3*] = 40 mM, and [HA*4*] = 30 mM in 3 mL of the acidified stationary phase is contained in the first three plates. The retaining acid with [TFA] = 0.05 mM is in the 1 mL of stationary phase in each of the 275 plates. [$NaOH_{aq}$]= 7.42 mM, vol_{org} = 275 mL, vol_{aq}= 50 mL, column volume = 325 mL, theoretical plates = 275. A plate contains 1 mL organic phase and 0.18 mL aqueous phase.

which no retaining acid was used. Recoveries of >99% pure acids were 69, 88, and 100% for HA*2*, HA*3*, and HA*4*.

In contrast, when four times as much retaining acid is used, the chromatogram (Figure 9) shows negligible overlap of the eluted compounds. Theoretical recoveries of >99% pure acids were 99% for HA*2*, HA*3*, and HA*4*.

The resemblance of the chromatograms in Figures 5, 7, and 9 to published experimental pH-zone-refining CCC chromatograms (*1-5*) indicates that the countercurrent distribution model is appropriate.

Chromatography of Mixtures of Monoprotic Acids with Several Major Components or One Predominant Component

pH-Zone-refining CCC is effective in purifying acids in mixtures containing several main components. As described above and shown in Figure 9, the theoretical separation of a mixture of three acids with a 20:40:30 mole ratio yielded >99% pure acids with recoveries of 99%. The technique is also effective in purifying the main component and isolating the minor components of an impure material. The theoretical separation of an analogous mixture of three acids with a 4:82:4 mole ratio (Figure 10) yielded a >99% pure major component with a recovery of >99.5%, and 98% pure minor components with recoveries of 98%.

Prediction of the Plateau pH for the Retaining Acid

When the retaining acid is dissolved in the stationary phase, then the model can be used to develop an equation to predict the plateau pH of the retaining acid. The initially basic first segment of the mobile phase extracts HA*1* from the stationary phase and becomes acidic as it advances from one tube to the next. As the now acidic first segment of the aqueous mobile phase passes through further segments of the organic phase,. it removes less and less $HA1_{org}$ until the concentrations of H^+_{aq}, $HA1_{aq}$, and $A1^-_{aq}$ are sufficiently high that equilibria with the original concentration of HA*1* in the organic phase have been reached. At this point, no more HA*1* will be removed from the organic phase and the first aqueous segment then passes unchanged through organic segments containing the original concentration of $HA1_{org}$. Other aqueous segments behind it are subjected to the same process and also reach the same equilibrium concentrations of H^+_{aq}, $HA1_{aq}$, and $A1^-_{aq}$. Thus a pH plateau is predicted. Because the Na^+_{aq} does not partition into the organic phase, its concentration in the aqueous phase is the $[NaOH_{aq}]$ in the eluting base. Therefore, $[HA1_{org}]$ and $[Na^+_{aq}]$ in the final tube are known. Equations 2 and 1 are used to successively substitute $[A1^-_{aq}]$ and $[HA1_{aq}]$ in Equation 3 ($i = 1$), thereby yielding Equation 7 which is used to calculate the pH of the HA*1* plateau from the ratio (K_D^{HA1}/K_a^{HA1}).

$$[H^+_{aq}] = -\frac{[Na^+_{aq}]}{2} + \sqrt{\left(\frac{[Na^+_{aq}]}{2}\right)^2 + K_W + \frac{K_a^{HA1} \times [HA1_{org}]}{K_D^{HA1}}} \qquad (7)$$

Downloaded by YORK UNIV on June 28, 2012 | http://pubs.acs.org
Publication Date: May 15, 1995 | doi: 10.1021/bk-1995-0593.ch015

Downloaded by YORK UNIV on June 28, 2012 | http://pubs.acs.org
Publication Date: May 15, 1995 | doi: 10.1021/bk-1995-0593.ch015

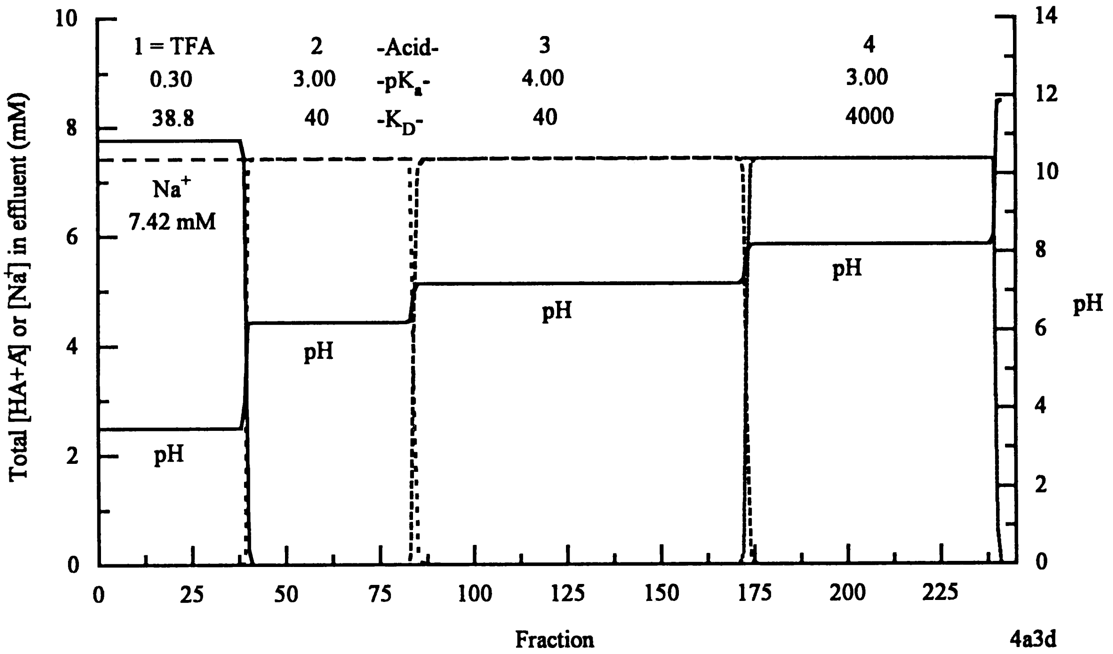

Figure 9. Simulated chromatogram of a mixture of three acids, plus sufficient retaining acid in the stationary phase for a good separation. [TFA] = 0.2 mM. Other conditions are as described for Figure 8.

Downloaded by YORK UNIV on June 28, 2012 | http://pubs.acs.org
Publication Date: May 15, 1995 | doi: 10.1021/bk-1995-0593.ch015

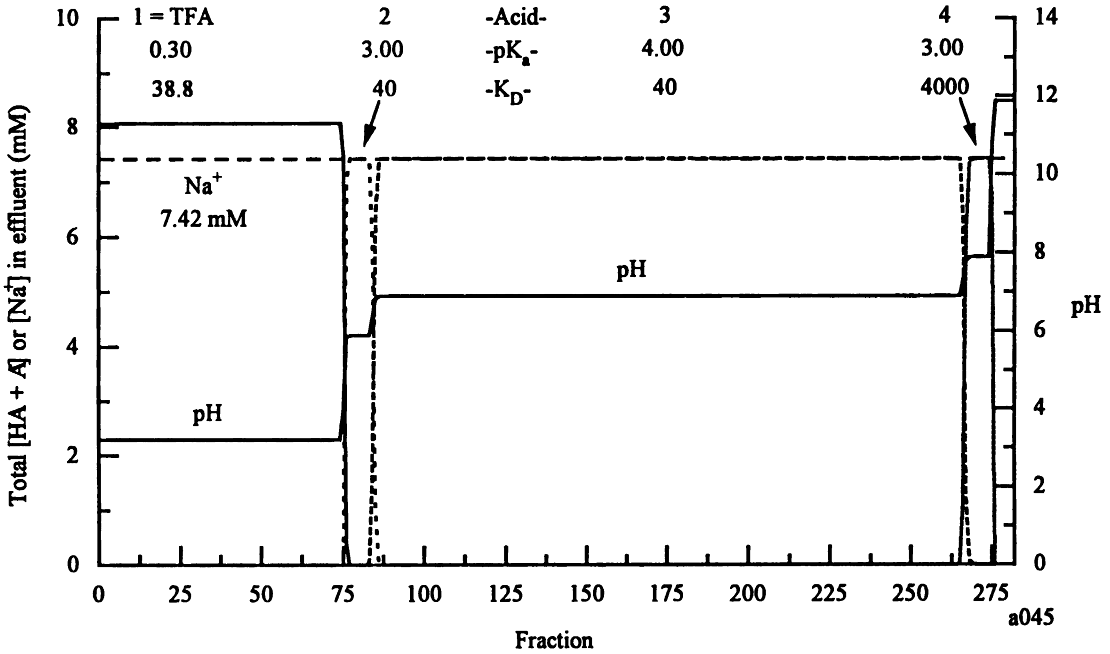

Figure 10. Simulated chromatogram of a mixture of one major and two minor acids, plus retaining acid in the stationary phase. [TFA] = 0.4 mM, [HA*2*] = 4 mM, [HA*3*] = 82 mM, [HA*4*] = 4 mM. Other conditions are as described for Figure 8.

Downloaded by YORK UNIV on June 28, 2012 | http://pubs.acs.org
Publication Date: May 15, 1995 | doi: 10.1021/bk-1995-0593.ch015

Equation 7 can be rearranged to Equation 8, which can be used to calculate the ratio $K_D^{HA\mathit{1}}/K_a^{HA\mathit{1}}$ from the measured pH of the HA*1* plateau.

$$\frac{K_D^{HA\mathit{1}}}{K_a^{HA\mathit{1}}} = \frac{[HA\mathit{1}_{org}]}{[H^+_{aq}]^2 + \left([H^+_{aq}] \times [Na^+_{aq}]\right) - K_W} \tag{8}$$

In a series of experiments, the concentration of the retaining acid (trifluoroacetic acid) in the stationary phase was varied. The measured plateau pHs and the predicted plateau pH curve from Equation 6 for the retaining acid, both vs. the initial concentration of acid in the stationary phase, are plotted in Figure 11. In an analogous series of experiments, the concentration of base in the aqueous eluent was varied. The measured plateau pHs and the predicted pH curve for the retaining acid, both vs. the concentration of base in the eluent, are plotted in Figure 12. The agreement is excellent, especially because both curves are calculated by fitting a single parameter, $K_D^{HA\mathit{1}}/K_a^{HA\mathit{1}}$, to Equation 7. This parameter was found to be 77.6. Based on a literature $pK_a = 0.3$, $K_D^{HA\mathit{1}} = 38.8$ for TFA was estimated.

Plateau Concentration of Monoprotic Acids in Effluent

In Figures 5, 7, and 9, it is notable that the calculated plateau concentrations of the monoprotic sample acids in the effluent are approximately equal to the concentration of NaOH in the basic eluent. In the simulations, the $[OH^-_{aq}]$ in the effluents were <0.01 mM (pH <9). The only counter ions other than OH^-_{aq} that are available for the >1 mM $[Na^+_{aq}]$ in the effluent are the anions of the sample acids. Also in the simulations, the sample acids elute at pHs that are two units greater than their pK_as; therefore, the ratio of anion to neutral acid in the effluent is >99%. Thus, under these conditions, $[Ai^-_{aq}] + [HAi_{aq}] \approx [Ai^-_{aq}] \approx [NaOH_{aq}]$. Thus pH-zone-refining CCC produces rectangular peaks with approximately the same concentration of the separated component. In contrast, displacement chromatography produces rectangular peaks containing increasing concentrations of separated components (*7*).

Plateau Concentration of Monoprotic Acids in Stationary Phase

The sample acids displace the preceding acids in the organic stationary phase. $HA\mathit{1}_{org}$ is displaced by HA*2*, which is displaced by HA*3*, etc. Therefore, the total concentration of sample and retaining acids in a section approximately equals the initial $[HA\mathit{1}_{org}]$ in the stationary phase. For the simulated chromatogram in Figure 9 with an initial $[HA\mathit{1}_{org}]$ of 0.2 mM, the sum $[HA\mathit{1}_{org}] + [HA\mathit{2}_{org}] + [HA\mathit{3}_{org}] + [HA\mathit{4}_{org}]$ in the effluent was in the range 0.187-0.200 mM. For an initial $[HA\mathit{1}_{org}]$ of 0.4 mM (simulated chromatogram not shown), $[HA\mathit{1}_{org}] + [HA\mathit{2}_{org}] + [HA\mathit{3}_{org}] + [HA\mathit{4}_{org}]$ in the final tube was 0.379-0.4 mM.

Prediction of Plateau pH for the Sample Acids

For a tube that contains only one acid, the pH is determined by $[Ai^-_{aq}]$ and $[HAi_{org}]$

Downloaded by YORK UNIV on June 28, 2012 | http://pubs.acs.org
Publication Date: May 15, 1995 | doi: 10.1021/bk-1995-0593.ch015

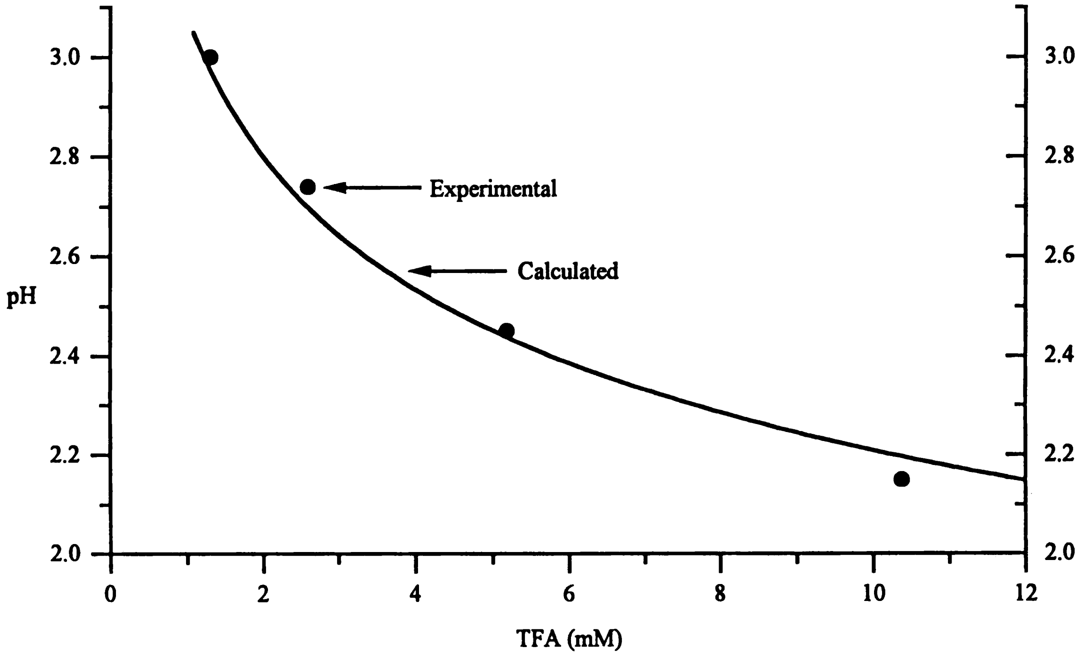

Figure 11. Dependence of the experimental and theoretical pH at the plateau of the retaining acid on the concentration of retaining acid.

Downloaded by YORK UNIV on June 28, 2012 | http://pubs.acs.org
Publication Date: May 15, 1995 | doi: 10.1021/bk-1995-0593.ch015

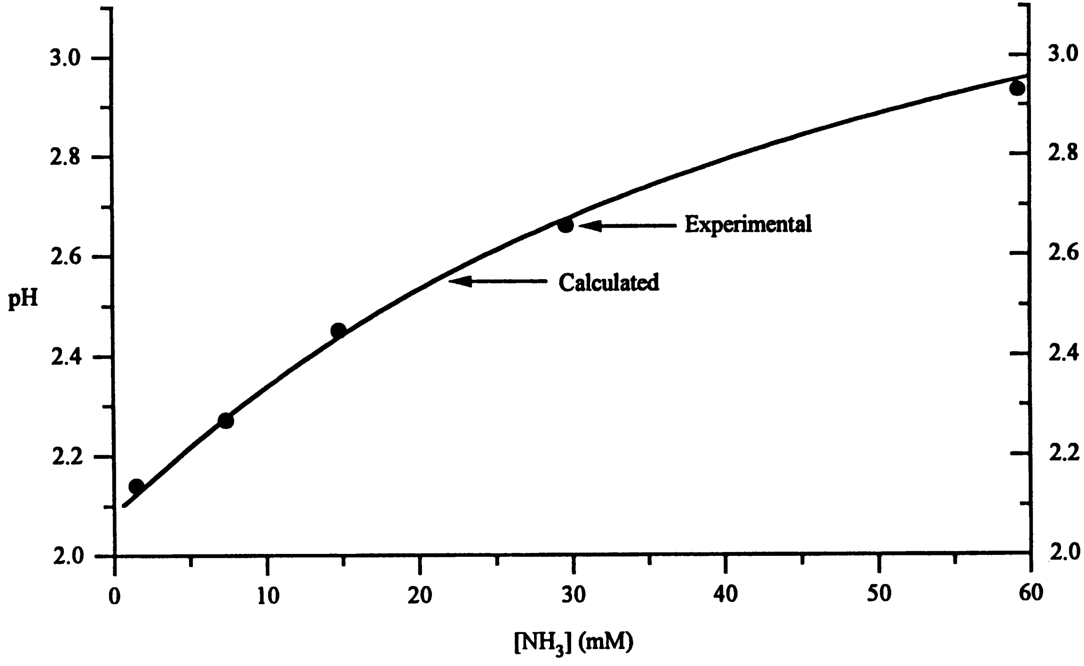

Figure 12. Dependence of the experimental and theoretical pH at the plateau of the retaining acid on the concentration of eluting base.

and the acid's pK_a and K_D. This is shown in Equation 9, which is derived by using Equation 1 to substitute $[\mathrm{HA}i_{aq}]$ in Equation 2.

$$[\mathrm{H}^+_{aq}] = \frac{K_a^{\mathrm{HA}i} \times [\mathrm{HA}i_{org}]}{K_\mathrm{D}^{\mathrm{HA}i} \times [\mathrm{A}i^-_{aq}]} \tag{9}$$

As discussed in a previous paragraph for the sample acids, the plateau $[\mathrm{A}i^-_{aq}] \approx [\mathrm{NaOH}_{aq}]$ in the eluting base and $[\mathrm{HA}i_{org}] \approx$ the original $[\mathrm{HA}1_{org}]$ for the retaining acid in the acidified stationary phase. Substituting these values into Equation 9 yields Equation 10.

$$[\mathrm{H}^+_{aq}] = \frac{K_a^{\mathrm{HA}i} \times [\mathrm{HA}1_{org}]}{K_\mathrm{D}^{\mathrm{HA}i} \times [\mathrm{NaOH}_{aq}]} \tag{10}$$

Within a pH-zone-refining CCC separation, the differences in the plateau pHs for the sample acids are approximately equal to the differences in the acid's (pK_a + log K_D). In different pH-zone-refining CCC separations with the same solvent system, the differences in plateau pHs for one sample acid are approximately equal to the differences in $\log([\mathrm{NaOH}_{aq}]/[\mathrm{HA}1_{org}])$.

Chromatography of Diprotic Acids

The model is not limited to monoprotic acids. Theoretical chromatograms of an analogous biphasic mixture of n monoprotic acids, HAi (i = 1 to n), m diprotic acids, $\mathrm{H_2B}j$ (j = 1 to m), and their sodium salts are similarly derived. A term (Equation 11) for the diprotic acids is added to the left side of Equation 6.

$$\sum_{j=1}^{m} \frac{\dfrac{TBj}{vol_{aq}} \times \left(2 + \dfrac{[\mathrm{H}^+_{aq}]}{K_{a2}^{\mathrm{H_2B}j}}\right)}{1 + \dfrac{[\mathrm{H}^+_{aq}]}{K_{a2}^{\mathrm{H_2B}j}} \times \left(1 + \dfrac{[\mathrm{H}^+_{aq}]}{K_{a1}^{\mathrm{H_2B}j}} \times \left(1 + \dfrac{K_\mathrm{D}^{\mathrm{H_2B}j} \times vol_{org}}{vol_{aq}}\right)\right)} \tag{11}$$

The resulting equation is expanded into a (2 + n + m × 2)-power polynomial equation in $[\mathrm{H}^+_{aq}]$. This equation is similarly evaluated to calculate the distribution of solutes in a two-phase mixture of monoprotic and diprotic acids.

A simulated chromatogram (Figure 13) of three diprotic acids and a retaining acid also contained rectangular peaks with steep slopes. For weak diprotic acids, the plateau concentrations of the acids were equal to approximately half the concentration of NaOH in the eluting base, because the acids elute predominantly as the dianions. If pK_{a1} and pK_{a2} for a diprotic acid are very different (acid 4 in

Downloaded by YORK UNIV on June 28, 2012 | http://pubs.acs.org
Publication Date: May 15, 1995 | doi: 10.1021/bk-1995-0593.ch015

Downloaded by YORK UNIV on June 28, 2012 | http://pubs.acs.org
Publication Date: May 15, 1995 | doi: 10.1021/bk-1995-0593.ch015

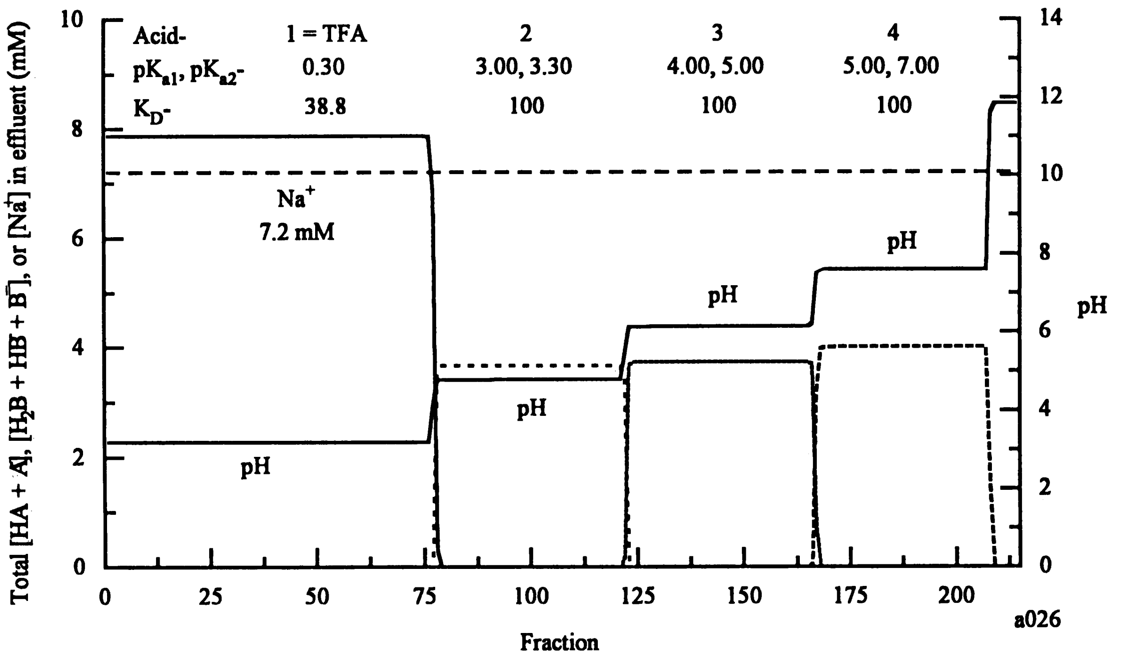

Figure 13. Simulated chromatogram of a mixture of three diprotic acids, plus retaining acid in the stationary phase. The sample in 3 mL of the acidified stationary phase is in the first three plates. [TFA] = 0.4 mM, [H_2B1] = 10 mM, [H_2B2] = 10 mM, [H_2B3] = 10 mM, [$NaOH_{aq}$] = 7.2 mM. Other conditions are as described for Figure 8.

Figure 13), then the plateau concentration of the acid is greater than half the concentration of NaOH in the eluting base, because the ratio of monoanion to dianion increases.

Conclusions

Simulations using countercurrent distribution as an equilibrium model for pH-zone-refining CCC produced the flat-top peaks with steep sides that are found in experimental chromatograms. These simulated chromatograms show that highly pure acids may be isolated with very high recoveries when sufficient retaining acid is used. The separation of acids is based on differences in pK_a and K_D. The plateau pH for the retaining acid can be calculated from its pK_a, K_D, and concentration in the stationary phase and from the $[NaOH_{aq}]$ in the eluting base. The plateau pH for a sample acid, HA*i*, can be estimated from its $(pK_a+\log(K_D))$ plus $\log([NaOH_{aq}])$ - $\log([HA1_{org}])$.

This model and calculations may be modified to simulate pH-zone-refining CCC of (1) acids when a retaining base in the aqueous stationary phase and an eluting acid in the organic mobile phase are used, (2) bases (e.g., organic amines) when a retaining base in the organic stationary phase and an eluting acid in the aqueous mobile phase are used, or (3) bases when a retaining acid in the aqueous stationary phase and an eluting base in the organic mobile phase are used.

Literature Cited

1. Weisz, A.; Scher, A.L.; Shinomiya, K.; Fales, H.M.; Ito, Y. *J. Am. Chem. Soc.* **1994**, *116*, 704-708.
2. Ito, Y.; Shinomiya, K.; Fales, H.M.; Weisz, A.; Scher, A.L. in *Countercurrent Chromatography*; Conway, W.D.; Petroski, R., Eds.; American Chemical Society Symposium Series; American Chemical Society: Washington, DC, 1995.
3. Weisz, A.; Andrzejewski, D.; Shinomiya, K.; Ito, Y. in *Countercurrent Chromatography*; Conway, W.D.; Petroski, R., Eds.; American Chemical Society Symposium Series; American Chemical Society: Washington, DC, 1995.
4. Weisz, A. in *High-Speed Countercurrent Chromatography*; Ito, Y; Conway W.D., Eds.; Chemical Analysis Series, Wiley: New York, NY (in press).
5. Ito, Y. in *High-Speed Countercurrent Chromatography*; Ito, Y; Conway W.D., Eds.; Chemical Analysis Series, Wiley: New York, NY (in press).
6. Kurz, J.L.; Farrar, J.M. *J. Am. Chem. Soc.* **1969**, *91*, 6057-6062.
7. Horváth, C.; Nahum, A.; Frenz, J.H. *J. Chromatogr.* **1981**, *218*, 365-393.

RECEIVED December 20, 1994

Downloaded by YORK UNIV on June 28, 2012 | http://pubs.acs.org
Publication Date: May 15, 1995 | doi: 10.1021/bk-1995-0593.ch015

Downloaded by COLUMBIA UNIV on June 29, 2012 | http://pubs.acs.org
Publication Date: May 15, 1995 | doi: 10.1021/bk-1995-0593.ch016

Chapter 16

Preparative Separation of Components of Commercial 4,5,6,7-Tetrachlorofluorescein by pH-Zone-Refining Countercurrent Chromatography

Adrian Weisz[1], Denis Andrzejewski[2], Kazufusa Shinomiya[3,4], and Yoichiro Ito[3]

[1]Office of Cosmetics and Colors and [2]Office of Scientific Analysis and Support, U.S. Food and Drug Administration, Washington, DC 20204
[3]Laboratory of Biophysical Chemistry, National Heart, Lung, and Blood Institute, National Institutes of Health, Building 10, Room 7N322, Bethesda, MD 20892

Samples of commercial 4,5,6,7-tetrachlorofluorescein (TCF) were subjected to pH-zone-refining countercurrent chromatography (pH-zone-refining CCC) to separate the main component and its contaminants. The study involved sample portions of 350 mg, 1 g, and 2 g, each with ~91% TCF, and a 5-g sample portion containing ~64.7% TCF. The separations were achieved with commercially available CCC centrifuges. The two-phase solvent systems used were diethyl ether-acetonitrile-10 mM aqueous ammonium acetate (4:1:5) and methyl *tert*-butyl ether-acetonitrile-water (4:1:5). Trifluoroacetic acid was added to either the sample solution or the (upper) stationary phase to serve as the retainer acid. Aqueous ammonia was added to the (lower) mobile phase to serve as the eluent base. The TCF separations required relatively short times (e.g., 5 h for the 5-g separation). The yield of the recovered TCF varied between ~65% for the 350-mg separation and 78.2 to ~89% for the gram-quantity separations. In all the separations, the recovered TCF had greater than 99.5% purity. Tetrachlorophthalic acid, 2,3,4-trichloro-6-hydroxyxanthone-1-carboxylic acid, 2-(2′,4′-dihydroxybenzoyl)tetrachlorobenzoic acid, and a new compound whose proposed structure is 10,11,12-trichloro-3H-[1]benzopyrano[2,3,4-k,l]xanthen-3-one were contaminants isolated from the 350-mg separation. A brief account of how each contaminant might be formed is also presented.

The compound 4,5,6,7-tetrachlorofluorescein (TCF), **1**, is a dye of the hydroxyxanthene class. It is synthesized by the condensation of two moles of

[4]Current address: College of Pharmacy, Nihon University, 7–7–1, Narashinodai, Funabashi-shi, Chiba 274, Japan

This chapter not subject to U.S. copyright
Published 1995 American Chemical Society

resorcinol with either one mole of tetrachlorophthalic anhydride (*1*) or one mole of tetrachlorophthalic acid in the presence of a condensing agent (*2*) (Figure 1). TCF is used primarily as an intermediate for the preparation of more highly halogenated dyes, such as tetrabromotetrachlorofluorescein, **2** [Colour Index (1971) No. 45410:1]; its disodium salt, Phloxine B, **3** [Colour Index (1971) No. 45410]; and Rose Bengal, **4** [Colour Index (1971) No. 45440] (Figure 1). Dyes in the same group as compounds **3** and **4** are widely used as biological stains (*3*) and, in fact, compound **1** itself is also sometimes used for this purpose (*4*). Compounds **2** and **3** have an additional important use; specifically, they are used as color additives for drugs and cosmetics in the United States, where they are designated as D&C Red No. 27 and D&C Red No. 28, respectively (*5*).

High-performance liquid chromatographic (HPLC) analyses revealed the presence of contaminants in each of several batches of TCF obtained from various distributors. HPLC results further indicated that the nature of the specific contaminants varied across batches (Figure 2). These contaminants of **1** can be carried over to the more highly halogenated dyes during the manufacturing process (Figure 1). The presence of contaminants in those dyes has significant ramifications for each of the areas of dye application. Before they may be used as color additives, **2** and **3** are subject to batch certification by the US Food and Drug Administration (FDA) to ensure compliance with chemical specifications and Good Manufacturing Practices (GMP) requirements set forth in the Code of Federal Regulations (CFR) (*5*). The nature and quantity of the contaminants present in the color additives can sometimes cause a given batch to be rejected for batch certification. The presence of contaminants in those dyes can also cause variations in their staining properties. This problem has been documented as the cause of anomalous histochemical staining results (*6-8*).

In order to overcome problems posed by the contaminants in TCF and its resultant dyes, the present study was initiated to develop a preparative method of purifying the compound. Purified samples of **1**, **2**, and **3**, and of the contaminants they contain were needed as reference materials to develop and validate an HPLC method for analyzing batches submitted to FDA for certification as D&C Red Nos. 27 and 28. Furthermore, purified dyes would enable the comparison of samples stained in different laboratories (*8-10*) and ultimately would enable standardization of biological stains (*8, 11, 12*).

One preparative method for the purification of TCF is reported in the literature (*13*). That method uses gel chromatography and separates relatively small quantities (10-30 mg) of dye in each trial. In the present study, high-speed countercurrent chromatography (HSCCC) (*14-16*) was chosen to purify TCF. HSCCC successfully separated **1** and its tribrominated analog (2′,4′,5′-tribromo-4,5,6,7-tetrachlorofluorescein) from other components in a synthetically prepared mixture that had been partially separated by preparative HPLC (*17*). HSCCC was also used previously to purify **2** and **3**, the tetrabrominated analogs of **1** (*18*). In that case, each purification trial involved only 50 mg of dye because of the highly concentration-dependent partition behavior of the dyes in the solvent system used. That problem was circumvented by using the improved HSCCC technique pH-zone-refining CCC (*19, 20*) in a later study (*21*) in which multigram quantities of **3** were

Downloaded by COLUMBIA UNIV on June 29, 2012 | http://pubs.acs.org
Publication Date: May 15, 1995 | doi: 10.1021/bk-1995-0593.ch016

Downloaded by COLUMBIA UNIV on June 29, 2012 | http://pubs.acs.org
Publication Date: May 15, 1995 | doi: 10.1021/bk-1995-0593.ch016

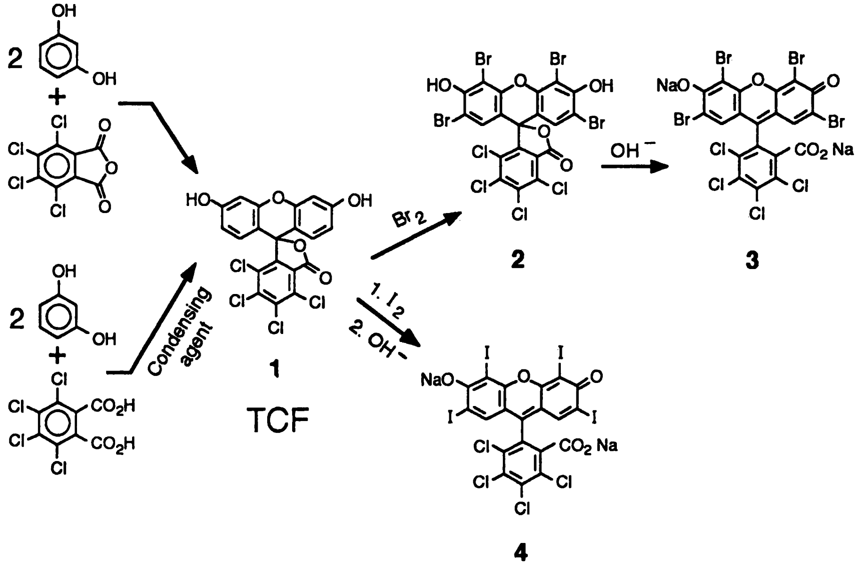
2
OH
OH
+
Cl
O
Cl
O
Cl
Cl
O
2
OH
OH
+
Cl
Cl
CO2H
Cl
CO2H
Cl
Condensing agent
HO
O
OH
O
Cl
O
Cl
Cl
Cl
1
TCF
Br2
1. I2
2. OH-
Br
Br
HO
OH
Br
Br
2
OH-
NaO
O
Br
CO2Na
3
I
I
NaO
O
I
I
CO2Na
4

Figure 1. Preparation of 4,5,6,7-tetrachlorofluorescein (TCF) and higher halogenated dyes.

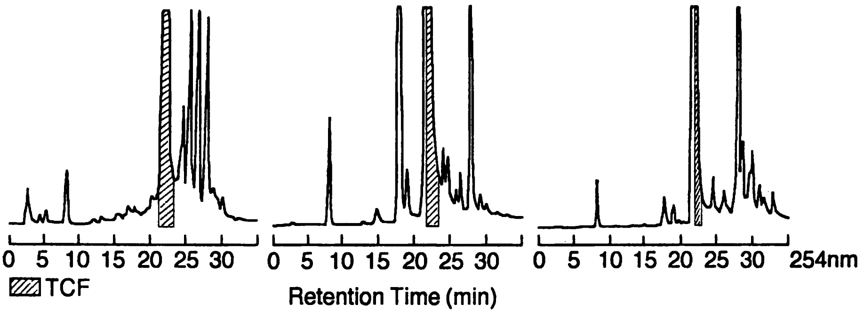

Figure 2. HPLC analyses of commercial batches of TCF obtained from three different sources.

successfully purified. pH-Zone-refining CCC involves the following procedure: A multigram mixture of acids (or bases) is isocratically eluted with aqueous base (or acid) through an acidified (basified) organic stationary phase in a CCC column; as the components of a mixture of acids (bases) are eluted, the pH of the eluent increases (decreases) in steps, with pH plateaus showing elution of single major components. A detailed description of pH-zone-refining CCC is presented in the chapter by Ito et al. in this volume. The present study concentrates on the application of this technique to the preparative separation of TCF and several contaminants in commercial TCF samples.

Experimental

Materials. The samples of commercial batches of TCF used in this study were from three American suppliers (Aldrich, Milwaukee, WI; K&K Lab., Inc., Plainview, NY; and Thomasset Colors, now Hilton-Davis Co., Cincinnati, OH). Ammonium acetate, methanol, water, and acetonitrile were chromatography grade. Diethyl ether (anhydrous) and hydrochloric acid (36.5-38.0%) were ACS reagent grade. Sodium sulfate anhydrous (granular) was analytical-reagent grade. Methyl *tert*-butyl ether and sodium deuteroxide (NaO^2H, 99.9%, ca. 40% in ^2H_2O, both from Fluka, Buchs, Switzerland), ammonium hydroxide (>25% NH_3 in water, Fisher Scientific, Pittsburgh, PA), trifluoroacetic acid (TFA, Sigma Chemical, St. Louis, MO), and deuterium oxide (^2H_2O, 99.9%, MSD Isotopes, Montreal, Canada) were used as received.

Instrumentation and pH-Zone-Refining CCC Procedure. The separations presented here were performed with a commercially available high-speed CCC centrifuge (Ito Multilayer Coil Separator/Extractor, P.C. Inc., Potomac, MD) unless otherwise specified. A schematic diagram of the apparatus was published previously (*19*). A multilayer column was constructed by one of the authors (Y.I.) from polytetrafluoroethylene tubing (ca. 165 m × 1.6 mm i.d., with a total capacity of approximately 325 mL). The β value (a centrifugal parameter) (*22*) ranged from 0.5 at the internal terminal to 0.85 at the external terminal. The column consisted of 16 coiled layers. (Similar columns are commercially available from P.C. Inc.; Pharma-Tech Research Corp., Baltimore, MD; and Shimadzu, Kyoto, Japan.) The experimental details are given in Table I. The two-phase solvent system was thoroughly equilibrated in a separatory funnel, and the two phases were separated shortly before use and degassed by sonication for 2-3 min. The lower (aqueous, mobile) phase was adjusted to the desired pH by addition of ammonium hydroxide (eluent base). The retainer acid, TFA, was added to the upper (nonaqueous, stationary) phase or to the sample solution. The sample solutions were prepared by suspending TCF in a minimum amount of solvent system (equal volumes of each phase) to which TFA was added. Alternatively, TFA was added only to the acidified upper phase. The separations were initiated by filling the entire column with the stationary phase, using a metering pump (Accu-Flo pump; Beckman, Palo Alto, CA), and then loading the sample solution into the column by syringe. The mobile phase was then pumped into the column at 3 mL/min while the column was rotated

Downloaded by COLUMBIA UNIV on June 29, 2012 | http://pubs.acs.org
Publication Date: May 15, 1995 | doi: 10.1021/bk-1995-0593.ch016

Downloaded by COLUMBIA UNIV on June 29, 2012 | http://pubs.acs.org
Publication Date: May 15, 1995 | doi: 10.1021/bk-1995-0593.ch016

Table I. pH-Zone-Refining Countercurrent Chromatography of Commercial 4,5,6,7-Tetrachlorofluorescein

Sample Size, mg	*TCF Recovered*[a], *% (mg)*	*Solvent System*		*Retainer Acid Location*	*Mobile Phase pH*[b]	*Sample Preparation*	*Column Rotation, rpm*	*Retention of Stationary Phase*[c], *%*	*TCF Separation Time, h*
350[d]	65.3 (208)	Et_2O[e] AcN[g] NH_4OAc[h] (10 mM)	4 1 5	TFA[f], 200 μL in sample solution	9.0	Suspension in 6 mL each of upper and lower phases	800	74.8	3
1000[d]	88.9 (809)	Et_2O AcN NH_4OAc (10 mM)	4 1 5	TFA, 250 μL in sample solution	9.3	Suspension in 18 mL each of upper and lower phases	800	70.0	4.5
2000[d]	78.2 (1424)	MTBE[i] AcN H_2O	4 1 5	TFA, 200 μL in (upper) stationary phase (500 mL)	10.6	Suspension in 100 mL of acidified upper phase	800	64.0	2
5000[j,k]	84.6 (2750)	MTBE AcN H_2O	4 1 5	TFA, 200 μL in (upper) stationary phase (500 mL)	10.7	Suspension in 110 mL of acidified upper phase	1000	60.0	5

[a] Recoveries were calculated on the basis of the amount of TCF in the sample as determined by HPLC. TCF was isolated in the lactone form (*17*) (greater than 99.5% purity) and identified by chemical-ionization mass spectrometry and by ^1H nuclear magnetic resonance spectroscopy. [b] Lower phase to which was added ammonium hydroxide. [c] % of total column capacity. [d] Commercial sample that contained approximately 91% TCF; the HPLC chromatogram of the sample is shown in Figure 2b. [e] Diethyl ether. [f] Trifluoroacetic acid. [g] Acetonitrile. [h] Ammonium acetate. [i] Methyl *tert*-butyl ether. [j] Commercial sample that contained approximately 64.7% TCF; the HPLC chromatogram of the sample is shown in Figure 2c. [k] This separation was performed with a Model CCC-1000 high-speed countercurrent chromatograph (Pharma-Tech Research Corp., Baltimore, MD) to which several improvements were made (e.g., continuous pH monitoring, computerized data acquisition) to facilitate chromatography (*23, 24*).

in the forward mode. The column effluent was monitored with a UV detector (Uvicord S; LKB, Stockholm, Sweden) at 206 or 254 nm and collected in fractions (3 mL) by using a fraction collector (Ultrorac, LKB). The pH of each eluted fraction was measured manually with a pH meter (Accumet 1001; Fisher Scientific Co.). In one case, the pH was monitored continuously (see Table I). When the separation was completed (that is, when the pH of the effluent was the same as the pH of the mobile phase), the pump and the column rotation were stopped. The inlet of the column was connected to a pressured N_2 line, and the column contents were forced into a graduated cylinder to measure the volume of stationary phase that was retained in the column at the end of the separation.

Downloaded by COLUMBIA UNIV on June 29, 2012 | http://pubs.acs.org
Publication Date: May 15, 1995 | doi: 10.1021/bk-1995-0593.ch016

Analysis of CCC Fractions. An aliquot of each selected fraction from the pH-zone-refining CCC separation was diluted with approximately 2 mL of methanol-water (25:75, v/v). The solution was filtered through a Uniprep 0.45-µm glass microfiber syringeless filter unit (Whatman, Clifton, NJ) and analyzed by reversed-phase HPLC. The HPLC system used was previously described (*17, 18*). It consisted of a Model 8800 ternary pump, Model 8500 dynamic mixer, Model 8780 autosampler, and Model 4270 integrator (all Spectra-Physics, San Jose, CA), and a Model 490 multiwavelength detector set at 254 and 530 nm (Waters Assoc., Milford, MA). The autosampler was equipped with a Model 7010 injector (Rheodyne, Cotati, CA) with a 20-µL injection loop. The column used was Hypersil MOS-1 RPC-8, 5-µm particle size, 250 × 4.6 mm i.d. (Keystone Scientific, Bellefonte, PA). The mobile phase consisted of 0.1 M aqueous ammonium acetate and methanol. The column was eluted with consecutive linear gradients of 25 to 90% methanol in 25 min, 90 to 100% methanol in 5 min, and 100% methanol for 5 min. The column was re-equilibrated with 25% methanol for 15 min. Other conditions were as follows: injection volume, 20 µL; full scale response, 0.128 absorbance units; and flow rate, 1 mL/min.

Isolation of the Separated Components from CCC Fractions. TCF was isolated in the lactone form as previously described for the brominated tetrachlorofluoresceins (*17*). Fractions with the same pH values and HPLC retention times were combined and concentrated to ca. 5 mL on a rotary evaporator at ca. 30 Torr and 50°C. The residue was acidified with 30-40 mL of 10% HCl, and the precipitated lactone was extracted into ethyl acetate. The organic layer was washed (2 × 20 mL water) and dried (anhydrous Na_2SO_4), and the solvent was evaporated. For the 5-g separation (see Table I), the concentration step was eliminated and the precipitated lactone was filtered, washed with water, and vacuum-dried (30 Torr) at ca. 50°C. Fractions corresponding to other separated components were freeze-dried.

Mass Spectrometry (MS). The low resolution positive ion chemical ionization (PICI) mass spectra were obtained on a Finnigan Mat TSQ-46 instrument interfaced to an INCOS 2300 data system with TSQ software (Revision D). The spectrometer had a source temperature of 100°C, emission of 0.35 mA at 70 eV, 0.25 Torr methane, preamplifier setting at 10^{-8} A/V, and conversion dynode of -5 kV, and was scanned from m/z 65 to 765 in 1.0 s. The sample portions were dissolved in either ethyl acetate or methanol, and the samples were introduced via the direct chemical ionization (DCI) probe at a heating rate of 20 mA/s. High-resolution mass-spectral measurements were made on a FISONS Auto Spec mass spectrometer with a VAX 4000 data system. Instrument operating parameters were 70-eV electron energy, 300-μA emission current, 8-kV accelerating voltage, and 100°C source temperature. High-resolution electron ionization data were acquired at 10,000 resolution (10% valley definition) by scanning the magnet from m/z 460 to 260 in 10 s. Perfluorokerosene, added via the heated batch inlet, was used as the reference standard. The sample was introduced on the solid probe, heated ballistically to 200°C.

^{1}H Nuclear Magnetic Resonance Spectroscopy (NMR). ^{1}H NMR spectra were obtained on a Varian XL 300 Fourier transform NMR spectrometer at 300 MHz. Typical concentrations were 1 to 4 mg of the sample (TCF in lactone form) in 0.5 mL of 0.5% NaO^2H in ^2H_2O.

Results and Discussion

The present study examined samples of commercial TCF from three different sources. Two of the samples were used for the present separations. The TCF content of the samples was assessed by HPLC (530 nm) using a previously purified TCF sample as the standard. One of the samples was found to contain ~91% TCF and the other, ~64.7% TCF. Portions of 350 mg, 1 g, and 2 g from the former sample and a 5-g portion from the latter sample were used for the separations described below.

The pH-zone-refining countercurrent chromatogram for the separation of the components in the 350-mg sample of TCF (for which the HPLC profile is shown in Figure 3a) is presented in Figure 3b. The solvent front (first fraction containing mobile phase) emerged at fraction 18. The retention of the stationary phase, calculated after the separation, was 74.8%. Other experimental details are described in Table I. A-E are the eluted fractions containing pure compounds that correspond to peaks A-E in the HPLC chromatogram of the commercial TCF (Figure 3a). Monitoring of the eluted fractions with a pH meter resulted in a long pH-plateau (dotted line) that corresponded to the main absorbance peak (solid line). The corresponding eluate was collected in fractions 116-168 (Figure 3b). Fractions 116-168 contained a single component whose HPLC peak corresponded to peak D in Figure 3a. The orange-colored compound was isolated as the lactone (208 mg, greater than 99.5% purity by HPLC at 254 and 530 nm) and identified by CI-MS and ^{1}H NMR as 4,5,6,7-tetrachlorofluorescein, 1 (~65.3% recovery). The eluates corresponding to the absorbance peaks A, E, B, and C (Figure 3b) were collected in fractions 78-80, 93-97, 102-103, and 105-109, respectively. These fractions contained single components that were isolated and identified by two or more of the following methods: CI-MS, ^{1}H NMR, high-resolution MS, and HPLC. The compounds obtained from this separation are shown in Figure 4. A short account of how each of these compounds may be formed during the manufacturing process and carried through to the final product--commercial TCF--is given below.

Downloaded by COLUMBIA UNIV on June 29, 2012 | http://pubs.acs.org
Publication Date: May 15, 1995 | doi: 10.1021/bk-1995-0593.ch016

Downloaded by COLUMBIA UNIV on June 29, 2012 | http://pubs.acs.org
Publication Date: May 15, 1995 | doi: 10.1021/bk-1995-0593.ch016

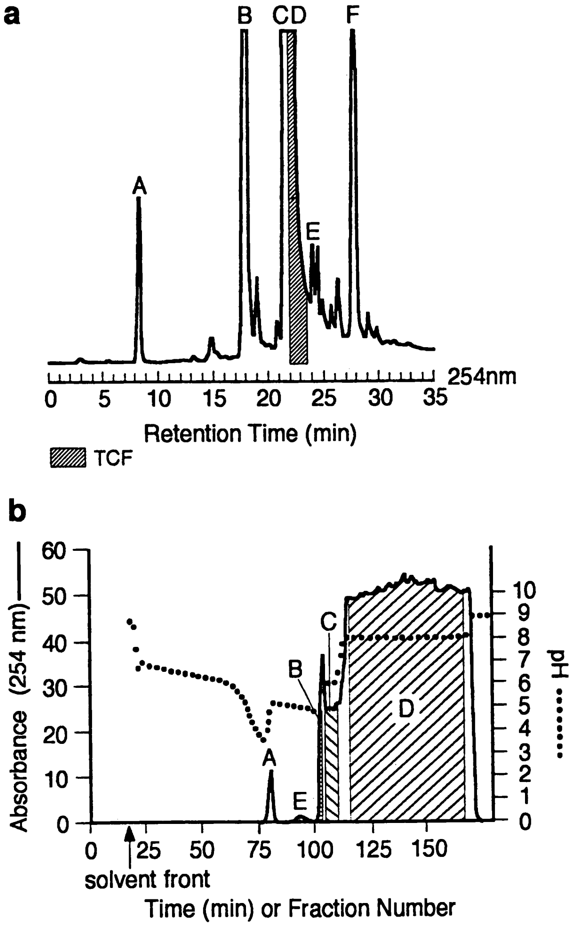

Figure 3. Separation of components of commercial TCF by pH-zone-refining CCC. (a) HPLC analysis of the commercial TCF, (b) pH-zone-refining countercurrent chromatogram of the separation of components in 350 mg of commercial TCF.

Downloaded by COLUMBIA UNIV on June 29, 2012 | http://pubs.acs.org
Publication Date: May 15, 1995 | doi: 10.1021/bk-1995-0593.ch016

Tetrachlorophthalic anhydride or its free acid is used as a starting material for the synthesis of TCF (Figure 1). The unreacted material, if carried over during the manufacturing process, would be present in the final product. Tetrachlorophthalic anhydride is hydrolyzed to tetrachlorophthalic acid, **5** (Figure 4), during the pH-zone-refining CCC separation (fractions 78-80, 24 mg).

Fractions 92-97 (peak E, Figure 3b) contained a single component whose HPLC peak corresponded to the minor peak E in Figure 3a. The compound was isolated (0.6 mg) and its elemental composition ($C_{19}H_7O_3Cl_3$) and exact mass (387.946200) were determined by high-resolution MS. The suggested 10,11,12-trichloro-3H-[1]benzopyrano[2,3,4-k,l]xanthen-3-one structure, **6**, and the proposed chemical pathway for its formation are shown in Figure 5. To obtain TCF, the aromatic H atom in position 4 of each of two molecules of resorcinol is involved in the elimination of H_2O during the condensation with tetrachlorophthalic anhydride (Figure 5a). If the elimination involves the H atom in position 2 of one of the resorcinol molecules and the H atom in position 4 of the other, the proposed intermediate **9** (Figure 5b) could be obtained. By loss of a molecule of HCl from intermediate **9** and by decarboxylation, the formation of contaminant **6** (Figure 5b) would result.

The effluent collected in fractions 102-103 (peak B, Figure 3b) contained a white crystalline precipitate. The crystalline material represented a single component. Its HPLC chromatogram (Figure 6a) corresponded to peak B in Figure 3a. The compound was isolated (3 mg) and characterized by CI-MS and ^1H NMR (Figure 6b-c) as 2,3,4-trichloro-6-hydroxyxanthone-1-carboxylic acid, **7**.

Fractions 105-109 (peak C, Figure 3b) contained a single component. Its HPLC peak retention time (Figure 7a) corresponded to peak C in Figure 3a. The colorless compound was isolated (5 mg) and identified by CI-MS and ^1H NMR (Figure 7b-c) as 2-(2′,4′-dihydroxybenzoyl)tetrachlorobenzoic acid, **8**. The isolated compound was further identified as **8** by comparing it with the synthetic material used as a standard by the Color Certification Branch of the FDA. It is noteworthy that **8** and TCF completely overlap and elute together in the reversed-phase HPLC system used, but are well separated by pH-zone-refining CCC (peaks C and D in Figure 3).

The contaminants **7** and **8** are by-products in the synthesis of TCF. They are produced when only one molecule of resorcinol reacts with tetrachlorophthalic anhydride (Figure 8). The pH-zone-refining CCC separation described here represents the first reported separation of **7** and **8** from commercial TCF. Previous references to **7** and **8** in the literature involve only the synthesis of **7** and **8** (*25*) and the observation of **7** as a decomposition product of TCF in strong alkaline solution (*26*).

The compound that corresponds to peak F in Figure 3a is less polar and, under the conditions used for this separation, remained in the stationary phase in the column (Figure 9). Its identity is currently under investigation and will be reported elsewhere (A. Weisz and D. Andrzejewski, US Food and Drug Administration, Washington, DC; and R.J. Highet and Y. Ito, National Institutes of Health, Bethesda, MD; unpublished results, 1994).

The pH-zone-refining CCC separation for the 1-g portion of commercial TCF resulted in increased peak width and a broadened pH plateau relative to those

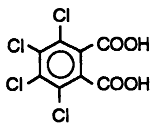

5

A, fr. 78-80
24 mg

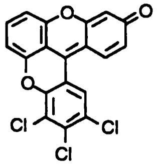

6

E, fr. 92-97
0.6 mg
$C_{19}H_7Cl_3O_3$

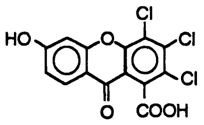

7

B, fr. 102-103
3 mg

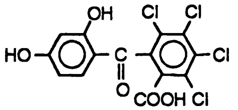

8

C, fr. 105-109
5 mg

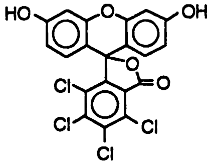

1

D, fr. 116-168
208 mg

Figure 4. Compounds isolated from a 350-mg sample of commercial TCF by the pH-zone-refining CCC separation shown in Figure 3.

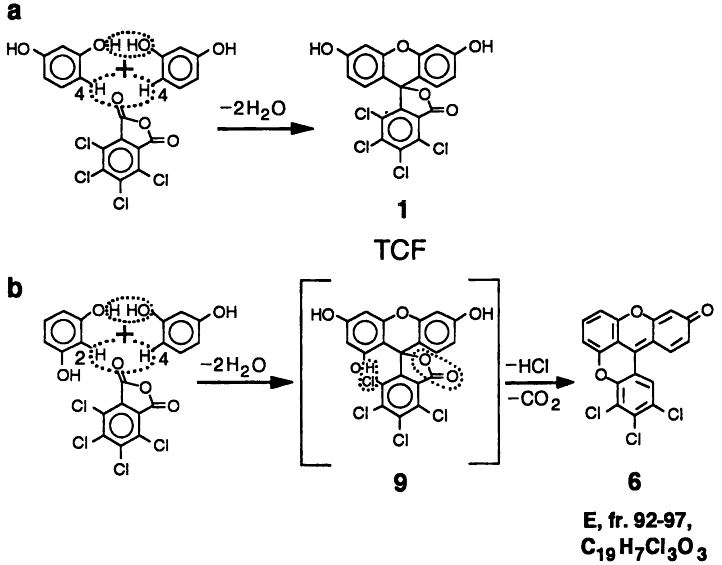

Figure 5. Schematic representation of the condensation of tetrachlorophthalic anhydride with two molecules of resorcinol. (a) Formation of TCF, (b) proposed pathway for the formation of 6.

Downloaded by COLUMBIA UNIV on June 29, 2012 | http://pubs.acs.org
Publication Date: May 15, 1995 | doi: 10.1021/bk-1995-0593.ch016

Downloaded by COLUMBIA UNIV on June 29, 2012 | http://pubs.acs.org
Publication Date: May 15, 1995 | doi: 10.1021/bk-1995-0593.ch016

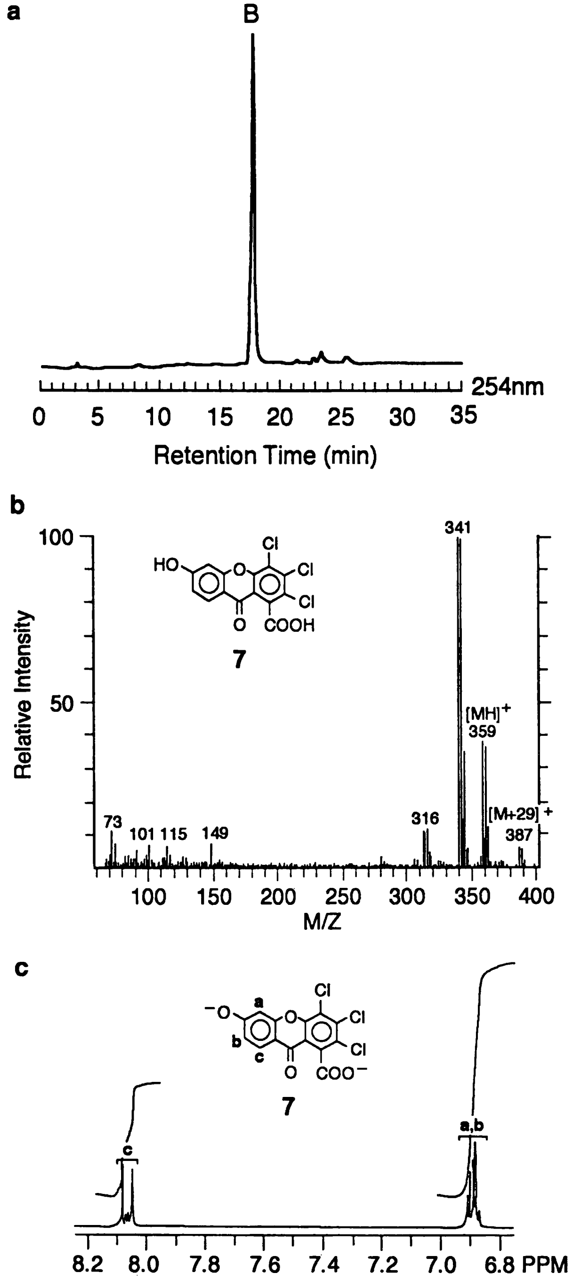

Figure 6. Characterization of the compound contained in fractions 102-103 of the pH-zone-refining CCC separation in Figure 3. (a) Analytical reversed-phase HPLC analysis, (b) positive ion chemical ionization (methane) mass spectrum, (c) ^{1}H NMR spectrum.

Downloaded by COLUMBIA UNIV on June 29, 2012 | http://pubs.acs.org
Publication Date: May 15, 1995 | doi: 10.1021/bk-1995-0593.ch016

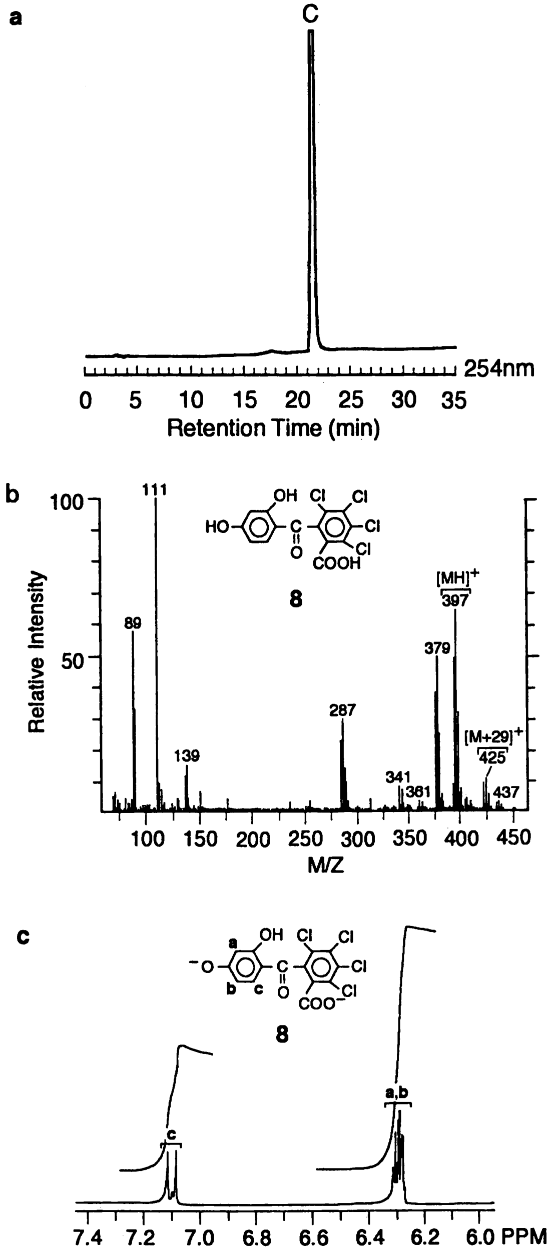

Figure 7. Characterization of the compound contained in fractions 105-109 of the pH-zone-refining CCC separation in Figure 3. (a) Analytical reversed-phase HPLC analysis, (b) positive ion chemical ionization (methane) mass spectrum, (c) ^{1}H NMR spectrum.

Downloaded by COLUMBIA UNIV on June 29, 2012 | http://pubs.acs.org
Publication Date: May 15, 1995 | doi: 10.1021/bk-1995-0593.ch016

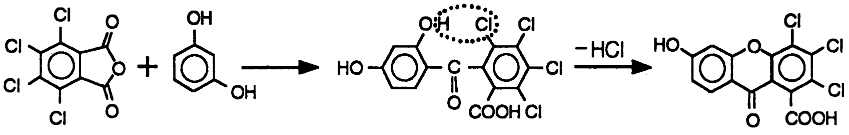

8

fr. 105-109
peak C

7

fr. 102-103
peak B

Figure 8. Schematic representation of the formation of by-products 7 and 8.

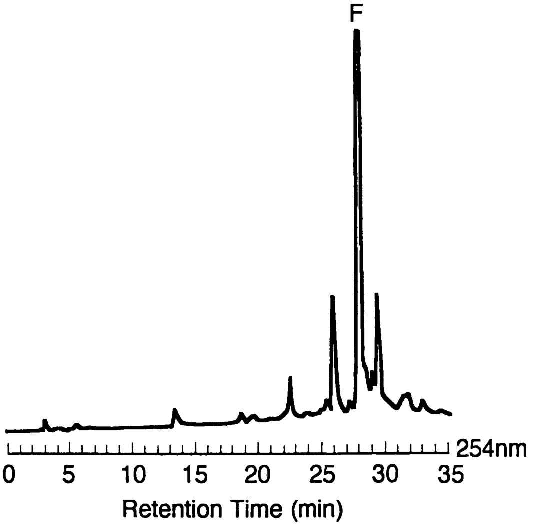

Figure 9. Reversed-phase HPLC analysis of the unfractionated column contents (stationary phase) collected at the end of the pH-zone-refining CCC separation shown in Figure 3.

Downloaded by COLUMBIA UNIV on June 29, 2012 | http://pubs.acs.org
Publication Date: May 15, 1995 | doi: 10.1021/bk-1995-0593.ch016

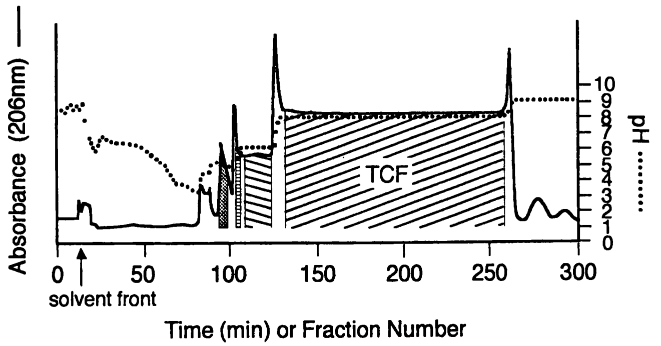

Figure 10. pH-Zone-refining countercurrent chromatogram of the separation of components in 1 g of commercial TCF (see Table I).

obtained from the separation for the 350-mg portion (Figure 10). Further proportionate changes in peak width and size of pH plateau occurred for the 2-g and 5-g portions of commercial TCF. This phenomenon was previously observed for pH-zone-refining CCC (*19*) and is further exemplified for TCF in the chapter by Shinomiya et al. The increase in sample size (with all other experimental conditions held constant) also resulted in improved recovery of the purified TCF (see Table I for recovery level from the 350-mg separation as compared with that from the 1-g separation, and that from the 2-g separation as compared with that from the 5-g separation). As was the case for the 350-mg separation, the purity of the isolated TCF in all gram-quantity separations was greater than 99.5% as measured by HPLC (254 and 530 nm). It is also noteworthy that the elution time for the purified TCF was relatively short (e.g., 5 h for the 5-g separation). Consistent with previously reported observations (*19*), an increase in the concentration of base in the mobile phase reduced the separation time (Table I).

Conclusion

The present study demonstrates that pH-zone-refining CCC is an effective method for the preparative-scale (multigram) purification of commercial 4,5,6,7-tetrachlorofluorescein and for the concentration and separation of minute amounts of its contaminants. The separations result in high-level recoveries of the highly purified TCF and can be accomplished within several hours even for multigram quantities.

Acknowledgments

The authors gratefully acknowledge Dr. Robert J. Highet, National Institutes of Health, Bethesda, MD, for producing and interpreting the nuclear magnetic resonance spectra.

Literature Cited

1. Graebe, C. *Liebigs Ann. Chem.* **1887**, *238*, 333.
2. Orndorff, W.R.; Hitch, E.F. *J. Am. Chem. Soc.* **1914**, *36*, 681.
3. Green, F.J. *The Sigma-Aldrich Handbook of Stains, Dyes and Indicators*; Aldrich Chemical Co., Inc.: Milwaukee, WI, 1990.
4. Tampion, J.; Wright, P.; Holt, G. *Stain Technol.* **1973**, *48*, 41-42.
5. *Code of Federal Regulations*, Title 21, Parts 74.1327-74.1328, U.S. Government Printing Office: Washington, DC, 1994.
6. Horobin, R.W. *Histochem. J.* **1969**, *1*, 231.
7. Marshall, P.N.; Lewis, S.M. *Stain Technol.* **1974**, *49*, 351.
8. Schulte, E.K.W. *Histochemistry* **1991**, *95*, 319.
9. Marshall, P.N.; Lewis, S.M. *Stain Technol.* **1974**, *49*, 235.
10. Marshall, P.N.; Bentley, S.A.; Lewis, S.M. *J. Clin. Pathol.* **1975**, *28*, 920.
11. Wittekind, D. *Anal. Quant. Cytol. Histol.* **1985**, 7, 6-30.
12. Lyon, H.O.; De Leenheer, A.P.; Horobin, R.W.; Lambert, W.E.; Schulte, E.K.W.; Van Liedekerke, B.; Wittekind D.H. *Histochem. J.* **1994**, *26*, 533-544.
13. Gandin, E.; Piette, J.; Lion, Y. *J. Chromatogr.* **1982**, *249*, 393.
14. Ito, Y. *CRC Crit. Rev. Anal. Chem.* **1986**, *17*, 65.
15. Ito, Y. In *Countercurrent Chromatography: Theory and Practice*; Mandava, N.B.; Ito, Y., Eds.; Chromatographic Science Series, Vol. 44; Marcel Dekker: New York, NY, 1988, Ch. 3, pp. 79-442.
16. Conway, W.D. *Coutercurrent Chromatography, Apparatus, Theory and Applications*, VCH: New York, NY, 1990.
17. Weisz, A.; Scher, A.L.; Andrzejewski, D.; Shibusawa, Y.; Ito, Y. *J. Chromatogr.* **1992**, *607*, 47.
18. Weisz, A.; Langowski, A.J.; Meyers, M.B.; Thieken, M.A.; Ito, Y. *J. Chromatogr.* **1991**, *538*, 157.
19. Weisz, A.; Scher, A.L.; Shinomiya, K.; Fales, H.M.; Ito, Y. *J. Am. Chem. Soc.* **1994**, *116*, 704-708.
20. Ito, Y.; Weisz, A.; U.S. Patent No. 5,332,504; July 26, 1994.
21. Weisz, A.; Andrzejewski, D.; Ito, Y. *J. Chromatogr. A* **1994**, *678*, 77-84.
22. Ito, Y. *J. Chromatogr.* **1984**, *301*, 387-403.
23. Weisz, A.; Scher, A.L.; Andrzejewski, D.; Ito, Y. *208th ACS National Meeting*, August 21-25, 1994, Washington, DC; Abstract ANYL77 in the Book of Abstracts.
24. Weisz, A. In *High-Speed Countercurrent Chromatography*; Ito, Y.; Conway, W.D., Eds.; Chemical Analysis Series; Wiley: New York, NY, in press.
25. Orndorff, W.R.; Adamson, W.A. *J. Am. Chem. Soc.* **1918**, *40*, 1235.
26. Kamikura, M. *Shokuhin Eiseigaku Zasshi* **1968**, *9*, 348; *Chem. Abstr.* **1969**, *70*, 79128z.

RECEIVED December 30, 1994

Downloaded by COLUMBIA UNIV on June 29, 2012 | http://pubs.acs.org
Publication Date: May 15, 1995 | doi: 10.1021/bk-1995-0593.ch016

Downloaded by PENNSYLVANIA STATE UNIV on June 28, 2012 | http://pubs.acs.org
Publication Date: May 15, 1995 | doi: 10.1021/bk-1995-0593.ch017

Chapter 17

Purification of 4,5,6,7-Tetrachlorofluorescein by pH-Zone-Refining Countercurrent Chromatography

Effects of Sample Size, Concentration of Eluent Base, and Choice of Retainer Acid

Kazufusa Shinomiya[1,3], Adrian Weisz[2,4], and Yoichiro Ito[1]

[1]Laboratory of Biophysical Chemistry, National Heart, Lung, and Blood Institute, National Institutes of Health, Building 10, Room 7N322, Bethesda, MD 20892
[2]Office of Cosmetics and Colors, Center for Food Safety and Applied Nutrition, U.S. Food and Drug Administration, Washington, DC 20204

Various factors involved in pH-zone-refining countercurrent chromatography were investigated in the purification of 4,5,6,7-tetrachlorofluorescein, using a two-phase solvent system composed of diethyl ether-acetonitrile-10 mM ammonium acetate (4:1:5). Trifluoroacetic acid (TFA) was added to the sample solution as a retainer acid. The results indicated that 1) increasing the amount of dye improved the yield of pure compounds; 2) increasing the concentration of ammonia in the solvent system increased the concentration of analytes in the mobile phase and shortened the retention time of the major peak; and 3) ammonium acetate in the solvent system could be eliminated and TFA in the sample solution could be replaced by acetic acid without significantly affecting the purification.

Countercurrent chromatography (CCC) is a form of liquid-liquid partition chromatography that does not use a solid support (*1*). The technique avoids complications caused by chromatographic supports, such as adsorptive sample loss and denaturation, tailing of solute peaks, contamination, etc. CCC has been widely used for many years to separate components of natural and synthetic products (*2*).

Recently, a new preparative CCC technique called pH-zone-refining CCC was developed (*3*) as a consequence of an incidental observation that, during the purification of a bromoacetylated thyroxine analog, the product formed an unusually sharp elution peak (*4*). Further studies revealed that bromoacetic acid present in the

[3] Current address: College of Pharmacy, Nihon University, 7–7–1, Narashinodai, Funabashi-shi, Chiba 274, Japan

[4] Guest researcher at Laboratory of Biophysical Chemistry, National Heart, Lung, and Blood Institute, National Institutes of Health, Bethesda, MD 20892

This chapter not subject to U.S. copyright
Published 1995 American Chemical Society

Downloaded by PENNSYLVANIA STATE UNIV on June 28, 2012 | http://pubs.acs.org
Publication Date: May 15, 1995 | doi: 10.1021/bk-1995-0593.ch017

sample solution as a reaction product formed a pH gradient in the mobile phase that concentrated the acidic solute at the steep rear border of the gradient zone. The introduction of various organic acids in the sample solution produced similar peak-sharpening effects for many other acidic compounds including the hydroxyxanthene dyes used in the present study.

When pH-zone-refining CCC was applied to the purification of a larger quantity of the hydroxyxanthene dye, the sharp elution peak underwent a drastic change (*3*): The major component in the sample mixture formed a flat broad peak with constant pH behind the pH-gradient zone in the aqueous phase because the mobile phase had become saturated with sample. Within this pH plateau, minor impurities were efficiently excluded according to their partition coefficients, moving toward either end of the plateau and forming sharp peaks. The method was found capable of purifying large quantities of compounds, even if they were only partially dissolved. One of the advantages of this method over other purification techniques is that the efficiency in terms of both yield and purity is improved as the amount of sample is increased.

In the chapter by Weisz et al., a quantitative aspect of the separation of components of commercial 4,5,6,7-tetrachlorofluorescein (TCF) is described in terms of recovery, yield, and purity as well as identification of contaminants from commercial TCF samples. The present chapter focuses on the effects of important experimental parameters such as amount of sample, concentration of eluent base in the mobile phase, and choice of retainer acid on purification of TCF. A series of experiments has been performed with a high-speed CCC centrifuge and a two-phase solvent system composed of diethyl ether-acetonitrile-10 mM ammonium acetate (4:1:5).

Experimental

Reagents. TCF was obtained from Aldrich (Milwaukee, WI). Diethyl ether, acetonitrile, methanol, and trifluoroacetic acid (TFA) were all glass-distilled chromatographic grade and purchased from Burdick & Jackson Laboratories (Muskegon, MI). Other chemicals including ammonium acetate, ammonium hydroxide (aqueous ammonia), and acetic acid were reagent grade and obtained from J.T. Baker Chemical Co. (Phillipsburg, NJ).

Apparatus. The present studies were performed using a commercial high-speed CCC centrifuge (P.C. Inc., Potomac, MD). The design of the apparatus is described in detail elsewhere (*5*). The column used for the present experiments was a semipreparative multilayer coil consisting of 16 coiled layers with a total capacity of about 325 mL. The entire column was made from a single piece of polytetrafluoroethylene (PTFE) tubing, 170 m × 1.6 mm i.d. (Zeus Industrial Products, Raritan, NJ). The β value (the ratio of the revolution radius to the distance from the holder axis to the coil), which is an important parameter determining the hydrodynamic distribution of the two solvent phases in the rotating coil, ranged from 0.5 at the internal terminal to 0.85 at the external terminal. The speed of the apparatus was regulated up to 1000 rpm by a speed control unit (Bodine Electric Co., Chicago, IL).

The solvent was pumped with a reciprocating pump (Accu-Flo pump, Beckman Instruments, Inc., Palo Alto, CA, or Milton Roy Minipump, LDC/Milton Roy Co., Riviera Beach, FL), the effluent was monitored with a UV detector (Uvicord S, LKB Instruments, Inc., Bromma/Stockholm, Sweden), and fractions were collected (Ultrorac, LKB Instruments, Inc.).

Preparation of Two-Phase Solvent System and Sample Solutions. The solvent system was prepared by mixing diethyl ether, acetonitrile, and 10 mM aqueous ammonium acetate at a volume ratio of 4:1:5. The solvent mixture was thoroughly equilibrated in a separatory funnel at room temperature. After the two phases were separated, aqueous ammonia (ca. 28%) was added to the lower mobile phase to adjust the pH to the desired level.

The sample solution was prepared by dissolving 350 mg of TCF in 10 mL of the solvent system consisting of equal volumes of each phase and then acidifying the solution by adding 200 μL of TFA, unless otherwise specified. The addition of TFA to the sample solution converted TCF to the hydrophobic lactoid form, which partitioned mostly into the upper nonaqueous phase. Because of reduced solubility at the lower pH, the sample formed a precipitate in the upper phase. To disperse the precipitate, the mixture was sonicated, and the resulting homogeneous suspension was injected into the CCC column without filtration. As described earlier, the present method permits loading an undissolved sample into the column (*3*).

CCC Separation Procedure. The purification was performed using a standard procedure previously described (*5*). The multilayer coil was first entirely filled with the stationary phase (upper nonaqueous phase), and the sample solution was injected through the sample port. Then the mobile phase (lower aqueous phase) was pumped into the column at a flow rate of 3 mL/min while the apparatus was rotated at 800 rpm. The absorbance of the effluent was continuously monitored at 206 nm with a Uvicord S detector, and 3-mL fractions were collected in test tubes. After the purification was complete, the apparatus was stopped and, by connecting the inlet of the column to a pressured N_2 line, the column contents were emptied into a graduated cylinder to measure the volume of the stationary phase retained.

Analysis of CCC Fractions. An aliquot of each fraction was diluted with a known volume of methanol, and the absorbance was manually determined at 254 nm with a Zeiss PM6 spectrophotometer. Fractions were also analyzed by reversed-phase high-performance liquid chromatography (RP-HPLC). The HPLC system consisted of a Model LC-6A pump (Shimadzu Scientific Co., Columbia, MD), a manual injector (Rheodyne, Berkeley, CA), a Model SPD-6A detector and a Model C-R5A recording data processor (both Shimadzu Scientific Co.), and a Capcell Pak C18 column, 13 cm × 0.46 cm i.d. (Shiseido, Tokyo, Japan). The flow rate of the mobile phase, composed of methanol-0.1 M ammonium acetate (1:1), was 1.0 mL/min, and the effluent was monitored at 254 nm.

Downloaded by PENNSYLVANIA STATE UNIV on June 28, 2012 | http://pubs.acs.org
Publication Date: May 15, 1995 | doi: 10.1021/bk-1995-0593.ch017

Downloaded by PENNSYLVANIA STATE UNIV on June 28, 2012 | http://pubs.acs.org
Publication Date: May 15, 1995 | doi: 10.1021/bk-1995-0593.ch017

Results and Discussion

Typical Elution Profile and HPLC Analyses of CCC Fractions. Figure 1A shows a typical chromatogram from CCC of TCF. The purification was performed with a solvent system of diethyl ether-acetonitrile-10 mM ammonium acetate (4:1:5) in which the pH of the lower mobile phase was adjusted to 9 by the addition of ammonium hydroxide. The other experimental conditions were as follows: Column, semipreparative multilayer coil with 16 coiled layers and 325-mL total capacity; revolution, 800 rpm; mobile phase, lower aqueous phase; flow rate, 3 mL/min; fractionation, 3 mL or 1 mL/tube.

In this chromatogram, the absorbance is shown by two solid lines: The thick line indicates the direct detection at 206 nm, and the thin line indicates the manual measurement (after dilution of an aliquot) of the absorbance at 254 nm with the PM6 Zeiss spectrophotometer. Although the two absorbance curves show similar trends, the direct tracing at 206 nm offers significant advantages as follows (Y. Ito et al., pH-Zone-Refining Countercurrent Chromatography: A New Technique for Preparative Separation, in this monograph): Direct monitoring of absorbance produces a smooth plateau, demonstrating a constant concentration of solute. In the manual measurement, dilution of concentrated solutions becomes a main source of error, resulting in an irregular plateau level. In addition, the sharp peaks at the plateau boundaries are well preserved in the direct tracing. In the manual measurement, these peaks become much broader because of the large volume of each fraction, 3 mL/tube. Because of these advantages, the chromatograms in Figures 2-4 were obtained by direct detection at 206 nm. (Direct detection at 254 nm produced an off-scale chromatogram at the plateau region.) One disadvantage of direct detection at 206 nm is that the absorbance, although responsive to changes in concentration, is not linear with concentration and no scale is given. The absorbance scale for manual measurement at 254 nm is adjusted for dilution of the fractions.

The dotted line in the chromatogram indicates the pH of the fraction as measured manually with a pH meter (Accumet 1001, Fisher Scientific Co., Fair Lawn, PA). The pH of the effluent decreases sharply at the mobile phase front (SF), and then decreases gradually until it rises sharply at 69 min, when an impurity (peak b) elutes. This first pH drop corresponds to elution of acetic acid from the ammonium acetate in the mobile phase. After the sharp rise from 5.6 to 6.5 (b), the pH again starts to fall (c). This second pH drop is produced mostly by the elution of TFA. The pH increases sharply at 95 min, when another impurity (peak d) elutes. Then the first pH plateau forms at pH 6.2 and 98 to 104 min, which corresponds to elution of a relatively large amount of a colorless impurity. At the end of this plateau, the pH rises to 8.1, forming a long second plateau that corresponds to the elution of the major component, TCF. At the beginning of this main pH plateau (f), impurities form a sharp peak. Finally, the pH curve returns to the original level after 170 min, which coincides with the elution of the last impurities (peak h).

HPLC analyses of aliquots of several of the fractions were performed as indicated by arrows in the chromatogram (b-h). As shown in Figure 1B-a, the original sample consisted of one major component, TCF (ca. 86% of the total peak area) and various impurities with a broad range of retention times. The HPLC

Downloaded by PENNSYLVANIA STATE UNIV on June 28, 2012 | http://pubs.acs.org
Publication Date: May 15, 1995 | doi: 10.1021/bk-1995-0593.ch017

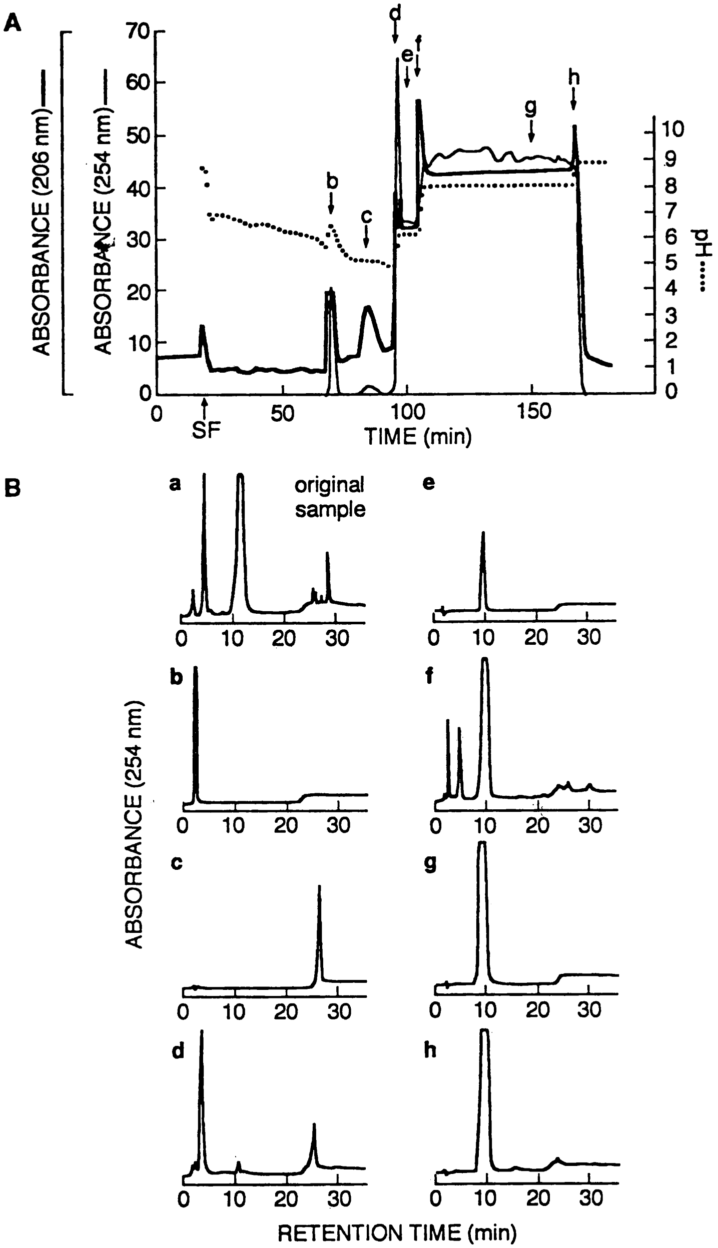

Figure 1. (A) Elution profile of 350 mg of TCF by pH-zone-refining CCC. Thick line: direct detection of absorbance at 206 nm. Thin line: manual measurement of absorbance at 254 nm. Dotted line: pH of CCC fraction, measured manually with a pH meter. SF: solvent front. (B) HPLC analyses of the original sample (a) and CCC fractions (b-h) corresponding to the points indicated in the chromatogram.

Downloaded by PENNSYLVANIA STATE UNIV on June 28, 2012 | http://pubs.acs.org
Publication Date: May 15, 1995 | doi: 10.1021/bk-1995-0593.ch017

conditions for the chromatograms in Figure 1B were as follows: Column, ODS-silica (250 × 4.6 mm i.d.); eluent, methanol-0.1M ammonium acetate (1:1) for 20 min and then changed to (3:1); flow rate, 1 mL/min; detection, 254 nm.

Figure 1B-b shows the chromatogram obtained for the first impurity (69 min), which consists of a single peak of a highly polar compound eluting at 2 min. The same peak is seen in the chromatogram of the original sample (a) as a very small peak. Chromatogram c (Figure lB) obtained for the fraction at 83 min under the broad absorption peak consisted of a single HPLC peak at 26 min. The width and location (not coinciding with the abrupt change of pH) of the CCC peak at 206 nm and the late HPLC retention time suggest that this impurity may be a hydrophobic neutral compound. Chromatogram d was obtained from HPLC analysis of the CCC fraction corresponding to the sharp peak (d) appearing before the main peak. It shows multiple peaks for impurities with a broad range of HPLC retention times. This finding clearly indicates the difference in elution order between HPLC and the present method. In RP-HPLC, analytes elute in order of increasing hydrophobicity regardless of their acidities. In contrast, the elution order of analytes in pH-zone-refining CCC is determined by two parameters, i.e., pK_a and hydrophobicity. For most organic acids, pK_a and hydrophobicity are correlated so that an analyte with higher hydrophobicity has a higher pK_a value. In such cases, the elution order of the analytes in pH-zone-refining CCC is similar to that in RP-HPLC. However, for a group of halogenated acids such as the hydroxyxanthene dyes the opposite relationship exists, so that the higher the hydrophobicity, the lower the pK_a value. In the present example, the elution order of the analytes in pH-zone-refining CCC is opposite to that in RP-HPLC; hence the more hydrophobic analytes elute earlier than the less hydrophobic analytes.

Chromatogram e (Figure 1B) obtained for colorless CCC fractions in the first plateau (98-104 min) shows a single peak which has the same retention time as the major peak. Thus, this impurity could not be separated from TCF by RP-HPLC under the applied conditions (see Figure 1B-f, g, and h).

Chromatogram f (Figure 1B) was obtained from HPLC analysis of the CCC fraction corresponding to the sharp peak appearing at the beginning of the major plateau (108 min). This fraction contained a group of hydrophilic subsidiary dyes and a few hydrophobic impurities that were eluted with the major component, TCF. Here again the result demonstrates the great potential of pH-zone-refining CCC for concentrating minor components.

HPLC analysis of the CCC fractions from the second plateau (110-167 min) (g) demonstrated the high purity of the major compound, TCF, which was greater than 99.9%. The CCC fraction corresponding to the sharp peak (h) at the end of the second plateau was found to contain an unidentified compound that produced a single HPLC peak.

Subsequent work focused on the effects of sample size, concentration of ammonia in the mobile phase, and choice of retainer acid on the purification of TCF.

Effects of Sample Size. A series of experiments was performed in which the sample amount was varied from 10 mg to 1 g under otherwise identical experimental conditions. The results are shown in Figure 2A-D. The experimental conditions for

Downloaded by PENNSYLVANIA STATE UNIV on June 28, 2012 | http://pubs.acs.org
Publication Date: May 15, 1995 | doi: 10.1021/bk-1995-0593.ch017

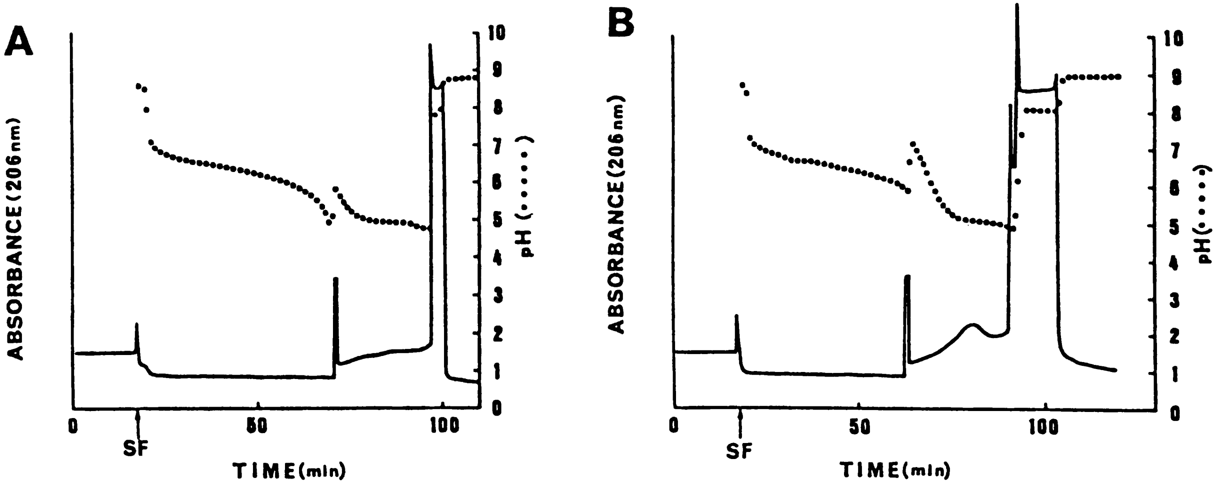

Figure 2. Effects of sample size on purification. These chromatograms were obtained from sample sizes of 10 mg (A), 50 mg (B), 350 mg (C), and 1 g (D) under otherwise identical experimental conditions. SF: solvent front.

Downloaded by PENNSYLVANIA STATE UNIV on June 28, 2012 | http://pubs.acs.org
Publication Date: May 15, 1995 | doi: 10.1021/bk-1995-0593.ch017

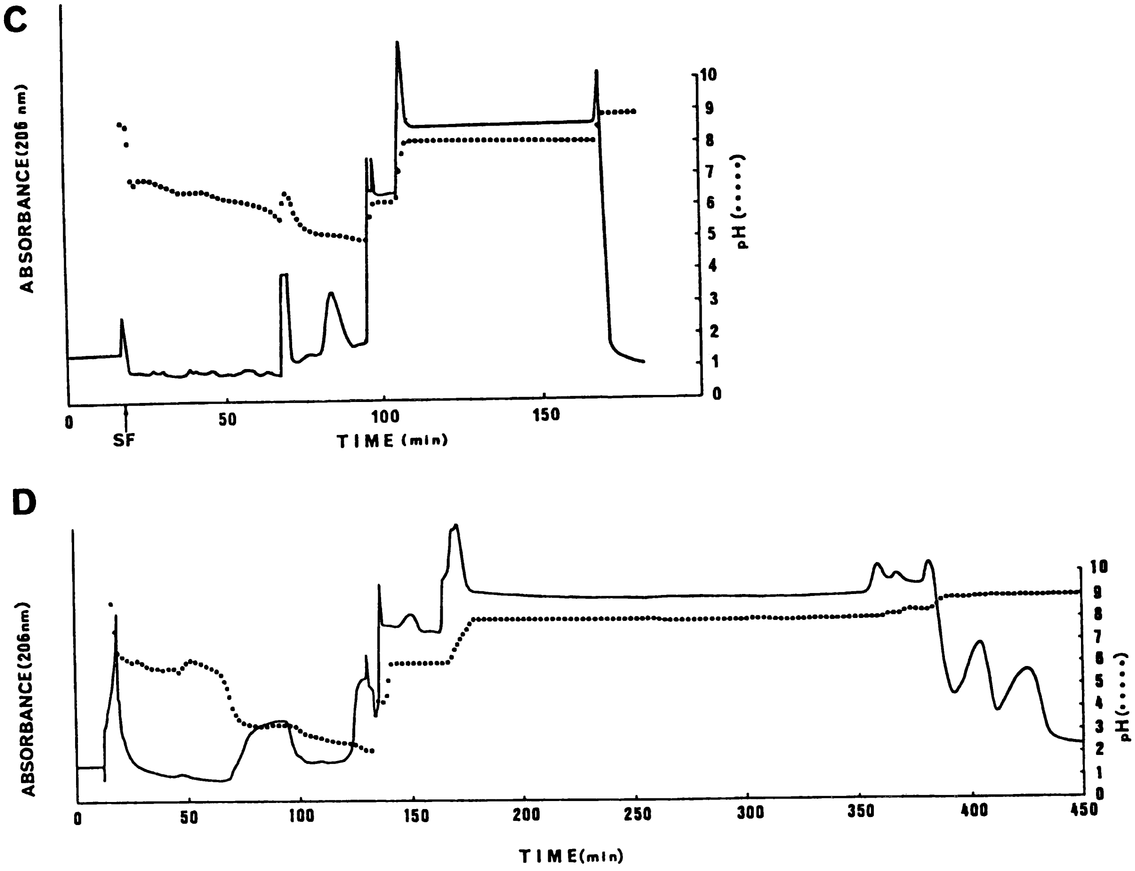

Figure 2. *Continued.*

the chromatograms in Figure 2 were as follows: Apparatus, high-speed CCC centrifuge with 10-cm revolution radius; column, multilayer coil of PTFE tubing (170 m × 1.6 mm i.d.) with a total capacity of about 300 mL; solvent system, diethyl ether-acetonitrile-10 mM ammonium acetate (pH 9) (4:1:5); mobile phase, lower aqueous phase; elution mode, head to tail; retainer acid, TFA, 200 μL in sample solution; revolution, 800 rpm.

An increase in sample amount from 10 mg to 1 g resulted in a nearly proportional increase in the length of the first and the second plateaus while the pH of each plateau remained the same. The retention time at the beginning of the main peak increased only slightly as sample size increased. The first sharp peak (around 70 min) became broadened in the 1-g purification where the abrupt pH shift was not produced. As documented in the chapter by Weisz et al., these results suggest that increasing the amount of the sample may increase the yield of pure compounds.

Downloaded by PENNSYLVANIA STATE UNIV on June 28, 2012 | http://pubs.acs.org
Publication Date: May 15, 1995 | doi: 10.1021/bk-1995-0593.ch017

Effects of Ammonia Concentration in the Mobile Phase. Experiments were performed to investigate the effect of ammonia concentration in the mobile phase on the CCC of TCF. In these experiments various amounts of ammonium hydroxide were added to the mobile phase to bring the pH to 8.7, 9.0, 9.5, and 9.7 while other conditions were unaltered. The experimental conditions were as follows: Apparatus, high-speed CCC centrifuge with 10-cm revolution radius; column, multilayer coil of PTFE tubing (170 m × 1.6 mm i.d.) with a total capacity of about 300 mL; sample, TCF (Aldrich), 350 mg; solvent system, diethyl ether-acetonitrile-10 mM ammonium acetate (4:1:5); mobile phase, lower aqueous phase; elution mode, head to tail; retainer acid, TFA, 200 μL in sample solution; revolution, 800 rpm.

The change in the ammonia concentration in the mobile phase produced profound effects on the elution profile as shown in Figure 3A-D. Increasing the concentration shortened the retention time of the main peak as well as the width of the first and second plateaus. The pH of each plateau was also raised as the ammonia concentration in the mobile phase increased. These changes may be a result of the increased number of ammonium ions in the mobile phase acting as counter ions for all anionic species including TCF, its subsidiary dyes, and TFA. Thus, the increased concentration of ammonia in the mobile phase increases the concentration of all anionic species in the mobile phase.

In practice, the use of a mobile phase with a higher pH increases the concentration of solute in the mobile phase and shortens the purification time. In contrast, the use of a mobile phase with a lower pH widens the plateau for each analyte and improves the purification.

Modification of Solvent Composition and Retainer Acid. In the previous purifications, the two-solvent system contained 10 mM ammonium acetate, and 200 μL of TFA was added to the sample solution. In this series, ammonium acetate (10 mM) was replaced by 0.05% (ca. 6 mM) ammonium hydroxide, and acetic acid (400 μL) was substituted for TFA in the sample solution. The results are illustrated in Figure 4, in which all chromatograms (A, B, and C) were obtained for 350 mg of sample under the standard CCC conditions.

Downloaded by PENNSYLVANIA STATE UNIV on June 28, 2012 | http://pubs.acs.org
Publication Date: May 15, 1995 | doi: 10.1021/bk-1995-0593.ch017

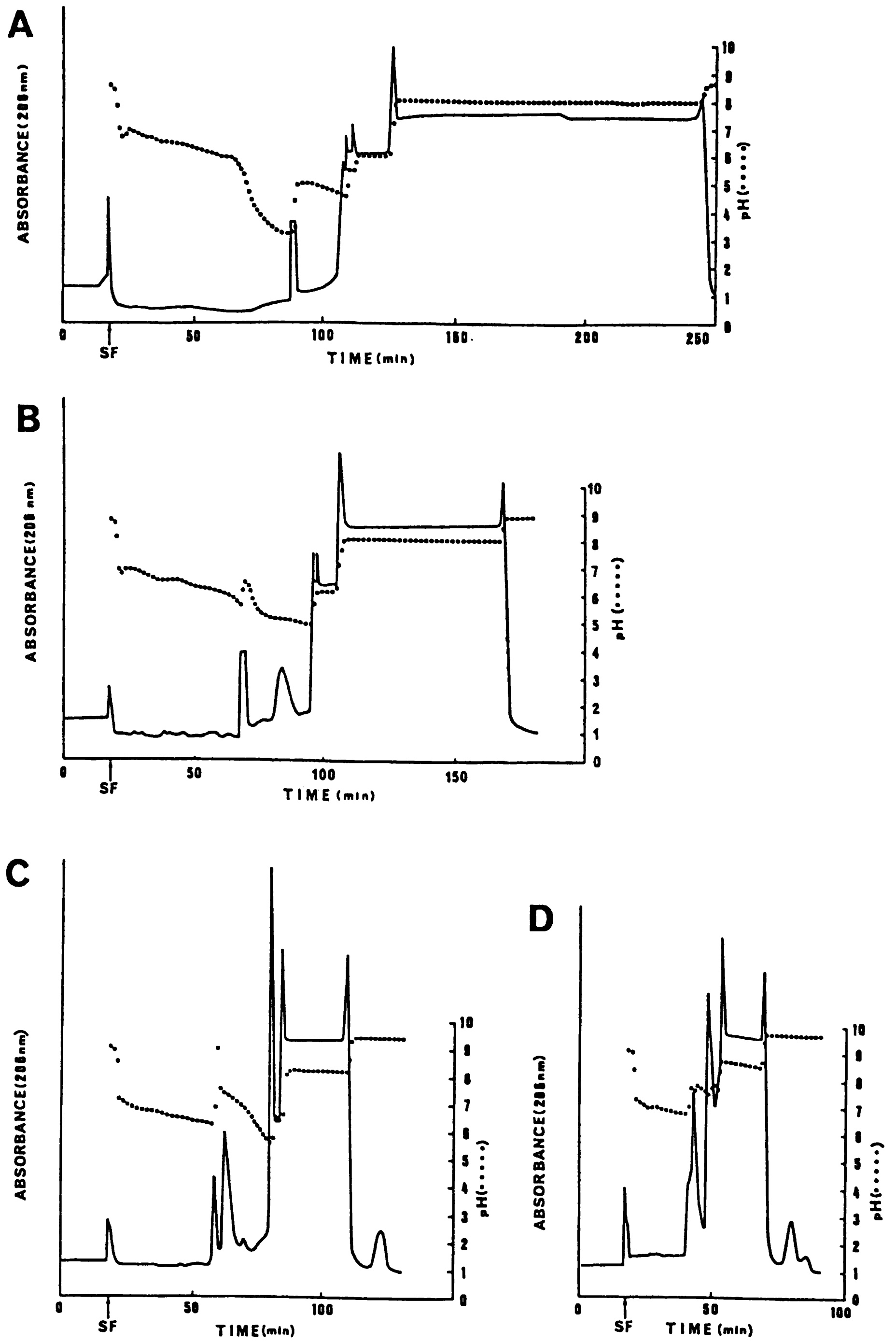

Figure 3. Effects of pH of mobile phase on purification: At pH 8.7 (A), 9.0 (B), 9.5 (C), and 9.7 (D). SF: solvent front.

Downloaded by PENNSYLVANIA STATE UNIV on June 28, 2012 | http://pubs.acs.org
Publication Date: May 15, 1995 | doi: 10.1021/bk-1995-0593.ch017

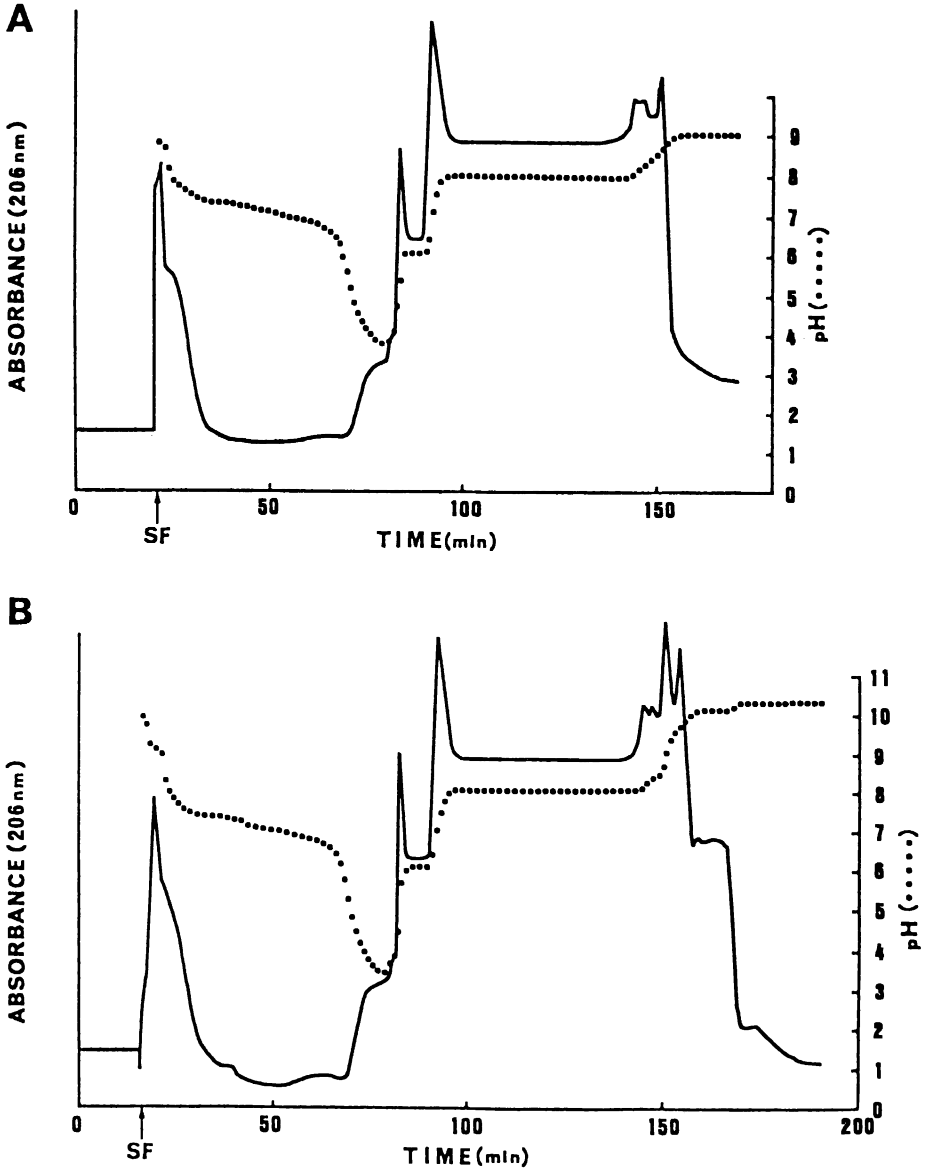

Figure 4. Effects of modified phase composition and choice of retainer acid on purification. (A) Solvent system, diethyl ether-acetonitrile-10 mM ammonium acetate (4:1:5) (pH 9.0); retainer acid, acetic acid (400 μL) in sample solution. (B) Solvent system, diethyl ether-acetonitrile-6 mM ammonia (4:1:5); retainer acid, acetic acid (400 μL) in sample solution. (C) Solvent system, diethyl ether-acetonitrile-6 mM aqueous ammonia (4:1:5); retainer acid, acetic acid (400 μL) and TFA (200 μL) in sample solution. Other experimental conditions were identical to those used for chromatograms in Figure 3. SF: solvent front.

Downloaded by PENNSYLVANIA STATE UNIV on June 28, 2012 | http://pubs.acs.org
Publication Date: May 15, 1995 | doi: 10.1021/bk-1995-0593.ch017

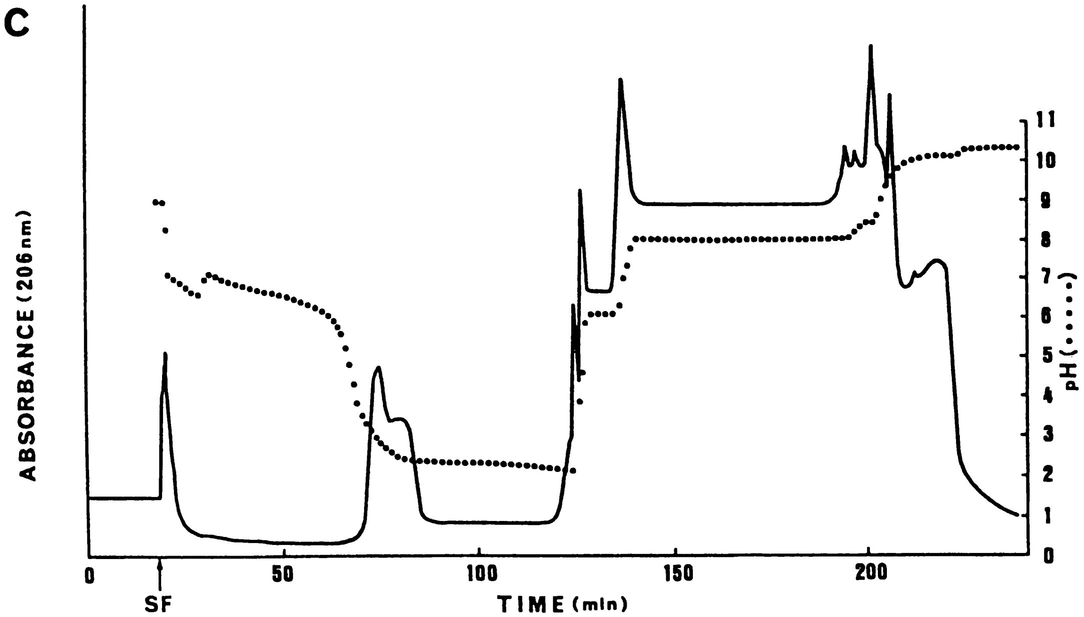

Figure 4. *Continued.*

Downloaded by PENNSYLVANIA STATE UNIV on June 28, 2012 | http://pubs.acs.org
Publication Date: May 15, 1995 | doi: 10.1021/bk-1995-0593.ch017

Chromatogram A (Figure 4) was obtained by using a solvent system composed of diethyl ether-acetonitrile-10 mM ammonium acetate (4:1:5) and adding 400 μL of acetic acid to the sample solution. The elution profile of the main peak is similar to that obtained with TFA in the sample solution (Figure 1A), except that the retention time is considerably shorter. The large amount of acetic acid added to the mobile phase formed a characteristic pH curve which shows a deep dip and a sudden rise at about 70 min along with an absorbance peak corresponding to this portion of the chromatogram.

Figure 4B is a chromatogram obtained by using a solvent system composed of diethyl ether-acetonitrile-6 mM ammonia (4:1:5) and adding 400 μL of acetic acid to the sample solution. The change from ammonium acetate (10 mM) to ammonia (6 mM) in the solvent system produced no significant change in the elution profile. Here again, acetic acid added to the sample solution produced a characteristic drop associated with an absorbance peak at about 70 min. Chromatogram C was obtained from the same solvent system, but both acetic acid (400 μL) and TFA (200 μL) were added to the sample solution to demonstrate the effect of TFA on the separation. Compared with chromatogram B, which was obtained with acetic acid alone, chromatogram C shows an increase in the retention time of the main peak, apparently caused by a prolonged low pH zone resulting from the addition of TFA to the sample solution. The decrease in pH produced by the acetic acid occurs at about 70 min, and the corresponding absorbance peak clearly indicates the elution of acetic acid. Therefore, the persisting low pH was evidently produced by the addition of TFA to the sample solution, which caused a delay in the elution of the main component.

The above results indicate that 1) ammonium acetate in the solvent system can be replaced by ammonium hydroxide without significantly changing the elution profile, and 2) acetic acid can be substituted for TFA in the sample solution.

Acknowledgments

The authors thank Dr. Henry M. Fales and Dr. Sandra J. Bell for technical review of the manuscript.

Literature Cited

1. Ito, Y.; R.L. Bowman. *J. Chromatogr. Sci.* **1970,** *8*, 315.
2. *Countercurrent Chromatography: Theory and Practice*; Mandava, N.B.; Ito, Y., Eds.; Marcel Dekker: New York, 1988.
3. Weisz, A.; Scher, A.L.; Shinomiya, K.; Fales, H.F.; Ito, Y. *J. Am. Chem. Soc.* **1994**, *116*, 704.
4. Ito, Y.; Shibusawa, K.; Fales, H.M.; Cahnmann, H.J. *J. Chromatogr.* **1992**, *625*, 177.
5. Conway, W.D. *Countercurrent Chromatography - Apparatus, Theory and Applications*, VCH: New York, 1990.

Received December 28, 1994

Downloaded by 89.163.35.42 on June 28, 2012 | http://pubs.acs.org
Publication Date: May 15, 1995 | doi: 10.1021/bk-1995-0593.ix001

Author Index

Andrzejewski, Denis, 203
Berthod, Alain, 16
Bordier, C. G., 62
Bully, Madeleine, 16
Cai, D.-G., 87
Carrupt, Pierre-Alain, 143
Chandrasekhar, Bhaskar, 111
Chiba, T., 119
Conway, Walter D., 1,129
Deroux, Jean Marc, 16
Du, Q. Z., 107
Fales, H. M., 156
Foucault, A. P., 62
Frias, E. Camacho, 62
Goupy, J., 47
Gu, M.-J., 87
Harada, K.-I., 92
Hayakawa, J., 92
Ikai, Y., 92
Ito, Yoichiro, 47,87,92,107,111,119,
156,184,203,218
Jin, T., 87
Knight, Martha, 111
Le Goffic, F., 62
Martin, D. G., 78
Matsumoto, U., 119
McGuire, James N., 129
Menet, J.-M., 35,47
Mukherjee, Anil B., 111
Nakazawa, H., 92
Oka, H., 92
Proefke, Mark L., 129
Rinehart, Kenneth L., 129
Rolet-Menet, M.-C., 35
Rosset, R., 35
Scher, Alan L., 156,184
Shibusawa, Y., 119
Shinomiya, Kazufusa, 47,156,203,218
Suzuki, M., 92
Takahashi, Kazuyuki, 111
Testa, Bernard, 143
Thiébaut, D., 35
Tsai, Ruey-Shiuan, 143
Weisz, Adrian, 156,203,218
Xiong, X. P., 107
Yamada, S., 92
Zhang, J.-D., 87
Zhang, T.-Y., 87
Zhu, G.-P., 87

Affiliation Index

Aichi Prefectural Institute of Public Health, 92
Beijing Institute of New Technology Application, 87
Centre National de la Recherche Scientifique 16,62
Chinese Academy of Agricultural Sciences, 107
Ecole Supérieure de Physique et Chimie Industrielles, 35,47
Meijo University, 92
National Institute of Public Health—Tokyo, 92
National Institutes of Health, 47,87,92,107,111,119,156,184,203,218
Nihon University, 47
Peptide Technologies Corporation, 111
Research Center of Pharmacy of People's Liberation Army's Navy, 87
State University of New York at Buffalo, 1,129
Tokyo College of Pharmacy, 119

In Modern Countercurrent Chromatography; Conway, W., et al.;
ACS Symposium Series; American Chemical Society: Washington, DC, 1995.

U.S. Food and Drug Administration, 156,184,203,218
Université de Lausanne, 143
Université de Lyon 1, 16
University of Illinois at Urbana–Champaign, 129
Upjohn Laboratories, 78

Subject Index

A

Acetyltylophoroside, purification by countercurrent chromatography, 85
Acquired immunodeficiency syndrome (AIDS),drug directed at reverse transcriptase enzyme, 111
Alkaloids, separation from *Senecio fuberi* Hemsl by high-speed countercurrent chromatography, 87–91
- applications, 91
- buffer pH vs. retention, 88,91
- chromatograms, 88,90*f*
- experimental procedure, 87–89
- TLC analysis of fractions, 88,90*f*

Ammonia, concentration in mobile phase, effect on CCC of 4,5,6,7-tetrachlorofluorescein, 226,227*f*
Apparent partition coefficient of retainer acid, calculation, 163–164
Apparent solute partition coefficient, calculation, 165,167
Aqueous alcohol–hydrocarbon solvent systems, optimization, 80
Aspartyl proteinase substrate peptide, purification, 111–117

B

Bond number values, 69–71*f*

C

Centrifugal partition chromatography
- flow pattern model of mobile phase, 62–74
- partition coefficient measurement, 143–153

Chambered plate chromatography, description, 5,8*f*
Coil planet centrifuge
- cross-axis, use of experimental design to determine optimal settings, 47–60
- description, 4–6*f*
- type J, comparison using orbital turns per theoretical plate, 35–45

Coil planet centrifuge chromatography, liquid flow, 5,7,8*f*
Count of orbital rounds per plate, definition, 37
Countercurrent chromatography
- advantages, 11,13,78,156
- applications, 1–2
- chambered plate chromatographs, 5,8*f*
- coil planet centrifuges, 4–6*f*
- comparison to other chromatographies, 2
- description, 218
- droplet countercurrent chromatography, 4,6*f*
- examples of coupled MS techniques, 129–130
- high- and low-density lipoprotein fractions from human serum, isolation, 119–128
- high speed, *See* High-speed countercurrent chromatography
- history, 3–4
- instrumentation, 129
- isolation of high- and low-density lipoprotein fractions from human serum, 119–128
- mobile phase, 16
- modern apparatus, 4–6*f*,8*f*
- optimization of solvent systems, 78–86
- overview, 1–13
- partition coefficient, 2

Downloaded by 89.163.35.42 on June 28, 2012 | http://pubs.acs.org
Publication Date: May 15, 1995 | doi: 10.1021/bk-1995-0593.ix001

U.S. Food and Drug Administration, 156,184,203,218
Université de Lausanne, 143
Université de Lyon 1, 16
University of Illinois at Urbana–Champaign, 129
Upjohn Laboratories, 78

Subject Index

A

Acetyltylophoroside, purification by countercurrent chromatography, 85
Acquired immunodeficiency syndrome (AIDS),drug directed at reverse transcriptase enzyme, 111
Alkaloids, separation from *Senecio fuberi* Hemsl by high-speed countercurrent chromatography, 87–91
  applications, 91
  buffer pH vs. retention, 88,91
  chromatograms, 88,90*f*
  experimental procedure, 87–89
  TLC analysis of fractions, 88,90*f*
Ammonia, concentration in mobile phase, effect on CCC of 4,5,6,7-tetrachlorofluorescein, 226,227*f*
Apparent partition coefficient of retainer acid, calculation, 163–164
Apparent solute partition coefficient, calculation, 165,167
Aqueous alcohol–hydrocarbon solvent systems, optimization, 80
Aspartyl proteinase substrate peptide, purification, 111–117

B

Bond number values, 69–71*f*

C

Centrifugal partition chromatography
  flow pattern model of mobile phase, 62–74
  partition coefficient measurement, 143–153
Chambered plate chromatography, description, 5,8*f*
Coil planet centrifuge
  cross-axis, use of experimental design to determine optimal settings, 47–60
  description, 4–6*f*
  type J, comparison using orbital turns per theoretical plate, 35–45
Coil planet centrifuge chromatography, liquid flow, 5,7,8*f*
Count of orbital rounds per plate, definition, 37
Countercurrent chromatography
  advantages, 11,13,78,156
  applications, 1–2
  chambered plate chromatographs, 5,8*f*
  coil planet centrifuges, 4–6*f*
  comparison to other chromatographies, 2
  description, 218
  droplet countercurrent chromatography, 4,6*f*
  examples of coupled MS techniques, 129–130
  high- and low-density lipoprotein fractions from human serum, isolation, 119–128
  high speed, *See* High-speed countercurrent chromatography
  history, 3–4
  instrumentation, 129
  isolation of high- and low-density lipoprotein fractions from human serum, 119–128
  mobile phase, 16
  modern apparatus, 4–6*f*,8*f*
  optimization of solvent systems, 78–86
  overview, 1–13
  partition coefficient, 2

Downloaded by 89.163.35.42 on June 28, 2012 | http://pubs.acs.org
Publication Date: May 15, 1995 | doi: 10.1021/bk-1995-0593.ix002

Countercurrent chromatography—*Continued*
  pH-zone-refining countercurrent chromatography, 10–12*f*
  purification of HIV–1 aspartyl proteinase substrate peptide, 111–118
  preparative technique, 3
  sample recovery, 3
  separation of alkaloids from *Senecio fuberi*, 87–91
  separation of cucurbitacin B and E from fruit base of *Cucumis melo*, 107–110
  separation of gardenia yellow components, 92–105
  solvent systems, 10
  stationary-phase retention, 16–34
  theory, 7,9–10,12*f*
  types, 156–157
Countercurrent distribution model
  mass balance equation, 185,187
  procedure, 185,186*f*
Crocin, separation by high-speed countercurrent chromatography, 92–105
Cross-axis coil planet centrifuge, use of experimental design to determine optimal settings, 47–60
Cucumis melo L., separation of cucurbitacin B and E from fruit base by high-speed countercurrent chromatography, 107–110
Cucurbitacin B and E, separation from fruit base of *Cucumis melo* L. by high-speed countercurrent chromatography, 107–110
  apparatus, 107
  chromatogram, 108,110*f*
  experimental procedure, 107
  HPLC analysis, 108,109*f*

D

D&C Orange No. 5, pH-zone-refining countercurrent chromatography, 174–176*f*
Dinitrophenylamino acids, pH-zone-refining countercurrent chromatography, 172–174
Dipeptides, on-line FAB MS detection in high-speed countercurrent chromatography through moving belt interface, 132–136
Diprotic acid, pH-zone-refining countercurrent chromatography, 200–202
Dispersion term, 66,69–71*f*
Displacement chromatography, comparison to pH-zone-refining countercurrent chromatography, 178,180–182
Droplet countercurrent chromatography, description, 4,6*f*

E

Effective section, definition, 37
Eluent base concentration, 4,5,6,7-tetrachlorofluorescein component purification, 226,228–230
Elution rate of trailing border of retainer acid, calculation, 163–164
Equilibrium model for pH-zone-refining countercurrent chromatography, 184–202
  countercurrent distribution model, 185–187
  diprotic acid, 200–202
  mathematical solution, 187
  monoprotic acid mixture, 194,196*f*
  plateau concentration of monoprotic acid, 197
  plateau pH prediction, 194,197–200
  retaining acid effect, 187–195
Erythromycins, on-line FAB MS detection in high-speed countercurrent chromatography through moving belt interface, 132–137
Ethyl acetate–hexane–aqueous methanol systems, optimization, 80
Experimental design to determine optical settings of cross-axis coil planet centrifuge, 47–60
  advantages, 47–48
  graphical analysis, 48–49
  interpretation by solvent, 54–59
  interpretation methods, 56,60
  methodology, 50–53

Downloaded by 89.163.35.42 on June 28, 2012 | http://pubs.acs.org
Publication Date: May 15, 1995 | doi: 10.1021/bk-1995-0593.ix002

Experimental design to determine optical settings of cross-axis coil planet centrifuge—*Continued*
  overall interpretation, 50,54
  solvents, 49–50

F

Fast atom bombardment MS detection in high-speed countercurrent chromatography through moving belt interface, on line, 129–142
Flow pattern of mobile phase in centrifugal partition chromatography, model based on Stokes law, 62–75
  apparatus, 62–63
  bond number, 69–71*f*
  consequence of Stokes' model, 70,72–74*f*
  dispersion term, 66,69–71*f*
  experimental procedure, 63
  interfacial area between phases in channels, 70,72
  linear velocities and diameter of Stokes droplets, 64,66*t*
  linear velocity–flow rate relationship, 64–65
  mobile-phase volume–flow rate relationship, 63–64,67*f*
  mobile-phase volume–rotational speed relationship, 66,67–68*f*
  systems used, 64,65*t*
Fractional volume of column occupied by stationary phase, definition, 36–37
Fruit base of *Cucumis melo* L., separation of cucurbitacin B and E by high-speed countercurrent chromatography, 107–110

G

Gardenia yellow components, separation by high-speed countercurrent chromatography, 92–105
  experimental procedure, 93–95
  HPLC identification, 95–101*f*
  photoisomerization of crocin, 105
Gardenia yellow components, separation by high-speed countercurrent chromatography—*Continued*
  purification, 102,104*f*
  selection of two-phase solvent system, 95,102–104*t*
Geniposide, separation by high-speed countercurrent chromatography, 92–105
Guadi, separation of cucurbitacin B and E by high-speed countercurrent chromatography, 107–110

H

Halocarbon–aqueous methanol systems, optimization, 80
Heptane–water systems, partition coefficients, 151
Hexane–aqueous methanol systems, optimization, 80
High- and low-density lipoprotein fractions from human serum, isolation by countercurrent chromatography, 119–128
  apparatus, 119–120
  composition of aqueous polymer phase systems, 120,121*f*
  experimental procedure, 119–123
  flow rate, 125,126*f*
  partition coefficients of lipoproteins and serum proteins, 123,124*f*
  polyacrylamide gel electrophoresis of fractions, 120–128
  polyethylene glycol molecular weight, 123,125*f*
High-performance liquid chromatography (HPLC)
  cucurbitacins B and E, 108,109*f*
  4,5,6,7-tetrachlorofluorescein, 204,205*f*,221–223
High-speed countercurrent chromatography
  separation of alkaloids from *Senecio fuberi* Hemsl, 87–91
  separation of cucurbitacin B and E from fruit base of *Cucumis melo* L., 107–110
  separation of gardenia yellow component, 92–105

Downloaded by 89.163.35.42 on June 28, 2012 | http://pubs.acs.org
Publication Date: May 15, 1995 | doi: 10.1021/bk-1995-0593.ix002

High-speed countercurrent chromatography—*Continued*
  on-line FAB MS detection through moving belt interface, 129–141
Human immunodeficiency virus 1 (HIV–1) aspartyl proteinase substrate peptide, purification, 111–117
  design of assay, 112–114
  experimental procedure, 114–115
  product generation, 115–116
  solvent system, 116,118
  tritiated peptide separation, 116,117*f*
Human serum, high- and low-density lipoprotein fraction isolated by countercurrent chromatography, 119–128

I

Indole auxins, pH-zone-refining countercurrent chromatography, 174,177*f*
Interfacial area between phases in channels, definition, 70,72
Isolation, high- and low-density lipoprotein fractions from human serum by countercurrent chromatography, 119–128

L

Linear velocity, definition, 63
Lipophilicity
  conceptual analysis, 143,147*f*
  relationship to biological activity, 143
  structural information encoded, 149,151
Lipophilicity-derived structural parameters, application to quantitative structure–activity relationships, 151–153
Lipoprotein fractions from human serum, isolation by countercurrent chromatography, 119–128
Liquid flow, coil planet centrifuge chromatography, 5,7,8*f*
Liquid–liquid partition coefficients
  measurement techniques, 144
  solute retention, 32,34
Liquid partition chromatography, limitations, 156
Liquid polarity
  and partition coefficient, 32–34
  and stationary-phase retention in countercurrent chromatography, 16–34
  indexes, 22–25*f*
  selection parameters, 20,22–24
Low- and high-density lipoprotein fractions from human serum isolation by countercurrent chromatography, 119–128

M

Mathematical model of pH-zone-refining countercurrent chromatography, 163–169
  apparent partition coefficient of retainer acid at plateau, 164
  elution rate of trailing border of retainer acid, 163–164
  multiple solute zones and mutual relationship, 167–169
  retention volume of retainer acid, 163–164
  solute zone formation behind sharp retainer border, 164–167
Measurement, partition coefficient, using centrifugal partition chromatography, 143–153
1-Methyl-4-methoxymethylcyclohexanecarboxylic acid, pH-zone-refining countercurrent chromatography, 178,179*f*
Mobile phase in centrifugal partition chromatography, flow pattern model, 62–74
Mobile-phase volume to column volume ratio, importance, 62
Model, flow pattern of mobile phase in centrifugal partition chromatography, 62–74
Monoprotic acids
  mixture, pH-zone-refining countercurrent chromatography, 194,196*f*
  plateau concentration, 197

Downloaded by 89.163.35.42 on June 28, 2012 | http://pubs.acs.org
Publication Date: May 15, 1995 | doi: 10.1021/bk-1995-0593.ix002

Moving belt interface
  on-line FAB MS detection in high-speed countercurrent chromatography, 129–141
  schematic representation, 130,131*f*

N

Neoplatyphylline, separation from *Senecio fuberi* Hemsl by high-speed countercurrent chromatography, 87–91
Nonaqueous solvent systems, stationary-phase retention in countercurrent chromatography, 32,33*f*
Number of theoretical plates, 35–36

O

Octanol–water system, partition coefficients, 149,151
On-line FAB MS detection in high-speed countercurrent chromatography through moving belt interface, 129–142
  advantages, 129
  dipeptides, 132–135*f*
  erythromycins, 133,137–141*f*
  experimental procedure, 130,132,135,137
  schematic representation, 130,131*f*
Optimal settings, experimental design for determination for cross-axis coil planet centrifuge, 47–60
Optimization of countercurrent chromatographic solvent systems, 78–86
  empirical partitioning in systems of varying polarity, approximate partition coefficients, 79–80
  initial need for semiquantitative monitoring system, 79
  optimization, various systems, 80
  tylophoroside isolation and purification, 81–86
Orbital turns per theoretical plate for comparison of countercurrent chromatographic devices, 35–46
  apparatus, 38
  count of orbital turns per plate, 44,45*f*
Orbital turns per theoretical plate for comparison of countercurrent chromatographic devices—*Continued*
  effective linear velocity of mobile phase, 39,42*f*
  efficiency, 39,43–44
  experimental conditions, 38–40*f*
  retention of stationary phase, 39,41*f*
  solvent systems and solutes, 38
  theory, 36–37

P

Partition coefficient
  and sample recovery, 2–3
  in heptane–water systems, 151
  in octanol–water systems, 149,151
  measurement using centrifugal partition chromatography, 143–153
Period of motion of column around central axis of apparatus, definition, 37
pH of mobile phase in equilibrated solute zone, calculation, 167
pH-zone-refining countercurrent chromatography
  advantages, 156,218
  apparatus, 169
  comparison to displacement chromatography, 178,180–182
  D&C Orange No. 5, 174,175–176*f*
  description, 10–12,184–185
  development, 218
  dinitrophenylamino acids, 172–174
  eluate analysis, 170,172
  equilibrium model, 184–202
  indole auxins, 174,177*f*
  mathematical model, 163–169
  1-methyl-4-methoxymethylcyclohexanecarboxylic acid, 178,179*f*
  number of components, 157,159–163
  preparative separation, 156–182
  principle, 157–163
  L-proline benzyl ester, 178,181*f*
  reagents, 169
  sample size, 157,159–163
  separation procedure, 170

Downloaded by 89.163.35.42 on June 28, 2012 | http://pubs.acs.org
Publication Date: May 15, 1995 | doi: 10.1021/bk-1995-0593.ix002

Downloaded by 89.163.35.42 on June 28, 2012 | http://pubs.acs.org
Publication Date: May 15, 1995 | doi: 10.1021/bk-1995-0593.ix002

pH-zone-refining countercurrent chromatography—*Continued*
  solvent phases to initiate model experiments, 157,158*f*
  4,5,6,7-tetrachlorofluorescein component separation, 203–216
  two-phase solvent system and sample solution, 170,171*t*
Plates, theory, 35
Platyphylline, separation from *Senecio fuberi* Hemsl by high-speed countercurrent chromatography, 87–91
Polarity of countercurrent chromatography solvents, definitions, 17
Preparative separation, 4,5,6,7-tetrachlorofluorescein components by pH-zone-refining countercurrent chromatography, 203–216
L-Proline benzyl ester, pH-zone-refining countercurrent chromatography, 178,181*f*
Purification
  HIV-1 aspartyl proteinase substrate peptide, 111–118
  4,5,6,7-tetrachlorofluorescein components by pH-zone-refining countercurrent chromatography, 218–230

Q

Quantitative structure–activity relationships, application of lipophilicity-derived structural parameters, 151–153

R

Raclopride, quantitative structure–activity relationships, 152*f*,153
Resolution, countercurrent chromatography theory, 9–10
Response, chromatographic, definition, 49
Retainer acid *or* retaining acid
  pH-zone-refining countercurrent chromatography, 187–195
  plateau pH prediction, 194,197–199*f*
Retainer acid *or* retaining acid—*Continued*
  4,5,6,7-tetrachlorofluorescein purification, 226,227*f*
Retention percentage, definition, 20
Retention volume of retainer acid, calculation, 163–164
Reverse transcriptase inhibitor drugs, examples, 111

S

Sample acids, plateau pH prediction, 197,200
Sample recovery, determination, 2
Sample size, 4,5,6,7-tetrachlorofluorescein component purification, 223–226
Senecio fuberi Hemsl, separation of alkaloids by high-speed countercurrent chromatography, 87–91
Separation by high-speed countercurrent chromatography
  alkaloids from *Senecio fuberi* Hemsl, 87–91
  cucurbitacins B and E from fruit base of *Cucumis melo* L., 107–110
  gardenia yellow components, 92–105
Serum lipoproteins, chromatographic separations, 119
Solubility parameter, definition, 20,24
Solute properties, determination by measurement of partition coefficient, 143–153
Solvent(s)
  composition, 4,5,6,7-tetrachlorofluorescein purification, 226,228–230
  list, 24,26–27*t*
  polarity, influencing factors, 20
  polarity indexes, 22–25*f*
  selection parameters, 20,22–24
  systems in countercurrent chromatography, 10
Squalidine, separation from *Senecio fuberi* Hemsl by high-speed countercurrent chromatography, 87–91
Stationary-phase loss rate, definition, 20
Stationary-phase retention
  in countercurrent chromatography, 16–34

Stationary-phase retention—*Continued*
  chromatographic system, 17–18
  experimental procedure, 16–20
  initial stationary-phase retention, 24,28–30
  liquid–liquid partition coefficient, 32,34
  nonaqueous solvent systems, 32,33*f*
  rate of stationary-phase loss, 30,32
  solvent polarity indexes, 22–25*f*
  solvent selection parameters, 20,22–24
  solvents used, 24,26–27*t*
  stable stationary-phase retention, 30,31*f*
  theoretical model, 20,21*f*
Stationary-phase volume, definition, 18
Stokes' law, basis of flow pattern model of mobile phase in centrifugal partition chromatography, 62–74
Structural determinants of solubility-related molecular properties of neutral organic solutes in solution, calculation, 149
Structural information, encoded in lipophilicity, 149,151

T

4,5,6,7-Tetrachlorofluorescein,
  HPLC analyses, 204,205*f*
  synthesis, 203–205*f*
4,5,6,7-Tetrachlorofluorescein
  purification by pH-zone-refining countercurrent chromatography, 218–230
    apparatus, 219–220
    elution profile, 220–221
    experimental procedure, 219–220
    HPLC analyses of fractions, 221–223
    mobile-phase ammonia concentration, 226,227*f*
4,5,6,7-Tetrachlorofluorescein—*Continued*
  purification by pH-zone-refining countercurrent chromatography—*Continued*
    retainer acid, 226,229–230
    sample size, 223–226
    solvent composition, 226,228–230
  separation by pH-zone-refining countercurrent chromatography, 203–216
    byproduct formation, 211,215*f*
    characterization of compounds, 211,213–214*f*
    chromatograms, 209,210*f*
    compounds isolated, 209,211,212*f*
    condensation of tetrachlorophthalic anhydride with resorcinol molecules, 211,212*f*
    experimental procedure, 206–209
    sample size, 211,215–216*f*
Theoretical plates, description, 35
Theory of plates, development, 35
Tylophoroside, isolation and purification by countercurrent chromatography, 81–86
  empirical partitioning, 81
  final purification, 84–85
  initial isolation, 84
  semiquantitative monitor development, 81,83*f*
  structures, 81,82*f*
Type J coil planet centrifuges, comparison using orbital turns per theoretical plate, 35–45

V

Versatility, countercurrent chromatography, 3

Downloaded by 89.163.35.42 on June 28, 2012 | http://pubs.acs.org
Publication Date: May 15, 1995 | doi: 10.1021/bk-1995-0593.ix002